Electrospun fibers for the prevention of human immunodeficiency virus

Cameron Ball

A dissertation

submitted in partial fulfillment of the

requirements for the degree of

Doctor of Philosophy in Bioengineering

University of Washington

2014

Reading Committee:

Kim A. Woodrow, Chair

Buddy Ratner

David F. Katz

Program Authorized to Offer Degree:

Bioengineering

University of Washington

Abstract

Electrospun fibers for the prevention of human immunodeficiency virus

Cameron Ball

Chair of the Supervisory Committee:
Professor Kim A. Woodrow, PhD
Bioengineering

HIV/AIDS education, testing, and treatment have thus far failed to cease the pandemic spread of the HIV virus. HIV prevention is hindered by a lack of protective options beyond the ABC approach of abstinence, being faithful, and using condoms. One approach to address this inadequacy is to develop antiviral products for vaginal or rectal application that provide receptive partner-initiated protection against viral infection during sex. Such products, termed anti-HIV microbicides, can especially empower young women to take control over their sexual health.

This work explored a new approach to anti-HIV microbicides: electrospun fibers for the delivery of small-molecule antiretroviral drugs. Electrospun microbicides are nonwoven fabrics made from polymer-based nanofibers. The wide array of polymers available for electrospinning allowed for the incorporation and release of chemically diverse agents. Since electrospun fibers have an extremely high surface area to volume ratio, they serve as excellent delivery systems for rapid drug delivery of both hydrophilic and hydrophobic agents. The flexibility in the design of electrospun fibers afforded by coaxial electrospinning further enabled the formulation of sustained-release microbicides. To demonstrate the power of electrospinning to deliver drugs over multiple timescales, composite microbicide fabrics were created to provide both rapid and sustained drug release from a single device.

This work has produced alternative microbicide formulations, while establishing methods for the thorough characterization of these systems and solutions for the needs of people at risk of HIV infection. By addressing problems in both HIV prevention and drug delivery, this work has expanded our capacity to engineer elegant solutions to complex and pressing global health challenges.

Table of Contents

List of Figures

List of Tables

Preface: Summary of Research Aims

Unsafe sex is the 2nd most important risk factor leading to disease, disability, or death in the developing world, and the 9th in the developed world[1]. Each year, an estimated 80 million women experience unintended pregnancy[1], and an estimated 2.5 million people become infected with human immunodeficiency virus (HIV)[2]. The spread of HIV is exacerbated by coincidence of other sexually transmitted infections (STIs), for which incidence rates are shockingly high amongst female youth in the developing world. Innovating new multipurpose prevention technologies (MPT) that simultaneously prevent HIV, other STIs, bacterial infections, and unintended pregnancy is a research priority. We hypothesized that electrospun fiber meshes could deliver diverse sets of drugs over either rapid (minutes) or prolonged (days) timescales for use in MPTs and anti-HIV microbicides. Electrospinning has been used extensively in the field of tissue engineering and drug delivery with a proven history of long-term safety and feasibility[3]. For this work, rapid release of high drug content from fibers was engineered based on polymer carrier aqueous solubility, polymer-drug compatibility and the physical state of active agents within electrospun materials. Controlled release of anti-HIV or anti-STI/BV compounds over 72 hours was achieved through the design of coaxial electrospun fibers with high drug loading in the fiber core and a sustained release polymer coating in the shell. Composite materials containing both rapid-release and prolonged-release fibers were capable of providing an initial burst release of drug, followed by sustained release of the compound over time. This technology might enable female-initiated dual protection/treatment against HIV, other STIs/BV, and unintended pregnancy, and could act as either a coitally dependent or coitally independent microbicide.

Aim 1.

Our first goal was to demonstrate electrospun fibers' ability to formulate and release diverse compounds for the prevention of HIV, unintended pregnancy, and HSV-2. Combining chemical and physical barriers offers the greatest potential to design effective MPTs, but integrating both functional modalities into a single device has been challenging. We showed that drug-eluting fiber meshes designed for topical drug delivery could function as a combination chemical and physical barrier MPT. Using FDA-approved polymers, we fabricated nanofiber meshes with tunable fiber size and controlled degradation kinetics that facilitated simultaneous release of multiple agents against HIV-1, HSV-2, and sperm. We observed that drug-loaded meshes

inhibited HIV-1 infection *in vitro* and physically obstructed sperm penetration. Furthermore, we reported on a previously unknown activity of glycerol monolaurate (GML) to potently inhibit sperm motility and viability. The application of drug-eluting nanofibers for HIV-1 prevention and sperm inhibition may serve as an innovative platform technology for drug delivery to the lower female reproductive tract.

Aim 2.

Our second research aim was to formulate maraviroc into rapidly dissolving solid dispersions for instantaneous drug release. Topical anti-HIV microbicides empower women to protect themselves against HIV infection by prophylactically self-administering antiretroviral drugs to the cervicovaginal mucosa. Pericoital drug delivery systems intended for use immediately before sex, such as microbicide gels, must deliver high drug doses for maximal effectiveness. The goal of achieving a high antiretroviral dose is complicated by the need to simultaneously retain the dose and quickly release drug compounds into the tissue. For drugs with limited solubility in vaginal gels, increasing the gel volume to increase the dose can result in leakage. While solid dosage forms like films and tablets increase retention, they often require more than 15 minutes to fully dissolve, potentially increasing the risk of acquiring epithelial abrasions during sex. In this aim, we demonstrate that water-soluble electrospun fibers, with their high surface area to volume ratio and ability to disperse antiretrovirals, can serve as an alternative solid dosage form for pericoital microbicides requiring both high drug loading and rapid hydration rates. We formulate maraviroc at up to 30 wt% into electrospun solid dispersions made from either polyvinylpyrrolidone or poly(ethylene oxide) nano- or micro-fibers, and investigate the role of drug loading, distribution, and crystallinity in determining drug release rates into aqueous media. We show that water-soluble electrospun materials can rapidly release high levels of maraviroc upon contact with moisture, and that drug delivery is faster (less than 6 minutes) when maraviroc is electrospun in polyvinylpyrrolidone fibers containing Tween 20 as a wetting agent. These materials offer an alternative dosage form to current pericoital microbicides.

Aim 3.

Next, we formulated maraviroc and metronidazole into electrospun fibers for sustained drug release out to 72 h. Maintenance of drug concentrations within their therapeutic windows requires controlled release of agents to replace metabolized or excreted actives. A useful

sustained release system would provide tunable control over the release rate of drugs by simple modulation of drug loading and polymer coating characteristics. This was achieved via coaxial electrospinning, a flexible method of creating polymer nanofibers from solution with discrete core and shell regions[4]. High maraviroc or metronidazole content in the coaxial fibers' cores established a depot of drug for release over 72 hours. A hydrophobic polymer shell controlled the rate of drug release primarily by slowing the rate of water penetration into the electrospun fabrics (through controlled surface wetting) and secondarily by acting as a release rate controlling membrane (through a diffusion mechanism). In Aim 3, we explored several important qualities of polymer-drug systems that determine the release rate of small molecule hydrophilic drugs, namely maraviroc and metronidazole, from electrospun fibers, including modulation of drug loading, core polymer type, and coaxial electrospinning parameters. Release properties were monitored *in vitro* using a variety of release media. The activity of formulated maraviroc was monitored *in vitro* to confirm no loss of efficacy against HIV following incorporation and release from fibers.

Aim 4.

Finally, the work reported in this thesis demonstrated instant and 72 h protection against HIV by creating composites of maraviroc-loaded electrospun materials developed in Aims 2 and 3. A major concern with pericoital products is that the drugs may no longer be active by the time of use if applied too far in advance of sexual activity. This is particularly true of maraviroc (and metronidazole for BV), which has a half-life on the order of several hours in plasma. In contrast, sustained release products must be in place long before exposure to sperm or HIV in order to be effective due to slow rates of drug release. Macro scale composites of rapidly releasing uniaxial fibers and slowly releasing coaxial fibers can fill the gap in the MPT pipeline for a product that deliberately produces a quick burst release of material followed by further, sustained release of multiple APIs. Composite materials containing maraviroc were produced by layering fiber formulations using various bonding or welding techniques. The effect of these methods on drug release and composite materials' ability to resist delamination during handling was evaluated. This work showed that post-electrospinning processes could generate composites that act as a superposition of component materials during *in vitro* release under sink conditions. These characteristics are consistent with "set it and forget it" microbicides, which may enjoy higher adherence among certain user populations than current pericoital or sustained release microbicides.

Acknowledgments

I have been extremely fortunate to work so closely with my supervisor, Prof. Kim Woodrow, over the last four years. I came to Kim's lab by serendipity and quickly became enamored by her dedication to translational research on HIV prevention, treatment, and vaccination. Kim is a brilliant and tireless scientist, and has inspired me to apply my training to the grand challenges of our time. I am grateful for her courage—for trusting me so much to explore my research interests and to act as a partner in growing her nascent research group into the successful and exciting organization it is today. Kim has worked endlessly to ensure that I had funding to pursue this research, and I can't thank her enough for her financial support and professional advocacy. It has been a long, sometimes arduous journey, and Kim deserves endless credit and appreciation for seeing me through the doctoral program. It has been an honor getting to know Kim, and I look forward to watching her change the world through her dedication to science and engineering.

I would also like to thank my supervisory committee for their many insightful conversations and difficult questions. They have served me both as mentors and as role models. I am especially grateful for their personal warmth and respect. Many thanks go to Prof. Buddy Ratner and Prof. David Katz for their willingness to serve on my reading committee and for their technical consultations on polymers, drug delivery, and anti-HIV microbicides. I would like to thank Prof. Suzie Pun for her razor-sharp mind, open attitude, and sincere feedback. Last but not least, I would like to thank Prof. Jared Baeten, a fellow Washington University in St. Louis alumnus and giant in the field of HIV prevention and microbicide research, for serving as my graduate student representative. Amidst managing some of the world's most important HIV research projects across multiple continents and three University of Washington departments, Jared has somehow effortlessly fulfilled the roles of advocate, consultant, and friend.

This work would not have been possible were it not for the support of Dr. Florian Hladik and his research staff. I am further indebted to Dr. Charles Muller and the staff of the University of Washington's Male Fertility Clinic, as well as Dr. John Amory for their assistance with my work on electrospun fibers for contraception. I am especially grateful for Dr. Elizabeth Micks for providing me with expert advice on issues related to women's health and for providing me with opportunities to shadow her in clinical practice. I owe a great deal of thanks to Dr. Lara Gamble, Gerry Hammer, and Scott Braswell at the UW's Nanotechnology User Facility and Surface Analysis Recharge Center for access to and training on several crucial instruments. Tuesday

Kuykendall deserves acknowledgement for her training and assistance with calorimetry experiments at the UW's Department of Materials Sciences.

This thesis reflects just one small part of a much larger effort on the part of my fellow group members and collaborators. Without their hard work, none of this work would have been possible. I am especially indebted to Dr. Thanyanan Chaowanachan, for her impeccable training and extraordinary heart. My sincerest thanks to my colleague and friend Emily Krogstad, for her exceptional commitment to quality research, human connection, and love. Anna Blakney has collaborated with me on numerous projects and publications, and I can't wait to see her take the scientific world by storm. Joe Phan and Renuka Ramanathan have been there for me though it all, helping me in lab when I ran into myriad problems requiring their expertise. Many thanks to the rest of the fiber research group—Dr. Huarong Nie, Rick Edmark, Arielle Steger, Daniel Carson, and Dr. Shih-Feng Chou—for long conversations, fruitful collaborations, and critical discoveries that helped advance my own work. Dr. Yonghou Jiang has buoyed me up with his good-natured help and virological expertise. I also need to thank the many former undergraduates in our lab, especially Deep Hathi, Rachel Lucero, Jennifer Wilson, and Qichen Xu, for granting me the opportunity to practice mentorship and collaborative learning.

I would not have made it this far without the wisdom and guidance given to me by former advisors and role models. In particular, I would like to thank Prof. Paul Yager for his relentless questioning of fundamental phenomena, and Prof. Barry Lutz for his brilliant engineering and dedication to students. I would also like to thank Prof. Wendy Thomas for keeping the faith in student-faculty relationships. I cannot say enough about my undergraduate advisor and friend, Prof. Robert Mecham, and all that he has given me. Prof. Brian Hedlund deserves credit for infecting me with the enthusiasm for biological research. Prof. Sharon Stahl and Dr. Bill Danforth have shaped my life in tremendous ways, and I owe them everything for a spectacular education and principles by which to live my life.

Graduate education is never without its struggles; laying siege to the ivory tower for a degree requires commitment, motivation, and perspective, for which I have to thank my many friends and family. Special thanks to Theodore Chen, Chin Jung Cheng, and Camilo Perez, as well as the UW Aikido club, Gary Barnett, and Carter Danne. My heartfelt appreciation goes out to Scott and Margaret Ball, as well as Kylie, Calvin, and Alex for their profound love and steadfast support. And of course, many thanks to Rochelle Nguyen, my eternal companion, for sharing her sublime wisdom, love, and laughter along this incredible journey through life.

What an illness
My life is meaningless
You make my life lifeless
You make me hopeless
What an illness

You don't care who you kill
It old and young
Big and small
Bad or good
What an illness

The sky was blue
Now it's black
People hate each other
Because of you HIV/AIDS
What an illness

By S.N.

Primary school KaNyamazane, South Africa

Dedication

To the young people of the world

May hope give you life

May life give you meaning

And may meaning help you love

Under the blue sky

Chapter 1. Introduction

Portions modified from Ball and Woodrow, in: Drug Delivery and Development of Anti-HIV Microbicides; J. das Neves, B. Sarmento; Eds., Singapore, Pan Stanford Publishing Pte. Ltd. (CRC Press) 2014.

1.01 HIV pathogenesis

Acquired immunodeficiency syndrome (AIDS) was first recognized as a new disease by the US Center for Disease Control in 1981, after large numbers of young men who have sex with men began suffering from opportunistic infections that led inexorably to death[5]. In 1984, researchers reached a consensus that the etiological agent of AIDS was a retrovirus, given the name human immunodeficiency virus (HIV)[6]. The virus was a zoonotic agent that is believed to have spread to humans from chimpanzees and gorillas. Unlike previous zoonoses from simian immunodeficiency viruses, the HIV-1 (M type) class of viruses spread rapidly through human populations with devastating effects[7]. HIV-1 is largely responsible for the current HIV/AIDS pandemic, which is thought to have reached its peak in the year 1999. Due in part to education, antiretroviral therapy, and other HIV prevention measures, the number of new HIV infections globally fell by nearly 19% from 1999 to 2011[2]. Today, HIV remains the most devastating virus to have emerged in recent history, having infected at least 60 million people and claimed 25 million lives[5].

The HIV virus is a lentivirus that primarily infects $CD4^+$ T-cells, macrophages, and dendritic cells of the human immune system[7]. Once HIV infects these cell populations, it leads to dramatic decreases in immune cell populations, particularly $CD4^+$ T-cells in mucosal tissues, due to viral killing of infected cells, inducing apoptosis in nearby immune cells, and targeted killing by anti-HIV specific $CD8^+$ cytotoxic T-cells[8]. Even during chronic stages of HIV infection, viral turnover remains dynamic[9], and constant immune activation, particularly of $CD4^+$ T-cells, is a hallmark of the disease[7,10,11]. As the affected cell types are crucial for regulating and effecting cellular immunity against infection and cancer, infection with HIV leads progressively toward more frequent and severe opportunistic infections and the development of cancers. For in depth reading on the pathogenesis of HIV, readers should refer to reviews in the HIV/AIDS literature[8,12-14]. The majority of new HIV infections occur during heterosexual intercourse, and the pathways for infection at the cervicovaginal mucosa are depicted in Figure 1.1.

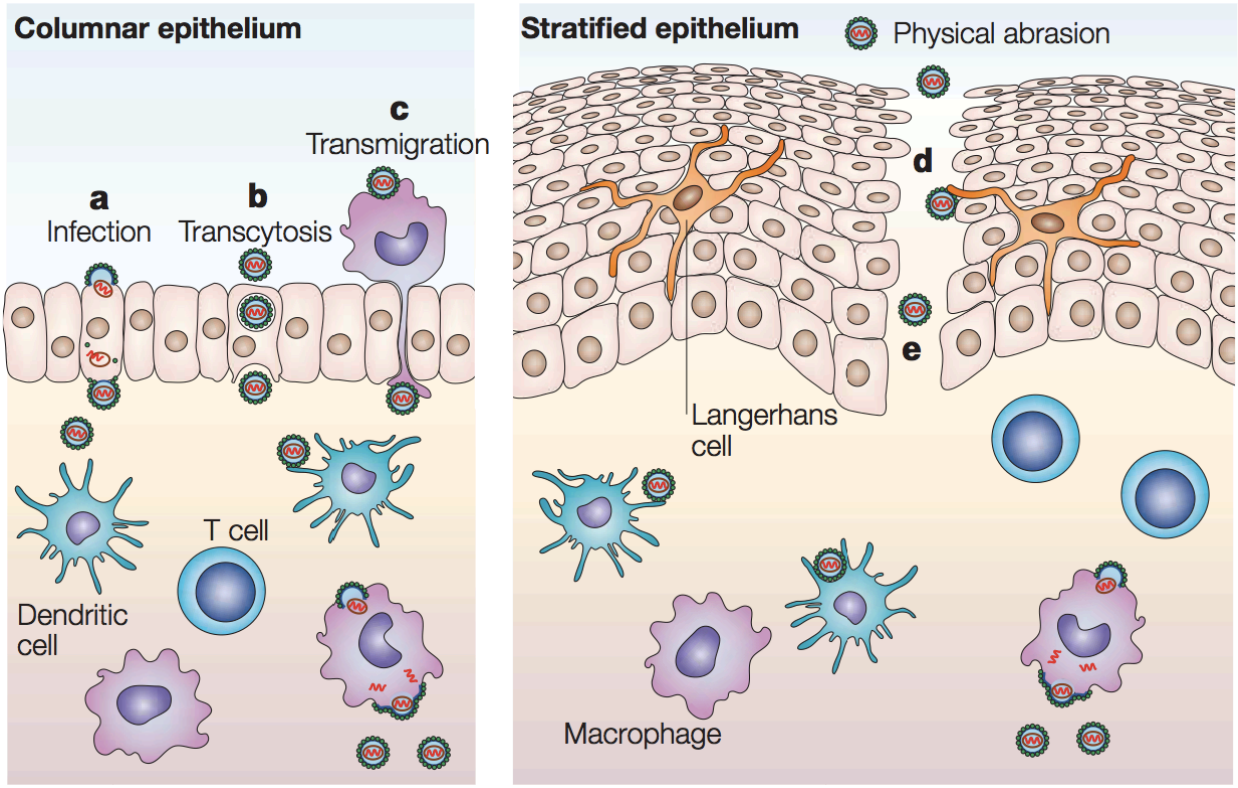

Figure 1.1—Possible mechanisms for HIV-1 infection at mucosal sites during intercourse. The endocervical and rectal epithelia are columnar, while the vaginal and ectocervical epithelia are stratified. **a)** Direct infection of epithelial cells. **b)** Transcytosis across epithelial cells or by specialized microglial (M) cells. **c)** Epithelial transmigration of infected donor cells. **d)** Uptake by intra-epithelial Langerhans cells. **e)** HIV viral particles can gain access to target immune cells via abrasions in epithelial tissue. Once they pass through the nonkeratinized squamous epithelium of the vaginal mucosa, they reach the stromal tissue, which contains immune cells: dendritic cells, $CD4^+$ T cells, and macrophages. These cells can traffic or *trans*-infect other immune cells both locally and in regional lymph nodes, leading to seroconversion. Reproduced with permission from Shattock and Moore, 2003[13].

As bioengineers, we can integrate our knowledge of materials, systems, biology and infectious disease, and bring that to bear on preventing HIV infections and premature death. Over the past decades, much has been learned about the mucosal transmission of HIV-1, and new discoveries in the immunology of HIV infection[14], antiretroviral therapy, drug delivery systems, and biomaterials for modulating immunity offer tools for creating innovative technologies to slow disease progression. Engineers will play a central role in applying scientific and medical principles to improve HIV prevention and treatment measures for decades to come.

1.02 The case for anti-HIV microbicides

HIV / AIDS is a devastating global pandemic that overwhelmingly afflicts Africa. Two-thirds of HIV-positive individuals live in Sub-Saharan Africa (22.5 million / 33.4 million), and prevalence rates among adults aged 15-49 is higher than 20% in three Sub-Saharan African countries[2]. In 2009, Africa saw 1.8 million new HIV infections and 1.3 million AIDS-related deaths. The numbers can be difficult to comprehend. 1.8 million new infections are the equivalent of every man, woman, and child in the Seattle area[†] being infected with HIV in a single year.

HIV transmission during sexual intercourse occurs by exposure of cervicovaginal, penile, or rectal mucosal tissues to free or cell-associated virus in mucosal secretions, semen, or blood. The physiology and numerous pathways by which HIV infection may occur are complicated, but our understanding continues to grow[12-15]. While numerous factors (both behavioral and biological) influence the risk of HIV acquisition, epidemiological studies demonstrate that the HIV viral load is the chief indicator of HIV-1 shedding and HIV transmission risk[16]. Thus, it is incumbent upon the global community that we seek out at-risk individuals to provide diagnosis and treatment for HIV-1 infection. HIV-1 viral loads are typically highest during acute infection and in late-stage AIDS, and can be lowered to undetectable levels through antiretroviral therapy, resulting in an estimated 96% reduction[17] in transmission rates to HIV negative partners[13]. The use of highly active antiretroviral therapy (HAART) to prevent the spread of HIV is well established[17], and has arguably led to the stabilization and sometimes decline of the epidemic in many countries across the globe[2]. While diagnosis and treatment are essential for controlling the pandemic, they will not be enough in isolation to eliminate the risk of viral transmission, since acute infections (high viral shedding) may not be diagnosed immediately, not all HIV-positive individuals will acknowledge their diagnosis and seek treatment, some who seek treatment may not wish to begin HAART, adherence to dosing regimens may be low, or viral resistance may develop in long-term HIV patients.

A proactive approach to preventing new infections must be taken in order to eradicate the disease. The most impactful prevention methods should be designed to combat the primary source of HIV transmission. Within Sub-Saharan Africa, the majority of new HIV infections are acquired through heterosexual transmission of the HIV-1 virus, and women are disproportionately infected[2]. While two-thirds of those infected with HIV live in the region, Sub-Saharan Africa is home to 80% of the world's HIV-positive women (12.1 million)[2]. Due to a

[†] The population of King County in 2010 was 1.88 million (U.S. Census 2010).

combination of social and biological[18] factors, women are much more likely to acquire HIV at a younger age than men in Sub-Saharan Africa[2]. The average prevalence among youth age 15-24 is 3.4% for women versus 1.4% for men. Abstaining from sex, being faithful to sexual partners, and using condoms, also known as the ABC approach, has been insufficient to prevent the continued spread of HIV. Without highly effective vaccines against the virus[12], alternative prevention measures that work for women are essential to control the epidemic[19].

It is crucial to develop female-initiated methods for HIV-prevention[19]. Most current prevention options, including male condom use or voluntary male circumcision, are either not female-initiated or require consent of the male partner. One approach is to develop topical products for vaginal or rectal application that provide receptive-partner-initiated protection against viral infection during sex by releasing protective levels of anti-HIV agents. Such products, which aim to prevent or significantly reduce the risk of HIV-1 acquisition[20], are known as anti-HIV microbicides. The challenge to researchers for the last two decades has been to develop topical intravaginal products that would allow at-risk women (and men) to protect themselves from HIV infection by either reducing the risk of epithelial lesions, maintaining a healthy vaginal environment, neutralizing the HIV virus, or blocking HIV replication in target cell populations[20]. The road has been long and bumpy as microbicides have evolved numerous times—1st generation surfactants, 2nd generation polymers, 3rd generation antiretrovirals, 4th generation co-receptor blockers[7], and now 5th generation controlled release systems.

1.03 Nonspecific microbicides

Once it was known that HIV was the etiologic agent of AIDS, clinical trials began with commercially available products shown to inactivate the virus *in vitro* and *in vivo* in animal models. The first microbicides tested were surfactants that could destabilize the viral envelope. These products, including nonoxynol-9[21], SAVVY[22], and the sodium lauryl sulfate (invisible condom)([23]), were often broadly acting against several STI causing pathogens and sperm. Unfortunately, the same physicochemical qualities that make detergents effective against HIV causes them to be toxic to mammalian cells[24]; these agents often remove stratified squamous epithelium from the cervix and vagina, increasing the risk of irritation and lesions[25]. From 1996 to 2000, researchers enrolled female sex workers in a definitive phase II / III clinical trial of COL-1492, a vaginal gel containing 3.5% of the spermicide nonoxynol-9, to test for an increase in the time to seroconversion[21]. Despite potent anti-HIV activity *in vitro*, nonoxynol-9 was found to have no efficacy, and treatment actually doubled the risk of HIV acquisition for those who used

the product more than an average of 3.5 times per day. It was shown that frequent use of the strong detergent N-9 compromised the integrity of the vaginal and cervical epithelium, making it easier for virus to reach target immune cells in an inflamed environment[21]. Thus, the microbicide community continued to search for products that could reduce the incidence of new HIV infections in women.

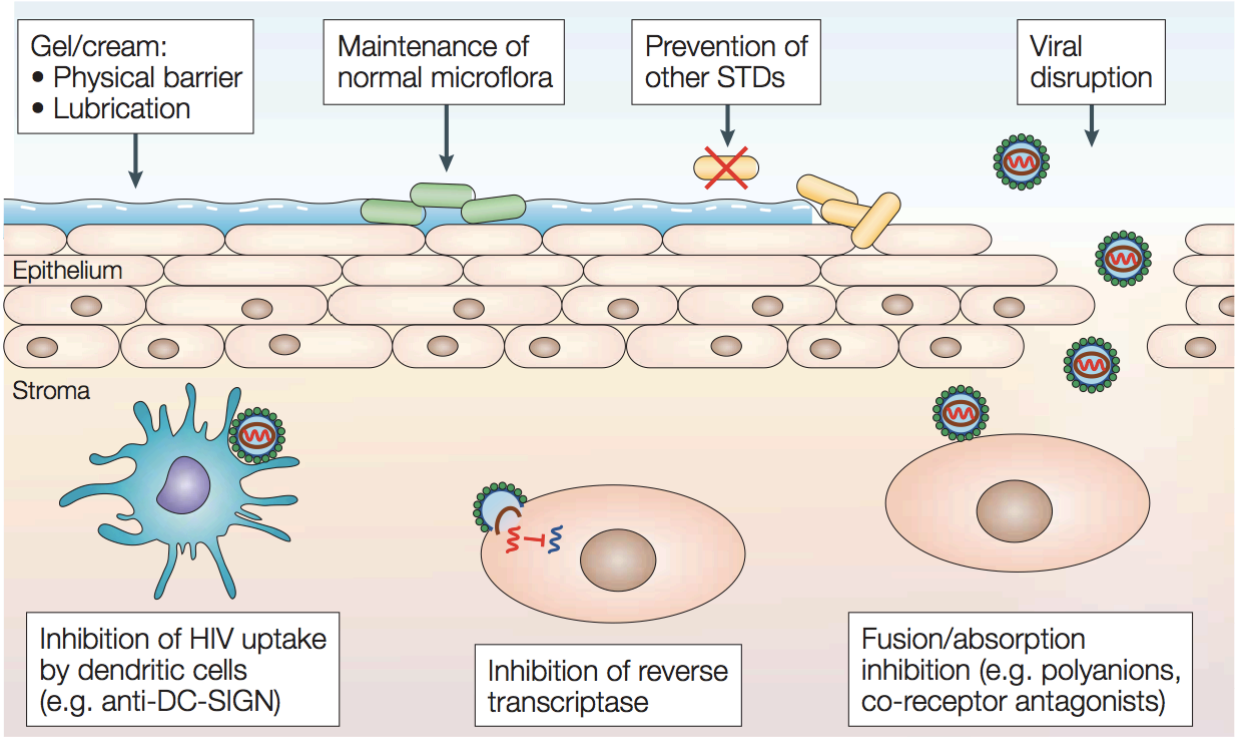

Figure 1.2—Potential modalities for anti-HIV vaginal microbicides. Anti-HIV microbicides may prevent HIV-1 transmission by disrupting the viral envelope, preventing other STIs that result in ulceration and increased transmission, maintaining normal bacterial populations or vaginal pH, providing a physical barrier to viral transport, lubricating sexual intercourse to reduce the frequency of micro-abrasions, inhibiting viral uptake, inhibiting viral proteins such as HIV reverse transcriptase or HIV protease, or by inhibiting viral fusion to immune cells. Reproduced with permission from Shattock and Moore, 2003[13].

Many years of *in vitro* research and work in animal models had lead to the discovery that anionic polymer hydrogels, many of them derived from carbohydrate biopolymers, could potentially serve as effective vaginal or rectal microbicides[26]. However, 15 years of subsequent clinical trials with polyanionic gels resulted in no evidence for reduced risk of HIV-1 transmission[26]. The basis for using polyanions to inhibit HIV-1 infection is that the positively charged viral gp120 electrostatically interacts with negatively charged polymers in the microbicide gels, prohibiting the virus from transporting into tissue. Thus, polyanions could act

as physical barriers to the entry of a broad spectrum of viral strains. In addition, vaginal gels could provide lubrication during sexual intercourse, and might reduce the frequency of micro-abrasions resulting from normal vaginal sex. Despite a sound theoretical basis for activity, three polyanionic gels failed to show efficacy in clinical trials—Carraguard (a blend of κ and λ carrageenans)[27], Ushercell (cellulose sulfate, potentially increased risk)[28,29], and PRO 2000 (naphthalene sulfonate)[30,31]. In response, the microbicide field has largely turned away from using polyanions in isolation to prevent sexual HIV-1 transmission[26]. While ineffective, some of these gels, like Carraguard, were found to be safe[32] for long term vaginal use and continue to be used to deliver other microbicidal agents against both HIV and other STIs[33,34]. The failure of polyanions to inhibit HIV infection *in vivo* resulted in a shift toward delivering antiretroviral medications with specific activity against the virus to those at risk for infection.

1.04 Specific, antiretroviral-based microbicides

Current microbicide strategies rely on the delivery of antiretroviral drugs to infectable cells in cervicovaginal or rectal tissues. Since the discovery of the HIV virus as the causal agent behind AIDS, the U.S. Food and Drug Administration (FDA) has approved 37 antiretroviral drug products (ARVs) for treatment of HIV. ARVs can target a number of pathways in the HIV replication cycle, including viral fusion to target immune cells (fusion inhibitors), reverse transcription of the viral RNA genome (nucleoside and non-nucleoside reverse transcriptase inhibitors), integration of the viral genome into the host genome (integrase inhibitors), or assembly of infectious viral particles (protease inhibitors)[35]. The microbicide community hypothesized that establishing clinically relevant levels of ARVs in at-risk HIV negative individuals could result in a protective effect. Since a number of these drugs have tolerable toxicity profiles, are highly potent, and have a long history of clinical use, there was low perceived risk involved in providing prophylactic treatment when weighed against the severity of the still-worsening HIV epidemic. Several studies have now shown that establishing protective levels of the ARVs tenofovir or the combination of tenofovir and emtricidabine in tissues at the site of their activity against HIV at the time of exposure can reduce the rate of HIV acquisition (Table 1). These studies include both oral pre-exposure prophylaxis (Oral PrEP) and topical application of antiretrovirals for pre-exposure prophylaxis.

Table 1.1—Selected anti-HIV pre-exposure prophylaxis (PrEP) clinical trials. The dose-relationship between efficacy and estimated user adherence is immediately apparent, and has hugely significant implications for the design of microbicide products. TFV = tenofovir; TDF =

tenofovir disoproxil fumarate; FTC = emtricidabine. *Adherence estimated by use of gel applicators, return of pills, or detectable levels of drug found in plasma of participants.

Trial	Active compound	PrEP regimen	Population	Reduction in HIV risk	Adherence*
CAPRISA 004[36]	TFV gel	Gel within 12 h before and after sex (BAT24)	Women	54% 38% 28%	> 80% 50-80% < 50%
TDF2[37]	TDF-FTC	Daily oral	Young heterosexuals	62.2%	80-85%
Partners PrEP[38]	TDF or TDF-FTC	Daily oral	HIV serodiscordant couples	67% (TDF) 75% (TDF-FTC)	82-92%
FEM-PrEP[39]	TDF-FTC	Daily oral	Women	None	< 40%
VOICE[40]	TDF-FTC TFV oral TFV gel	Daily oral Daily oral Daily gel	Women	None None None	29% 28% 23%

As evident in Table 1.1, both topical application and oral administration of ARVs can result in protection against HIV infection when used consistently. These trials provided the first evidence that women could take HIV prevention into their own hands and proactively reduce their risk of HIV acquisition—a major breakthrough! The CAPRISA 004 trial of an intravaginal 1% tenofovir gel dosed before and after sex showed a 54% risk reduction among high adherence users[36]. This has led to renewed interest in developing microbicides that rely upon the delivery of drugs with specific action against HIV to prevent infections. With millions of women becoming newly infected with the virus every year, ARV-based microbicides are in a position to make a huge impact on the burden of HIV and other STIs[41].

Despite the recent successes with ARV-based microbicides and oral PrEP studies, similar clinical trials continue to fail due to challenges associated with human behavior. For example, the VOICE trial (vaginal and oral interventions to control the epidemic), which was meant to determine women's preference for either daily oral or daily gel pre-exposure prophylaxis methods, was seen as a major disappointment[42]. Low (20-30%) user adherence to both oral and vaginal daily dosing regimens meant that the same products that worked in the CAPRISA 004 and Partners PrEP trials (different women/nationalities, different dosing schedules, etc.) were ineffective and undesirable to young African women. As noted by Shattock and Moore, while the incidence of HIV transmission between discordant couples per sexual act is not remarkably high (estimated to be between 0.0001 – 0.0040 per sexual act), HIV can easily transmit over the long term due to the long duration of HIV-1 shedding, the frequency of sexual intercourse in many couples, and the large range in varying infectiousness and susceptibility

associated with human physiological cycles or the general state of genital health in different populations[13]. With every sex act, there is a stochastic risk for infection[18]. It is therefore paramount that microbicides be acceptable, even desirable, to end users, since they will have to commit to long-term product use with every sex act in order to maintain protective levels of drug in tissue.

Poor adherence can be intimately connected to technical challenges of drug formulation. For example, tenofovir's solubility is greater at basic pH values due to a phosphate group in the molecule, but intravaginal gels are preferentially formulated at mildly acidic pH values to match the homeostatic pH of the "average" healthy vagina. This results in lower drug content in aqueous gels in order to preserve their clarity, which in turn increases the volume of the gel that must be administered to achieve adequate dosing. Intravaginal gel volume is a prime determinant of dose leakage during ambulation and sex[43]. Therefore, the unfortunate compromise between formulation requirements and drug pH-dependent solubility properties leads to likely extravaginal excretion of tenofovir gel before it can play an active role in inhibiting HIV replication *in vivo*. Such an outcome is problematic both biologically and behaviorally. Vaginal leakage can significantly reduce a woman's satisfaction with a product and lead to discontinued use.

Formulation toxicity and side effects must also be considered. While tenofovir gels are reportedly "well-tolerated" and safe for repeated use, they have nevertheless been shown to induce inflammation in the vagina and lead to vaginal irritation[44,45]. This irritation may be due to excipients in the gel formulation, or even to the drug itself. It is important to note that specific action against HIV replication is not equivalent to a lack of relevant side effects that can impact adherence to ARV microbicides. In order for anti-HIV microbicides to succeed, they must possess characteristics that will make young women want to use them regularly and often, regardless of their perceived risk for HIV infection[46].

The technical challenges associated with ARV-based microbicide development are nontrivial. At the outset, we must have some understanding of the required concentrations of active agents in order to achieve efficacy. This changes based on the location of the protective action—whether it be in vaginal fluid, cervicovaginal mucus, vaginal tissue, or blood plasma, and may be a function of women's age, time in the menstrual cycle, contraceptive use, and so on. Furthermore, the pharmacokinetics and mass transport of antiretrovirals in the human female reproductive tract are not well characterized for most compounds, but are crucial for understanding how to best design drug delivery systems. Sophisticated models of *in vitro-in vivo* extrapolation pharmacokinetics (IVIVE PB/PK) have been developed at great cost for

gastrointestinal delivery, and the investments are beginning to pay off in terms of reducing the number of poorly designed clinical trials based on *in vitro* data, even for ARV drug delivery[47]. Variability among at-risk women must be studied seriously to understand how inter-person and intra-person variability will influence the bioavailability of intravaginally administered ARVs.

1.05 The current microbicide pipeline

Current microbicide products in the pipeline span numerous drugs and drug delivery systems[48]. Traditional modes of vaginal drug delivery include tablets or pessaries[49], foams[50], films[51], gels[52], and elastomeric rings[53] (Figure 1.3). Anti-HIV microbicides have now been developed in nearly all of these classic vaginal drug delivery forms with the goal of providing protection against HIV infection during or immediately after sexual exposure to the virus. Each of these formulations has unique advantages and disadvantages related to ease of drug formulation and release, drug residence time, cost, and user acceptability within a given population. Currently, vaginal gels and vaginal rings dominate the list of microbicides in clinical trials. In particular, vaginal rings and gels containing tenofovir[52-54], dapivirine[54,55], UC781[56], maraviroc[57], or their combinations offer considerable promise for showing efficacy, since they do not require daily dosing and are coitally independent. It is likely that a mixture of coitally dependent, rapid ARV delivery systems and coitally independent, short to long term ARV delivery systems will be necessary to provide comprehensive coverage against heterosexual transmission of HIV-1. While the competitive nature of procuring funding and academic publishing put pressure on those developing each microbicide delivery system to make claims of superiority, the reality is that no one product will ever satisfy the needs of all women. Rather, each microbicide will contribute to a portfolio of technologies that can meet market demand.

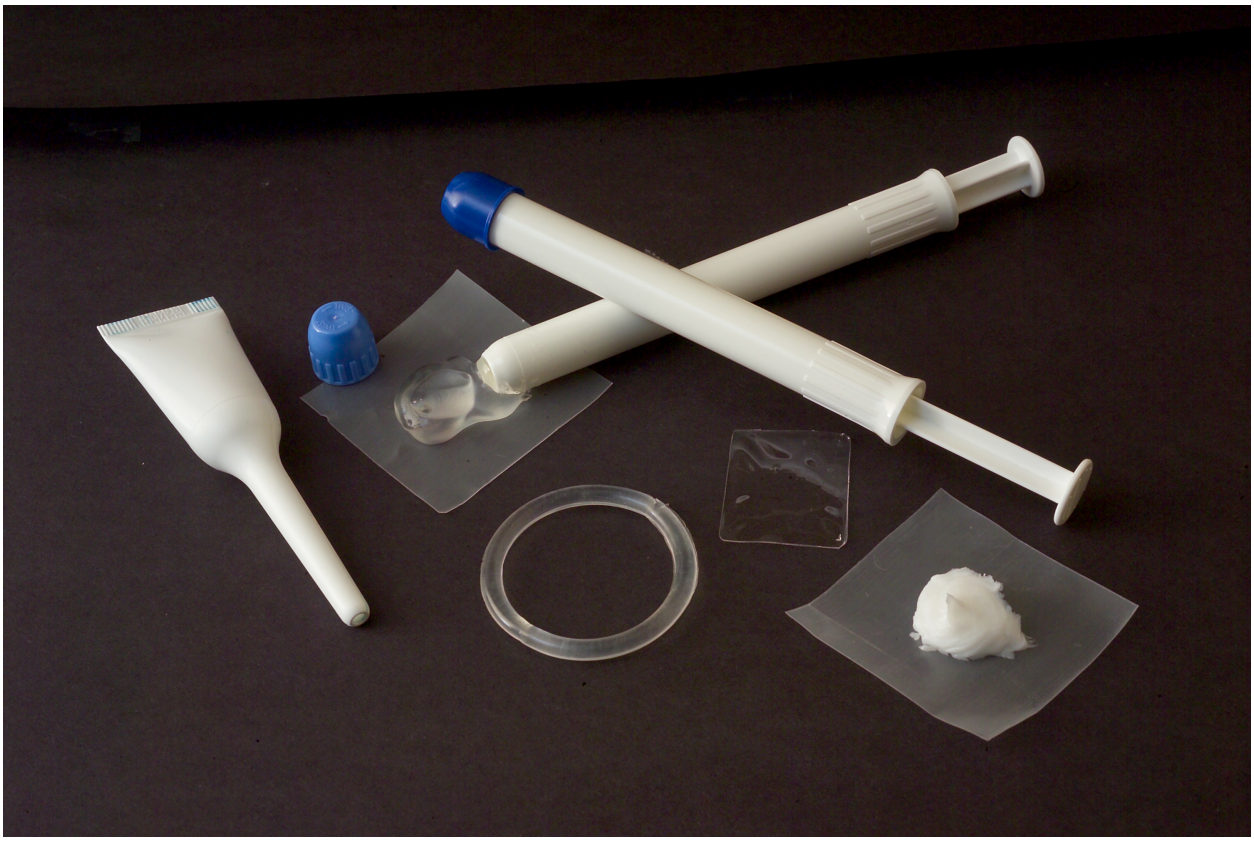

Figure 1.3—Microbicides come in many forms. Microbicide products are formulated in a variety of ways, including gels in various intravaginal applicators, square vaginal films both clear and translucent, vaginal rings, vaginal foams, and tablets (not depicted in this image). New additions to the microbicide toolkit include nanoparticles, nanofibers, and injectables. Image from the Microbicide Trials Network, www.mtnstopshiv.org.

1.05.1 Vaginal gels and creams

Vaginal gels were adopted early on for the delivery of microbicides. Water based vaginal gels are typically developed to have a smooth, lubricating texture and sufficient viscosity to minimize vaginal leakage[52,58,59]. Typically, hydrogel delivery systems are only well suited for the delivery of fairly soluble antiretrovirals, dendrimers (e.g., Viva gel), or nonspecifically active polymers. The intended timing of gel usage is pericoital, but efforts have been made to extend the window of time between delivery and successful HIV challenge out to 12 h or even 24 h by choosing drugs or prodrug strategies to extend the half life of actives in mucosal tissue. Microbicidal vaginal gels have a long history, and are the most extensively studied class of microbicide delivery systems. The main challenges for microbicide gels are dealing with vaginal leakage, drug insolubility, and coformulation of multiple active pharmaceutical ingredients[60]. A

minority of vaginal gels has been developed using silicone-based elastomers for the delivery of hydrophobic agents[61].

It is worth noting that vaginal cremes have a long history of use in pharmaceutics for small molecule drug delivery[62] but have not been aggressively pursued for use as microbicides. Cremes are typically oil in water emulsions with high viscosity, optically opaque appearance, and highly adjustable "feel" (i.e., oily, slick, light, etc.). Since crèmes are emulsions, they are suitable for the delivery of water soluble and water-insoluble drugs or drug particles, and may be useful for the delivery of nanoparticle microbicides. Cremes, if used for microbicides, would likely be meant for pericoital or daily use. The major hurdles for the development of creme-based microbicides are a funding agency aversion to topically opaque products and broad-based concern about the effects of emulsification agents, particularly surfactants, on epithelial integrity. It should be noted, however, that most common emulsification agents, particularly fatty acid excipients, have a long history of safe use in vaginal products.

1.05.2 Vaginal films

Polymer films are another promising microbicide delivery system. Vaginal films are thin, flexible, and water soluble delivery systems. Films are optimized for their texture, flexibility, appearance, and dissolution capabilities[51,63]. The most common method for application of vaginal films is digital insertion into the vagina. Due to the nature of film casting methods and required film flexibility, films contain numerous ingredients including polyvinyl alcohol as a polymer base and glycerol. Films may also include disintegrants and solubilizing agents. Amorphous drug compounds or those with good compatibility with water-soluble excipients are best suited for film formulation. Hydrophobic and highly crystalline compounds present a significant challenge due to their propensity to phase separate from the excipients during curing and form brittle films if loaded at levels above a few wt%. The intended timescale for intravaginal film microbicide use is pericoital, preferably at least 20 minutes before sex to ensure adequate dissolution. The development of anti-HIV microbicide films is a relatively new endeavor, but multiple formulations have been described in the literature[51,63,64]. Film-specific hydration characterization methods have also been pioneered in recent years[65]. Major challenges for successful film development include increasing drug loading while maintaining both dose flexibility and rapid dissolution times, particularly for very insoluble actives like dapivirine.

1.05.3 Vaginal tablets

Tablets are commonly used for oral delivery, and have also been developed for vaginal administration of microbicides. Tablets are manufactured by mixing actives with manifold excipients like binders, and then compacting them under high pressure to form monolithic structures. One of the advantages to tablet formulations is that they allow for easy encapsulation of nearly any active. However, the properties of the drug and the effect of excipients on solubility and release rate ensure that the resulting release behavior is often complex. Depending upon tablet composition, coating, drug loading, etc., the intended time of use in relation to sex can range from just minutes (rapid dissolution tablets) to several days (osmotic pump tablets), with a strong dependence upon the API of interest and its physical state within the excipient matrix[49,58,66-69]. Tablet delivery systems have been extensively tested both *in vitro* and *in vivo* in animal models for actives including tenofovir, UC781, and dapivirine, but only Praneem Polyherbal tablets have advanced to Phase II clinical trials in humans. The main challenges for tablet formulation include achieving uniform dosing in tablets with very low drug content and achieving rapid dissolution of poorly soluble APIs in small volumes of vaginal fluid.

1.05.4 Vaginal rings

Vaginal rings are exciting systems for long-term microbicide delivery[55]. Vaginal rings are thin, flexible rings made from polymers. The ring diameter, a couple of inches, is large enough to ensure retention within the vagina. Vaginal rings are optimized for their mechanical strength, compressibility, stability, and drug release characteristics. Vaginal rings are typically constructed by melt extrusion or by casting and curing of thermoplastic or thermosetting polymers, respectively. Typical polymers include ethyl vinyl acetate, polyurethanes (both hydrophilic and hydrophobic), and silicones. Rings may be constructed as monolithic matrices or as core-shell vaginal rings with a drug slurry core or secondary polymer matrix core. Furthermore, rings may contain multiple fused segments or inserted pods for the delivery of multiple APIs. Vaginal rings may therefore be used to encapsulate and release a wide range of agents, but they are typically more suitable for the formulation of poorly soluble hydrophobic compounds with high potency *in vivo*. This way, the release of the drug is limited by the solubility of the drug in the surrounding fluid, and nearly constant release kinetics may be achieved. Hydrophilic compounds in vaginal rings tend to display accelerated burst release during the first few days of release before providing low level release for the next 30-90 days. Due to the long-term release capabilities of these rings, they are intended for continuous use over 1-3 months, and are coitally independent.

In some cases, it may even be possible to remove the ring for sexual activity (if the active is long-acting, like tenofovir). This approach has been tested extensively *in vivo* in animal models for both PK and SHIV challenge. Rings have been developed for maraviroc[57,70], tenofovir (also in combination with levonorgestrel)[53,54,71,72], tenofovir disoproxil fumarate[73], dapivirine (also in combination with maraviroc)[70,74], UC781[56], and other antiretroviral compounds. The dapivirine vaginal ring is currently in two Phase III clinical trials in Africa for the prevention of HIV (ASPIRE and The Ring Study by MTN/IPM). The main challenges for this approach include improving correlations between *in vitro* and *in vivo* drug release data, reducing initial compound burst release, and maintaining drug stability over long periods of storage and use in the vagina. For example, recent results from the Phase I trial MTN-013/IPM 026 have shown that dapivirine/maraviroc combination rings fail to release significant levels of maraviroc into cervicovaginal tissue, despite good release profiles *in vitro*[70,75]. It is unclear if this is due to a rapid depletion of maraviroc from the ring over the first few days *in vivo* or from a failure of the ring to release the drug entirely. Vaginal rings, which have been widely used in the U.S. and elsewhere for contraception, will likely become standard products for long-term HIV prevention.

1.06 Toward "Set It And Forget It" microbicides

Despite the variety of vaginal microbicide delivery systems, none have been developed explicitly for programming adjustable levels of burst and subsequent sustained release of APIs. I was interested in addressing this gap by formulating APIs for both rapid and sustained delivery from a single device over 3 to 5 days. Such a microbicide product has been called a "set it and forget it" or "weekend warrior" product by the microbicide development community. Women could place the product intravaginally even minutes before sex to trigger rapid drug release and transport into tissues. Alternatively, they could apply the product as far as 3 to 5 days in advance of sexual activity and rely upon the sustained release of drug to maintain protective concentrations in tissue at the time of sex. Behavioral focus groups in a population of US women have found that such capabilities might improve the desirability and adherence to microbicide gel formulations[76]. With the failure of recent daily dose microbicides due to adherence problems, any product feature that may enhance user efficacy should be pursued with great interest. While gels, films, tablets, and rings address many of the challenges present in vaginal drug delivery applications, none of them explicitly incorporates the "set it and forget it" functionality into their design. In addition, the development of intermediate-term sustained release products (days to a couple weeks) has only just begun[61,69].

My approach is to combine rapidly dissolving microbicide fabrics with sustained release fabrics to create composites that will rapidly establish high levels of drug in tissue and then maximize the duration of the therapeutic window through additional sustained release (Figure 1.4). This approach is based on a common understanding of pharmacokinetics. As shown in the diagram, drug release kinetics are intricately linked to the pharmacokinetics in fluid, tissue, or plasma. In rapid drug delivery, as in intravenous injection, a bolus of drug is delivered to the site of administration all at once. Typically this results in a rapid rise in plasma and tissue concentrations to a maximum concentration (C_{max}) at time T_{max}. Then drug is removed from the plasma or tissue by excretion, metabolic degradation, etc. with a certain half-life ($T_{1/2}$) that is characteristic of the individual patient, the drug, and the specific delivery environment. This can be thought of as the impulse response of the tissue system to rapid administration of drugs.

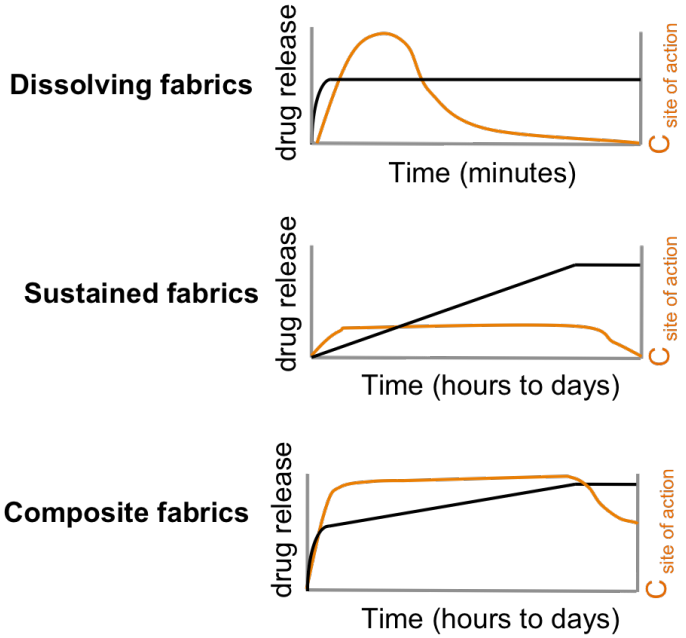

Figure 1.4—Schematic for the rationale behind developing combination rapid and sustained release electrospun microbicides for HIV-prevention.

In the case of sustained release products, there is a continuous flux of drug into the system, and a proportional elimination out of the system. The result is that a steady state level of drug is reached in the tissue until the end of the release phase. By combining both rapid and sustained release approaches, the resulting response can establish protective levels of drug at the site of action and then maximize the time spent within the therapeutic window. Ideally, such a delivery

system would also permit seamless integration of coformulation or co-delivery of actives with multiple mechanisms of action or clinical indications, especially contraception.

1.07 Electrospun fibers as a dosage form for anti-HIV microbicides

The recent growth in the number of microbicide ARV drug delivery systems is partially in response to a desire to co-formulate drug compounds with different chemical properties and control drug release over the duration of minutes to several months. With clever engineering, researchers have been able to achieve multiple drug release over variable timescales using familiar dosage forms[54,77]. Intensive study of microbicides in animal models, particularly in rabbits, sheep, and macaques, have demonstrated that many currently available microbicides are effective at delivering high drug levels to tissue and at preventing HIV, SHIV, or SIV transmission. Nevertheless, microbicides have thus far struggled to show efficacy in human populations most at risk of infection, perhaps due to low levels of specific anti-viral activity[27], low drug levels in tissue due to poor user adherence (particularly in young, unmarried women)[36,40], or combinations thereof. The grand challenge for microbicides is now addressing user adherence. Therefore, next generation microbicides must be more desirable to use or less dependent upon consistent usage, while maintaining or improving upon the drug delivery characteristics of traditional dosage forms.

This thesis applies electrospun fibers to microbicide formulation. Electrospinning is a process whereby one can transform polymer melts or solutions into collections of fine fibrous strands of material using a strong electric field. The resulting materials are typically opaque, soft, foldable sheets of polymer capable of taking nearly any shape. For the purposes of microbicide development, the polymer can possess innate anti-viral properties[78], encapsulate anti-HIV compounds[79], or be decorated with anti-HIV compounds after electrospinning is complete. Our recent work with electrospun fibers has shown that these materials are capable of preventing HIV infection *in vitro* through efficient delivery of ARV compounds, and are nontoxic to macaque ectocervical tissue explants[49,79]. Our current research is focused on developing both rapidly dissolving and persisting fiber formulations. Rapidly dissolving fibers are meant to establish supersaturated concentrations of drugs within the vagina in less than 10 minutes, driving rapid transport of drugs into tissue. Persisting fibers are meant to extend the release of compounds over multiple days without requiring the macroscopic geometry of a ring or implant. The overall goal of current electrospun microbicide research is to develop translatable, realistic solutions to problems faced by other microbicide dosage forms based on

an understanding of materials science, drug pharmacokinetics, and drug transport processes in the reproductive tract.

Electrospinning is an elegant technique for formulating a solid-dosage microbicide. Electrospinning has long been used to create tissue engineered scaffolds or drug delivery devices for topical treatment of burns, antibiotic delivery in fiber-based surgical gauze, oral drug delivery, and ocular drug delivery in addition to applications in nanotechnology unrelated to the biomedical field, such as filtration and energy production[4,80,81]. The process of manufacturing electrospun materials is efficient (low drug and polymer loss) and scalable, so manufacturing costs should be low. Most synthetic polymers and several biopolymers can be electrospun, so drug formulation is nearly unlimited by the polymer space. Since electrospinnable polymers span vast ranges in hydrophilicity, crystallinity, and hydrolyzability, drug release from electrospun fibers can be adjusted by controlling the physical properties of polymers or their composites. In addition, a growing body of electrospinning research provides numerous formulation methods for a broad range of drug classes, including small molecules and biologics. Additives such as common biomedical plasticizers (e.g., polyethylene glycol, polypropylene glycol, glycerol, lipid derivatives etc.) may be added to fiber formulations to adjust the overall feel of materials, which is typically soft and highly flexible even without plasticizers due to the fibers' interwoven microstructure. These characteristics of electrospun fibers make them suitable for the delivery of anti-HIV agents, either as single drugs, as antiretroviral combinations, or as combinations of antiretrovirals with drugs preventing or treating other STIs or providing contraception. There are several excellent reviews on electrospinning processes and applications, and readers should consult literature for a comprehensive list of electrospinning polymers and techniques[4,80,81].

Electrospinning is capable of producing composite drug delivery materials with near 100% encapsulation efficiency of incorporated drug compounds by simultaneous spinning of multiple solutions, layering of electrospun fibers, coaxial spinning, or emulsion spinning. Thus, electrospun microbicides offer a viable platform for combined ARV delivery as topical HIV prevention. Once dissolved, polymeric matrices are, like some hydrogels, capable of solubilizing and stabilizing drugs formulated at, above, or near their aqueous solubility due to chemical compatibility or complexation with small molecule compounds, which are often highly water insoluble[82-86]. Insoluble polymer matrices can be used effectively as drug depots, providing nearly constant rates of drug release over long periods of time, particularly in instances where a rate controlling polymeric membrane facilitates swelling-dependent release of active compounds[53,54]. While gel microbicides lack the ability to co-formulate hydrophobic drugs like

etravirine, darunavir, ritonavir, dapivirine, or maraviroc in combination with the hydrophilic drug tenofovir, solid dosage forms can theoretically combine water soluble compounds with poorly soluble compounds by providing physically separate drug depots or stabilizing molecules in solid emulsions or amphiphilic polymer systems. For solid dosage forms like vaginal rings, increasingly complex geometries with small features, such as pods or inserts, add significant cost and complexity to product design[55]. Electrospinning and other nanofabrication techniques allow for the creation of intricate geometries (coaxial fiber, particles in fibers, composite fiber blends) in single-step processes[87].

It is still unclear how fiber based materials will compare to microbicide gels, films, tablets, or rings for vaginal or rectal application. Like other solid dosage forms, electrospun fibers may provide some significant advantages over vaginal or rectal gels for product stability. This is because solid dosage forms can stabilize some drugs that would otherwise precipitate, decompose, or become chemically modified if stored in a gel or liquid suspension for extended periods or at high ambient temperatures. In addition, fiber based microbicides will likely not suffer from significant vaginal leakage during normal activity such as walking or urination, which occurs (or is at least a significant perceived nuisance) with use of many microbicide gels[88-90]. On the other hand, fiber based microbicides must become wetted by vaginal fluid before they feel slippery, so they lack inherent lubrication properties. Once wet, however, encapsulated lubricants such as glycerol or PEG and soluble polymers may enhance sexual lubrication. It is likely that hydrophobic fibers in particular must be designed with rapidly hydrating coatings requiring minimal fluid volumes or break up into small hydrophobic “rafts” of material after insertion to avoid sensations or perceptions of large, dry materials interfering with intercourse. Both increased vaginal “dryness” and “just the right amount” of lubrication have been reported after vaginal film acceptability studies, with impacts on perceived pleasure varying by population[67]. Because the fibers provide a solid dosage form and have a macroscopically silky appearance and texture, they will likely look opaque (due to the length scale of the individual fibers) and feel like soft, ultrafine cloth to product users. Fibers would lack the sharp corners of vaginal films, and may be easier to fold over a finger. Recent interest in developing pericoital products for rapid delivery of small molecule ARVs has led to the creation of a dapivirine film that can release nearly 100% of the encapsulated dapivirine within 10 minutes incubation in aqueous buffer[51]. Once inserted, fibers have similar potential to dissolve quickly, but may also dissolve slowly or not at all depending upon the choice of materials for the intended application. Fibers may swell, or experience surface erosion or hydrolysis. These different behaviors could tune the properties of electrospun materials to provide sustained release over multiple days or

even weeks, although the user acceptability of such a device is questionable. In the short term, electrospun fibers may provide a new dosage form for pericoital prevention of HIV in combination with unintended pregnancy, HSV-2, HPV, or bacterial infections.

The rationale for using electrospinning to create rapidly protective microbicides is multifaceted. First, the high surface area to volume ratio of electrospun fibers allows for more rapid ingress of water into hydrophilic electrospun materials than into films cast from identical solutions. Second, electrospinning allows drugs to become molecularly dissolved or dispersed throughout the polymer solution. Recrystallization of drugs in the final product may be minimized due to rapid evaporation of the solvent from fibers versus films. Molecular dispersion of drugs into rapidly dissolving nanofibers has been shown to enhance the solubility and transport rate of drugs into mucosal tissues[91]. For insoluble or sparingly soluble drugs with melting temperatures at or above 200°C, the lattice energy found in a drug crystal presents a significant thermodynamic barrier to the drug entering into aqueous solution[82]. By dispersing the drug throughout a solid matrix, one can temporarily increase the solubility limit of the drug, creating a larger chemical gradient to drive diffusive flux. The ability to disperse drugs in an amorphous phase is by no means unique to electrospun materials, and not all electrospun formulations are solid dispersions. Work by Johnson et al. has demonstrated that amorphous dispersion of tenofovir in polyurethane vaginal rings was responsible for significantly enhancing the release of tenofovir compared to release from a polyurethane ring formulation in which tenofovir existed in a crystalline state[54]. Research on the transport of drugs from gels into tissue has shown that drug transport into tissue may be limited by the rate of gel spreading, drug diffusion through the gel, or drug penetration into tissue[92-95]. Drug loading in gels is limited by the often-poor aqueous solubility of the active compound. Thin mats made from electrospun fibers, by comparison, may provide an alternative pericoital dosage form that can release both hydrophilic and hydrophobic drugs at high levels (even above solubility limits) while providing coverage over a large surface area within the reproductive tract. A third justification for the use of electrospun fibers as pericoital microbicides is the ability to create fiber materials in a wide variety of shapes and configurations. Unlike films, tablets, or vaginal rings, electrospun materials can be processed into sheets, tubes, pessaries, or coatings without altering the microscopic structure, formulation, or release properties of the materials[4,87]. Finally, electrospun fiber materials are soft, flexible, non-abrasive, and lack sharp corners. Thus, the “feel” of electrospun materials may be more attractive to users than that of films with an identical composition.

Microbicide Trials Network study 001 (MTN-001) found that tenofovir delivered in a gel established 130 times higher tissue levels of active drug (tenofovir diphosphate) and much

lower levels of drug in the blood than did oral dosing, and tissue levels of drug remained high for more than 24 hours after use[96]. Theoretically, pericoital usage of such products should dramatically reduce the rates of HIV infection in users. Unfortunately, while both once daily oral dosing for PrEP (iPrEx, Partners PrEP, TDF2) and microbicide gel usage before and after sex (CAPRISA 004) have been found effective in clinical trials with high user adherence, similar trials in different study populations have failed due in large part to a lack of adherence (VOICE, FEM-PrEP). Since any given user's adherence to a microbicide may be minimal, it behooves biomedical teams to create products that not only establish high but safe tissue levels of active drugs as rapidly as possible following deployment, but that also maintain those drug levels over long time periods.

Electrospun fibers hold promise as an alternative formulation to vaginal rings or nanoparticles for sustained release of antiretrovirals, particularly for release over several days (a time scale in between pericoital products and vaginal rings). This is because it is possible to electrospin polymer fibers with tunable erosion rates, allowing control over drug release through polymer engineering. Compared to nanoparticles, nanofibers are theoretically less suited to rapid release of drug compounds due to their lower surface area to volume ratio for a given radius and material composition. Thus, fibers may provide less bursting of drugs if care is taken to minimize enrichment of drug concentrations on the surface of fibers. Fibers may also be used to deliver nanoparticles, which may then persist and release drugs[97]. There are multiple reports of ARV-loaded nanoparticles for use in HAART and in microbicides (see other chapters in this book), but there are few options for efficient particle delivery. Future application of electrospun fibers to sustained vaginal drug delivery should benefit from current knowledge of drug transport through vaginal rings. Through uniaxial, coaxial, or emulsion electrospinning, the macroscopic arrangement of materials within vaginal rings may be recapitulated in miniature. The reduction in size will lead to more rapid compound release, providing an intermediate-length microbicide to vaginal rings with similar capacity to deliver drugs in significant quantities. Fibers can facilitate sustained release of both small molecules and biologics, especially proteins[98-100]. Consequently, microbicide fibers will be capable of delivering biologics like broadly neutralizing antibodies, lectin fusion inhibitors like CVN and griffithsin, or antimicrobial peptides. While the recent innovation in vaginal ring technology of filling a hollow polyurethane tube with a drug paste may be amenable to use in a protein-releasing vaginal ring, coaxial electrospinning of polyurethane sheath and protein solution core fibers could produce the same effective release system as a flexible, porous sheet in a single step process with minimal processing equipment. Alternatively, antibodies[101], rate controlling coatings[102], or responsive coatings[103] may be used to functionalize

or modify the surface of fibers, acting as a dual-functional drug delivery vehicle and viral capture system.

1.08 Electrospinning technology and application to drug delivery

The most commonly used setup for electrospinning consists of a viscous polymer solution, a nozzle through which the polymer passes, a high voltage source to charge the nozzle, and a collection surface set a short distance away (Figure 1.5). The polymer may be heated into a polymer melt or dissolved in a solvent (more common) to achieve solution properties amenable to electrospinning. The polymer solution is pushed through the nozzle at a steady rate by either a syringe pump or pressurized gas in the polymer container, producing pendant droplets at the nozzle tip. The voltage source typically applies a positive voltage between 5-50 kV to the polymer, and the collection surface is typically held at 0 kV. This potential difference between the nozzle and the collector creates an electric field, the strength and direction of which depend upon the potential difference, the nozzle-collector gap distance and the nozzle and collector geometries. In some cases, polymers are electrospun using either a negative or an alternating current source. In addition, the collector may possess a negative voltage bias (e.g., -1 to -5 kV) to discourage fiber collection onto nearby grounded surfaces. A large variety of collector surfaces and styles can be used to achieve different fiber orientations and shapes through manipulation of the electric field. Once charged and suspended in a strong electric field, the pendant droplet of polymer accelerates toward the collector, deforming into a so-called Taylor cone. If the electric forces are capable of overcoming the surface tension of the solution, a jet of polymer erupts from the tip of the cone. Here, the polymer solution begins to stretch as it continues accelerating, relying upon sufficient extensional viscosity and polymer chain entanglement along with low surface tension to avoid breakup into microparticles. A short distance away from the Taylor cone, the jet becomes unstable due to repulsion of like charges along the polymer surface. This instability, known as Rayleigh instability, leads to chaotic whipping of the fibers as they move generally toward the collector surface. This whipping is responsible for the dramatic reduction in fiber diameter, from millimeters to tens of micrometers or tens of nanometers (10^1-10^5 fold reduction in size). Solvent evaporates rapidly during this entire process (accompanied by rapid cooling), forming solid fibers on the collector surface.

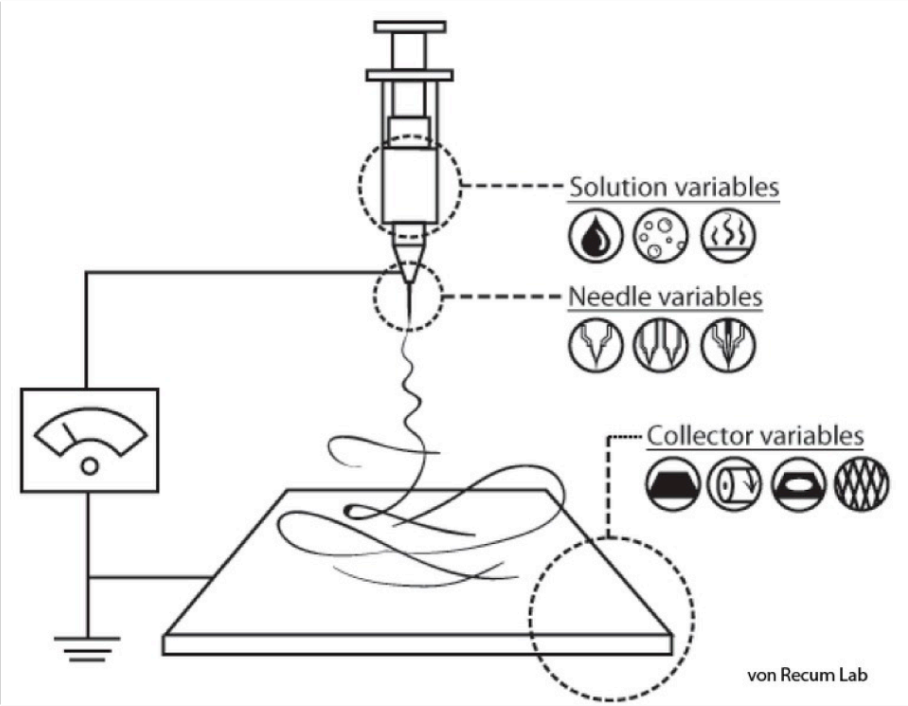

Figure 1.5—Schematic of typical electrospinning setup. Electrospinning is controlled by varying solution, needle, and collector variables. Credit: the von Recum Lab; used with permission.

Electrospinning can be performed at small scales on a laboratory bench top, or at large scales using multi-nozzle systems or needle-free electrospinning. At least 11 corporations provide industrial equipment for large-scale manufacture of electrospun fibers[50,87]. Several reviews have been written on the electrospinning process, and readers are referred to these sources for an in depth introduction to the technique[4,51,80,104]. Below, we highlight two examples of exciting electrospinning technologies that have been developed for drug delivery: coaxial electrospinning and tunable polymer design for sustained drug release.

One example of electrospun fibers for drug delivery is a coaxial nanofiber solid dispersion of acyclovir for oral delivery developed by Yu et al.[52,91]. Acyclovir is a hydrophilic small molecule drug often used to treat Herpes simplex virus (HSV). Despite being hydrophilic, acyclovir has poor aqueous solubility in PBS (around 12 mcg/mL), leading to low bioavailability[53,86]. Repeated dosing to establish effective drug levels can result in high levels of side effects, such as nausea or gastrointestinal problems. Yu et al. developed hydrophilic polyvinylpyrrolidone (PVP) fibers containing sucralose as a sweetener, sodium dodecyl sulfate (SDS) as a transmembrane penetration enhancer, and acyclovir[54,77,91]. Yu et al. prepared fibers using coaxial electrospinning, a method by which two solutions (a core solution and a sheath solution) may be

simultaneously incorporated into fibers in a concentric fashion (Figure 1.6). This electrospinning technology allows for simultaneous loading of multiple components with different physicochemical properties into a single dosage form, as well as customization of fiber surface properties or structural properties. For example, Yu et al. employed different solvents in the fiber core and sheath solutions to ensure the molecular dispersion and solubility of the included compounds. The core of Yu's fibers, spun from a mixture of ethanol and dimethylacetamide, contained ~20 wt% acyclovir molecularly dispersed in PVP. Meanwhile, the sheath of the fibers, spun from a mixture of water and ethanol, contained the highly water soluble compound sucralose and the permeabilizing agent SDS. Yu et al. found that these coaxial PVP nanofibers readily dispersed acyclovir, sucralose, and SDS, such that no crystalline compounds were present in the final materials. By making acyclovir amorphous, Yu et al. removed the thermodynamic barrier of overcoming crystal lattice energy before the drug could enter solution (significant, as acyclovir has a melting point well above 200 °C[27,82]). As a result of the fiber's hydrophilicity, high surface area to volume ratio, solid dispersion of acyclovir, and inclusion of SDS, the coaxial nanofiber formulation released 100% of the formulated acyclovir in 1 minute (compared to 50% dissolution of pure acyclovir particles in 60 minutes) and increased the rate of porcine sublingual mucosa penetration over 6-fold[36,40,91]. Similar results might be expected for delivery to the female reproductive tract or the rectum if such technology (containing multiple ARVs rather than SDS and sucralose) were developed for pericoital anti-HIV microbicides.

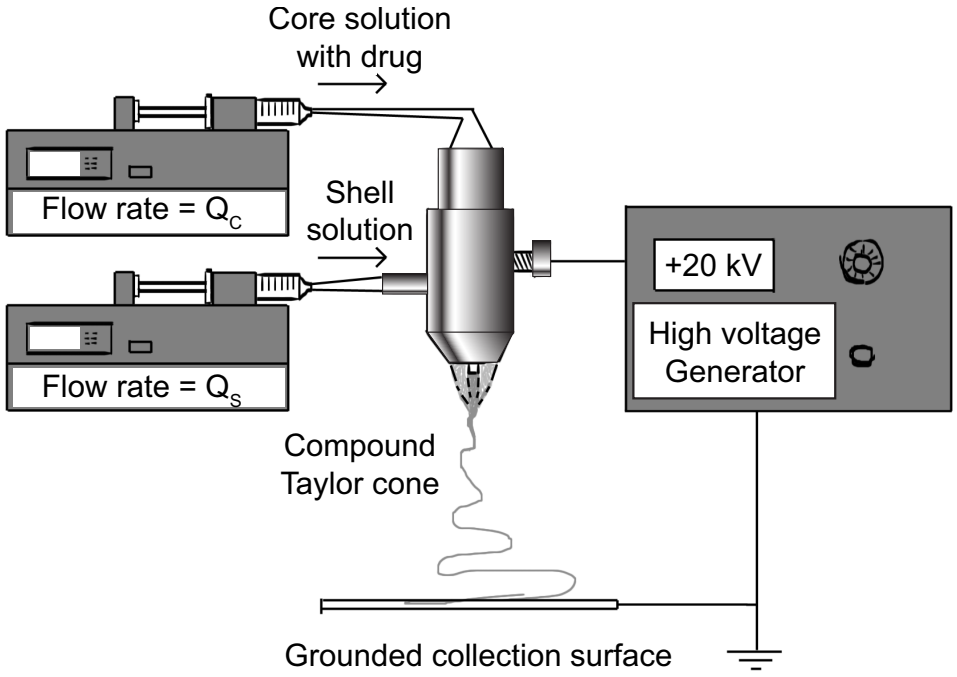

Figure 1.6—Schematic for coaxial electrospinning. Core and shell solutions are pumped out of concentric nozzles. The entire nozzle is charged with a high voltage, initiating spinning and collection onto a grounded substrate.

Yu et al.'s acyclovir-loaded PVP fibers were capable of delivering the drug in one minute or less, which could have advantages for microbicides used at the time of or immediately following unprotected sex. However, pericoital or even daily dosing strategies have suffered from poor user adherence in clinical trials with gels and oral tablets[36,40]. Dosage forms capable of persisting for days, weeks, or months may help assuage concerns over adherence to microbicide use. Our second example of electrospun fibers for drug delivery focus on providing sustained release of drugs over longer periods of time (8 h to 4 days) based on polymer erosion rate. Macri et al. recently published work on peptide delivery from electrospun scaffolds composed of tyrosine-derived polycarbonate terpolymers for topical application to burn injuries[98]. Fibers containing up to 5 wt% peptide were electrospun from glacial acetic acid. The release of the so-called P12 peptide, a cationic hydrophilic peptide with 14 amino acids (MW = 1780 Da), was controlled by the rate of polymer erosion (dissolution into solution), and provided either zero-order peptide release for 8 hours or diffusion controlled release from fibers over 4 days[98]. The tyrosine-derived polycarbonates used in the study had tunable erosion rates based on variable incorporation of PEG units and alkyl pendant groups on desaminotyrosyl-tyrosine alkyl ester units, and all polymers were reduced to very low molecular weight species within one

week of incubation in PBS at 37 °C. Previous work with tyrosine-derived polycarbonates has shown that it is possible to design polymers that erode over timescales of hours to months[105]. Macri et al. went on to show that electrospun scaffolds were nontoxic to epithelial tissue in a porcine incisional wound model[98]. These polymers resemble the more hydrophobic poly(ortho esters) in their ability to control drug release over variable timescales (hours to months) through rational design of polymer chemistries[106]. Developing novel bioresorbable polymers that are capable of controlled erosion and degradation rates will undoubtedly revolutionize the field of drug delivery, which has long depended upon less-tunable polymers like poly(lactic-*co*-glycolic acid) for drug release. Bioresorbable fiber materials could be used to deliver peptides or macromolecules like cyanovirin-N or griffithsin into the vagina over similar timescales (several hours to 1 week) without the need for device recovery from the vagina.

1.09 Previous work on electrospun fiber microbicides

Work at Ghent University, conducted concurrently with the beginning of this work, is the only known early application of electrospun fibers for topical microbicides outside of our group (Woodrow laboratory, University of Washington). Huang et al. formulated pH-responsive electrospun microbicides containing the anti-HIV drugs tenofovir disoproxil (free base of tenofovir disoproxil fumarate, or TDF), and etravirine (ETR), in addition to neutralizing cellulose acetate phthalate (CAP). Drugs were chosen as model compounds based on varying physicochemical properties and their different mechanisms of action against HIV.

Huang et al. explored the use of electrospun CAP fibers for formulating tenofovir disoproxil (as a free base) and ETR into semen-responsive nanofibers. CAP is a common polymer used as an enteric coating to prevent drug release in the acidic stomach. The CAP used in this study became water soluble only at pH greater than 5.2. As a result, electrospun cap fibers are stable at most normal vaginal pH levels, but dissolve rapidly following the introduction of semen, which has a high buffering capacity and a pH between 7 and 8[78]. This semen-responsive behavior is useful for delaying the release of encapsulated drugs until they are exposed to very high levels of virus present in seminal fluid. Semen-dependent release of ARVs has some significant disadvantages. In particular, ARVs may not be delivered if the male partner did not ejaculate, depending upon the volume, pH, and buffering capacity of any pre-ejaculate released into the vagina. Since HIV can still be present in pre-ejaculatory fluids, it is possible that unprotected sex without male ejaculation could result in HIV challenge. Tenofovir disoproxil fumarate (TDF), is an ingredient in multiple oral antiviral tablets, and is the prodrug form of the active tenofovir

diphosphate. TDF was not used in previous clinical trials with 1% tenofovir gel[36]. Huang et al. purified tenofovir disoproxil as a free base from Viread® through liquid-liquid extraction into dichloromethane, followed by purification on a column. Compared to tenofovir monophosphate (simply known as tenofovir), TDF is more hydrophobic, but possesses similar solubility at low pH (tenofovir is highly soluble at neutral and basic pH). The other drug studied by Huang et al. was ETR, an NNRTI with good ability to avoid drug resistance.

CAP was electrospun at 25 %wt/vol in a 3:1 mixture of acetone and dimethylformamide (DMF). Electrospun CAP fibers had a regular, smooth morphology with diameters from 500 to 800 nm. The authors reported that typically 1 mL of solution was spun per electrospinning session, producing a maximum yield per spin of around 250 mg (depending upon drug loading). While the efficiency of the process is unreported, the study required the use of at least tens of milligrams of fiber. Tenofovir disoproxil was incorporated into fibers in amounts up to 17.8 % wt drug per weight CAP. While no loading studies were completed to verify drug loading, our work and that of other electrospinning researchers has consistently found that nearly the entire drug content within the electrospinning solution makes it into the final fibers. ETR was incorporated into fibers in much lower amounts than tenofovir disoproxil, up to 0.75% wt drug per weight CAP. The high drug loading of tenofovir disoproxil into CAP fibers means that in order to deliver the same amount of tenofovir as is found in a 1% tenofovir gel (accounting for differences in molecular weight, neglecting considerations of pharmacokinetics or drug transport), ~300 mg of CAP fibers must be inserted into the vagina. Huang et al. provided no physical characterization of the fibers beyond imaging.

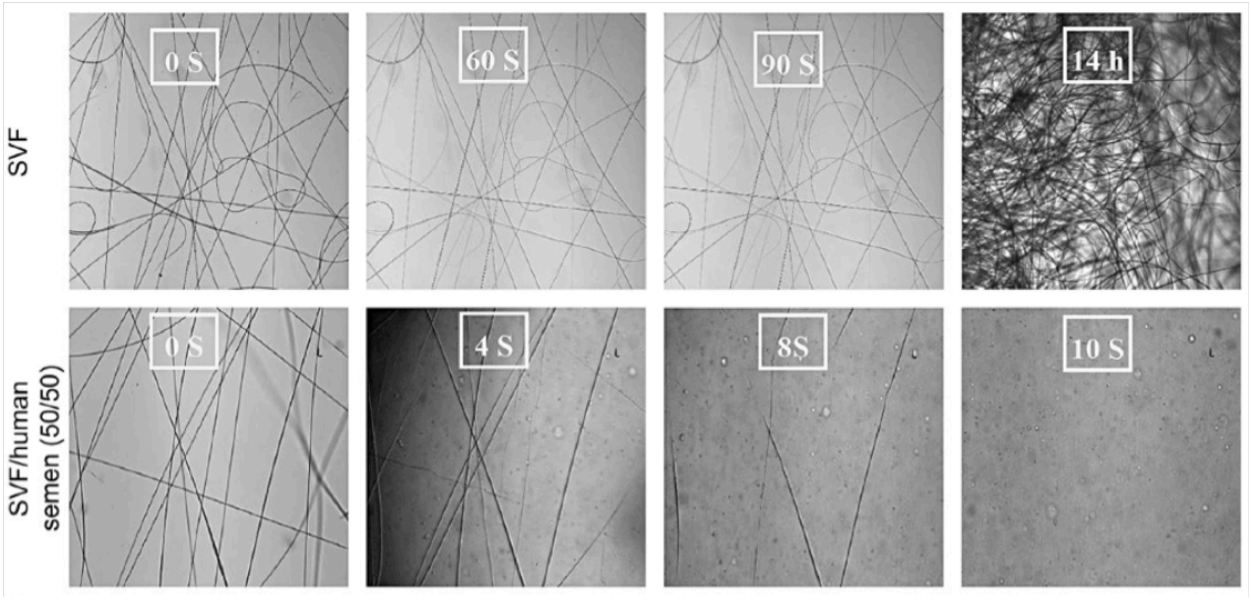

Figure 1.7—CAP fibers are semen-responsive. CAP fibers were shown to be stable in simulated vaginal fluid (SVF, top) for at least 14 hours. Upon addition of an equal volume of seminal plasma, fibers dissolved within 10 seconds, releasing encapsulated antiretrovirals. Figure adapted with permission from Huang et al., 2012[78].

One very interesting aspect of the work by Huang et al. was that CAP fibers dissolved within seconds upon exposure to small amounts of human semen, but did not dissolve in simulated vaginal fluid (Figure 1.7). The rationale behind this approach is ostensibly that the encapsulated drugs would not be delivered too far in advance of intercourse, which may result in premature elimination of the drug. A potential drawback to this strategy is that drug release immediately following potential virus challenge might not allow for rapid enough transport of tenofovir disoproxil to target cells to have a protective effect. In general, ARVs have been shown to transport rapidly through vaginal fluid and into vaginal tissue and blood plasma. Once within cells of interest, tenofovir disoproxil must be metabolized into tenofovir, and then into tenofovir diphosphate. Although the authors did not report the pH of semen/SVF mixtures, it is likely that all of the mixtures had a pH that was above 5.3, since all fibers eventually dissolved in the presence of semen. Although not explicitly stated in the article, seminal plasma rather than whole semen was likely used, since no sperm were visible in microscopic images of the fibers dissolving after the addition of semen to SVF. Next, Huang et al. demonstrated release of rhodamine 6G (a small molecule dye with similar molecular weight and solubility to tenofovir disoproxil) from CAP fibers in PBS and SVF, finding that no rhodamine was released from fibers in SVF over 1 hour, but that all rhodamine released within 2 minutes of incubation in PBS. Further microscopy results suggested that the vast majority of rhodamine remained in fibers

following 24 h incubation in SVF. It is unclear if longer incubation periods would result in some release of rhodamine from CAP fibers at pH 4.2. No drug release data was provided for tenofovir disoproxil or etravirine[78].

Before testing the bioactivity of CAP fibers loaded with ARVs, Huang et al. tested the toxicity of CAP fibers against both immortalized vaginal epithelial cells and TZM-bL cells. No toxicity was found at polymer concentrations at or below ~1 mg/mL of polymer. Data from higher treatment concentrations was not shown. They also showed that CAP had no effect on the growth of vaginal *Lactobacilli* at CAP concentrations up to 0.1 mg/mL[78]. Given that fibers would likely be used in concentrations nearer 100-50 mg/mL following vaginal sex and ejaculation of semen, these tested concentrations are very low, and effects on human and bacterial cells may occur at higher concentrations.

Huang et al. reproduced results from earlier papers demonstrating the CAP possesses inherent antiviral properties through interactions with viral Gp41[107]. They found that CAP was capable of fully neutralizing HIV virus when incubated with HIV-BaL virus at concentrations of 0.2 mg/mL CAP and 220 pg/mL P24 (10^6 fold excess CAP) for 1 hour[78]. This is exciting, since CAP concentrations might be higher if an actual product were used depending upon dosing. In addition, the authors found that CAP at 0.1 mg/mL with 0.5 µg/mL of tenofovir disoproxil was capable of fully neutralizing virus. Unfortunately, neutralization data was shown for neither free tenofovir disoproxil, nor for any treatments containing ETR. Interestingly, the authors postulate that if the fibers were plentiful enough or if the composition of the polymer were altered, they might last for repeated exposures to semen[78]. This would likely be difficult, since alteration of CAP's pH responsive behavior (through modulation of percent of hydroxyl substitution) would not only alter the kinetics of dissolution, but also change the pH at which fibers would be soluble, potentially affecting their responsiveness to semen. While pH 5.3 is higher than that of SVF, normal vaginal fluid exudate can have pH of up to 6 in healthy women[108]. Thus, these CAP fibers may not be responsive to semen in all women, particularly in those women with bacterial vaginosis, which is common among populations at risk of HIV infection[109]. The authors acknowledged that the fibers would dissolve before semen is present in women with abnormally high vaginal pH.

1.10 Producing electrospun materials at scale and technology translation

To date, our work on electrospun fibers for intravaginal drug delivery has been academic and focused on providing proof-of-concept. Funding agencies and the microbicide community

have expressed strong interest in the technology, particularly in the feasibility of scale-up and the predicted cost of creating such materials. Answering these questions requires a complex consideration of product design, material sourcing, mass production methods, and commercialization/distribution plans. We have attempted to provide answers to these many questions in our recently published perspective on the use of electrospun fibers for vaginal drug delivery[110]. Summarizing very briefly, we believe that there is real potential for the cost-effective scale up production of microbicide fibers. Commercial machines for large-scale, GMP manufacture of electrospun fibers have been developed by a number of corporations, including Elmarco (whose instrument we use in lab to demonstrate at-scale production of fiber microbicide formulations). Recent work with free-surface electrospinning has shown that it is also possible to produce coaxial fibers at scale from a nested slit extrusion system for both rapid delivery of poorly soluble drugs from solid dispersions and sustained release of drugs from proprietary formulations[111]. The per dose cost of a fiber-based microbicide, assuming a dose of 0.3-4 g•dose^{-1}, is estimated to be \$0.003 - \$0.6 dose^{-1}. We caution that these estimates do not include the API, other excipients, and the costs associated with GMP pharmaceutical manufacturing. Therefore, the estimate of dosage cost is likely to be too low. Commercialization plans would likely include partnering with pharmaceutical companies, international aid organizations, and world governments to provide access to active pharmaceutical ingredients, expertise in product manufacture and regulatory approval, and product distribution to at-risk populations.

1.11 Maraviroc as a model drug compound for electrospun microbicides.

Maraviroc is a CCR5 antagonist that blocks the fusion of CCR5-tropic HIV-1 virions to the CCR5 co-receptors on CD4$^+$ cells, including CD4$^+$ T-cells, macrophages, and dendritic cells[112]. Maraviroc has been approved by FDA as an oral dose drug for HIV treatment since 2007[113]. As a result, much is known about the PK of maraviroc in women following oral dosing with Selzentry (the oral product produced by ViiV Healthcare)[114]. In addition, the PK of maraviroc in men (oral/IV dosing only) and nonhuman primates following the administration of maraviroc-containing oral pills[115,116], vaginal gels[61,117,118] and vaginal rings[57,70] has been reported in multiple peer-reviewed publications over the past five years. Maraviroc looks promising as a microbicide because of its potency, good toxicity profile, and CCR5-tropism[61,70,117]. However, recent evidence for maraviroc-mediated CD4+ T-cell activation in rectal tissues and poor efficacy in nonhuman primate models dampen the enthusiasm for its use as a microbicide[11,115]. From a

pharmaceutics and materials perspective, our choice of maraviroc as a model microbicide compound is appropriate based on its similarity to other ARVs and allows us to investigate the delivery of compounds that are either hydrophilic or hydrophobic by simply adjusting the pH of media.

1.11.1 Physicochemical Properties

Maraviroc is a small molecule (molecular weight 513.7 g/mol) with fair solubility within the range of healthy vaginal pH values (3-6)[108]. As shown in below in Figure 1.8, maraviroc has two pKa values that determine its ionization state. The pKa of the triazole ring is 3.31, so at a vaginal pH of ~4.31 (average from Ravel et al.[108]), nearly 91% of the maraviroc triazole rings will be deprotonated (and therefore neutral). The pKa of the tropane ring, however, is much higher (7.84), such that in healthy human vaginal fluid, nearly all of the drug will be protonated and hence positively charged. The ionization state of the drug has a direct effect upon the solubility of the drug compound, as well as how the drug partitions into an oil phase (log *P*). In mildly basic media and in blood plasma, maraviroc is slightly soluble (up to 1 mg/mL) and can be considered a hydrophobic drug (log $D_{7.4}$ = 2.1[119]). My personal experience is that maraviroc's aqueous solubility drops off precipitously at pH > 10, such that the drug is practically insoluble. In an acidic to near neutral pH range, maraviroc is fairly soluble (up to 25 mg/mL at 37°C, depending upon polymers and other components in solution[120]) and is a moderately hydrophilic drug (logP = -0.34)[57]. The melting point of crystalline maraviroc is near 200°C, suggesting that maraviroc's enthalpy of fusion (~72 J/g[120]) may significantly retard the dissolution of the crystalline drug as compared to the amorphous drug[82], particularly if the vagina has a pH at or greater than the pKa of the tropane ring (e.g., in macaques, or in humans following the ejaculation of semen, infection with some bacterial pathogens, douching, heavy menstruation, or frequent tampon use). Our work on solid dispersions of maraviroc showed that large particles of maraviroc dissolved very slowly (24 h) in a sink of pH 7 PBS but rapidly in a sink of pH 4 media (20 min). In addition, dispersion into PVP or PEO fibers maintained rapid dissolution even in neutral PBS[120].

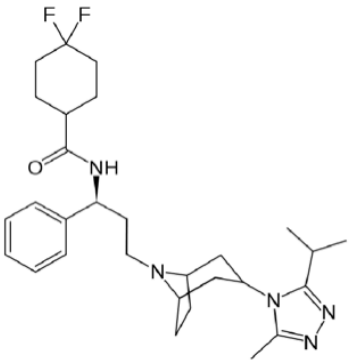

MW = 513.7 g/mol
MP = 197 - 198 °C
Solubility in various media:
Unbuffered water = 1.03 ± 0.07 mg/mL
2.2% HEC in PBS, pH 7.2 = between 300 mcg/mL and 1 mg/mL
pKa = 3.31 ± 0.05 (triazole) and 7.84 ± 0.01 (tropane)
log *P* = 2.55 ± 0.04 (X) and -0.32 ± 0.12 (XH^+)
Micronized drug size (ViiV) D_{50} = 567 nm

Figure 1.8—Data on physicochemical properties compiled from Malcolm et al., 2012[57], Malcolm et al., 2013[118], and ViiV Healthcare.

1.11.2 Modes of Delivery and Resulting Pharmacokinetics (PK)

Pfizer completed the first extensive studies of maraviroc's PK following oral and intravenous dosing in humans. Abel et al. studied the amount of drug related radioactivity in the blood, plasma, urine, and feces following a ^{14}C-labeled dose of oral maraviroc and characterized the PK, safety and tolerability of intravenously delivered maraviroc to determine the drug's absolute bioavailability. They also looked at the main metabolites of maraviroc after administration[119]. After oral dosing, T_{max} was reached by 2 hours. There was a higher level of radioactivity in plasma than in blood (blood/plasma ratio ~0.6 for AUC_t and C_{max}), showing that maraviroc was not taken up into red blood cells. Intravenous doses of 3-30 mg of maraviroc showed that drug exposure and PK were linear with the administered dose[119]. In contrast, previous studies with oral dosing had shown that maraviroc has nondose-proportional oral PK (although this nonproportionality is very small over the relevant dose range)[121]. As a result, it is convenient to think of maraviroc delivery to the body as a linear system with a particular transfer function—a rapid peak by 0.5 to 4 hours followed by an exponential decay clearance with half-life around 10-12 hours[119].

Maraviroc is extensively metabolized and is excreted through the feces and the urine. Following a 300 mg oral dose, 42% of the radioactivity in plasma was unmodified maraviroc. 76.4% and 19.6% of radioactivity were recovered in feces and urine, respectively. Similarly, 23% of the total intravenous dose clearance was renal. Profiling of these samples showed extensive metabolism. Excreted radioactivity was mostly unmodified maraviroc (33%). Major metabolites included oxidized and N-dealkylated metabolites. The mean volume of distribution of maraviroc was 194 L, and the absolute bioavailability of a 100 mg oral dose, compared to a 30 mg IV dose, was 23.1%[119].

Soon after maraviroc was released on the market, there was considerable interest in using the drug for oral PrEP against HIV-1. Dumond et al. examined the concentration of maraviroc in cervicovaginal fluid, vaginal tissue, blood plasma in HIV-negative women following oral dosing with 300 mg maraviroc twice daily for 7 days[116]. On day 1 and day 7, the AUC for maraviroc in cervicovaginal fluid was 1.9- and 2.7-fold higher, respectively, than for the AUC of maraviroc in blood plasma. Furthermore, maraviroc was detectable at concentrations exceeding the protein-free IC_{90} in cervicovaginal fluid only 1 hour after oral dosing. Peak concentrations in cervicovaginal fluid were reached at 6 hours after dosing. The level of protein binding was only 7.6% in vaginal fluid, and the half-life of the drug was longer than in plasma. The concentration of maraviroc in cervicovaginal fluid 72 hours after dosing was similar to blood plasma levels only 12 hours after dosing. Dumond et al. also found that maraviroc concentrated in vaginal tissue. The AUC of maraviroc in vaginal tissue was 1.9-fold higher than in blood plasma[116], which might be expected given the drug's large volume of distribution. While Dumond et al.'s PK study informed potential use for PrEP in women, it did not provide information about the concentration of maraviroc in rectal tissues following oral dosing—crucial information for use with receptive anal intercourse.

In order to evaluate the potential for using maraviroc as an oral PrEP measure for men who have sex with men, as well as for evaluating the usefulness of testing saliva as a measure of adherence to oral PrEP with maraviroc, Brown et al. characterized the PK of single and multiple dose oral 300 mg maraviroc in the saliva, seminal plasma, and rectal tissue of healthy, HIV-negative men[122]. The enrolled men took 300 mg of maraviroc orally twice daily for 8 days. The AUC of maraviroc in seminal plasma was 50% of the AUC in blood plasma. However, Brown et al. found that protein binding of maraviroc in seminal plasma was low, ranging from 4% to 25%. Consequently, the protein-free concentration of drug was about twice as high in seminal plasma as in blood plasma. Rectal tissue AUC was 7.5- to 26-fold higher than blood plasma AUC, suggesting that maraviroc may be protective against rectal challenge with HIV following oral dosing. As discussed later, however, it isn't that simple with maraviroc. The saliva AUC was 70% lower than in blood plasma, but correlated decently with blood plasma AUC (R^2 = 0.58). As a result, Brown et al. concluded that monitoring drug levels in saliva might be useful for assessing adherence to oral PrEP with maraviroc in clinical trials.

Malcolm et al. evaluated the PK of maraviroc delivered from 4 mL volumes of an intravaginal HEC gel[118]. Concentrations of maraviroc were measured in vaginal fluid, vaginal tissue, and blood plasma over 72 h after a single application of maraviroc gel with concentration ranging from 0.003% to 3.3% w/w. Malcolm et al. found that maraviroc concentrations in vaginal fluid,

vaginal tissue, and blood plasma were highly dependent upon the dose of maraviroc administered in the HEC vaginal gels[118]. Interestingly, the concentrations in plasma and vaginal fluid increased even after the solubility limit of maraviroc was reached in the gels. Thus, the most effective gels contained insoluble maraviroc (could be problematic from the perspective of a user's perception). The tissue concentration was well below the solubility limit of maraviroc, and the vaginal fluid concentration remained high above the solubility limit for at least 12 hours. Concentrations of maraviroc in vaginal fluid and blood plasma peaked around 0.5 and 2 hours, respectively, after administration and then declined steadily over 72 hours.[118] The decay rate was around 10-fold per 24 hours in vaginal fluid and around 100-fold per 24 hours in blood plasma.[118] PK parameters for vaginally administered maraviroc gels in macaques are presented below.

Table 1.2—Measured PK parameters of vaginally delivered maraviroc from a 2.2% HEC gel in macaques. The results of the PK analysis suggest that efficacy is directly correlated with dose, which must remain around 1 mg/mL in vaginal fluid. Table reproduced with permission from Malcolm et al., 2013[118].

Maraviroc gel conc. / dose (% w/w / total dose)	Vaginal fluid			Plasma		
	C_{max} (ng/mL)	T_{max} (h)	AUC (ng·h/mL)	C_{max} (ng/mL)	T_{max} (h)	AUC (ng·h/mL)
0.003 / 0.12 mg	18960	12	314400	0.16	2	0.658
0.01 / 0.4 mg	149700	0.5	583800	0.32	2	3.774
0.03 / 1.2 mg	122300	0.5	833500	1.32	0.5	8.371
0.10 / 4.0 mg	394400	2	2420000	3.33	0.5	41.12
0.30 / 12 mg	1387000	0.5	5351000	18.18	2	60.40
3.3 / 132 mg	6564000	0.5	57450000	147.9	2	626.5

Correlations between dose and maraviroc plasma and vaginal fluid concentrations were very strong and positive. As in previous studies of oral dosing in humans, the PK of maraviroc was nearly linear in vaginal fluid and in blood plasma. In macaques used in the Malcolm study, plasma levels were 5 orders of magnitude below the vaginal fluid concentration, and tissue levels were 4 orders of magnitude lower than the vaginal fluid concentration[118]. It is likely that this would be the case for maraviroc delivered from other dosage forms. It is unknown how the PK in pH of 7.2 of the gel and vaginal fluid in macaques would differ from the PK of maraviroc in vaginal fluid of pH 4.5 in a human subject[118]. There was no mention of how vaginal gel leakage (likely for 4 mL of gel in a macaque) may have impacted results.

In order to provide sustained maraviroc release from a vagina gel, Forbes et al. developed a non-aqueous silicone-elastomer gel containing 3.3% wt/wt maraviroc (the same loading that

was found 100% protective by Malcolm et al. in a HEC gel)[61]. The lead elastomeric gel identified as the lead candidate contained 80% w/w ST Elastomer 10 and 20% w/w cyclomethicone. This formulation was 20 times more viscous than the HEC gel, and so may have greater vaginal retention. However, the gel was also thin shearing, so the spreadability and syringeability of the gel would be only about twice as difficult as with a HEC gel. The elastomeric gels were found to lack mucosal irritancy and released maraviroc *in vitro* at rates dependent upon the swellability of the polymer in the release media. Fluid, tissue, and plasma levels of maraviroc were higher and more sustained in macaques given a silicone maraviroc gel than a HEC gel, despite the fact that the in vitro release studies showed lower release of maraviroc[61]. These results implied that maraviroc formulated into non-aqueous gels may be more efficient at providing protection against HIV per unit mass of drug. The results of this work seemed to show that retention of and sustained release from the microbicide product containing maraviroc is crucial for favorable PK, and, by extension, efficacy.

Malcolm et al. expanded upon the need for a sustained maraviroc dosage form by developing a matrix-type silicone elastomer vaginal ring (mass of 1.85 g) for the sustained release of maraviroc (400 mg)[57]. Previous studies had shown that the efficacy of gels was highly dependent upon the amount of time between dosing and SHIV challenge. A vaginal ring could provide continuous long-term release of maraviroc, and may offer better protection against SHIV challenge. Maraviroc vaginal rings showed a burst release of drug *in vitro* in a sink of simulated vaginal fluid of about 20 mg on the first day, which quickly dropped to a daily release between 5 mg after day 4 and 2.5 mg on day 29. A cumulative 127 mg of maraviroc was released over 30 days. The PK study of the ring in macaques found that the steady state concentration of maraviroc in vaginal fluid were ~10^6-fold greater than the IC_{50} of maraviroc with PBMCs *in vitro* (solubility limit of maraviroc). An important feature of this study was the comparison between the PK of maraviroc in animals with and without Depo-Provera treatment. The use of Depo-Provera in macaques resulted in a significant difference in the biodistribution of maraviroc released form vaginal rings. With Depo-Provera treatment, plasma levels of maraviroc ranged from 1.4 ng/mL at the beginning of the month to undetectable levels by day 21 (consistent with previous studies of gels in hormone treated macaques). Maraviroc was undetectable in macaques that did not receive Depo-Provera[57]. This is exciting data, since it shows that a sustained release of maraviroc within the vagina can result in minimal systemic circulation of the CCR5-antagonist, which was shown in oral dosing to alter the macaque's immune system[115]. Without Depo-Provera treatment, the concentration in vaginal *fluid* was 10^5 to 10^6 ng/mL; with Depo-Provera treatment, the concentration was 10^4 to 10^5 ng/mL. Without Depo-Provera treatment, the

concentration in vaginal *tissue* was 5,000 to 20,000 ng/mL; with Depo-Provera treatment, the concentration was around 2,500 ng/mL. These data support the idea that the thickness of the epithelium is key to how the drug distributes and ultimately how the protection against infection might occur. In summary, the vaginal rings provided protective tissue and fluid levels of maraviroc in both macaques with and without Depo-Provera treatment for 1 month.

Fetherston et al. have since developed a matrix-type silicone elastomer vaginal ring containing both dapivirine and maraviroc[70]. A ring containing 25 mg of dapivirine is currently in phase III clinical trials, with results expected in 2015[74]. The combination of two ARVs may provide better protection while resisting the development of drug resistant viral strains. Fetherston et al.'s lead formulations contained 25 mg of dapivirine and 100 mg of maraviroc in two different silicone elastomers. Maraviroc and dapivirine were not extremely soluble in the elastomers (~0.2 mg/g), and melting endotherms were present in DSC analysis of rings with 10% wt/wt drug, suggesting that the drug exists in a crystalline form within the silicone elastomers typically used for vaginal rings. The 100 mg maraviroc ring released 10 mg cumulative over 30 days from either ring type, but about 50% of this was released as a rapid burst in the first day due to drugs on the surface of the ring. The rate of drug release following the burst was consistent with a diffusion process[70]. Compared to the maraviroc ring previously formulated by Malcolm et al., the dual dapivirine maraviroc ring appears to have released drug much more slowly, and it is uncertain if protective concentrations of maraviroc would be established in the vaginal tissue. A ring containing 400 mg of maraviroc (Fetherston et al.) released only 4.6% of the maraviroc in 30 days from the 400 mg maraviroc ring, compared to 31.8% from the 400 mg maraviroc ring produced by Malcolm et al[57]. While the same elastomer (for at least one formulation by Fetherston et al.) and production method were used in both cases, there were key differences between the two studies. First, the volumes and compositions of release media were different. Second, the cross-sectional diameters of the two rings were slightly different (7.6 mm vs. 6 mm). In addition, the difference in release rate between the 400 mg maraviroc rings could be due to the physical state of the maraviroc in the ring (untested by Malcolm et al.), or by the presence of dapivirine in the matrix used by Fetherston et al.[70].

1.11.3 Efficacy Studies

The first proof-of-concept test of maraviroc for oral PrEP was performed in humanized mice by Neff et al.[123]. Neff et al. orally dosed humanized mice with 62 mg/kg of oral maraviroc for 4 days before vaginal challenge with HIV, followed by a further 3 days of treatment. The mice with

treatment showed complete protection against HIV, while those mice without treatment all seroconverted within 5 weeks[123]. While data from humanized mice are not necessarily predictive of success in humans, this proof-of-concept study showed that oral PrEP with maraviroc was possible. Oral PrEP using maraviroc was evaluated later in a macaque model of repeated low dose rectal exposure.

Massud et al. recently completed an oral PrEP study with maraviroc in macaques using a low dose multiple rectal challenge of $SHIV_{162p3}$[115]. A human equivalent dose of maraviroc was given orally 24 hours before virus exposure followed by a booster post-exposure dose. Maraviroc concentration in rectal *secretions* peaked 24 h after dose with a concentration of 10,242 ng/mL and remained 40 times higher than levels required to block infection of PBMCs *in vitro* at 48 hours. Maraviroc concentration in rectal *tissue* at 24 h after dosing had a median value of 1,404 ng/g and was 30 and 10 times higher than levels in vaginal and lymphoid tissues, respectively. The authors showed that maraviroc efficiently bound to CCR5 on rectal lymphocytes, with a half-life of CCR5-bound maraviroc of 2.6 days. Despite a favorable concentration profile and the observation that maraviroc was bound to target cells, 5/6 macaques treated with maraviroc were infected over 5 challenges, as were 3/4 controls. A similar model was used to previously predict efficacy of TDF/FTC oral PrEP with rectal exposure[124], which was then validated in iPrEX clinical trial with men who have sex with men[125]. Thus, the failure of maraviroc to provide effective oral PrEP to macaques suggests that maraviroc may not be effective in human clinical trials for rectal HIV transmission. Interestingly, maraviroc treatment was seen to increase the percentage of $CD3^+/CCR5^+$ cells in mucosal tissue. It could be that maraviroc treatment results in an increase in the virus' target cells, thus eliminating the protective effect of the drug. However, maraviroc has been effective against HIV clinically when used for treatment, and has shown protective efficacy when formulated in gels, as discussed below. It remains to be seen if systemic vs. local dosing or rectal vs. vaginal application/challenge influence maraviroc's use as an HIV prophylactic.

There is strong preliminary evidence from human clinical trials that intensive oral dosing in humans may negatively impact oral PrEP outcomes. An excellent study by Hunt et al. in 2013 found that oral maraviroc administered to HIV patients with incomplete CD4+ T-cell recovery and currently receiving ART induced elevated T-cell activation in peripheral blood and rectal tissues[11]. In addition, maraviroc caused a redistribution of CD8+ T-cells from GALT into the peripheral blood. Naturally occurring CCR5 antagonists, such as MIP-1β, were found in high concentrations in the blood, indicative of competitive inhibition by maraviroc. These elevated antagonists may have been responsible for immunological changes seen in the study. The

study's results implied that although oral PrEP with maraviroc would block CCR5-mediated viral entry into cells, it might increase the abundance of activated CD4+ T-cells. This could be problematic for users with low adherence (seemingly the vast majority) or for those exposed to CXCR4-tropic virus.

Despite a lack of efficacy when used for oral PrEP in macaques, maraviroc has been successful at preventing infection via vaginal challenge in nonhuman primates. Local delivery of maraviroc is particularly attractive considering the reduction in systemic side effects (potentially including the dramatic immunological changes and CD4+ T-cell activation seen in rectal tissue following oral dosing) and the reduction in the amount of drug required per dose (and hence, lower cost). Veazey et al. used a vaginal gel containing up to 6 mM maraviroc (i.e., 3.3 mg/mL, or 0.33% wt/wt) in 2.2% HEC as a protective measure against vaginal challenge with 500 $TCID_{50}$ of $SHIV_{162P3}$, a CCR5-tropic virus engineered to be mucosally transmissible, and found that 5/6 animals were protected when given a 6 mM gel 30 minutes prior to challenge[117]. Veazey et al. showed that the extent of coverage was highly dependent upon the time before challenge. They showed that the efficacy dropped to 50% and 0% for 4 h and 12 h post-dosing challenge with a 0.3% gel. Furthermore, they showed that efficacy declined from 86% to 75%, 50%, and 0% when dose was decreased to 0.1% (1 mg/mL), 0.01% (100 mcg/mL), and 0.003% (30 mcg/mL). Gel volume was 4 mL[117]. The gel did not protect against challenge with a CXCR4 using strain of SHIV. Veazey et al. therefore showed that maraviroc should be used in high doses (> 6mM in 4 mL of gel) within a short time before challenge with the virus. The efficacy of maraviroc appears to drop precipitously when maraviroc falls below its solubility limit and is no longer a saturated solution or dispersion. Maraviroc levels must therefore be maintained as high as possible in the vagina to protect against a high dose SHIV challenge in Depo-Provera-treated macaques. Despite showing some efficacy, this study by Veazey et al. failed to show 100% protective efficacy against viral challenge in a model that was predictive of success with a 1% tenofovir gel.

Malcolm et al. subsequently followed up on the study performed by Veazey et al. by measuring the PK of maraviroc in macaques following administration of even higher levels of HEC based maraviroc gels (see above)[118]. This kind of PK study was not performed by Veazey et al[117]. Malcolm et al. also tried to specifically correlate the PK data with efficacy in the same single high-dose vaginal $SHIV_{162P3}$ challenge model as used previously. Malcolm et al. found vaginal protection was effective with > 1mM maraviroc gels, but confirmed that the protection was lost if the gel was applied 6-12 h before virus challenge (in a high dose challenge model, not repeated low dose)[117,118]. This points to a potential need for sustained release of maraviroc

following an initially high maraviroc dose at the time of challenge. Alternatively, these results may point to similar immunological changes observed following oral administration of maraviroc.

1.12 Summary of introduction

Electrospun fibers can incorporate and deliver a variety of anti-HIV compounds. The polymer space for developing electrospun microbicides is vast, and a number of electrospinning techniques developed for other drug delivery applications have yet to be adapted for anti-HIV microbicides. Perhaps the most attractive aspect of electrospun fibers for microbicide development is their ability to facilely incorporate multiple compounds into composites or nano-structured carriers (e.g., layered mats or coaxial fibers). Future research into electrospun microbicides should focus both on developing dosage forms in familiar polymer systems for vaginal drug delivery and on designing fibers with unique polymers, including “smart” polymers that are responsive to pH, enzymes or HIV virions and polymers with tunable erosion rates. Ultimately, we must move toward rational design of drug carriers based not only on materials science, thermodynamics, and engineering, but also on social science and product acceptability studies to develop products that are technically sound and highly desirable for end users.

Chapter 2. Drug-eluting fibers for HIV-1 inhibition and contraception

Adapted from Ball and Krogstad et al., PLOS ONE 7(11): e49792. doi:10.1371/journal.pone.0049792.

2.01 Abstract

Multipurpose prevention technologies (MPTs) that simultaneously prevent sexually transmitted infections (STIs) and unintended pregnancy are a global health priority. Combining chemical and physical barriers offers the greatest potential to design effective MPTs, but integrating both functional modalities into a single device has been challenging. As in our previous publication[79], here we show that drug-eluting fiber meshes designed for topical drug delivery can function as a combination chemical and physical barrier MPT. Using FDA-approved polymers, we fabricated nanofiber meshes with tunable fiber size and controlled degradation kinetics that facilitate simultaneous release of multiple agents against HIV-1, HSV-2, and sperm. We observed that drug-loaded meshes inhibited HIV-1 infection *in vitro* and physically obstructed sperm penetration. Furthermore, we report on a previously unknown activity of glycerol monolaurate (GML) to potently inhibit sperm motility and viability. The application of drug-eluting nanofibers for HIV-1 prevention and sperm inhibition may serve as an innovative platform technology for drug delivery to the lower female reproductive tract.

2.02 Introduction

HIV-1 infections and unintended pregnancies are inextricably linked by unprotected sex and represent a major health burden for women worldwide[1]. Access to MPTs combining safe, effective, and easily reversible options for contraception are essential for women who are also at risk for STIs including HIV-1. To date, no single commercialized product exists that women can use discreetly for simultaneous and effective prevention of STIs and pregnancy[126], although such products are in development[127]. Women would also benefit from more options for chemical contraceptives that are nonhormonal[128,129]. In particular, an alternative to nonoxynol-9 (N-9) that is safe and non-toxic, does not alter the vaginal microflora, and does not enhance the risk for HIV-1 infection would have a major impact on women's sexual and reproductive health[21].

The materials chemistry and process of fabricating MPTs have a significant influence on their design and function. Existing MPTs are classified by their function as physical, chemical, or

combined physical/chemical barriers to prevent STIs and unintended pregnancy[77,130]. Chemical barrier methods are the front-line approach being evaluated in clinical trials for multipurpose protection, and include dosage forms such as gels, films, tablets, and intravaginal rings (IVRs)[55,85]. Gels containing tenofovir[36], UC781[52], dapivirine[131], and MIV-150[132] are among the many anti-HIV-1 microbicides under development. Typically, vaginal gels are unable to formulate water-insoluble drugs at high loadings. This limits their application to drugs that are hydrophilic, such as nucleotide analog reverse transcriptase inhibitors, or extremely potent. Vaginal films have long existed for the prevention of pregnancy (Vaginal Contraceptive Film® by Apothecus) as well as the treatment of fungal and bacterial infections[85]. Unlike water-based vaginal gels, films are delivered dry, which may confer the benefit of increased vaginal retention on a delivered drug. Recently, researchers have begun to formulate vaginal films and tablets that can provide quick release of antiviral compounds as an alternative dosage form to microbicide gels. For example, Akil et al. developed thin vaginal films that release 0.6 mg of dapivirine within 10 minutes following hydration[51]. IVRs, which are designed to provide sustained release of a combination of agents over several weeks or months, are the leading technologies being evaluated currently for multipurpose prevention[54,70]. However, IVRs are unlikely to satisfy all women's prevention needs, and may not be suitable for addressing the prevention needs of men who have sex with men. Greater flexibility in the choice of dug delivery system platforms and their fabrication processes could lead to innovative new dosage forms for a larger number of pharmaceutical agents.

Emerging technologies that integrate physical and chemical barriers provide the greatest potential for new MPT designs. To be effective, these technologies must address five fundamental design requirements: 1) deliver multiple drugs with differing physicochemical or pharmacokinetic properties from a single device, 2) provide extensive coverage of mucosal tissue, 3) be female-controlled and discreet, 4) deliver contraception that is fully reversible, and 5) be inexpensive so as to reach the most relevant populations. Based on these requirements, we have developed an innovative dosage form for vaginal drug delivery using drug-eluting nanofibers. Electrospinning is an elegant method to deliver combination drug therapies because polymers can be selected based on their drug compatibility as well as their degradation or dissolution rates[133]. In addition, controlling processing parameters (applied voltage, polymer flow rate, capillary-collector distance), nozzle configuration (single, multijet, coaxial), and choice of materials (non-degradable, biodegradable, water-soluble) allows greater versatility and flexibility to design topical prevention strategies[87].

To demonstrate the versatility of drug-eluting fibers for topical delivery to the vaginal mucosa in applications for multipurpose prevention, we generated nanofiber meshes that elute small molecule agents that target HIV-1, HSV-2, and sperm function. We demonstrated that these drug-eluting fibers deliver antiviral drugs with diverse physicochemical properties and mechanisms of action. Fibers loaded with antiretroviral drugs showed potent inhibition of HIV-1 infection *in vitro*. To address the need for contraception in a multipurpose prevention strategy, we screened multiple non-hormonal chemical contraceptive alternatives to N-9 that have been reported previously in the literature and discovered an unreported function of glycerol monolaurate (GML) to inhibit sperm motility and viability in a dose-dependent manner. We also showed that fiber meshes acted as a physical barrier to sperm penetration despite their porosity. The fiber meshes were readily electrospun in a geometry designed to provide physical coverage of both the vaginal epithelium and cervix. The functional combination offered by our drug-eluting nanofibers cannot be accomplished with any single technology currently in the development pipeline.

2.03 Materials and Methods

2.03.1 Ethics statement.

All animals were obtained and cared for in accordance with the University of Washington Institutional Animal Care and Use Committee (IACUC) guidelines, and animal studies were approved by the University of Washington IACUC. Human semen samples were obtained according to guidelines approved by the Institutional Review Board of the Human Subjects Division at the University of Washington. All subjects provided written, informed consent prior to participation, and the University of Washington Institutional Review Board approved the study protocol.

2.03.2 Polymer preparation.

Polymers used for electrospinning included poly(L-lactide) with an inherent viscosity of 0.90–1.20 dL g^{-1} (MW ~117 kDa) (Lactel Absorbable Polymers), poly(ethylene oxide) with MW 100 kDa (Sigma-Aldrich), polycaprolactone of M_n 70-90 kDa (Sigma-Aldrich), and acid terminated poly(D,L-lactide) of M_w 18-24 kDa (Sigma Aldrich). Maraviroc was obtained from the NIH AIDS Research & Reference Reagent Program, Division of AIDS, NIAID, NIH. 3'-Azido-3'-

deoxythymidine, methyl-β-cyclodextrin (M_n=1310), acyclovir, iron(II) D-gluconate, and L-ascorbic acid were purchased from Sigma-Aldrich. Glycerol monolaurate was purchased from MP Biomedicals, LLC. VFS was made according to methods described by Owen and Katz, et al.[134]. Potassium hydroxide, calcium hydroxide, lactic acid, acetic acid, and glycerol were purchased from Fisher Scientific. Bovine serum albumin, urea, and glucose were obtained from Sigma-Aldrich. Sodium chloride was purchased from Mallinckrodt Chemicals. The pH for VFS was adjusted to 4.2 with HCl and filter sterilized.

2.03.3 Electrospinning.

PLLA and PEO were dissolved at 5%, 10%, 15% (wt/vol) in mixtures of 1:1 or 3:1 (vol/vol) chloroform (EMD Chemicals) and 2,2,2-trifluoroethanol (Sigma-Aldrich). PCL was dissolved at 10% and 15% (wt/vol) in 2,2,2-trifluoroethanol. PDLLA and PLLA were dissolved at 15% (wt/vol) in 1:1 chloroform and 2,2,2-trifluoroethanol. Drugs were mixed with polymers at 1 or 10% (wt/wt) prior to addition to solvent. Polymer solutions were loaded into glass gastight syringes (National Scientific) and set into a precision syringe pump (KD Scientific Inc.). Unless otherwise specified, fibers were produced with the following parameters. We dispensed 500 μL at a flow rate of 5 μL min^{-1} through a gauge 22 stainless steel dispensing needle (Integrated Dispensing Solutions, Inc.) that was clamped to +15 kV using a high voltage generator (Gamma High Voltage Research). The aluminum mandrel collector was machined at the University of Washington to have a diameter of 1.27 cm. The collector was placed 12 cm horizontally from the tip of the needle and set to 3,000 r.p.m. (linear rotational speed of 200 cm s^{-1} at the surface of the collector) with a 5.08 cm horizontal travel at a speed of 2.54 cm s^{-1}. A copper or graphite brush electrically grounded the mandrel. 3.4 μm 70:30 PLLA/PEO fibers were produced as above except polymers were dissolved at 25% (wt/vol) and spun at 100 μL min^{-1} at 1,200 rpm. 1.5 μm 70:30 PLLA/PEO fibers were produced as 3.4 μm fibers except a 20% (wt/vol) solution of polymer was used. PDLLA/PLLA fibers were produced as above except for the flow rate and mandrel speed, which were 100 μL min^{-1} and 1,200 rpm, respectively. PCL fibers were produced by dispensing 500 μL at a flow rate of 100 μL min^{-1} from a 25 G needle clamped to +12 kV voltage and set 8 cm from the collector, which was rotating at 1,200 rpm. Electrospun meshes were removed from the collector and lyophilized for at least 24 h before imaging or use in biological assays.

2.03.4 Material characterization.

Polymer recovery was determined by dividing the mass of polymer removed from the mandrel by the theoretical mass of polymer and drug present in 500 μL of polymer solution. Meshes were sputtered with gold/palladium for 70 s and imaged with a scanning electron microscope at 500x and 5,000x magnification. Two scanning electron microscopes were used to complete imaging: a Sirion SEM at the University of Washington Nanotechnology Facility (funded by National Science Foundation), and a JSM-7000F SEM (JEOL Ltd.) at the Materials Science and Engineering Department at the University of Washington. Fiber size was determined in ImageJ (NIH) by measuring fibers that intersected a diagonal line drawn across each 5,000x micrograph to eliminate bias. At least 100 fibers from at least three separate micrographs were measured for each sample. Degradation in VFS was analyzed by placing 5 mg samples of mesh in 6 mL of VFS at 37°C for up to 15 days. Samples were removed at times up to 15 days, immersed gently in distilled water, inverted three times to remove salts, and lyophilized. The fibers were massed again, and percent mass loss was calculated as (original mass – current mass) / (original mass) x 100%. Fiber mesh thickness was measured using calipers. Dog bone shaped samples were cut from collected meshes with a D1708-96-MET die (ODC Tooling and Molds) such that the long axis of the dog bone corresponded to the circumferential direction of the mandrel collector. Uniaxial tensile testing was performed with an Instron model 5543 instrument and model 2712-03 grippers (Instron). Samples were stretched at a rate of 10 mm/min until failure. Young's modulus was estimated by fitting stress-strain curves with a line for 0-15% of maximum stress. Samples with a mass of 5-10 mg (n = 1) were placed into aluminum pans (T-Zero, TA Instruments) and analyzed with a TA Auto Q20 DSC instrument (TA Instruments) for thermal analysis. Samples were heated from 30°C to 250°C at a rate of 10°C/min with a nitrogen flow of 50 mL/min. Peak integration was performed using TA Thermal Analysis software and sigmoidal tangential integration. Percent crystallinity of the polymer or the drug was calculated by normalizing the measured enthalpy per unit mass of polymer or drug to the measured heat of fusion of the pure substance.

2.03.5 Drug release and loading.

Triplicate samples of mesh approximately 10 mg each containing AZT or MVC were placed into 6 mL glass vials, immersed in 6 mL of VFS, and incubated at 37°C on an orbital shaker at 200 r.p.m. At set time points (1h, 4h, 8h, 12h, 24h, 48h), 500 μL of buffer was removed and replaced with fresh VFS. A Shimadzu Prominence LC20AD UV-HPLC system equipped with a

Phenomenex Luna C18 column (5 µm, 250x4.6 mm) and LCSolutions software were used to quantify drug levels in samples. Methods for MVC were based on those as described[135]. The mobile phase consisted of HPLC grade 0.01 M KH_2PO_4 buffer and acetonitrile (60:40, vol/vol) (EMD Chemicals) at isocratic flow rate of 1.0 mL min^{-1} for 10 min. Column oven temperature was 25ºC. Standards were made in VFS, with linearity established from 0.001 to 0.02 mg mL^{-1} with 20 µL injection volume. MVC was detected at 193 nm with a retention time of 3.1 to 4.1 min. AZT was detected using an isocratic mobile phase was composed of HPLC grade water with 0.045% trifluoroacetic acid and acetonitrile with 0.036% trifluoroacetic acid (72:28) at a flow rate of 1.0 mL min^{-1} for 15 min, with column oven temperature of 30ºC. AZT was detected at 265 nm at retention time of 4.4 min. Standards were prepared in water, with a linear range from 0.001 to 0.5 mg mL^{-1} with 10 µL injection volume. GML release from fiber meshes was detected using thin-layer chromatography (TLC). 10 mg pieces of either 30:70 PLLA/PEO or 70:30 PLLA/PEO with 10% (wt/wt) GML were added in triplicate to 6 mL of PBS at pH 4.2. Samples were incubated at 37°C, and 500 µL were removed at periodic intervals and replaced with fresh PBS (pH 4.2) for 48 h. 5 µL of release media (n=3) were added onto duplicate TLC plates. After drying, plates were baked at 100°C for 10 min, then allowed to cool to room temperature. Plates were then immersed in 0.025% (wt/vol) Coomassie blue (Fisher) in 20% (vol/vol) methanol for 10 s and allowed to dry for 1 h. Plates were then digitized using a scanner. Drug loading and stability was measured using fibers stored at room temperature (19-22°C) for at least five months. 10 mg pieces of fiber mesh were dissolved in 2.5 mL acetonitrile, centrifuged for 10 min at 10,000g, and added to 0.01 M KH_2PO_4 buffer or water at a 1:1 ratio for MVC or AZT fibers, respectively. UV-HPLC was used to quantify amount of drug in samples as previously described. Encapsulation efficiency was calculated as the amount of drug in drug-loaded fibers relative to the amount of drug detected in dissolved blank fibers spiked at 1% (wt/wt) drug loading.

2.03.6 Mouse fiber coverage study.

Two eight-week old female Balb/cByJ mice (Jackson Laboratories) were cycled with injections of medroxyprogesertone acetate (Greenstone LLC) four days prior to fiber insertion. Fiber meshes of dimensions 2 x 2 cm were folded around an applicator and inserted into the mouse vagina. The control mouse received blank 30:70 PLLA/PEO fibers, and the experimental mouse received 30:70 PLLA/PEO fibers electrospun with 1% (w/w) indocyanine green (Sigma-Aldrich). Mice were anesthetized during the procedure with isoflurane administered through

nose cones. Mice were sacrificed after 30 minutes, and reproductive tracts were excised for imaging. Fiber meshes were removed after dissection and imaged with excised reproductive tracts. A Xenogen in vivo imaging system (IVIS) was used to measure fluorescence at 745/820 nm as a surrogate for fiber coverage.

2.03.7 HIV inhibition assay.

TZM-bL cells and HIV-1 BaL isolate were obtained from the NIH AIDS Research and Reference Reagent Program, Division of AIDS, NIAID, NIH (http://www.aidsreagent.org/). TZM-bL cells, a derived HeLa cell line that expresses CD4, CCR5, and CXCR4[136-139], were added to black 96-well plates (Corning, Corning, NY) with Dulbecco's Modified Eagle Medium (DMEM) (Gibco Life Technologies) with 10% fetal bovine serum (Hyclone), 1% 100X penicillin/streptomycin (Invitrogen), and 1% 200 mM L-glutamine (Invitrogen) with 50 μL/well at a density of 5,000 cells/well. Cells were incubated in 5% CO_2 and 37°C for 24 h prior to exposure to drugs or fibers. Fibers were sterilized by UV irradiation for 2 h (1 h per side). Treatments were added in 50 μL volumes. For the HIV-infectious inhibition assay, 100 μL of HIV-BaL (240 TCID/well) was added to wells 1 h after drug treatment. Media was removed from cells after 48 h post-treatment, and 100 μL of phosphate buffered saline (Gibco Life Technologies) and 100 μL of Bright-Glo Luciferase reagent (Promega) were added to wells. Infectious activity was quantified by measuring luminescence on a plate reader (Tecan). IC_{50} values of drug compounds were estimated using sigmoidal regression and bootstrapping in MATLAB version 7.11 (Mathworks).

2.03.8 Explant toxicity assay.

Macaque ectocervical tissues (Tissue Banking and Distribution Program, University of Washington National Primate Research Center) were processed for polarized explant cultures in duplicate on the day of surgery as previously described[45,140,141]. Briefly, a circular tissue punch was inserted through the transwell membrane with the luminal side up. The edges around the explant were sealed with Matrigel™ (BD Biosciences, San Jose, CA). A 0.6 mm diameter disc of either 30:70 PLLA/PEO, 70:30 PLLA/PEO, or 30:70 PLLA/PEO with 10% (wt/wt) GML fiber was placed on the apical side of the tissue with 200 μL of culture media (DMEM with 10% fetal bovine serum, 1% 100X penicillin/streptomycin, and 1% 200 mM L-glutamine). For controls, explants were untreated (culture media) or treated with a 0.4% dilution of nonoxynol-9 (N-9) gel. The explant cultures were maintained at 37°C in a 5% CO_2 atmosphere. After 18-24 h, the

explants were washed and one of each duplicate was incubated in RPMI containing 250 μg/ml MTT [1-(4,5-dimethylthiazol- 2-yl)-3,5-diphenylformazan] for 4 h. The explants were removed and placed in 1 mL of methanol overnight to extract the formazan dye produced by live tissue. The next day, the explants were removed from methanol and placed on a marked paper towel to dry and be weighed. The color extracted in the methanol was read for optical density at 595 nm. The percent viability of the treated explants was determined by correcting the optical density (OD) with the weight of the corresponding explant. The other explant was frozen in an embedding medium (Tissue-Tek, Sakura Finetek USA Inc., CA) and processed for histology by cryosectioning and hematoxylin-eosin staining.

2.03.9 Sperm motility and viability assays.

Sperm was obtained from two donors for sperm motility experiments. A third donor was recruited for sperm viability assays with glycerol monolaurate. Swim out sperm were obtained as described previously[142]. Briefly, we placed 0.5 mL aliquots of semen below 3 mL of Ham's F-10 media (Sigma-Aldrich) with 0.5% human serum albumin (Sigma-Aldrich) for 75 min in 5% CO_2 and 37°C. The aspirate, enriched for motile sperm, was centrifuged at 300 RCF for five min and resuspended in fresh Ham's F-10 to a concentration of 20 x 10^6 sperm mL^{-1}. The effect of drug dilutions on sperm motility were performed both in whole semen and in swimout sperm by adding 5 μL each of sperm and drugs to a slide and observing sperm motility with phase contrast either at 200x and 37°C (ECLIPSE Ti, Nikon), or by adding 200 μL of drug to 100 μL of semen and quantifying sperm motility with computer aided motility analysis for up to 7 min after the addition of drug. Multiple media only controls were run to ensure that any observed change in motility was minimally dependent upon time since ejaculation. Sperm viability was measured by adding 20 μL of semen to 20 μL of Trypan blue (Sigma-Aldrich) and counting 100 live or dead sperm based on head staining after a 10 min incubation using 1000x brightfield microscopy.

2.03.10 Sperm migration assay.

Millicell cell culture insert membranes (Millipore) with 3 μm pores were removed with forceps and replaced with square pieces of electrospun mesh. The mesh was attached to the inserts by applying firm pressure with a gloved finger. The thicknesses of cell culture insert membranes and electrospun meshes were measured using a micrometer. Modified and unmodified inserts were placed in a 12 well plate. Swimout sperm were diluted 1:10 in Ham's F-10 with no protein.

600 µL of Ham's F-10 was added to each of the twelve wells, and 400 µL of diluted sperm was added to each insert. Sperm were incubated for 2 h at 37 °C and 5% CO_2. The solutions from the inner and outer chambers of the wells were aspirated and used for counting to measure sperm concentration in media inside and outside of the inserts. Sperm were fixed by dipping membranes into ice cold ethanol and were then lyophilized for 24 h. Meshes were imaged using SEM with the same settings used to image blank meshes.

2.03.11 Statistical methods.

Fiber diameters were plotted as geometric mean with 95% CI and reported in writing as geometric mean with standard deviation. As fiber diameters had lognormal distributions, they were transformed by taking the log of the diameters in nm prior to hypothesis testing. One-way ANOVA and Bonferroni t tests were used to compare the diameters of log-transformed fiber diameters. Drug release was reported as mean with standard deviation, and 6 d release values were compared by one-way ANOVA with Bonferroni t tests or compared to zero release with a one sample t test. Differences in amount of drug release were reported as mean difference with 95% confidence interval. Sperm viability in the presence of GML was analyzed using one-way ANOVA and a Bonferroni t test. The numbers of sperm counted in the transwell migration assay were reported as mean and standard deviation of log transformed data, except in the case where the number of sperm detected was zero. We used two-sided tests at a significance level of $\alpha=0.05$ for all hypothesis testing. Actual p values are reported unless $p < 0.0001$.

2.04 Results

2.04.1 Electrospun fibers incorporate antiviral compounds with high drug loading.

We electrospun fibers from mixtures of hydrophilic polyethylene oxide (PEO) and hydrophobic poly-L-lactic acid (PLLA), two polymers with proven biocompatibility and FDA approval for use in medical implants[143,144]. We hypothesized that fibers with partially hydrophilic and partially hydrophobic composition would enable encapsulation of agents with high and low aqueous solubility, respectively. Previous studies with PLLA-PEO polymer blends found that blends act as a single material with averaged properties when mixed at a ratio up to 30:70 or 70:30 (wt/wt), but act as a composite of two materials with discrete properties when mixed at ratios approaching 50:50 (wt/wt)[145]. We therefore attempted to fabricate homogeneous fibers with well mixed PLLA and PEO components by electrospinning 70:30 (wt/wt) PLLA/PEO and

30:70 (wt/wt) PLLA/PEO meshes[‡]. We also electrospun pure PLLA and pure PEO meshes. Polymer concentration in the electrospinning solution had a significant impact on the resulting fiber diameters between formulations with the same PLLA/PEO ratio and solvent choice, as assessed by ANOVA ($P < 0.0001$) (Figure 2.1).

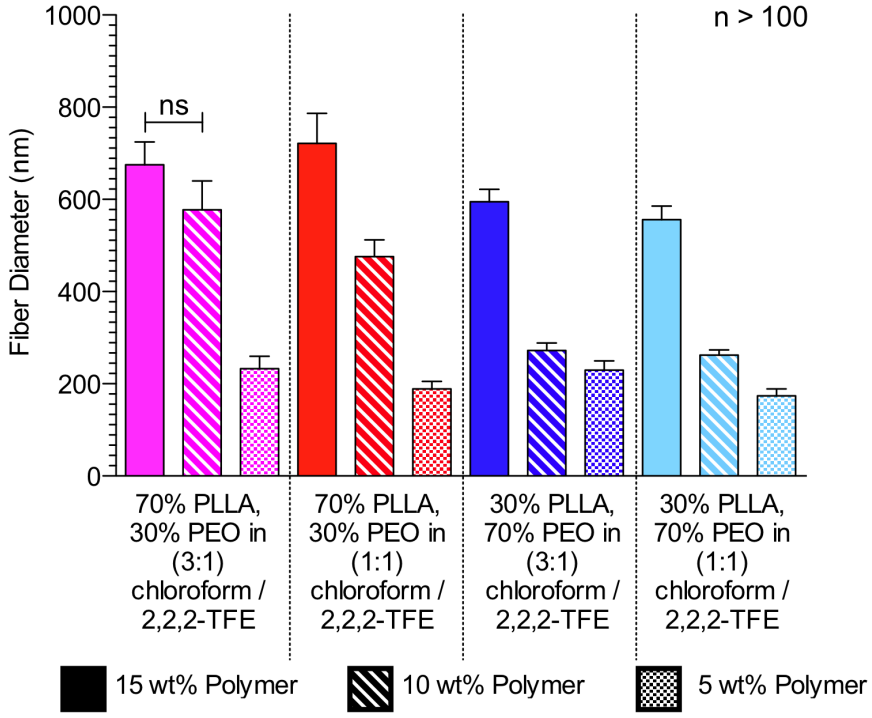

Figure 2.1—Fiber diameters depend upon polymer viscosity, composition, and solvent. Geometric mean fiber diameters with 95% confidence intervals are shown for 70:30 PLLA/PEO fibers (red) and 30:70 PLLA/PEO fibers (blue) made from polymers dissolved in either 1:1 or 3:1 (vol/vol) chloroform/2,2,2-trifluoroethanol). Geometric mean fiber diameter was found to vary significantly between all groups based on the concentration of polymer in the electrospinning solution (solid = 15% wt/vol, dashed = 10% wt/vol, dots = 5% wt/vol) ($P < 0.0001$), except as indicated.

Electrospinning parameters were modified to yield fibers with reproducible size and high polymer recovery (Figure 2.1, Figure 2.2), and two blends were identified for further study: 70:30 PLLA/PEO in 1:1 chloroform/2,2,2-trifluoroethanol and 30:70 PLLA/PEO in 3:1 chloroform/2,2,2-trifluoroethanol. These compositions produced fiber diameters of 200 - 700 nm and polymer recovery of >50%.

[‡] As it turned out, calorimetry measurements revealed poor compatibility and mixing between the PLLA and PEO phases in 70:30 and 30:70 electrospun fibers (2.06).

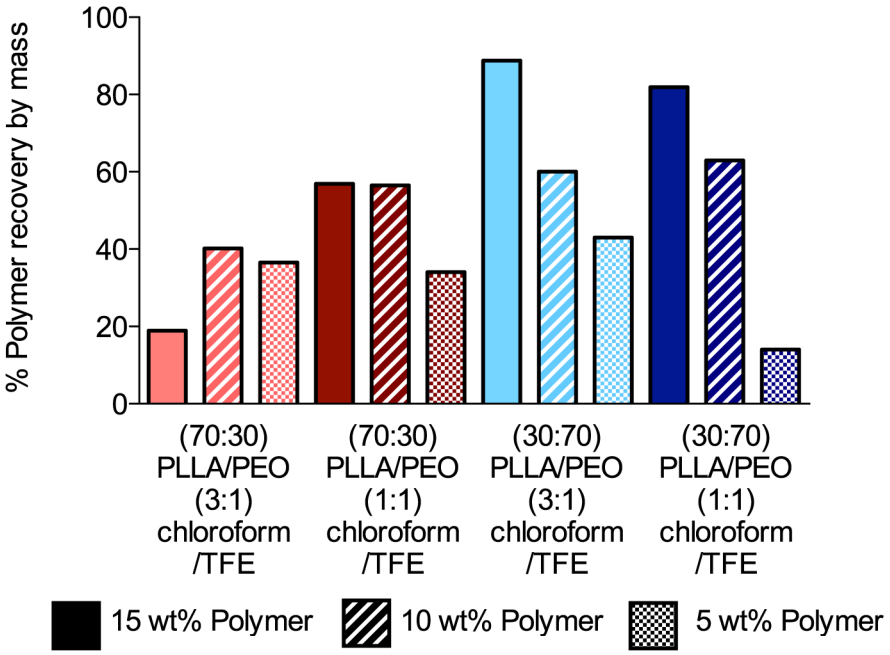

Figure 2.2—Material efficiency was positively correlated with % wt/vol of polymer in solution for most polymer blends. Here we define material efficiency as the percent polymer recovered from the mandrel by mass. For 30:70 PLLA/PEO blends, material efficiency increased with the % wt/vol of polymer in solution. Material efficiency is important for cost effectiveness. Based on these results, we chose the 15% (wt/vol) 70:30 PLLA/PEO in 1:1 chloroform/TFE and 15% wt/vol 30:70 PLLA/PEO in 3:1 chloroform/TFE as the base formulations for all further work with drug encapsulation.

The fibers were collected on a mandrel designed in the geometry of a tampon applicator (Figure 2.3, a-b) and resulted in fiber meshes in the shape of a hollow tube (Figure 2.3, c), which we were able to incorporate into a standard tampon applicator (Figure 2.4). By controlling the axial deposition of the fibers near the apex of the collector, we could also form a thick barrier mesh (~2-3 mm thick) that is continuous with a thinner inner mesh (down to ~10 μm thick).

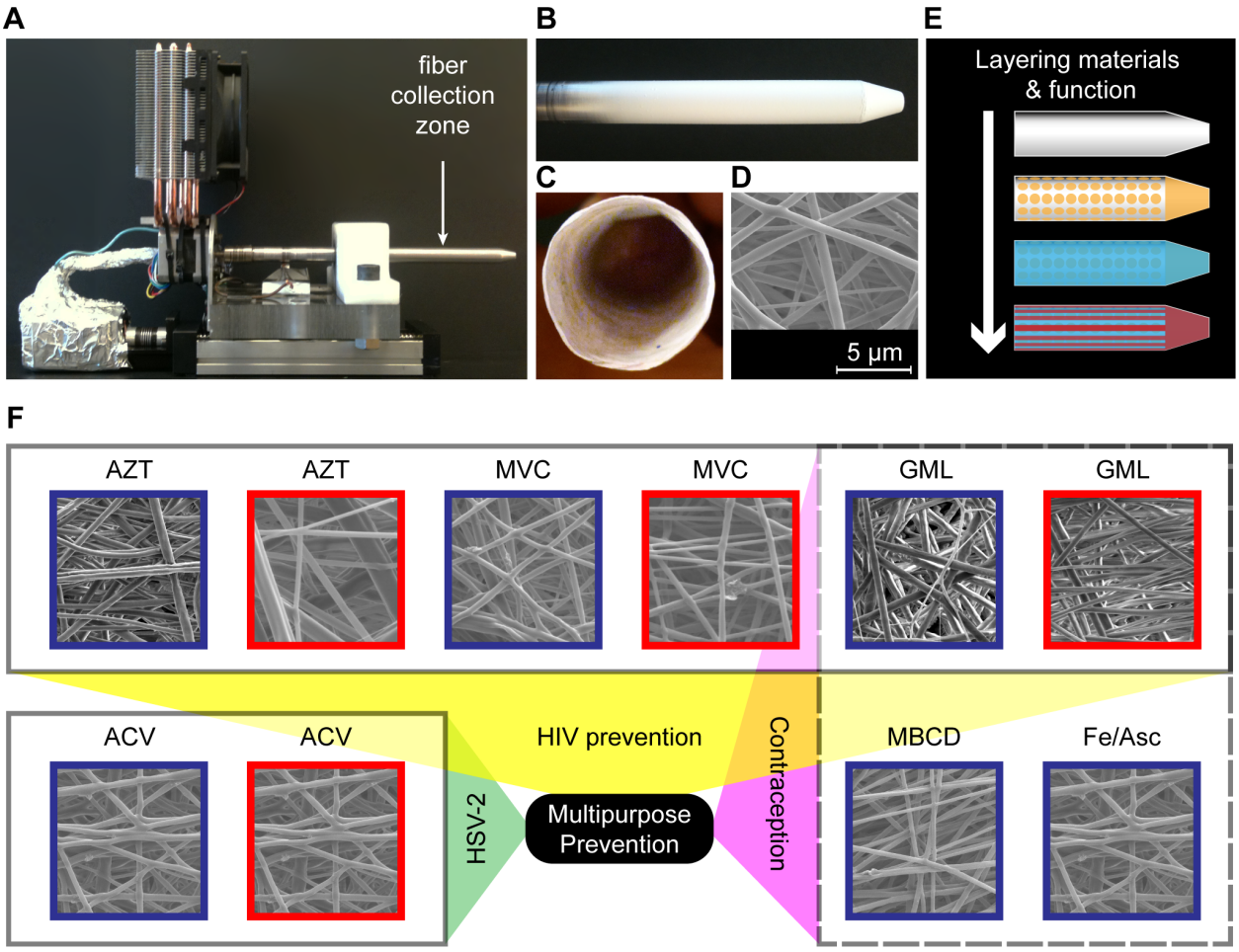

Figure 2.3—Electrospun fibers incorporate drugs for multipurpose prevention. (a) Two-axis mandrel electrospinning rig for fiber collection. (b) Controlled fiber deposition along a grounded aluminum collector produces a geometry that may be suitable for vaginal drug delivery. (c) Mesh abstracted from mandrel has a hollow interior. (d) Fiber meshes have porous microstructure. (e) Combining fiber meshes produces a multifunctional material. (f) Diverse agents with action against HIV, HSV-2, or sperm are incorporated into blends of PLLA and PEO. PLLA/PEO (30:70, blue) and PLLA/PEO (70:30, red); AZT = 1 wt% 3'-azido-3'-deoxythymidine, MVC = 1 wt% maraviroc, ACV = 1 wt% acycloguanosine, GML = 10 wt% glycerol monolaurate, MBCD = 10 wt% methyl-β-cyclodextrin, Fe/Asc = 10 wt% iron (II) D-gluconate with 10 wt% ascorbic acid.

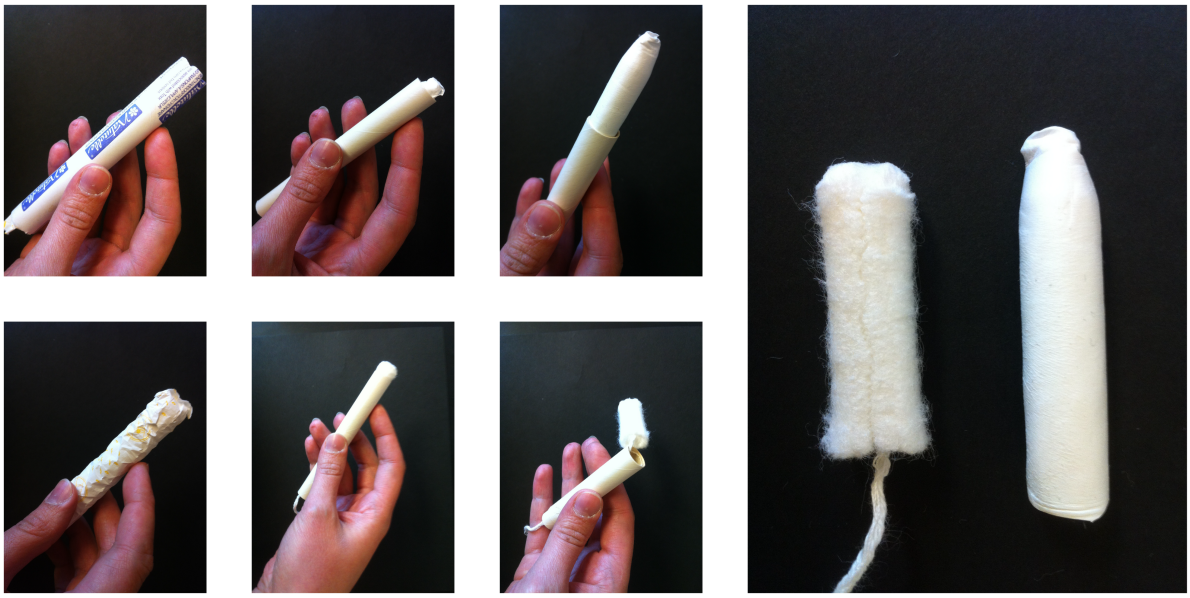

Figure 2.4—Electrospun fibers can be made sufficiently thick to be easily pushed out of a tampon applicator. The mesh device can be loaded into standard packaging (top and bottom images on the left), and resembles a tampon once opened (2nd to left, top – mesh, bottom – tampon). The device is delivered by pushing the inner cardboard tube through the outer cardboard tube of the applicator, revealing the fiber mesh, which would then hydrate and release active agents (3rd to left, top – mesh, bottom – tampon). A side-by-side comparison of a tampon and the tubular mesh reveals comparable geometry (right).

We selected several model compounds to demonstrate the versatility of electrospun fibers to deliver agents with differing solubility and mechanisms of action against either HIV-1 or HSV-2 (Figure 2.3, f). We electrospun fibers containing either 1% (wt/wt) maraviroc (MVC), which inhibits CCR5-mediated HIV fusion, 1% (wt/wt) 3'-azido-3'-deoxythymidine (AZT), which inhibits viral reverse transcriptase, or 1% (wt/wt) acyclovir (acycloguanosine), which has antiviral activity against HSV-2. Collectively, these compounds vary in aqueous solubility (0.01–50 g L^{-1}) and span a wide range of log P values (-1 to 4). We assessed drug loading of MVC or AZT-loaded fiber meshes stored at room temperature (19-22°C and 40-60 % relative humidity) for at least five months by dissolving them in acetonitrile and measuring drug content with HPLC. MVC and AZT were incorporated successfully into fibers at >95% drug encapsulation efficiency for both PLLA/PEO blend compositions. ARVs eluted from the polymer fibers were identical to the unformulated drugs as measured by UV-HPLC (Figure 2.5), suggesting that the compounds are stable during electrospinning and during shelf storage for at least five months. Fiber meshes also retained the same white color and soft, flexible texture over this five month period.

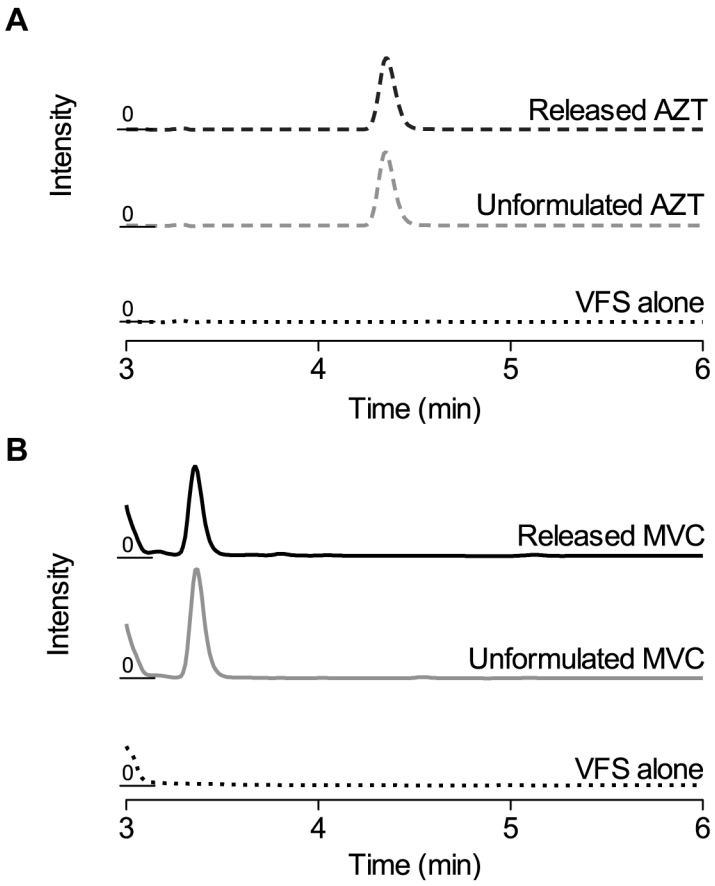

Figure 2.5—Electrospinning does not alter drug retention time with HPLC. (a) Representative chromatogram for AZT. (b) Representative chromatogram for MVC. Peak shapes and retention times do not change for unformulated drugs (gray lines) compared with drugs released from fibers (black lines).

We found that drug incorporation into polymer fibers influenced fiber size, fiber alignment, and polymer recovery (Figure 2.6, Figure 2.7, Figure 2.8, Figure 2.9). The fact that this was true even at 1% drug loading showed that electrospun fiber materials could be very responsive to changes in the material composition of the spinning solution.

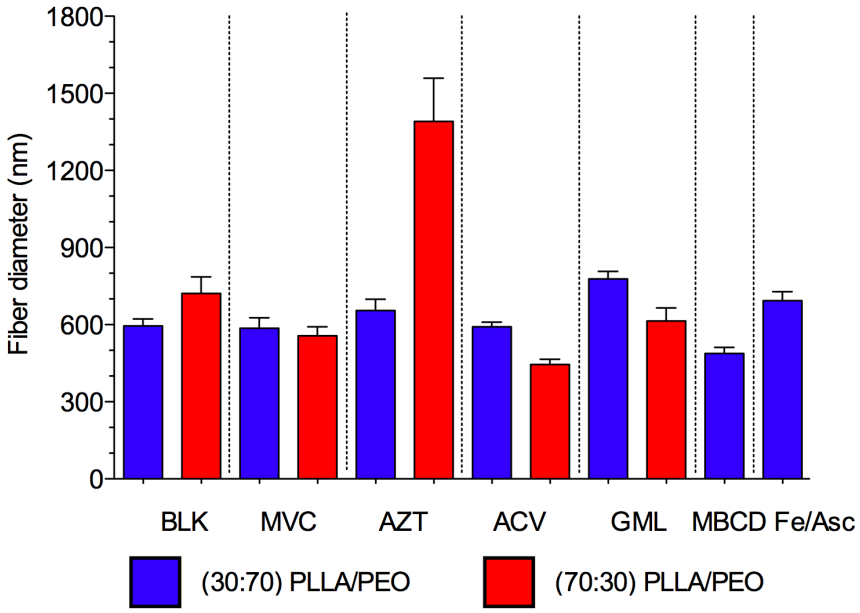

Figure 2.6—Drug incorporation into 30:70 and 70:30 PLLA/PEO electrospun fibers can alter fiber diameter distributions. Geometric mean fiber diameters with 95% confidence intervals are shown for 70:30 PLLA/PEO fibers (red) and 30:70 PLLA/PEO fibers (blue) incorporating MVC, AZT, ACV, GML, MBCD, or Fe/Asc compared to blank fibers.

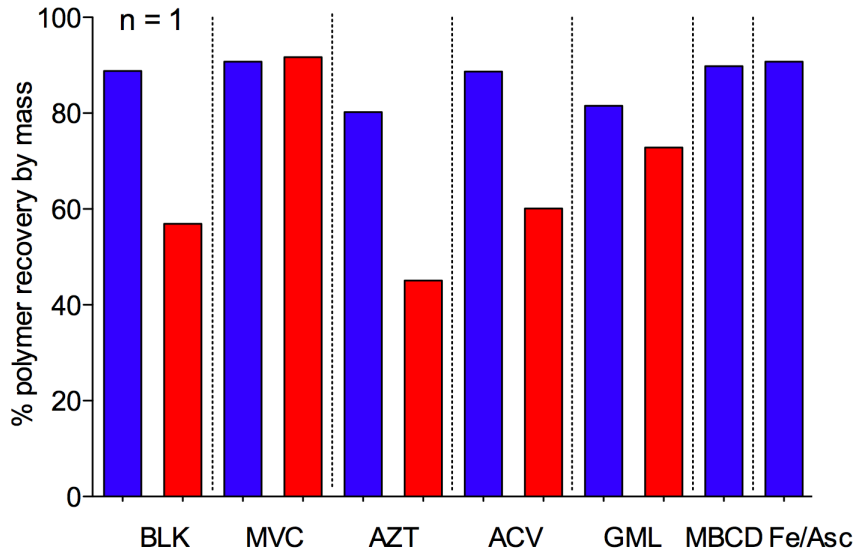

Figure 2.7—Drug incorporation into fibers influences material efficiency. Incorporating drugs into 30:70 and 70:30 PLLA/PEO blends (blue and red, respectively) affected polymer recovery. Interestingly, MVC dramatically increased material efficiency for 70:30 PLLA/PEO fibers.

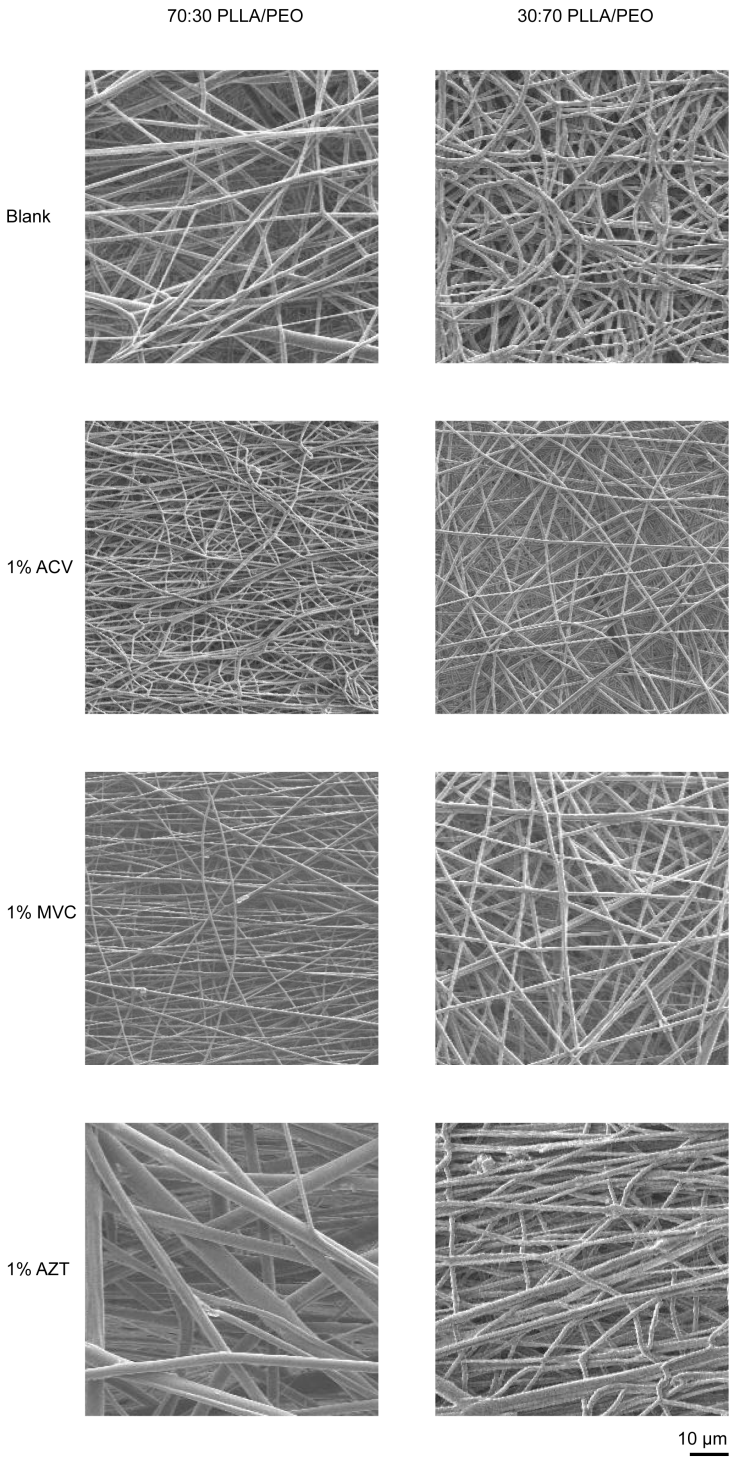

Figure 2.8—Fiber morphology and alignment for antiviral compounds ACV, MVC, and AZT. Increased alignment of 70:30 PLLA/PEO fibers is apparent in 1% MVC samples. Increased alignment of 30:70 PLLA/PEO fibers is apparent in 1% AZT samples. Differences in fiber diameter, previously shown in Figure 2.6, are also apparent.

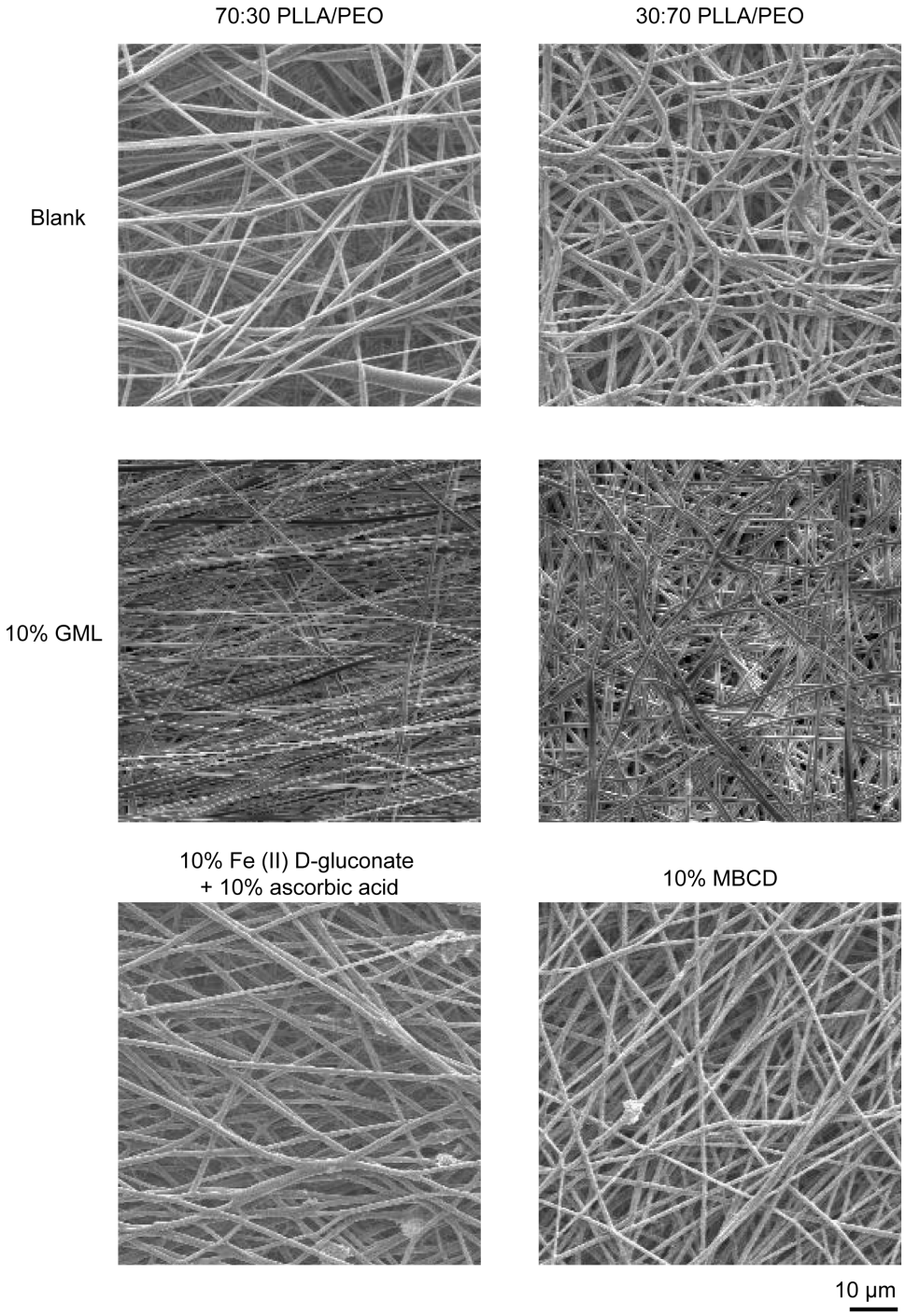

Figure 2.9—Fiber morphology and alignment for contraceptive compounds GML, Fe/Asc, and MBCD. Increased alignment of 70:30 PLLA/PEO fibers is apparent in 10% GML samples. Increased alignment of 30:70 PLLA/PEO fibers is apparent in 10% MBCD samples. Differences in fiber diameter, previously shown in Figure 2.6, are also apparent.

2.04.2 Drug-loaded fibers erode and release agents to potently inhibit HIV-1 activity *in vitro*, and show no toxicity in an *ex vivo* macaque cervical tissue model

We had hoped that our first foray into developing electrospun microbicides would produce materials capable of releasing drug either slowly or rapidly, depending upon the specific formulation. It is thought that microbicides that release drugs over weeks or even months, like intravaginal rings, have a greater potential for adherence than daily use products like gels, since the women using them would not have to remember or decide to reapply the microbicide on a frequent basis. We wanted to demonstrate that electrospun fibers could be designed to provide sustained release of antiretroviral compounds for at least 48 hours, and therefore overcome potential problems with adherence associated with daily use. In addition, we believed that fibers might be ideally suited for rapidly releasing encapsulated compounds. This burst release of active agents may be desirable for pericoital prevention[126]. Since degradation of polymeric delivery systems can influence drug release properties, we fabricated fibers with varying degradation rates by modulating the hydrophilic and hydrophobic content of the fibers. We monitored fiber degradation in VFS over two weeks by recording mass loss and imaging with SEM (Figure 2.10). Fiber meshes with greater hydrophilic content showed the most pronounced change in individual fiber and overall mesh morphology. We observed that fibers decreased in diameter within hours to days, and then appeared to fuse into large fiber bundles. These observations were confirmed by measuring a 30% (95% CI = 25% to 35%, n = 117) reduction in 30:70 PLLA/PEO and a 32% (95% CI = 23% to 40%, n = 103) reduction in 70:30 PLLA/PEO fiber diameters after 3 days and over 30% mass loss of the meshes within one week. The percent mass loss corresponded with the percent PEO composition in the fibers. Pure PLLA fibers showed no mass loss after a one-hour incubation in VFS, whereas pure PEO fibers dissolved in less than 10 minutes upon contact with water.

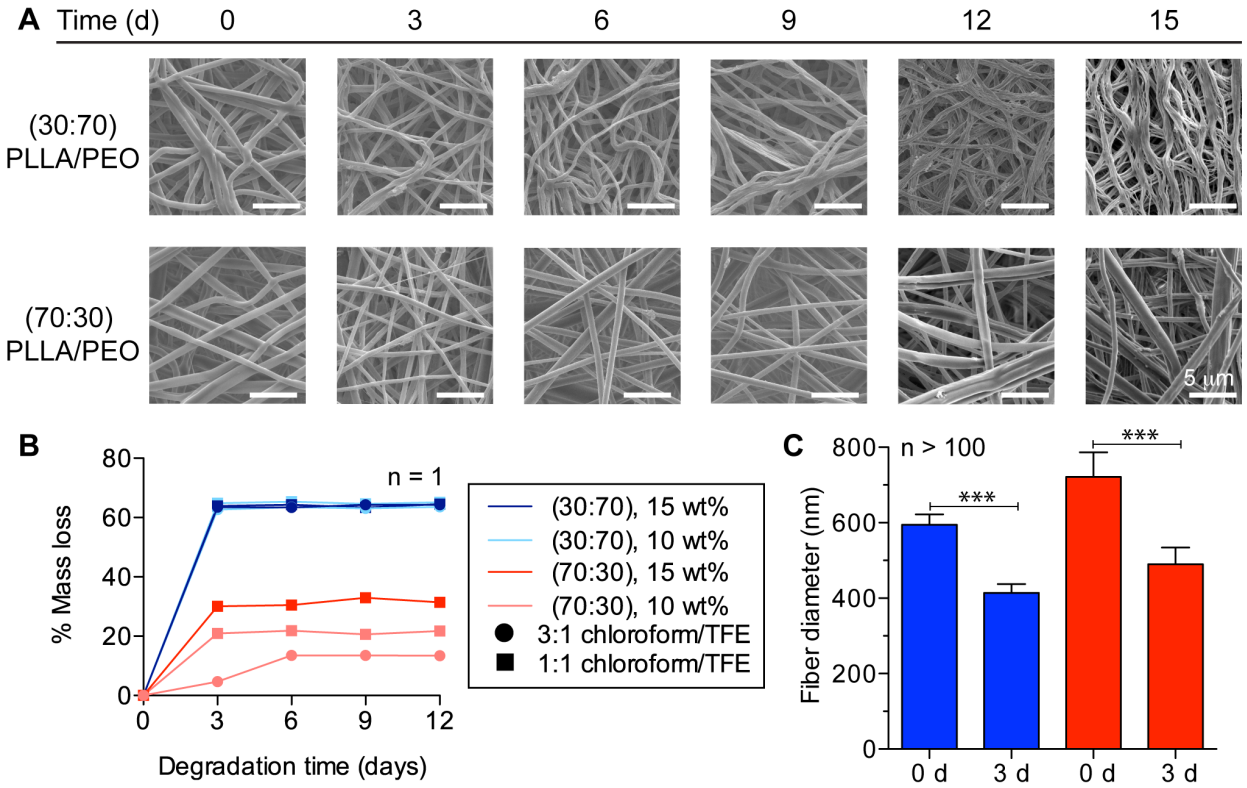

Figure 2.10—Fiber composition influences degradation properties. (a) SEM micrographs show that fiber and mesh morphology changes markedly over 15 d in VFS. (b) Mass loss of fibers over time is controlled by PEO content in fibers. (c) Fiber diameters, displayed as geometric mean with 95% confidence interval, and decrease significantly over three days of degradation in VFS ($p < 0.0001$ for 30:70 and 70:30 PLLA/PEO fibers). 30:70 PLLA/PEO (blue) and 70:30 PLLA/PEO (red) for (b) and (c).

To investigate if drug release kinetics recapitulated polymer degradation kinetics, we monitored drug release from meshes incubated in VFS (Figure 2.11). We observed that AZT and MVC burst released from fibers within 1 h, but that the drug release profiles differed based on PLLA and PEO content of the fibers. For example, fibers with greater hydrophilic content (30:70 PLLA/PEO) released 2.1% more AZT (95% CI = 0.68% to 3.5%, n = 3) and 13% more MVC (95% CI = 6.8% to 20%, n = 3) over 6 d than corresponding meshes with greater hydrophobic content (70:30 PLLA/PEO) (Figure 2.11**, a**). In 6 d, 70:30 PLLA/PEO fibers released 92 ± 0.75% of encapsulated AZT and 80 ± 3.9% of MVC into VFS (n = 3). The 30:70 PLLA/PEO fibers released 94 ± 0.48% of encapsulated AZT and 93 ± 0.98% of MVC into VFS (n = 3). We did not detect MVC release from pure PLLA fibers over 96 h in VFS (Figure 2.11, **c**). These results suggest that controlling polymer-drug interactions and the rate of polymer swelling and dissolution may alter the release kinetics of different active agents. Given the burst release

of AZT and the aqueous solubility of indocyanine green (ICG) dye, we chose to electrospin ICG-loaded fibers to investigate the extent of fiber coverage and agent release in mice. After inserting 30:70 PLLA/PEO fibers loaded with 1% (wt/wt) ICG into mice, we observed that dye completely coated the vaginal tract after 30 minutes (Figure 2.11**, d**). This study provides initial evidence that fibers are able to sufficiently hydrate and release agents to coat the vaginal mucosa *in vivo*.

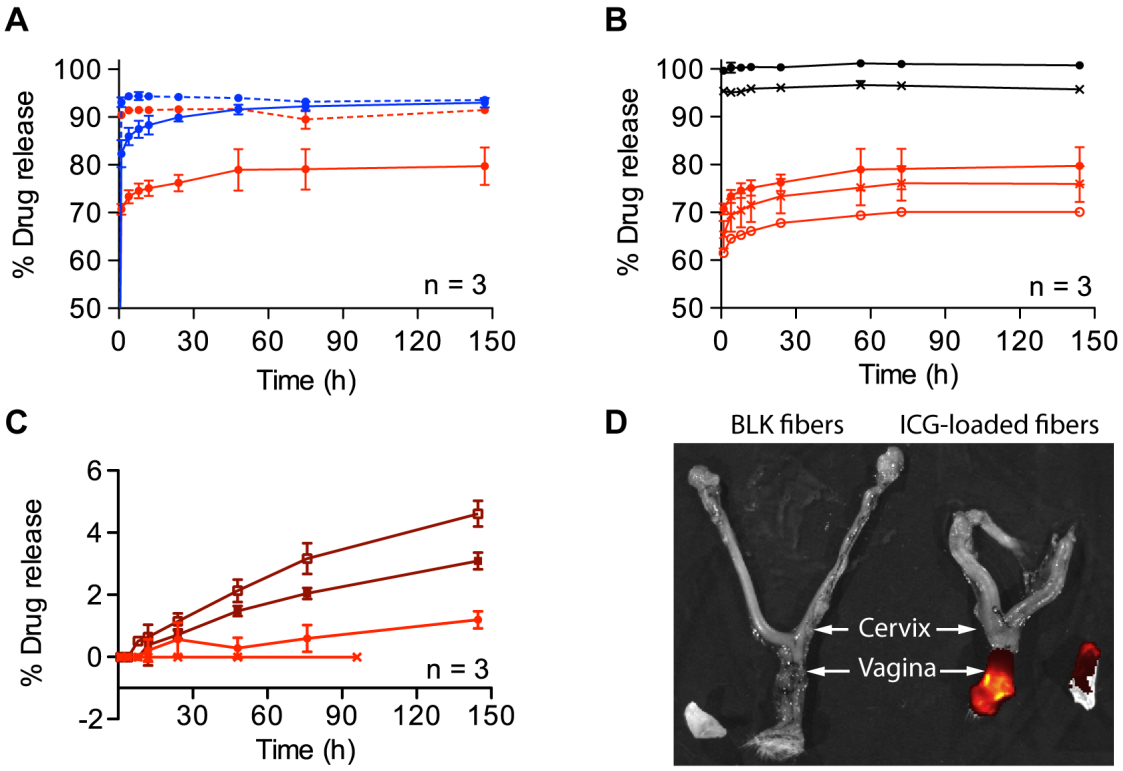

Figure 2.11—Fibers release active antiretroviral agents. (a) Cumulative drug release in VFS was measured for 30:70 PLLA/PEO (blue) and 70:30 PLLA/PEO (red). AZT (dashed line) and MVC (solid line) showed rapid burst release from blended fibers within 1 h. (b) Varying fiber diameter resulted in MVC burst release from PCL fibers (black) and 70:30 PLLA/PEO fibers (red). PCL meshes with two fiber diameters (• =370 nm and × =1.3 μm) and 70:30 PLLA/PEO fibers with three fiber diameters (• =560 nm, **o** = 1.5 μm, × = 3.4 μm) were tested. (c) Sustained release of MVC is achieved from PDLLA/PLLA blends and from 99:1 PLLA/PEO, but not from PLLA fibers. 50:50 PDLLA/PLLA (□), 25:75 PDLLA/PLLA (■), 99:1 PLLA/PEO (•), and 100% PLLA (×). (d) Insertion of fibers into mouse vagina and subsequent fluorescent imaging reveal release of dye within 30 minutes for ICG-loaded fibers (right) compared with blank fibers (left). Fiber meshes are shown next to excised reproductive tracts.

We evaluated the activity and toxicity of our drug-loaded fibers in several relevant *in vitro* assays. MVC, AZT, and fibers were shown to be nontoxic to TZM-bL cells, and no difference between treated cells and media controls was found (Bonferroni post test, α = 0.05) (Figure 2.12).

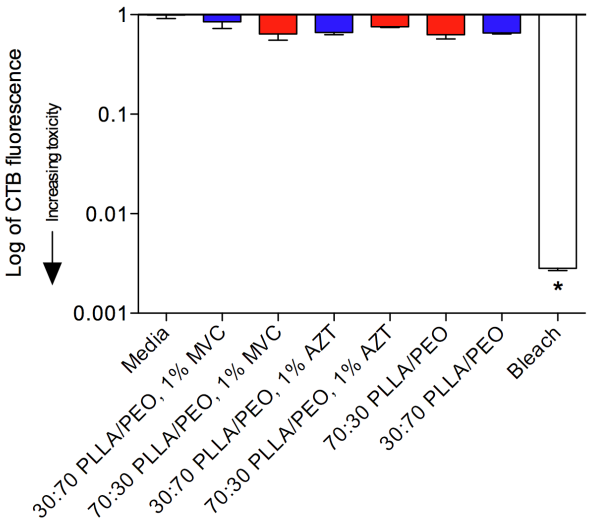

Figure 2.12—Fibers are not cytotoxic to TZM-bL cells. Cytotoxicity was tested using the CellTiter-Blue(TM) cell viability assay by culturing TZM-bL cells with disks of blank and drug-loaded meshes (n = 3) for 48h. Fluorescence signals for each condition are plotted as log-transformed values. Media-only treated cells and fiber-treated cells show significantly less cytotoxicity than bleach-treated cells ($p<0.05$).

We tested the ability of both the drug *eluates* released from 70:30 PLLA/PEO and 30:70 PLLA/PEO fibers and the *drug-loaded fibers themselves* to inhibit HIV-1 BaL infection in TZM-bL cells. First, we determined the specific antiviral activity of drug eluates released from the fibers to confirm that the absolute drug activity was not diminished by electrospinning. We measured an IC50 value of 0.90 nM and 2.3 nM for unformulated and eluted MVC, respectively. The IC50 of unformulated and eluted AZT was found to be 120 nM and 84 nM, respectively (Figure 2.13**, a**). The order of magnitude agreement between drug IC50 values before and after spinning suggests that the stabilities of MVC and AZT are maintained during electrospinning. Incubating TZM-bL cells with drug-loaded fiber discs significantly inhibited HIV-1 infection compared to blank fibers (P value < 0.0001) (Figure 2.13**, b**). The polymer composition of the mesh at this dosing did not impact their anti-HIV activity, and we saw equivalent viral inhibition for both drugs using the 30:70 and 70:30 PLLA/PEO meshes (Bonferroni post test, α = 0.05). Fiber toxicity was evaluated in an *ex vivo* tissue explant model using macaque cervical tissue. In

contrast to tissue treated with N-9, we observed no reduction in tissue viability due to exposure to blank fibers or fibers loaded with 10% (wt/wt) GML as determined using an MTT assay and by histological examination of tissue morphology (Figure 2.13**, c and d**).

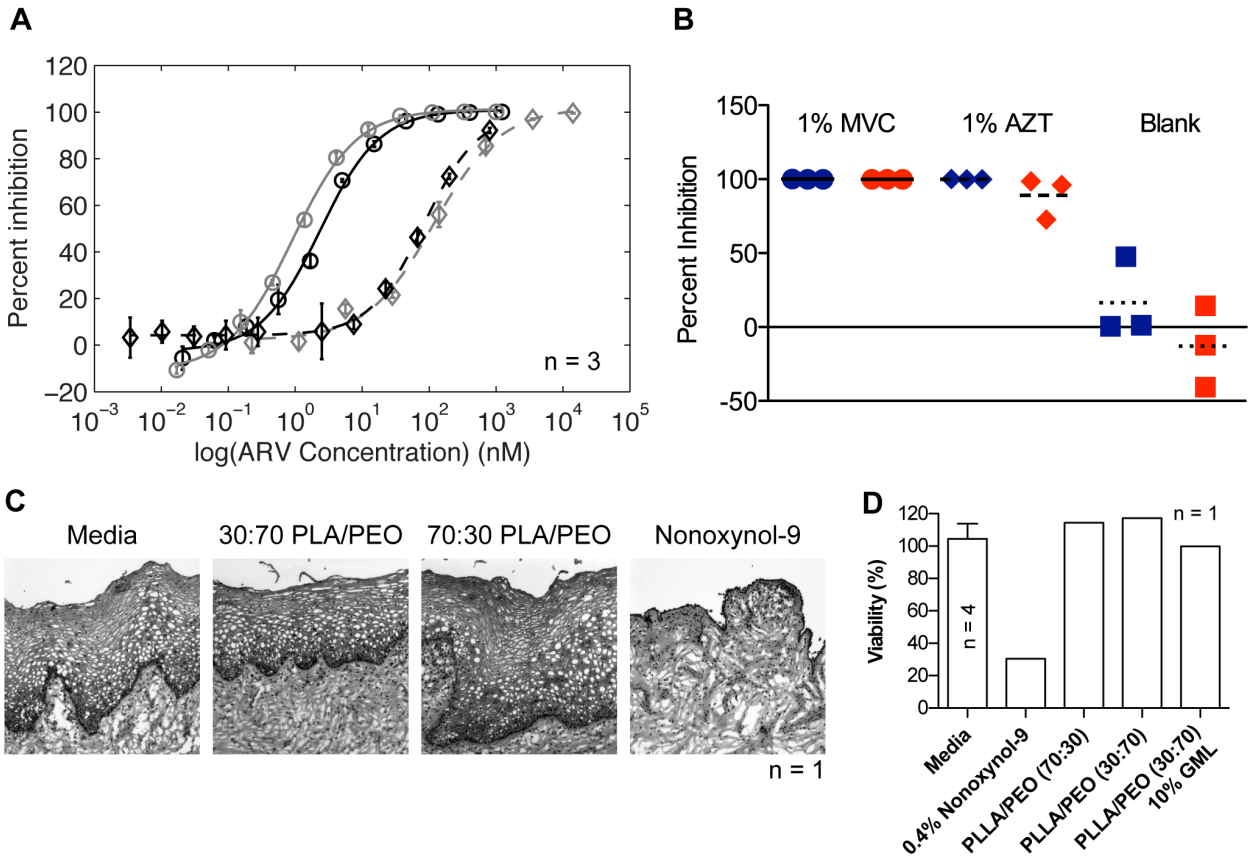

Figure 2.13—Fiber meshes inhibit HIV *in vitro* and are nontoxic to macaque cervical tissue explants. (a) Dose-response assay indicates that AZT and MVC released from fibers have similar potency to unformulated drugs (drug eluates, black and unformulated drug, gray). (b) Drug loaded fiber blends (30:70 PLLA/PEO (blue) and 70:30 PLLA/PEO (red)), but not blank fiber controls, show equivalent inhibition of HIV infection. (c) Histology indicates that 30:70 PLLA/PEO, 70:30 PLLA/PEO, and 30:70 PLLA/PEO fibers with 10% (wt/wt) GML are nontoxic to macaque cervical tissue explants compared to nonoxynol-9 control. (d) MTT assay confirms fibers, including those containing 10% (wt/wt) GML, are nontoxic to tissue explants. Note that for media controls n=4, and for all other groups n=1.

2.04.3 GML fibers are a chemical and physical barrier against sperm function.

To address the need for contraception in a multipurpose prevention strategy, we sought to identify non-hormonal chemical alternatives to N-9. We first evaluated the spermicidal capabilities of ferrous D-gluconate (FeGluc) and ascorbic acid (Asc) to corroborate findings from literature that the metal compound and ascorbic acid cause rapid spermiostasis due to lipid peroxidation of sperm[146]. We also evaluated methyl-β-cyclodextrin (MBCD), which we hypothesized might sequester cholesterol from semen and lead to premature sperm capacitation[147]. FeGluc and MBCD were readily incorporated into electrospun fibers (Figure 2.3, Figure 2.6, Figure 2.7, Figure 2.8, and Figure 2.9), but these agents were ineffective at inhibiting sperm function as assayed by measuring motility of purified (swim-out) human sperm (Table 2.1). Previous reports of the spermicidal activity from the combination of FeGluc and L-ascorbic acid appeared to be due primarily to the effects of ascorbic acid on solution pH.

Table 2.1—GML inhibits sperm motility in swimout sperm at 0.05 and 0.5% (wt/vol). We tested the contraceptive agents for their ability to inhibit sperm motility in a dose response motility experiment. Equal amounts of drug solution and human swimout sperm were combined on a glass slide. Changes in sperm motility over 2–5 min were recorded using a microscope and video recording system. Time point controls with PBS were performed to ensure drug effects on motility were independent of sperm incubation time. PBS percent motility at 2 min reflects average over all PBS control measurements, with range from 72%–100%.

Solution	Concentration (wt/vol)	Percent Motility at 2 min	Complete Inhibition within 5 min
PBS	1x	89	No
Nonoxynol-9	0.4%	0	Yes (< 30 s)
Glycerol Monolaurate	0.5% (pH 7)	30	Yes (< 4 min)
	0.05%	28	Yes (< 5 min)
	0.005%	55	No
	0.0005%	84	No
	0.00005%	75	No
Fe(II) D-gluconate	5%	52	No
L-ascorbic acid	5% (pH 2)	0	Yes (< 30 s)
	0.5% (pH 4)	21	No
Fe(II) D-gluconate + L-ascorbic acid	5% / 5%	0	Yes (< 30 s)
	0.5% / 0.5% (pH 4)	12	No
	0.05% / 0.05% (pH 5.5)	85	No
Methyl-β-cyclodextrin	5%	94	No

Based on the amphiphilic properties of glycerol monolaurate (GML) and its reported function to interact with lipid bilayers[148], we were motivated to evaluate GML activity on sperm function. We hypothesized that GML could potentially interact with sperm plasma membranes to reduce sperm viability and motility. Using human swim-out sperm, GML inhibited sperm motility at concentrations of 0.05–0.5% (wt/vol) (Figure 2.14-**a**). At these concentrations, complete spermiostasis was measured in < 5 min (Video S2, 3). Reduction in motility was also observed at concentrations down to 0.00005% (wt/vol) but did not result in complete spermiostasis during the measurement time (Figure 2.14-**a,** Table 2.1). GML also reduced viability of human sperm in whole semen by 33.1% (95% CI = 24.0% to 42.2%, n = 2) when tested at a 5% (wt/vol) concentration and by 19.6% (95% CI = 10.7% to 28.9%, n = 2) (Figure 2.14-**b**).

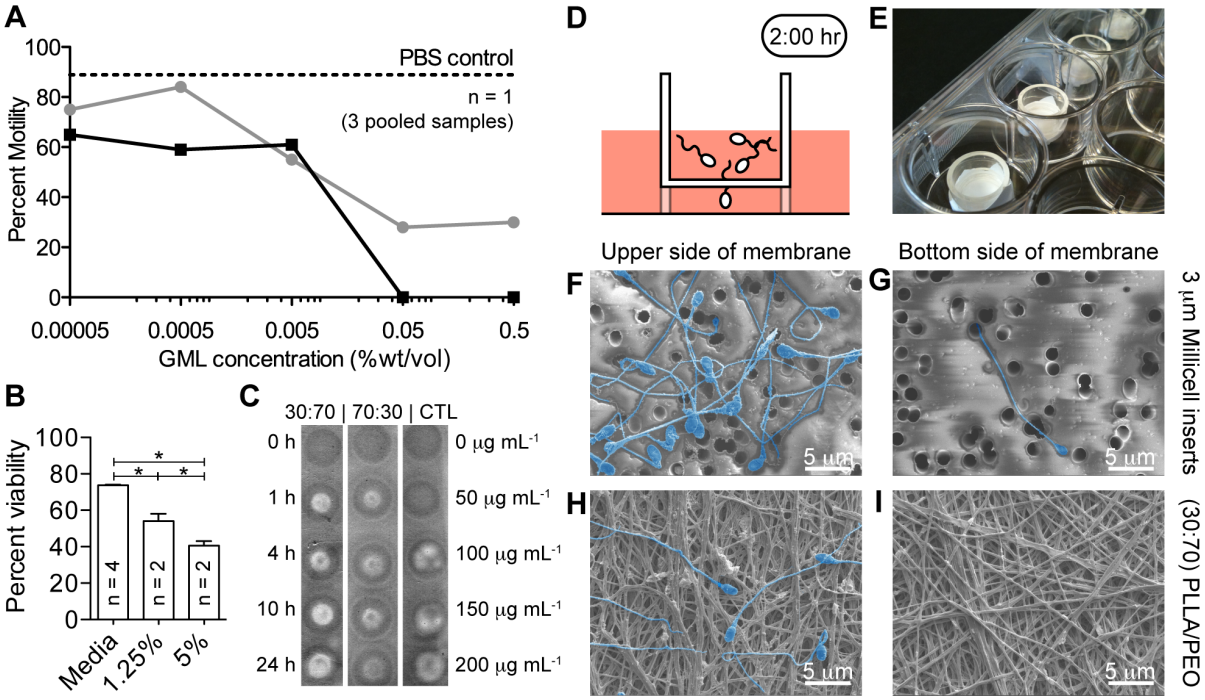

Figure 2.14—Fiber meshes are a physical and chemical barrier against sperm. (a) Motility of human swim-out sperm was completely inhibited within 5 min for 0.05 and 0.5% GML. Data show counts of motile and immotile sperm at 2 min (gray line) and 5 min (black line). Baseline sperm motility (~89%) was measured at the beginning and end of experiment using a PBS control (dotted line). (b) Sperm viability is reduced in whole semen incubated with GML compared with media control. (c) GML release from fiber meshes was qualitatively measured using TLC. (d, e) A transwell assay was used to test the physical barrier properties of the fiber meshes by replacing Millicell cell culture insert membranes (3 μm pore diameter) with a blank fiber mesh (n=3). (f, g) SEM micrographs of the upper (f) and lower (g) side of Millicell control membrane. (h, i) SEM micrographs of upper (h) and lower side (i) of fiber mesh show that no sperm penetrate through the fiber mesh.

We also fabricated fibers loaded with 1% or 10% (wt/wt) GML using both PLLA/PEO blends. GML fibers were reproducibly electrospun to achieve polymer recoveries of >70% and fiber diameters between 600–800 nm (Figure 2.6, Figure 2.7). Fibers loaded with 10% (wt/wt) GML released ~100-200 μg mL^{-1} into VFS within 1 h, suggesting that 100% GML released from fibers within 1 hour of incubation with VFS (Figure 2.14**-c**).

In addition to encapsulating agents that chemically inhibited sperm function, the fibers served to physically block sperm penetration. We used a transwell assay to measure the ability of sperm to penetrate electrospun meshes in the absence of drugs (Figure 2.14). The thicknesses of the tissue insert controls and electrospun meshes used as barriers were 30 μm and 150 μm, respectively. We found that motile sperm placed onto electrospun mesh were unable to swim through the fiber meshes despite the presence of numerous pores greater than 3 μm. In contrast, tissue culture insert controls with 3 μm diameter pores allowed sperm to penetrate into the bottom chamber. Approximately 58,000 sperm mL^{-1} (~1.7% of sperm) penetrated the commercial membranes in 2 h, whereas no sperm penetrated the fiber meshes (Table 2.2).

Table 2.2—Electrospun fibers effectively block sperm migration in a transwell assay. We tested the ability of electrospun fiber mats to block sperm migration in a transwell assay. 30:70 PLLA/PEO fibers without drug were used to replace existing membranes in transwell cups. Motile sperm collected by swimout into media were added to the upper chamber (inside of the cup) and allowed to attempt to enter the bottom chamber for 2 hours. Sperm were then counted in both chambers to assess if sperm could penetrate the meshes.

	30:70 PLLA/PEO fibers	Control membranes
Upper chamber	$10^{6.05 \pm 0.036}$ sperm mL^{-1}	$10^{6.52 \pm 0.25}$ sperm mL^{-1}
Bottom chamber	0 sperm mL^{-1}	$10^{4.76 \pm 0.405}$ sperm mL^{-1}

SEM image analysis confirmed these results, as we observed sperm on the underside of the control membranes but not the electrospun fiber meshes (Figure 2.14**-f thru i**). To assess the material strength of the electrospun meshes, we performed uniaxial tensile testing on samples of PCL containing 1% MVC that were spun at 5, 50, or 100 μL min^{-1} (n=2). We found that all materials had a Young's modulus between 25 to 120 MPa (Figure 2.15). In addition, materials were able to withstand at least 50% strain before failure. There was a statistically significant difference in Young's moduli between fibers spun at different flow rates, as determined by ANOVA (P

= 0.048). A Bonferroni corrected t test was used to compare 5 μL min^{-1} and 50 μL min^{-1} fibers. It was found that fibers spun at a flow rate of 50 μL min^{-1} were on average 68 MPa stiffer than those spun at a flow rate of 5 μL min^{-1} (95% C.I = 2.8 to 130 MPa stiffer).

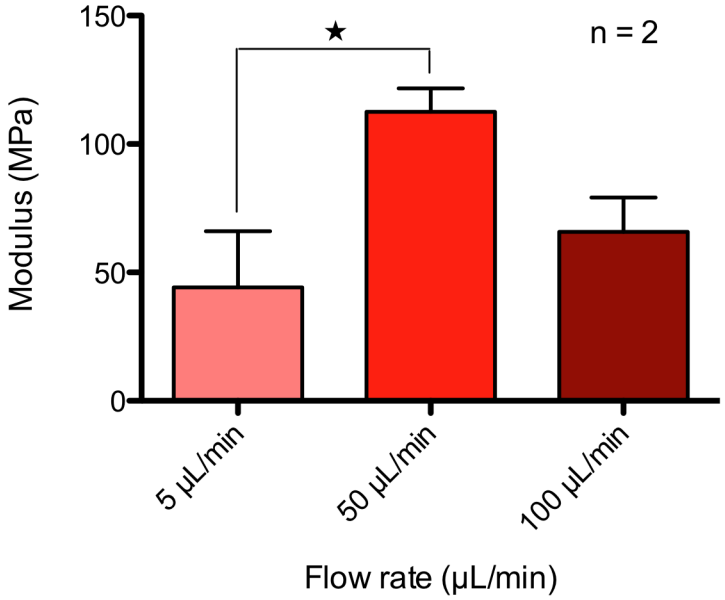

Figure 2.15—Flow rate influences modulus of PCL fibers incorporating 1% (w/w) MVC. Moduli of PCL fiber meshes made from electrospinning at varying flow rates (5, 50, and 100 μL/min) were measured. The modulus of PCL fibers electrospun at a flow rate of 50 μL/min is significantly different than the modulus of PCL fibers electrospun at 5 μL/min ($p<0.05$).

2.05 Discussion

We have developed an innovative dosage form for intravaginal drug delivery using drug-eluting fibers fabricated by electrospinning. We show that electrospun fibers deliver agents that inhibit both HIV and sperm *in vitro* in addition to physically preventing sperm penetration. We also report on a novel function of GML to act as a spermicide and potential non-hormonal chemical contraceptive. This finding adds to the characteristics that make GML an attractive candidate for use in topical microbicides for multipurpose prevention[149]. Polymer fibers may provide a single dosage form that is readily amenable to encapsulating an array of small molecule hydrophobic and hydrophilic compounds. The diversity and number of polymers that can be electrospun should enable a correspondingly large number of active agents to be encapsulated for delivery[133]. We hypothesize that drug-eluting fibers formulated with a single

agent can be assembled into a composite mesh to deliver drug combinations or temporal combinations of drug release (Figure 2.3). Combined with the ability to control device geometry (Figure 2.4), we expect that layered chemical function will enable delivery of specific drugs to defined regions within the lower female reproductive tract. The application of drug-eluting fibers for drug delivery to prevent HIV-1 and inhibit sperm function is unprecedented, and should have wide implications for the design of next generation multipurpose prevention technologies.

Topical delivery systems that combine potent and broadly active inhibitors have the greatest likelihood of protecting against the global diversity of STI and HIV variants that are transmitted sexually. The compounds that we incorporated into our fibers have different mechanisms of action against HIV and HSV-2. MVC prevents HIV entry by binding to CCR5[112] and is already in clinical trials for use as a microbicide (MTN-013/IPM 026). While AZT is not currently a leading candidate for use in topical microbicides[§], its physicochemical properties are similar to those of tenofovir, which has been used in recent and ongoing clinical trials of microbicide gels[36,40]. GML, which we report has activity against sperm function, has also been shown to inhibit HIV infection *in vitro* and SIV infection of macaques *in vivo* by inhibiting the production of MIP-3α and other pro-inflammatory cytokines[149]. Finally, we also incorporated ACV into fibers, since HSV-2 infection is of great concern in its own right and in relation to risk of acquiring HIV and other STIs[150]. Together, these four compounds provide a strong proof of principle that electrospun fibers may be a useful platform for vaginal drug delivery and topical prevention of STIs.

For this work, we chose to electrospin fibers from mixtures of PEO and PLLA. We expected PEO to rapidly hydrate and dissolve in vaginal fluid and that PLLA would degrade slowly via hydrolysis at low pH into lactic acid[145], a natural component of vaginal fluid important for maintaining vaginal homeostasis[151]. Unfortunately, PLLA takes years to degrade in this way, so this system is not ideally suited for a “dissolving” delivery system (see 0). We found that the magnitude of MVC release from PLLA/PEO blends was highly dependent upon the amount of PEO present. Over six days, 78% of encapsulated MVC was released from 70:30 PLLA/PEO fibers, compared with 93% of encapsulated MVC from 30:70 PLLA/PEO fibers. In contrast, approximately 90% of encapsulated AZT was released from both 70:30 and 30:70 PLLA/PEO fibers (Figure 2.11). This suggested that MVC could disperse throughout both PEO and PLLA, while the majority of AZT partitioned into PEO. Furthermore, the release and degradation behavior implied that there was significant phase separation between PLLA and PEO polymer regions within the fibers. We discuss this in depth below. Small diameter hydrophilic fibers may be an improvement on current film devices that provide coitally dependent protection against

[§] In fact, AZT is seen as a rather terrible antiretroviral drug due to its harsh side effects.

STIs and pregnancy, and this is the focus of the work presented in Chapter 3. The current data show that substantial amounts of hydrophilic and hydrophobic drugs can be delivered very quickly from nanometer diameter fibers. Meshes made from hydrophilic polymers have previously been found to dissolve and release encapsulated agents more rapidly than films cast from the same materials[152,153]. Yu et al. showed that 100% of encapsulated ferulic acid dispersed with sodium dodecyl sulfate and sucralose was released within 2 minutes from 250 nm polyvinylpyrrolidone fibers, compared to 20 minutes from equivalent masses of thin films produced by casting. Furthermore, *in vitro* testing of ferulic acid permeation across the sublingual mucosa demonstrated a doubling of permeation rate for the fiber dosage form over the film dosage form[152]. Due to the high surface area-to-volume ratio of electrospun fiber meshes, water may ingress more rapidly into hydrophilic electrospun materials than into cast films. Rapid hydration and a shorter diffusion distance offered by a nanofiber can create a very steep concentration gradient of encapsulated molecules, thus enhancing the rate of mass transport into mucosal tissues[153]. While we did not compare drug release from PLLA/PEO films to fibers, future studies should investigate how nanofibers can enhance the dissolution and mucosal delivery of ARVs in *ex vivo* and *in vivo* models of vaginal drug delivery (see 0).

The ability to hydrate rapidly upon insertion can aid in fast drug release and effective spreading of dissolved materials along the vagina. Material spreading can result in more complete coverage of the mucosal tissue that is vulnerable to infection by HIV and other pathogens[154]. We showed that insertion of indocyanine green loaded 30:70 PLLA/PEO fibers into the vagina of a mouse resulted in high levels of fluorescence throughout the vaginal tract (Figure 2.11). This suggests that fibers can sufficiently hydrate in small volumes of vaginal fluid and release encapsulated agents within 30 minutes *in vivo*. Hydrophilic polymer-based fiber meshes, including those made from PEO, may therefore provide a useful dosage form for pericoital prevention methods.

In addition to releasing ARVs, it is also critical that fibers are safe and effective in biological systems. We evaluated the antiviral activity of fibers loaded with either AZT or MVC using an *in vitro* TZM-bL assay. This model has previously been used to evaluate drug candidates for topical microbicides[131,155]. Both the drug eluates from *in vitro* fiber release studies and drug-loaded fibers themselves were found to potently inhibit HIV compared to blank fibers. The IC50 values of unformulated ARV versus eluted ARV were of a same order of magnitude (Figure 2.13). Our results suggest that fibers are able to release sufficient levels of drug in cDMEM to prevent HIV infection in TZM-bL cells over 48 hours, which is consistent with the release profiles obtained from *in vitro* release studies in VFS. Furthermore, these studies demonstrate that both

drugs are in a bioavailable form after the electrospinning formulation process. The toxicity of fibers was measured with a macaque cervical explant model using histological examination and an MTT viability assay (Figure 2.13). A similar model has previously been used to evaluate the safety of microbicide candidates using human cervical or colorectal explant tissues[45,140,141]. Tissue exposed to either 30:70 or 70:30 PLLA/PEO fibers was found to have similar epithelial layer integrity and cell viability compared with untreated control tissue, indicating the biological suitability of the polymer blends for additional studies in vaginal drug delivery.

Long-term shelf stability is another quality imperative to the design of effective dosage forms for multipurpose prevention. Ham *et al*. performed an extensive characterization of the long-term stability of pyrimidinedione vaginal film, measuring drug release, toxicity, and activity at specified time points over 12 months at both standard and elevated temperature and humidity[63]. We detected >95% of the initially-loaded AZT and MVC in fiber meshes stored at room temperature for at least five months and observed that fiber meshes retained similar appearance and texture over this period. While this data suggest that ARVs remain stable in PLLA/PEO fiber meshes under standard storage conditions, more comprehensive studies of drug stability are needed for the polymer-drug combinations chosen for future studies. We expect that the solid dosage form of drug-loaded fibers will be advantageous for long-term stability compared with semi-solid dosage forms like vaginal gels.

There is a great need to develop multipurpose prevention strategies that provide contraception in addition to protecting against STIs including HIV. Topically applied non-hormonal chemical contraceptives for pericoital use would address an important gap in contraception needs for women. While N-9 is a highly effective spermicide*,* the same detergent properties responsible for immobilizing sperm are also known to promote vaginal inflammation and increase the risk of STI infection[21,156]. We first evaluated non-hormonal contraceptives described previously in the literature to be potent inhibitors of sperm function. We tested the function of FeGluc, Asc, and their mixture because these agents had been reported previously to potently inhibit sperm motility in solution and after elution from a vaginal ring[146,157]. At the highest concentration tested, FeGluc alone inhibited motility of ~37% of sperm within 2 minutes but did not result in complete spermiostasis (Table 2.1). Combining FeGluc with L-ascorbic acid (FeAsc) resulted in rapid spermiostasis in <30s. However, we observed equally rapid spermiostasis upon treatment with L-ascorbic acid alone. We conclude that the reported spermicidal effect of FeGluc when combined with L-ascorbic acid was likely due to the decrease in pH upon dissolution of L-ascorbic acid (pH ~2), since pure L-ascorbic acid was just as effective as its mixture with iron. Indeed, L-ascorbic acid at a pH of 5.5 had no effect on sperm

motility (Table 2.1). MBCD was also evaluated as a non-hormonal chemical contraceptive but showed no effect on sperm function at the concentrations tested. In addition, due to the high amounts of free cholesterol present in whole semen, we estimate that the high concentration of MBCD required to induce sperm capacitation would exceed the concentration that causes inflammation when applied to the buccal epithelium[147,158].

We were motivated to evaluate GML's activity on sperm function based on its amphiphilic properties and its reported interaction with lipid bilayers[148]. GML, a glycerol ester of lauric acid that is used commonly as an emulsifier in foods and cosmetics, is regarded by the FDA as safe for topical use at doses up to 100 mg mL^{-1} [159]. Additionally, GML is inexpensive, possesses documented anti-inflammatory properties, and is antimicrobial for a number of vaginal pathogens[159,160]. We show for the first time that GML potently reduces sperm motility in a dose-dependent manner (EC_{50} ~ 0.005% wt/vol, or 50 μg mL^{-1}, at 2 min) and significantly lowers sperm viability at concentrations equivalent to those used in recent microbicide studies with macaques (5% wt/vol, or 50 mg mL^{-1}) (Figure 2.14). Although its spermicidal mechanisms are as yet unknown, interference with signal transduction by incorporation into plasma membranes has been suggested as a mechanism for its antibacterial and anti-inflammatory properties[159,161,162] and may also be involved in sperm inhibition. Future studies should perform an in-depth characterization of how GML causes spermiostasis. Our findings add to the list of properties that make GML an attractive candidate for use in topical microbicides for multipurpose prevention, including anti-inflammatory mediated prevention of SIV infection in macaques[149] and the capacity to prevent bacterial infections[163]. The low aqueous solubility of GML (50–100 μg mL^{-1} at pH 7) precluded our ability to evaluate the activity of higher concentrations of GML on human sperm in whole semen, but provided a strong rationale to formulate GML in polymer fibers. A dosage form that enhances the bioavailability of GML could potentially enhance the spermicidal potency of the compound. Recent work with lipid-loaded electrospun fibers has shown that such systems are capable of rapidly releasing lipid molecules as micelles in water [164]. This might provide an effective way of dispersing large amounts of GML into the small fluid volumes present in the vagina during sex.

The potential of GML to act as a surfactant has raised controversy within the microbicide field over its safety as a topical product. Schlievert et al. provided extensive characterization of the safety of 5% GML in KY warming gel for daily use in macaques for up to 12 weeks (n=9)[159]. Using an MTT viability assay and histological examination of polarized cervical explants from macaques, we found that 30:70 PLLA/PEO fibers loaded with 10% (wt/wt) GML were nontoxic *ex vivo* and had similar epithelial layer integrity to untreated controls (Figure 2.13). Nonoxynol-9

has been found to increase the frequency of genital lesions, which, it is thought, subsequently increase the risk of HIV infection[21]. In contrast, GML actually stabilizes eukaryotic cell membranes and reduces production of IL-8, an inflammatory cytokine. Furthermore, GML does not negatively impact the growth of lactobacilli or the production of lactic acid *in vivo*[159]. In contrast, nonoxynol-9 irritates and removes vaginal and cervical epithelial cells (Figure 2.13) and disrupts the normal vaginal flora[165,166]. While Moench et al. demonstrated that GML increased susceptibility to HSV-2 infection in mice, they acknowledged that the vaginal epithelium of medroxyprogesterone acetate treated mice is quite different from that of humans and nonhuman primates[167]. Depoprovera-treated murine vaginal lining is similar to endocervical columnar epithelium, which is much thinner and less robust than the non-keratinized stratified squamous epithelium of the ectocervix or vaginal wall in humans and non-human primates. Since HSV-2 infection may occur through the vulva, the vagina, or the cervix, the mouse model developed by Moench et al. may be too sensitive to draw conclusions about how GML may affect HSV-2 acquisition in humans or nonhuman primates. Despite the surfactant nature of GML, the compound has been shown to have several protective qualities, including the ability to neutralize the toxic effects of pathogenic gram-positive bacteria[168]. Recently, Li et al. provided preliminary evidence that GML is not only safe for chronic use in rhesus macaques, but actually prevents SIV mucosal transmission with repeated high dose challenge[149].

In addition to the chemical inhibition provided by GML, we also demonstrated that blank fibers block sperm migration in a transwell assay (Figure 2.14**,** Table 2.2). Since the electrospun fibers used as a physical barrier were five times as thick as the tissue culture inserts, the tissue culture inserts cannot serve as a control to discern why the fiber meshes formed a functional barrier against sperm transport. Nevertheless, they do still provide a control to demonstrate that the sperm were motile and capable of traversing a membrane with 3 μm diameter pores. Relying upon a porous mesh to block sperm penetration differs from current barrier approaches, which rely on nonporous materials to block sperm entry into the cervical os[127,169]. Our results showed that a porous mesh fabricated by electrospinning could efficiently block sperm entry. This suggests that, if fabricated in the appropriate geometry and given the appropriate mechanical strength, electrospun fibers may serve as an effective barrier contraceptive. While the materials we presented are not yet suitable to be turned into a final barrier device, analysis of their mechanical properties does shed some light on potential product configurations. In particular, the Young's moduli of electrospun materials made from 70:30 PLLA/PEO fibers with 1% (wt/wt) MVC were around 50-100 MPa, and electrospun meshes withstood at least 50% extensional strain before failure (Figure 2.15). For comparison, latex rubber condoms have a

Young's modulus of approximately 2 MPa and can withstand inflation to volumes greater than 20 L[170]. Dapivirine films have a tensile modulus of 5.4 to 7.8 MPa[51]. Based on the mechanical properties of these electrospun materials, it is unlikely that they would be effective as a condom-like device, but they may be suitable as devices similar to vaginal sponges or diaphragms. Alternatively, fibers could be spun from elastic materials for incorporation into a flexible condom.

2.06 In depth analysis of release mechanisms from fibers and implications for the design of future sustained release fibers

2.06.1 Introduction

The work just presented demonstrated that electrospun fibers made from blends of PEO and PLLA burst released encapsulated compounds, including maraviroc, azidothymidine, acyclovir, and glycerol monolaurate[79]. Interestingly, the degree of initial burst release and the presence of a secondary release phase were dependent upon the specific combinations of drugs with polymer blend ratios (Figure 2.11). While modulating the ratio of hydrophilic PEO and hydrophobic PLLA polymers in the fibers changed the overall amount of drug released in the case of both maraviroc and azidothymidine, only maraviroc-loaded fibers showed a secondary release phase. Interestingly, beyond the initial burst release associated with the erosion of PEO from PLLA/PEO matrices, PEO content had little effect on the rate or the degree of release of maraviroc from the fibers. These observations appeared to be consistent with release of compounds from phase-separated blocks of rapidly dissolving PEO, and water impermeable PLLA. The extent to which either drug was released after two weeks appeared to depend upon the partition coefficient of the drug between the PEO and the PLLA phases. In this in depth discussion, we probe the mechanisms governing release of azidothymidine and maraviroc from PLLA/PEO fibers by critically evaluating the drug release and fiber degradation data presented above in 2.04. We also provide further analysis of pure PLLA, pure PEO, and PLLA/PEO blend fibers containing maraviroc to confirm our hypothesis of polymer phase separation and the role that drug sequestration in PLLA plays in determining the ultimate extent of drug release.

Several factors may affect drug release rates from polymer materials. Here, we present multiple strategies for achieving sustained release for at least 72 hours without an initial burst release of drug based on our in-depth analysis of maraviroc release from PLLA/PEO fibers and comment on their success or failure in terms of proposed underlying release mechanisms. These experiments allow us to develop a qualitative model to describe the release of maraviroc

from electrospun fibers. The sustained release strategies we evaluate include increasing the fibers' diameters (increasing the diffusion distance through the matrix to the media), reducing the hydrophilic polymer content (decreasing hydrophilicity, reducing erosion, and shrinking regions of phase separated PEO), encapsulating maraviroc in poly(ε-caprolactone) (PCL) (decreasing crystallinity and glass transition temperature), and doping PLLA with lower molecular weight PDLLA (decreasing crystallinity and allowing more access of water into the hydrophobic matrix). Ultimately, we succeed in providing sustained release of maraviroc from fibers over 72 hours without an initial burst release of drug. The low degree of release, however, warrants future efforts to reformulate maraviroc into sustained release fibers, which I address in later chapters of this thesis.

2.06.2 Re-analysis of drug release from 70:30 and 30:70 PLLA/PEO fibers

While rapid release of antivirals from electrospun fibers is desirable for pericoital anti-HIV microbicides[78,79], sustained release of agents like maraviroc would theoretically extend the duration of protection against HIV infection and reduce the dependence of product efficacy upon user adherence at each sex act[57,61,70]. We hypothesized that polymer fibers with a partially hydrophobic composition would enable encapsulation and sustained release of hydrophobic agents. Above, we showed that electrospun PEO/PLLA fibers could successfully incorporate and sustain the release of maraviroc (which is hydrophobic in its non-ionized form, at pH > 7.8, and slightly soluble at pH 4.2 in vaginal fluid simulant) for 72 hours. However, neither 70% nor 30% PLLA content in fibers prevented a large burst release of maraviroc prior to achieving a sustained release profile (Figure 2.11). In addition, the release of maraviroc from electrospun fibers was incomplete. Here, we seek to understand why these phenomena occurred.

Many publications on drug release from electrospun fibers explain their results by citing Fickian diffusion of a homogeneously distributed drug out of a uniformly swollen polymer matrix. Such an explanation is often too simplistic to accurately capture the prolonged release behavior of drugs from polymer fibers[171,172]. Drugs are often enriched at the surface of electrospun fibers, and the rates of water influx, polymer swelling, drug dissolution, and drug interactions with insoluble polymer matrix all play a role in determining the release profile of a compound. In particular, the frequently observed phenomena of an initial burst release of drug and the incomplete release of drugs from fibers are wholly inconsistent with a model of fibers as a system described by Fickian diffusion of drug from a homogeneous polymer matrix. We observed both rapid burst release and subsequent incomplete release of azidothymidine and

maraviroc from PLLA/PEO blend fibers. Such release behavior is consistent with multiple models of drug release. In order to evaluate the validity of potential models for describing release from PLLA/PEO fibers, we begin by thoroughly analyzing the evidence.

Azidothymidine rapidly released from fibers in less than one hour. Beyond the initial burst release of azidothymidine (94% from 30:70 PLLA/PEO, 92% from 70:30 PLLA/PEO), no more azidothymidine was released. In addition, more maraviroc was released from 30:70 PLLA/PEO fibers than from 70:30 PLLA/PEO fibers. These observations are consistent with at least three simple models.

1) AZT exists mostly on the fiber surface, and therefore rapidly dissolves when fibers are put in solution. A small amount of AZT remains sequestered inside the blended PLLA/PEO polymer matrix.
2) AZT is distributed throughout the polymer matrix, which is phase separated into large (several nanometers in size) domains of PLLA and PEO. AZT has partitioned between the phases and is largely associated with PEO. All of the PEO hydrates, swells, and dissolves, as does the PEO-encapsulated AZT. The AZT in the PLLA is inaccessible to water and remains sequestered.
3) AZT is insoluble in PLLA and is therefore completely partitioned into phase-separated PEO. Once in solution, much of the PEO hydrates, swells, and dissolves, releasing encapsulated AZT. Small islands of PEO, along with associated AZT, remain sequestered within contiguous regions of PLLA.

The AZT release profiles support model 3 more strongly than models 1 or 2. Since AZT is soluble and hydrophilic, its presence on the surface of fibers should result in a rapid release of the drug. The different extent of surface presence on the fibers could be due to changes in the drug interaction with the polymers. The incomplete release could be explained by either a lack of water penetration into homogeneous PLLA/PEO blends due to the hydrophobic nature of PLLA or a lack of water penetration into phase separated regions of PLLA or PEO (either of which could contain drug). Thus, model 1 is consistent with release data. Nevertheless, it is rare that a drug loading as low as 1%, particularly into a polymer matrix with at least some solubility with the drug (PEO is also hydrophilic) would result in all of the drug moving to the fiber surface during spinning (see Chapter 3). Rather, we can expect modest but incomplete enrichment of drugs on the fiber surface. Model 2 is less convincing than model 1. If AZT partitions between PLLA and PEO with a partition coefficient K ($K = C_{PLLA}/C_{PEO}$), and it is assumed that the partitioning is at equilibrium due to the long time allowed for preferential association with PEO versus PLLA within the polymer solution just prior to electrospinning and the short time allowed

for phase separation as the solvent evaporates and fibers are formed, then the percent of AZT released should be equal to the amount of drug in PEO divided by the total amount of drug present in both polymers:

$$\%\ \text{release} = \frac{C_{\text{AZT in PEO}} \times\ \text{wt\% PEO}}{C_{\text{AZT in PEO}} \times\ \text{wt\% PEO} + C_{\text{AZT in PLLA}} \times\ \text{wt\% PLLA}} = \frac{\text{wt\% PEO}}{\text{wt\% PEO} + K \times \text{wt\% PLLA}}$$

Thus, if the proportion of PEO in the fibers is 100%, then 100% of AZT is burst released. Alternatively, if fibers are entirely PLLA, then 0% of AZT is released. One can solve for the partition coefficient K given the measured percent release, and the known polymer composition of fibers. Let's now apply this to the release data shown in Figure 2.11. For 70:30 PLLA/PEO fibers, K = 0.037. For 30:70 PLLA/PEO fibers, K = 0.15. Since these two values are not the same (a 5-fold difference is beyond the level of experimental error using HPLC, which is precise to within 5%), it is unlikely that the release of AZT from fibers can be described simply by partitioning of AZT between fully dissolvable PEO and water impermeable PLLA (although differences in the solvent composition used to spin the two could lead to variable partitioning). Thus, model 2 seems insufficient to describe the observed behavior.

Model 3, on the other hand, is more consistent with observed drug release. As in model 2, AZT is assumed to partition into PEO. However, here the partition is total—no AZT resides within PLLA. The amount of AZT released is determined solely by the fraction of phase-separated PEO that is accessible to water. In this case, drug release would be consistent with 94% or 92% of the PEO in 70% or 30% PEO fibers, respectively, having access to water and dissolving—resulting in a 65.8% or 27.6% mass loss. In order to validate model 3, we can refer to the mass loss of PLLA/PEO blend fibers over 2 weeks in vaginal fluid simulant. These data support the hypothesis that the release of AZT from PLLA/PEO fibers is due to the extent of water access to PEO, which contains 100% of the drug content due to the drug's insolubility in PLLA. 70:30 PLLA/PEO fibers spun from 15 wt% solutions lost 63.9% of their mass and 30:70 PLLA/PEO fibers lost 31.2% of their mass. These values are very close to the 65.8% and 27.6% mass loss predicted by model 3, which assumes no AZT on the fiber surface or in PLLA, and assumes equal distribution of drug within the fiber center and in the outer regions of the fiber. In conclusion, the likely mechanism governing the release of AZT from PLLA/PEO fibers is the complete partitioning of AZT into PEO, and the incomplete dissolution of phase separated PEO

domains within the fibers due to sequestration of PEO islands within domains of water-impermeable PLLA. There is likely some surface-AZT component involved in release as well, but it is negligible at the low 1% loading. Could such a mechanism also describe the biphasic release of maraviroc from fibers?

As just discussed, the release behavior of AZT from PLLA/PEO fibers suggested that release of water-soluble molecules was affected by phase separation of the polymers, preferential partitioning of the drugs into PEO, the rapid erosion of the PEO from the fibers, and entrapment of residual PEO and AZT within water-excluding PLLA domains. Maraviroc fibers also showed an initial burst release from fibers. However, the extent of initial release was very different depending upon the PEO content of the fibers (5 times larger than the difference in burst amount from AZT fibers). In contrast with azidothymidine-loaded fibers, maraviroc-loaded fibers also displayed a biphasic release profile. Following the 1st hour of burst release (70-80% of the encapsulated maraviroc), the PLLA/PEO fibers released another 10% of the encapsulated maraviroc before reaching a plateau at 72 h. The model used to describe release of AZT from fibers was insufficient to describe maraviroc release. We evaluated the following, more nuanced models for maraviroc release, which assume that maraviroc, more compatible with PLLA than AZT, was able to partition into PLLA:

1) Maraviroc is partially soluble in PLLA, and the drug is able to permeate amorphous regions of PLLA and release by diffusion to provide a secondary release phase. A plateau is reached because some of the drug remains sequestered with amorphous PLLA or hydrophilic PEO in regions surrounded by water-impermeable, crystalline PLLA.
2) Maraviroc is partially soluble in PLLA, but the drug is not able to release by diffusion from PLLA. A rapid burst release of maraviroc from PEO results from partitioning of the drug into solvent-accessible PEO regions. The secondary release phase is produced by reduced hydrophilicity of PEO-maraviroc regions due to the drug content or the minute size of PEO domains within hard-to-access or tortuous regions of the fibers, thus slowing the erosion of PEO from the phase separated fibers. A plateau is reached because some of the drug remains sequestered with amorphous PLLA or hydrophilic PEO in regions surrounded by water-impermeable, crystalline PLLA.
3) Maraviroc is partially soluble in PLLA, but the drug is not able to release by diffusion from PLLA. A rapid burst release of maraviroc from PEO results from partitioning of the drug into solvent-accessible PEO regions. The secondary release phase is produced by desorption of maraviroc from the surface of PLLA pores left behind after

the erosion of PEO. Thus, the rate of maraviroc release is due to the interactions of maraviroc with the PLLA surface. A plateau is reached because some of the drug remains sequestered with amorphous PLLA or hydrophilic PEO in regions surrounded by water-impermeable, crystalline PLLA.

We began by testing these models' assumption of phase separation directly with differential scanning calorimetry (DSC). DSC detects minute differences in heat flow into and out of an experimental sample compared to a reference standard as the temperature of the environment increases steadily. DSC analysis of 30:70 and 70:30 fibers containing maraviroc showed that PEO and PLLA maintained their individual melting peaks, and were therefore immiscible in the electrospun fibers (Figure 2.16). This observation is interesting, because the original motivation for using 30:70 and 70:30 blends of PEO and PLLA was to achieve homogeneous polymer blends. Clearly, this was not accomplished. This confirmed the validity of models for drug release that were based on phase-separated domains of PEO and PLLA within the fibers (AZT models 2-3, all maraviroc models). Based on the size of the peaks relative to pure PLLA and pure PEO, it appears as though the PEO and PLLA were immiscible and entirely phase separated. Maraviroc could not be detected in fibers by DSC measurements, likely due to low loading as opposed to amorphous dispersion (see Chapter 3). In combination with the fiber erosion data in Figure 2.11, the data in Figure 2.16 provide good evidence to support the hypothesis that incomplete release of maraviroc (and AZT) occurs due to sequestration of PEO and drug within water-impermeable regions of PLLA.

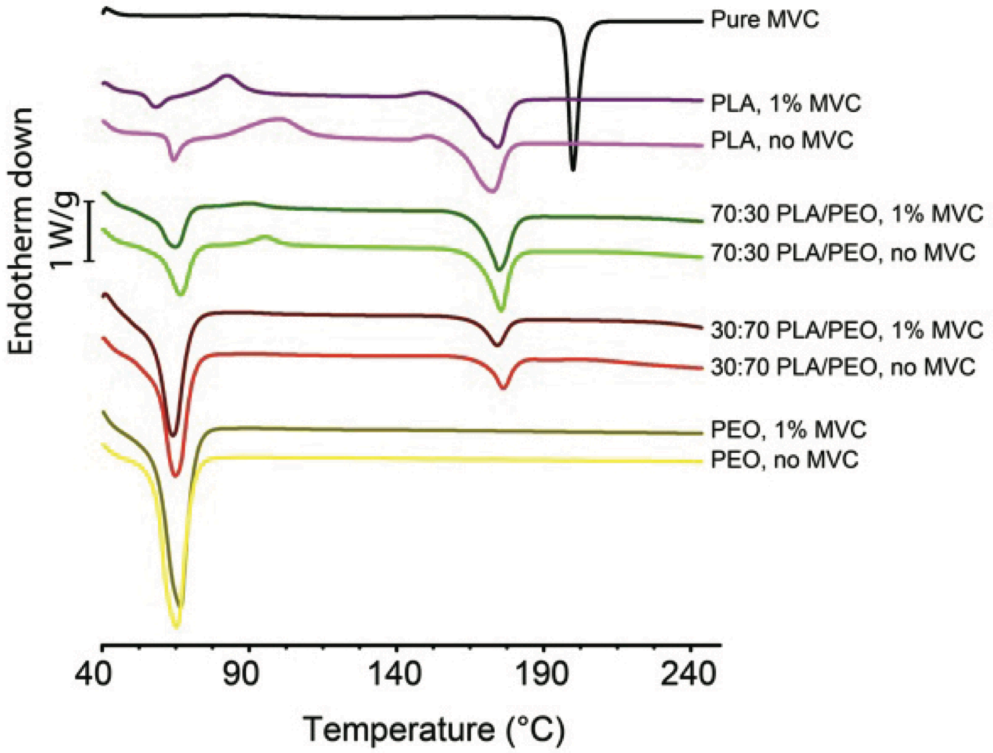

Figure 2.16—Thermal analysis of PEO, PLLA, and PLLA/PEO blend fibers with and without maraviroc. DSC traces reveal phase separation between PLLA and PEO. PLLA displays a T_g at 50 °C, a recrystallization exotherm at around 90 °C, and T_m at 170°C. PEO displays a T_m at 65 °C. Thanks to Jennifer Wilson for her assistance in collecting data for this figure.

In order to test whether or not sustained release of maraviroc was occurring by diffusion of maraviroc out of PLLA and provide further evidence for the sequestration model of incomplete drug release, we electrospun pure PLLA fibers loaded with 1% maraviroc. Pure PLLA fibers containing 1% maraviroc indeed did not release any maraviroc over multiple days (Figure 2.11). In order to eliminate the confounding variable of whether or not fibers wet out quickly (shown to be a factor in release from hydrophobic fibers in work by Yohe et al.[173]), a small amount of surfactant (SDS) was added to the release media and the experiment was repeated, still yielding zero percent maraviroc release (data not shown). Thus, model 1 for maraviroc release was inconsistent with our experimental observations. It is unlikely that maraviroc was able to readily diffuse through PLLA. This might have been expected, since the release temperature of 37°C is well below the T_g of PLLA (50°C), meaning that the PLLA polymer exists in a glassy state with little polymer chain flexibility.

Models 2 and 3 were tested by monitoring drug release from pure PEO fibers and by calculating the apparent partition coefficient for maraviroc in PLLA/PEO mixtures using the equation given above for AZT. Pure PEO fibers containing 1% maraviroc hydrated rapidly, and 100% of the maraviroc content was released within minutes (data not shown, but similar data is found in Chapter 3). This suggested that one of the proposed mechanisms for sustained maraviroc release in model 2, that maraviroc within PEO reduces the matrix hydrophilicity to sustain release for 72 hours, was incorrect. PEO with 1% maraviroc hydrated nearly as rapidly as pure PEO fibers. It was still possible, however, that model 2 could describe sustained release from fibers The apparent partition coefficient of maraviroc into PLLA versus maraviroc, calculated based on the initial burst release, was K = 0.18 for 70:30 PLLA/PEO fibers and K = 0.58 for 30:70 PLLA/PEO fibers. These values are not entirely dissimilar (2.5-fold difference), supporting the idea that maraviroc, unlike the more hydrophilic AZT, is capable of partitioning into both PLLA and PEO. This is not surprising, since the solubility of maraviroc in chloroform, a good solvent for PLLA, is quite high. The fact that the calculated K values are different for each of the fiber blends suggests that partitioning alone is not entirely responsible for the observed release profile. Accounting for the possibility that some regions of PEO are not accessible to solvent, we can rewrite the expression for K as:

$$K = \frac{\text{wt\% PEO} \times (\alpha - \text{\% release})}{\text{\% release} \times \text{wt\% PLLA}}$$

Where α is the fraction of PEO that is accessible to water. This α value can be calculated by comparing the actual mass loss from materials to their theoretical material composition. Recalculating K with this approach based on the initial burst of maraviroc results in K = 0.32 for 30:70 PLLA/PEO fibers and K = 0.21 for 70:30 PLLA/PEO fibers. Calculating the same K values based on the total maraviroc released at 72 hours yields K = 0.026 and K = 0.12 for those fibers, respectively. Thus, the partitioning of maraviroc into rapidly dissolving, water accessible PEO can reasonably explain the extent of initial burst release, but is inadequate to describe the total extent of maraviroc release (as proposed in model 2), unless a change from 75% to 50% chloroform in electrospinning solvent has an order-of-magnitude effect on maraviroc partitioning into PEO (which it might; the amount of mass loss from 70:30 PLLA/PEO materials changes significantly depending upon the solvent mixture and concentration of polymer used to spin, Figure 2.10). Thus, model 3 seems more apt at describing the mechanism of drug release from PLLA/PEO fibers.

In conclusion, the release of maraviroc from PLLA/PEO blend fibers consists of three regions—an initial burst release, a secondary sustained release, and a plateau region with no further drug release (Figure 2.11). The initial burst release is likely a result of preferential partitioning (2 to 3 times) of maraviroc into PEO combined with the fast erosion of water accessible and phase-separated PEO domains from the fibers. The secondary sustained release of maraviroc is likely due to desorption of the maraviroc from the surface of PLLA nanopores, created when PEO was dissolved out of the electrospun fibers. The secondary release phase only is shown in Figure 2.17.

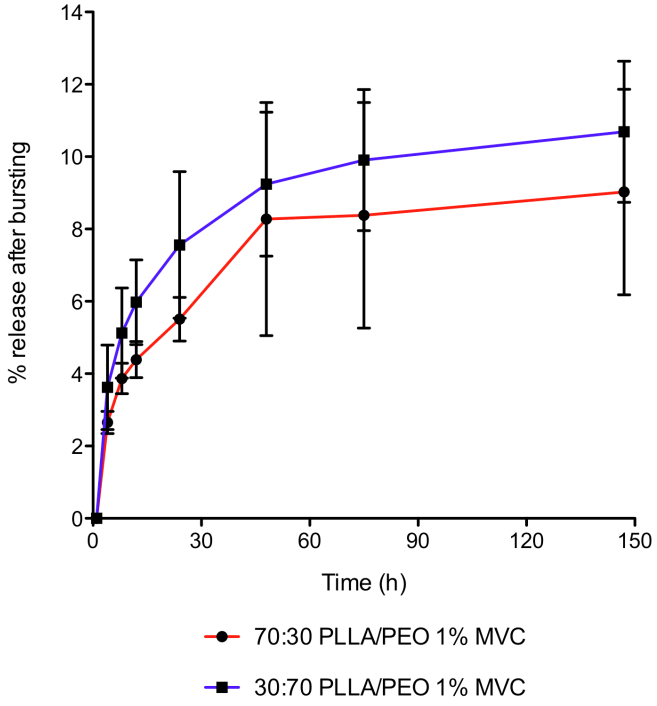

Figure 2.17—The release rate is independent of PEO content, but the extent of release is dependent upon PEO content. These results are consistent with constant desorption energy of maraviroc from PLLA surfaces and a variable porosity of materials based on the amount of PEO interspersed within the PLLA. Data shown has been transformed by subtracting release after 1 hour, shown as mean with standard deviation of the transformed data.

As described by Srikar et al., desorption limited release of drugs from electrospun materials is a function of the thermodynamics of drug-polymer interactions, the amount of drug on the surface of pores within the fiber, and the porosity of the fiber[172]. The rate of desorption-limited release of drugs from electrospun fibers is dependent upon the change in free energy of the system following solvation of polymer surface bound drug. Srikar et al. described this as the

desorption enthalpy, but it is likely that both changes in enthalpy and entropy contribute to the rate of drug desorption from the surface of PLLA nanopores. Interestingly, this model of drug release from electrospun fibers suggests that the drug-polymer combination is responsible for the rate of drug release, and can be controlled through the modification of insoluble polymer surfaces through blending compatible insoluble polymers (Srikar et al. blended PMMA and PCL to tune drug release rate[172]). Since, in the model proposed by Srikar et al., drugs cannot be released from within water-impermeable polymers (solid state diffusion would be too slow), the overall extent of drug release is determined by the porosity of the material, which is a function of the solvent volatility, polymer molecular weight, and polymer concentration in the electrospinning solution[172].

While Srikar's model was only formulated for single component fibers, the effect of porosity on the extent of release may be extended to two-component phase separated polymer fibers, since degradation studies suggested that changes in solvent and polymer concentration could alter the pore network of PEO domains within PLLA. Importantly, we have shown that the extent and quality of phase separation can result in large burst release of polymer. While, the rate of drug release from desorption-limited release systems can be controlled by increasing porosity or by increasing drug concentration on the pore surfaces, the time constant with which that release occurs cannot be changed unless the polymer material is altered. Combined with the incomplete release of drugs from such systems, this makes PLLA/PEO blends for sustained maraviroc release an inflexible system for engineering different release rates and an inefficient use of drug.

2.06.3 Strategies for sustaining maraviroc release without an initial burst

We tested multiple strategies to obtain sustained release of MVC from fibers by increasing fiber diameter, reducing hydrophilic polymer content, and modulating PLA crystallinity. First, we tested the hypothesis that increasing fiber diameter would slow release of MVC from 70:30 PLLA/PEO fibers. If such an approach were successful at slowing the time course of release from 70:30 fibers, it would imply that the release of maraviroc from PLLA/PEO fibers was describable by a Fickian diffusion process. We increased fiber diameters by raising the polymer concentration in 70:30 PLLA/PEO solutions (Figure 2.18, Figure 2.19). Despite three- and six-fold increases in fiber diameter, all 70:30 PLLA/PEO fibers burst released MVC within one hour in VFS (Figure 2.11). Comparison of mean MVC release from variably sized 70:30 PLLA/PEO fibers with ANOVA showed that the fibers released significantly different amounts of MVC based

on fiber size (P = 0.0261). The data suggested a trend for larger fiber diameters to release less MVC into VFS over six days. For example, 3.4 μm diameter fibers released 9.6% less MVC (95% CI = 1.17% to 18.1%, n = 3) than 560 nm diameter fibers. While Cui et al. showed that increasing PDLLA fiber diameter from 212 to 551 nm led to slower release of the highly water-soluble compound acetaminophen[174], we observed MVC release from 70:30 PLLA/PEO fiber meshes was not altered by increasing fiber diameter six fold from 560 nm to 3.4 μm. If the release of MVC from 70:30 PLLA/PEO fibers were diffusion controlled, an increase in diameter by a factor of six should have decreased release rates by a factor of approximately 36. These results are consistent with a rapid burst release from phase separated PEO followed by desorption-limited release from porous PLLA. Increased polymer concentration appears to decrease the amount of PEO that is accessible to water, thus reducing the burst release of maraviroc. The rate constant for release from PLLA pores appears identical for all fibers, as expected, and there is a hint that increasing polymer concentration (and thus diameter) reduces porosity and thus the magnitude of the secondary release phase. The discrepancy between Cui et al.'s results with PDLLA fibers and our results with PLLA fibers are likely due to differences in polymer crystallinity and chain mobility, as discussed later.

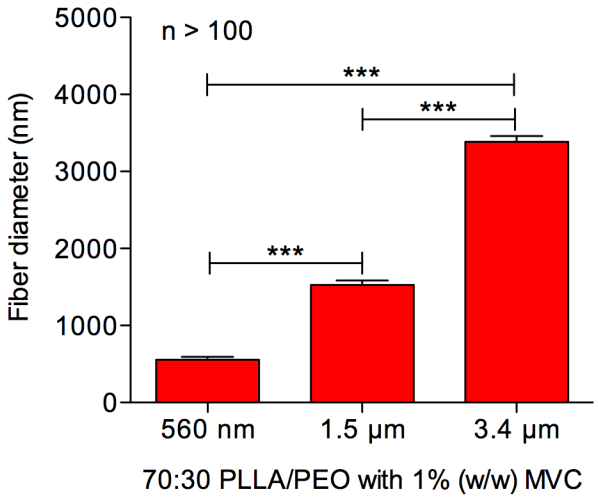

Figure 2.18—Fiber diameters of 70:30 PLLA/PEO with 1% (w/w) MVC. Geometric mean fiber diameters with 95% confidence intervals are displayed for 70:30 PLLA/PEO fibers with 1% (w/w) MVC made by varying polymer concentration and electrospinning parameters. Geometric mean fiber diameters of all three mesh types are significantly different from each other ($p<0.0001$). These fibers correspond to cumulative release curves displayed in Figure 2.11-b.

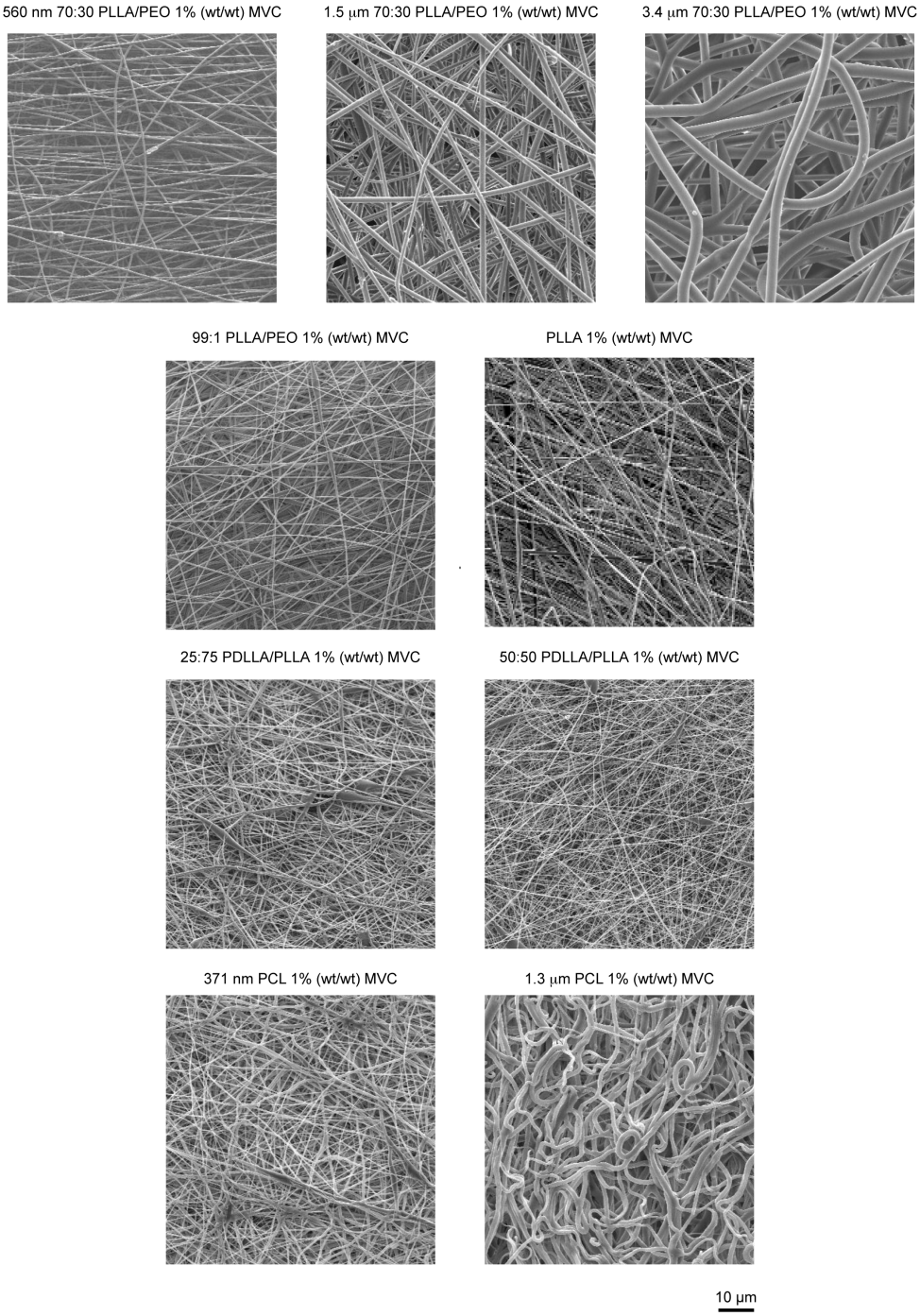

Figure 2.19—Morphology of additional polymeric fibers incorporating 1% (wt/wt) MVC. Scanning electron micrographs of fibers made from different polymers incorporating 1% (wt/wt) MVC are shown, including 70:30 PLLA/PEO of three fiber diameters (560 nm, 1.5 μm, and 3.4 μm), 99:1 PLLA/PEO, PLLA, 25:75 PDLLA/PLLA, 50:50 PDLLA/PLLA, and PCL of two fiber diameters (371 nm and 1.3 μm). These fibers correspond to cumulative release curves displayed in Figure 2.11-b,c.

Given that the desorption-limiting release model reasonably described our data, we hypothesized that severely reducing the PEO content in fibers should eliminate burst release (minimal fiber maraviroc would be solubilized) yet maintain a low-level sustained release of maraviroc though the creation of small PEO pores in the PLLA. Thus, our second strategy was to reduce hydrophilic polymer content by electrospinning fibers from a 99:1 PLLA/PEO blend containing 1% (wt/wt) MVC. The resulting fibers were smooth, regular, and similarly sized to 70:30 and 30:70 PLLA/PEO fibers (Figure 2.19). When placed into VFS, the fibers showed no burst release of MVC. Rather, the fibers provided sustained release over six days, eluting an average of only 1.19% of encapsulated MVC into VFS (95% CI = 0.51 to1.88 %, n = 3) (Figure 2.11). The small fraction of PEO present in fibers meant that very little PEO was likely to be accessible to water through pores extending through the polymer matrix. 1% loading into 1% PEO that partitions at 2:1 with PLLA would effectively result in a maximum burst release of 4.8% drug according to maraviroc release model 3 in section 2.06.2, assuming 100% of PEO were solvent accessible. Thus, the total amount released from these fibers was miniscule, and would likely have reached a plateau near the measured value of 1.19%. This amount of MVC corresponds to an average concentration of 360 ± 120 nM (n = 3) maraviroc in the VFS sink release assay, two orders of magnitude greater than maraviroc's IC_{50} *in vitro*, but far below the effective concentration (10^6 times IC50 value) in vaginal fluid or tissue *in vivo*[115,118].

Since the release of maraviroc from PLLA/PEO fibers was constrained by interactions with PLLA, we sought to change the hydrophobic component of the fibers while dropping the PEO from the mixture to prevent rapid and extensive burst release. Consequently, for our third strategy, we encapsulated 1% (wt/wt) MVC into fiber meshes made from polycaprolactone (PCL) or blends of poly-(D,L)-lactic acid (PDLLA) and PLA to investigate the influence of polymer T_g and crystallinity on release rate. PCL is a bioabsorbable hydrophobic polymer with a long history of use in electrospinning[4,175,176]. PCL has a much lower melting temperature than PLLA, and it's glass transition temperature is near -50 °C, reflecting weaker polymer-polymer interactions than in PLLA, and much greater molecular flexibility in the polymer strands at physiological temperature, where the PCL should be rubbery instead of glassy[173]. Such material properties meant that maraviroc and water would be able to move more readily through PCL materials. We electrospun PCL meshes containing 1% (wt/wt) MVC with two different fiber diameters: 371 nm and 1.3 µm (Figure 2.19). Upon incubation in VFS, all PCL meshes burst released more than 95% of the encapsulated MVC within 1 hour with no secondary release phase (Figure 2.11**-b**). Larger PCL fibers released 5.04% less MVC over 6 days (95% CI = 3.92% to 6.17%, n = 3) than small PCL fibers. These data are consistent with other reports of

drugs burst releasing from PCL due to a high level of nanoporosity in PCL matrices and a high degree of drug migration to the surface of rubbery-state PCL fibers[171]. We believe that the rapid burst of maraviroc from PCL is due to the low T_g of PCL, which allows for phase separation and ultimately dissolution of drug from the fiber surface. Evidence for phase separation of maraviroc to the fiber surface and subsequent release includes the observation that these materials wet out very quickly, while blank PCL fiber mats retain air for a several months[173]. Exposed drug on the fiber surface helped wick water into the PCL fiber network, leading to rapid drug release.

We modulated the crystallinity of pure PLA fibers by blending PLLA with varying amounts of lower molecular weight poly(D,L-lactide) (PDLLA). PDLLA is chemically identical to PLLA, but displays key structural differences. In particular, PDLLA is amorphous, and allows for greater penetration of water into PLA meshes[145]. The PDLLA used in this study had a mass average molecular weight of 18-24 kDa (much smaller than the ~117 kDa PLLA), but retained a glass transition temperature of between 50°C and 60°C, similar to PLLA. We hoped that PDLLA, as a glassy but amorphous analogue of PLLA, would provide release intermediate between PCL and PLLA. We electrospun 25:75 and 50:50 PDLLA/PLLA blends containing 1% MVC. The resulting fibers showed regular morphology with similar fiber size (265 ± 145 nm and 190 ± 159 nm, respectively) to pure PLLA fibers (478 nm ± 287 nm) (Figure 2.19). When placed into VFS, these PDLLA/PLLA meshes showed no burst release, and released MVC linearly over six days (Figure 2.11**-c**). The amount of encapsulated MVC released after six days was 3.09 ± 0.27% from 25:75 PDLLA/PLA fibers and 4.61 ± 0.41% from 50:50 PDLLA/PLLA fibers. 50:50 PDLLA/PLLA meshes released significantly more MVC than 25:75 PDLLA/PLLA meshes (P value = 0.0059, n = 3). Therefore, modulating the polymer crystallinity by blending PDLLA with PLLA provided small, but sustained, linear release of MVC from electrospun fibers.

Based on results shown in Figure 2.11**-c**, it is unlikely that the hydrophobic nature of PLLA alone was responsible for the lack of MVC release from pure PLLA fibers or PLLA domains in PLLA/PEO blends. Forbes et al. documented release of MVC from a silicone based elastomer gel both into VFS and into the vaginal fluid of rhesus macaques, providing evidence that MVC can release from hydrophobic formulations[61]. We hypothesized that the semi-crystalline structure of PLLA is responsible for preventing MVC release from the hydrophobic portions of blended fibers by occluding water penetration. PDLLA is comprised of a racemic mixture of the D- and L- stereoisomers of lactic acid and has an amorphous nanostructure that allows increased water entry and accelerated polymer degradation compared to PLLA[145]. We found that electrospinning 25:75 and 50:50 blends of PDLLA and PLLA allowed the ingress of water and the subsequent sustained release of MVC over six days. 25:75 and 50:50 PDLLA/PLLA

fibers had similar sizes; 25:75 fibers were around 20% larger than 50:50 fibers (Figure 2.19). The rate of MVC release from PDLLA/PLLA fibers increased with the PDLLA content, but remained small. Cui et al. achieved sustained release of acetaminophen (a drug with similar properties to maraviroc) from electrospun PDLLA fibers over six days and found that >70% of encapsulated drug could be released[174]. We found that 50:50 PDLLA/PLLA fibers only released 4.61 ± 0.41% of MVC into VFS over 6 days. Our results may differ from those of Cui et al. because of maraviroc's lower hydrophilicity, inclusion of PLLA, or variation in polymer molecular weight. Despite the low levels of drug release, our results provide proof of principle that electrospun fibers made from biodegradable materials can sustain the release of ARVs over multiple days. It is likely that encapsulating MVC in glassy amorphous polymers like PDLLA, PLGA, or ethyl cellulose would result in improved sustained release of MVC.

2.06.4 Summary of analysis of sustained release fiber formulations.

By thoughtfully analyzing data obtained from formulating azidothymidine and maraviroc into 70:30 and 30:70 PLLA/PEO blend electrospun fibers, we were able to develop a number of qualitative models to describe the mechanisms controlling the release of ARVs from two-component electrospun fibers. Further characterization of electrospun materials by monitoring fibers' mass loss, performing thermal analysis, and quantitatively considering the implications of simple partitioning of drugs into phase-separated materials on expected release profiles enabled us to identify which models most accurately described the observed release behavior. Release of maraviroc from blended fibers was determined by a rapid dissolution of PEO containing preferentially partitioned maraviroc followed by a desorption-limited release of maraviroc from the surface of PLLA pores created by PEO dissolution. Based on this knowledge, we successfully eliminated burst release of maraviroc from blended fibers by reducing the PEO component to 1% by weight. Unfortunately, this also resulted in minimal drug release. Higher sustained release without an initial burst was achieved with PDLLA/PLLA blends. These results warrant further investigation of the use of PLLA and other biodegradable polyesters, such as PLGA, as materials to provide sustained release of maraviroc from electrospun fibers for the prevention of sexual HIV-1 transmission. In particular, a controlled release system that will enable high drug loading, 100% release of encapsulated maraviroc, and eliminate the burst release of maraviroc should be developed.

2.07 Conclusion

We have presented a versatile platform for topical drug delivery to the lower female reproductive tract. The electrospun fiber meshes were fabricated in geometries suitable for intravaginal drug delivery, and we showed that our fibers incorporate agents with differing aqueous solubility and mechanisms of action against HIV-1, HSV-2, or sperm. Layering or co-electrospinning drug-loaded fibers may create composite materials that are multifunctional by virtue of simultaneous delivery of multiple agents with different mechanisms of action. In particular, fibers incorporating inhibitors of viral reverse transcriptase and CCR5 binding prevented HIV infection *in vitro*. We also screened non-hormonal chemical contraceptive alternatives to N-9 and identified a novel function of GML to inhibit sperm motility and reduce sperm viability. In addition to chemically inhibiting sperm function, fibers also physically inhibit sperm penetration by creating a tortuous path that sperm cannot navigate. This system is expected to provide enhanced coverage of the mucosal tissue and vaginal rugae by covering both the vaginal wall and the cervix, supported by the extent of coverage demonstrated when fiber meshes were applied to mice. We envision that the fiber meshes could be inserted simply with a tampon applicator, rendering it discreet, female-controlled, and wholly reversible. Further research will be conducted to investigate the mechanical properties of the fibers and explore other methods to modulate drug release. The functional combination offered by our drug-eluting fibers cannot be accomplished with any single technology currently in the development pipeline. We envision other applications for drug-eluting fibers along with prevention technology, including mucosal vaccine delivery, STI treatment, rectal microbicides, and other reproductive health applications.

2.08 Acknowledgments

We thank J. Amory, C.H. Muller and the University of Washington Male Fertility Laboratory for technical assistance with the sperm function assays and critical discussions of the manuscript. Collection of human semen samples from volunteers was performed at the University of Washington Male Fertility Laboratory. We also thank F. Hladik and R. Astronomo for assistance with the cervical tissue explant models. We thank A. Chen for technical assistance with tensile testing of electrospun materials.

Chapter 3. Electrospun solid dispersions of maraviroc for rapid intravaginal pre-exposure prophylaxis of HIV

3.01 Abstract

The development of topical anti-HIV microbicides may provide women with strategies to protect themselves against sexual HIV transmission. Pericoital drug delivery systems intended for use immediately before sex, such as microbicide gels, must deliver high drug doses for maximal effectiveness. The goal of achieving a high antiretroviral dose is complicated by the need to simultaneously retain the dose and quickly release drug compounds into the tissue. For drugs with limited solubility in vaginal gels, increasing the gel volume to increase the dose can result in leakage. While solid dosage forms like films and tablets increase retention, they often require more than 15 minutes to fully dissolve, potentially increasing the risk of inducing epithelial abrasions during sex. Here, as in our recent publication[120], we demonstrate that water-soluble electrospun fibers, with their high surface area to volume ratio and ability to disperse antiretrovirals, can serve as an alternative solid dosage form for microbicides requiring both high drug loading and rapid hydration. We formulate maraviroc at up to 28 wt% into electrospun solid dispersions made from either polyvinylpyrrolidone or poly(ethylene oxide) nano- or micro-fibers, and investigate the role of drug loading, distribution, and crystallinity in determining drug release rates into aqueous media. We show that water-soluble electrospun materials can rapidly release maraviroc upon contact with moisture, and that drug delivery is faster (less than 6 minutes under sink conditions) when maraviroc is electrospun in polyvinylpyrrolidone fibers containing an excipient wetting agent. These materials offer an alternative dosage form to current pericoital microbicides.

3.02 Introduction

The development of more effective topical anti-HIV microbicides might provide women with products that reduce the risk of HIV-1 transmission during heterosexual intercourse. Recent clinical trials of anti-HIV microbicides and oral pre-exposure prophylaxis (PREP) have demonstrated that prophylactic delivery of small molecule anti-HIV compounds can significantly reduce HIV acquisition rates, and that adherence to microbicide use is correlated with protective outcomes [36-40]. Current lead delivery systems for microbicides include intravaginal rings, gels,

tablets, and films. While rings provide the advantage of long-term delivery, they may not be most appropriate for use during infrequent sex acts. Tablets and films, while they can be used immediately before sex, often require thirty minutes to dissolve fully before the start of intercourse. Moreover, microbicide films reported in literature have low drug loadings (less than 1.5 wt%) [51,63], which when coupled with their small dosage size, limits their application to only highly potent ARV drugs. Recently, Ball *et al.* and Huang *et al.* demonstrated that electrospun fibers could release a range of active ARV drugs and spermicides [79], and that such release could occur in response to stimuli, such as a semen-induced rise in pH [78]. Furthermore, Huang et al. demonstrated high loading (15 wt%) of tenofovir disoproxil into electrospun fibers [78], which would reduce the required dosage size.

Maraviroc, another antiretroviral drug, is of interest for use in a microbicide due to its effectiveness at treating HIV [113], high potency in animal models [118], and favorable toxicity profile. Maraviroc works by binding to CCR5 coreceptors on HIV target cells, thereby inhibiting viral entry [112]. Since the majority of new HIV infections are CCR5-tropic, maraviroc may be particularly suited for use as a microbicide. Maraviroc is also not a first-line HIV medication, so the development of HIV resistance to maraviroc [177] would not necessarily preclude the use of frontline HAART treatments. While maraviroc has been loaded into a HEC gel [118], two vaginal rings (one also containing dapivirine) [57,70], and a silicone based elastomer gel [61] for testing as a microbicide, it has yet to be formulated into fully soluble disintegrable fibers for the purpose of pericoital protection. Previous pharmacokinetic and efficacy studies have shown that maraviroc can be delivered and absorbed intravaginally, but that protection against high dose SHIV-162P3 challenge in macaques requires a large dose (3.3 wt% in HEC gel) just 30 minutes prior to viral exposure [117,118]. Thus, solid pericoital delivery systems should be designed in part to maximize drug release speed.

Within pharmaceutics, it is often the case that drugs with melting temperatures near or above 200 °C will display improved solubility and release rates when formulated into amorphous solid dispersions, since crystalline active pharmaceutical ingredients must overcome the enthalpic energy barrier of “melting” their crystalline lattice structure before solvating [82,178]. The melting point of crystalline maraviroc is near 195 °C [70], suggesting that dispersion of maraviroc within appropriately compatible polymer fibers might aid in achieving high drug dosing in less than 30 minutes prior to viral challenge. Solid dispersions most often utilize polymers like poly(ethylene oxide) (PEO, also known as PEG) and polyvinylpyrrolidone (PVP) to serve as carriers that can formulate active compounds as a “dissolved solid”. Our previous, unpublished work demonstrated that maraviroc existed in a semicrystalline state within PEO fibers even at

loadings as low as 1 wt% (Chapter 2). PVP, which has often been used to accelerate drug release or increase apparent drug solubility in both electrospun fibers and oral tablets [91,179,180], may improve the extent of amorphous dispersion of maraviroc within electrospun materials, even at 15 wt% or higher drug content.

Additionally, incorporating hydrophilic surfactants like Tween 20 into electrospun microbicides might lower the entropic cost of solvating maraviroc's hydrophobic moieties through complexation with drug molecules in solution, thereby further accelerating drug release. However, the incorporation of a surfactant into a potential microbicide raises the potential for increased risk of HIV transmission, so it is important to investigate how their use to alter release behaviors may be balanced with toxicity concerns.

Here, we design and evaluate electrospun fibers containing the antiretroviral drug maraviroc for rapid, pericoital prevention of HIV-1. We demonstrate that maraviroc may be loaded to at least 28 wt% into PVP and PEO nano- and microfibers. These materials hydrate rapidly (less than 15 min [126]) and release high levels (10^6 x $IC_{50,\ in\ vitro}$ for maraviroc [118]) of active agents both in sink conditions and on agar gels. Since maraviroc constituted such a large portion of the fiber mass, we reasoned that maraviroc's ability to hydrate and enter solution would have a large influence on the time required to complete release. We also examine how drug loading, polymer choice, and inclusion of Tween 20 (at levels deemed to be an upper limit for safe use) would affect the crystallinity, distribution, and release rates of maraviroc from the fibers. Our studies show that the inclusion of the wetting agent Tween 20, drug loading, and polymer choice impacted the distribution, crystallinity, drug solubility, and release rates of maraviroc from electrospun fibers. While all fiber formulations achieved rapid drug delivery through dispersion of maraviroc (increased surface area for drug dissolution), the most rapid delivery of maraviroc was achieved through a combination of PVP and 2.5 wt% Tween 20, which allowed for the complete release of 28 wt% maraviroc in just 6 min under sink conditions. Crucially, the maraviroc released from electrospun fibers was shown to retain its original potency against HIV *in vitro*. These rapidly dissolving fibers could be ideally suited for use as a pericoital delivery system, since they have a very high surface area to volume ratio, can be made of the same polymers as films and tablets, and, unlike other nano-systems like nanoparticles, are easily handled. Electrospun fibers are smooth (materials appear textured on a micrometer scale), fabric-like materials (capable of repeated folding without breakage and post-production shaping) that could be inserted vaginally either with a finger or with an applicator[79].

3.03 Materials and Methods

3.03.1 Preparation and composition of electrospinning solutions

Maraviroc was purchased through the University of Washington's Investigative Drug Services facility, and was purified and recrystallized from Selzentry® (ViiV Healthcare) through extraction into dichloromethane and recrystallization in ethyl acetate (see supplementary materials). Selzentry tablets (6 tablets, 1.8 g maraviroc) were crushed by hand using a mortar and pestle. Due to the brittle nature of the pill's core and the more flexible properties of the pill's film-coat, the core was ground into a fine white powder while the film-coat remained in larger blue flakes. Then a fine copper mesh (75 lines/inch, Home Depot) was used to separate the film-coat fragments from the interior powder. 100 mL of dichloromethane (Sigma Aldrich) and 1 g of anhydrous $MgSO_4$ (Fisher Scientific) were added to the powder and stirred with a magnetic stir bar for 10 minutes to dissolve the maraviroc into the dichloromethane. This suspension was filtered through cellulose filter paper (Whatman) into a 250 mL round bottom flask. The filtrate was clear and colorless. The dichloromethane was evaporated using a rotary evaporator (Rotovap) to produce a white foam (maraviroc-DCM polymorph). Refluxing ethyl acetate (Sigma Aldrich) was added slowly to the white foam while keeping the round bottom flask at a temperature of 70°C. Gentle swirling helped dissolve the maraviroc foam into the ethyl acetate. Once all of the maraviroc was dissolved, the round bottom flask was allowed to cool slowly to room temperature, then again to 4°C. White maraviroc crystals formed in the ethyl acetate. Finally, the ethyl acetate was removed under vacuum using a rotary evaporator to yield pure crystalline maraviroc. Identity and purity (>99%) were confirmed by comparing proton-NMR spectra of the sample dissolved in CDCl3 (University of Washington Chemistry Supplies Store) to that described previously [181]. Common contaminants (<1% molar composition) were polyethylene glycol (from pill film-coat fragments) and ethyl acetate, identified by peaks on NMR spectra. HPLC, DSC, and XPS further verified drug identity and purity. Polyvinylpyrrolidone (PVP) with a M_W of ~1,300,000 Da was purchased from Sigma Aldrich (St. Louis, MO). Poly(ethylene oxide) (PEO) with a M_w of ~400,000 Da was purchased from Scientific Polymer Products, INC (Ontario, NY). 100% ethanol (USP grade) was purchased from the University of Washington's biochemistry supplies store. Distilled, deionized water was obtained using a Milli-Q-water purifier (Millipore). Tween 20 (Polysorbate 20) was purchased from Fisher Scientific. PVP, PEO, Tween 20, maraviroc, and solvents were added to 20 mL glass scintillation vials with gas tight lids. Solutions were mixed by gentle tumbling overnight on a rotisserie shaker (Labquake, Thermo Scientific). Solution density was measured by massing triplicate 500 µL

samples, taking the mean of the measurements, and dividing by the sample volume. Solution conductivity was measured using a calibrated conductivity probe (Thermo Scientific). Solution surface tensions were measured using an AquaPi surface tensiometer (Kibron). Rheological data were measured using an AR G2 series rheometer (TA Instruments) with a 40 mm 2° cone geometry in frequency sweep oscillation mode with a constant small strain of 4%. Measurements of G'' were converted to viscosity measurements by dividing G'' by the angular frequency. Comparisons of solution parameters between solutions with and without Tween 20 were made using paired, two-sided T-tests with $\alpha = 0.05$, matching for drug loading. Correlations between solution parameters and drug loading were tested using a Pearson's correlation test with $\alpha = 0.05$.

3.03.2 Electrospinning and SEM characterization

PVP solutions were electrospun at 15 kV over a 20 cm gap using flow rates of 25, 50, and 100 µL/min. PEO solutions were electrospun at 15 kV over a 25 cm gap using flow rates of 10, 25, and 50 µL/min. Solutions were spun with a charged 15 cm by 15 cm metal screen at the base of the needle to promote a spatially homogeneous electric field and increase polymer recovery. For each run, 1 mL of solution was spun from a glass syringe fitted with a 2.54 cm long 25 G stainless steel blunt dispensing needle. Fibers were collected onto a flat, grounded, aluminum surface covered with a single layer of wax paper. The wax paper substrate facilitated easy removal of the fiber samples from the collector with tweezers. After electrospinning, fiber samples were lyophilized for at least 24 hours. Then their final mass was recorded to determine yield.

Electrospun fibers were examined by SEM using a Sirion SEM (NTUF, UW). Fibers were examined after sputtering with gold and palladium for 90 seconds to minimize charge buildup on fibers. Imaging settings of 5 kV, spot size 3, and working distance of 6.5 mm were used to obtain images. Fields of view were randomly selected in order to eliminate bias in selecting which fibers to image. Fiber diameters were measured in ImageJ (NIH) by bisecting the SEM image diagonally with a line and manually measuring the diameters of fibers that intersected that bisecting line. At least 25 fibers were measured per sample, and fiber diameters were reported using the median and coefficient of variation as measures of the population's center and distribution, respectively. Correlations between median fiber diameters and drug loading were tested using a Pearson's correlation test with $\alpha = 0.05$.

3.03.3 Measuring drug loading by HPLC

A Shimadzu Prominence LC20AD UV-HPLC system equipped with a Phenomenex Luna C18 column (5 µm, 250x4.6 mm) and LCSolutions software were used to quantify drug levels in samples. The actual loading of maraviroc in electrospun fibers was measured with UV-HPLC (Shimadzu) by dissolving 2.5 mg pieces of mesh (n=1, containing 0.25 mg to 1 mg of maraviroc) in 50 mL of the HPLC mobile phase, which consisted of a 60% 10 mM KH_2PO_4 buffer and 40% acetonitrile, filtered through 0.45 µm, 0.22 µm, and glass frit filters to remove particulates. Polymers and maraviroc were freely soluble in the mobile phase. A fresh maraviroc standard curve was prepared by dissolving 20 mg of maraviroc in mobile phase to a concentration of 1 mg/mL and diluting serially at 1:2 until at concentrations of approximately 10 ng/mL. Spiked samples were prepared by adding maraviroc from 1 mg/mL stock solution to dissolved blank fibers with and without Tween 20. The maraviroc standard, spiked samples, and unknown samples were detected by UV-HPLC as described previously [79,135]. The calibration curve was prepared in Prism (GraphPad) using $1/C^2$ weighting to minimize residuals. The linear range was found to be from 64,000 ng/mL to 400 ng/mL.

3.03.4 Thermal analysis by differential scanning calorimetry (DSC)

Samples with a mass of 5-10 mg (n = 1) were placed into aluminum pans (T-Zero, TA Instruments) and analyzed with a TA Auto Q20 DSC instrument (TA Instruments). Samples were heated from 30°C to 250°C at a rate of 10°C/min with a nitrogen flow of 50 mL/min. Peak integration was performed using TA Thermal Analysis software and sigmoidal tangential integration. Percent crystallinity of the polymer or the drug was calculated by dividing the measured specific heat of fusion for the sample by the mass fraction of drug or polymer and the reference heat of fusion of the pure crystalline substance (reference value for maraviroc was measured directly; reference value for purely crystalline PEO was estimated as 197 J/g, according to TA Instruments' thermal application note TN048 [182]). The lower limit of detection of crystalline maraviroc was approximately 0.5 wt%. Correlations between T_m values or PEO crystallinity and drug loading were tested using a Pearson's correlation test with $\alpha = 0.05$. The impact of Tween 20 on the T_m or percent crystallinity of PEO or maraviroc was tested using paired, two-sided T-tests with $\alpha = 0.05$, matching for drug loading.

3.03.5 Fiber surface analysis by X-ray photoelectron spectroscopy (XPS)

XPS was performed using a Surface Science Instruments S-Probe at the University of Washington's NESAC/BIO surface analysis recharge center. Due to the surface sensitivity of XPS measurements, care was taken to prepare samples with no surface contamination. Freshly electrospun materials were collected onto aluminum foil and immediately lyophilized. Samples were analyzed in triplicate and illuminated with low intensity electrons to reduce charging of the insulated materials. In addition to survey scans, high-resolution carbon scans and detailed nitrogen and fluorine scans were taken for all materials. Peak assignment and integration were performed using XPS analysis software (CasaXPS). Theoretical atomic percentages for C, N, O, and F were calculated assuming a uniform distribution of materials within electrospun fibers. The percent of the fiber surface covered by maraviroc molecules was calculated by normalizing the total fluorine content in each fiber sample to the fluorine content in pure maraviroc crystal. Enrichment of Tween 20 in PVP materials was assessed using atomic % oxygen, and was calculated only for blank PVP fiber materials. Pure PVP fibers and PVP fibers with Tween 20 were compared by subtracting atomic % O, and based on the 95% confidence intervals after error propagation.

3.03.6 Determination of *in vitro* maraviroc solubility following release from fibers

Drug release from fibers into saturated drug conditions was carried out to assess the solubility limit of maraviroc following release from electrospun fibers loaded with approximately 28 wt% maraviroc. 21 ± 3.5 mg or 42 ± 5.3 mg (mean ± SD) of crystalline maraviroc or maraviroc-loaded fibers, respectively, were added to pH 4.0 10 mM citrate (sodium) buffer with 154 mM ionic strength at 50 mg of drug per 1 mL of buffer (n = 3 per group). Fibers were vortexed for 1 min, heated to 37 °C for 24 h, vortexed again for 1 min, and centrifuged to pellet insoluble drug and polymer. A clear, viscous supernatant was present in all samples. This supernatant was diluted 1:1000 into citrate buffer for quantification of drug concentration by UV-HPLC. Pure PVP and PEO were also added to identical buffer to verify that they did not alter solution pH. A one-way ANOVA was used to test the null hypothesis that drug solubility was equivalent across all formulations of maraviroc ($\alpha = 0.05$), and performed Dunnett's post-test comparisons to test for solubility differences between fiber formulation groups with the pure drug control group ($\alpha = 0.05$).

3.03.7 *In vitro* drug release into sink conditions

Sink release was studied in ambient conditions (20 °C, 50% RH) in a pH 4.0 10 mM citrate (sodium) buffer with 154 mM ionic strength. PBS (pH 7.0) was also used to assess the effect of drug ionization on release rate from highly loaded PVP fibers without Tween 20. Media was filter sterilized before use. Studies were carried out by adding 5 mg of fiber to a 50 mL conical tube secured to a rotisserie shaker (Labquake, Thermo Scientific). 25 mL of media was added (maximum [maraviroc] = 0.06 mg/mL, >50 times lower than the drug's solubility limit) and a timer was started when fibers first touched fluid. Materials were tumbled gently at 7 RPM, and 50 µL samples were removed at 2 min intervals for 20 min (total of 500 µL). A 24 h time point was taken the next day as an approximation of infinite time. Spiked samples as well as pure drug crystal controls were also analyzed to validate quantitative methods. Spiked drug controls yielded full drug recovery at the 2 min time point. Purified maraviroc was micronized using a mortar and pestle, and particle size was assessed by SEM and imaging software (ImageJ, NIH). Release samples were quantified by UV-HPLC as described above.

3.03.8 In vitro dissolution of electrospun fibers on a moist, porous surface

Electrospun fibers were cut into 1.27 cm diameter circles using a metal die (Grainger), and their mass and thickness were measured with an analytical balance and calipers. PVP samples had a mass of 8.2 ± 4.2 mg (thickness of 0.49 ± 0.25 mm, basis weight of 65 ± 35 g/m^2, density of 0.13 ± 0.02 g/cm^3), and PEO samples had a mass of 2.0 ± 0.89 mg (thickness of 0.11 ± 0.04 mm, basis weight of 16 ± 7 g/m^2, density of 0.15 ± 0.07 g/cm^3). Fiber discs were gently dropped onto black agar plates (1.5% agar with 1% v/v of India ink) incubated at 37 °C. No pressure was applied to fibers to force contact with the gels. When the fibers absorbed water from the gels, the black plate clearly showed through the hydrated fibers (opaque and white prior to wetting). The degree of fiber hydration was assessed visually every 30 seconds from time-lapse photos taken on a smartphone (iPhone 4, Apple).

3.03.9 *In vitro* Tween 20 cytotoxicity anti-HIV activity of dissolved electrospun fibers

The *in vitro* cytotoxicity of the surfactants Tween 20 (Fisher), Tween 80 (Fisher), glycerol monolaurate (Sigma Aldrich), and nonoxynol-9 (Options Conceptrol) were evaluated using a cell titer blue assay (Promega) according to manufacturer instructions. The *in vitro* activity of maraviroc in fiber eluates (from sink release assays) was evaluated using a cell-based reporter assay described previously [79,183]. Briefly, TZM-bL cells and HIV-1 BaL isolate were obtained

from the NIH AIDS Research and Reference Reagent Program, Division of AIDS, NIAID, NIH (http://www.aidsreagent.org/). TZM-bL cells, a derived HeLa cell line that expresses CD4, CCR5, and CXCR4 [136-139], were added to black 96-well plates (Corning, Corning, NY) with Dulbecco's Modified Eagle Medium (DMEM) (Gibco Life Technologies) with 10% fetal bovine serum (Hyclone), 1% 100X penicillin/streptomycin (Invitrogen), and 1% 200 mM L-glutamine (Invitrogen) with 50 μL/well at a density of 5,000 cells/well. Cells were incubated in 5% CO_2 and 37°C for 24 h prior to exposure to surfactants or fiber eluates. For the surfactant cytotoxicity assay, compounds were dissolved or suspended with slight heating in cDMEM at 5 %wt/vol, and then diluted serially. 50 μL volumes of the dilutions were added into duplicate wells and cells were incubated an additional 24 h. Finally, per manufacturer specifications, 20 μL of cell titer blue reagent were added to each well and incubated for 4 h before reading fluorescence on a plate reader (Tecan). LD_{50} values of the surfactants were estimated using sigmoidal regression in Prism (GraphPad Software, Inc.) and compared using an extra sum-of-squares F-test ($\alpha = 0.05$). For the antiviral activity assay, treatments were diluted serially. A second operator, blinded to the identity of the treatments, added each in 50 μL volumes into duplicate wells (n = 1 was used for PVP and PEO Tween 20 formulations only due to space limitations on the 96-well plate). Polymer, surfactant, and drug concentrations were at least 1,000 times below toxic concentrations. 100 μL of HIV-BaL (240 TCID/well) was added to wells 1 h after drug treatment. Media was removed from cells after 48 h post-treatment, and 100 μL of phosphate buffered saline (Gibco Life Technologies) and 100 μL of Bright-Glo Luciferase reagent (Promega) were added to wells. Infectious activity was quantified by measuring luminescence on a plate reader (Tecan). IC_{50} values of the 5 drug formulations were estimated using sigmoidal regression in Prism (GraphPad Software, Inc.) and compared using an extra sum-of-squares F-test ($\alpha = 0.05$).

3.04 Results

3.04.1 Electrospinning solutions, fiber characterization, and drug loading determination

Our results show that it is possible to incorporate high levels of maraviroc (identity and purity confirmed in Figure 3.1) into PVP and PEO solutions without compromising fiber production by electrospinning. Electrospinning solution properties (Table 3.1) correlated with finished fiber characteristics (Table 3.2) and drug loading (Table 3.3). HPLC analysis of PVP and PEO fibers incorporating maraviroc had measured drug loadings of 94.2% ± 1.2% (n=8) and 98.0% ± 1.8%

(n=8), respectively. Maraviroc loading efficiency was not reduced even when drug precipitate was visually detected in the formulation solutions, such as in the case with solutions containing both Tween 20 and 40% wt drug/wt polymer maraviroc. Material efficiency was high for all PVP and PEO formulations with measured polymer recoveries of up to 95%. As expected, the lower PEO concentrations used in the solution formulations resulted in a reduced basis weight for PEO fiber materials (16 ± 7 g/m^2, thickness of 0.11 ± 0.04 mm) compared to PVP materials (65 ± 35 g/m^2, thickness of 0.49 ± 0.25 mm). PVP fibers loaded with maraviroc appeared large, cylindrical, and slightly wrinkled (Figure 3.2). We observed that increasing maraviroc content correlated highly with increased conductivity of PVP solutions with and without Tween 20 (Pearson's R = 0.95, 0.91 respectively, P < 0.05), and predicted that drug incorporation would lead to the formation of smaller diameter fibers. While we did observe that PVP fiber diameter decreased with increasing maraviroc concentration for formulations without Tween 20, the correlation was not statistically significant (Pearson's R = -0.80, P = 0.11). In contrast, when maraviroc was added to formulations containing Tween 20, the median fiber diameter decreased by up to 3-fold, and SEM images revealed a distinct population of both large (diameter ~2000 nm) and small (diameter ~400 nm) fibers (Figure 3.2).

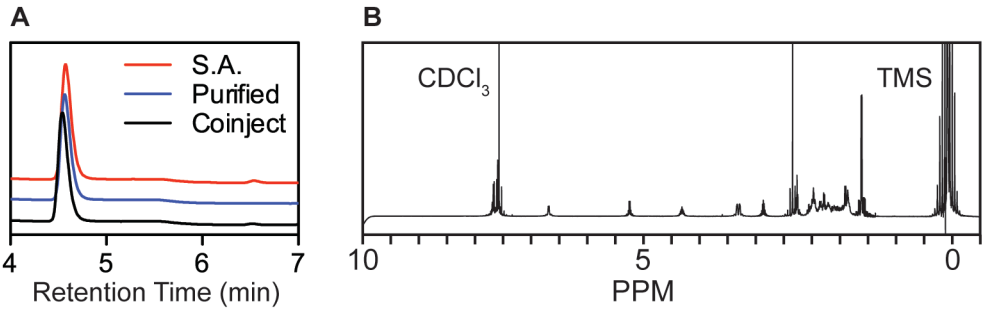

Figure 3.1—Maraviroc purified from Selzentry is pure and chemically identical to a maraviroc standard. (A) HPLC traces of maraviroc from Sigma Aldrich, purified maraviroc, and coinjection shows identical peak shape and retention time. (B) 1H NMR (CDCl3, 400 MHz) δ 7.37-7.27 (m, 5H), 6.60 (br, 1H), 5.13 (q, 1H), 4.29 (m, 1H), 3.38 (d, 2H), 2.98 (m, 1H), 2.50 (s, 3H), 2.44 (t, 2H), 2.17-1.64 (m, 19H), 1.38 (dd, 6H).

Table 3.1—Properties of PVP or PEO electrospinning solutions containing maraviroc. Density, conductivity, viscosity (η), and surface tension (γ) of electrospinning solutions are important parameters that affect the morphology of electrospun fibers. Viscosity is reported as the viscosity at an angular frequency of 1 rad/s. All values are taken from single experiments (n = 1).

Polymer	Tween 20 concentration (%wt Tween/wt polymer)	MVC concentration (%wt drug/wt polymer)	Density (g/mL)	Conductivity (μS/cm)	η (Pa.s)	γ (mN/m)
PVP	0	0	0.86	0.86	0.87	32.0
PVP	0	10.30	0.86	1.94	0.94	32.2
PVP	0	20.38	0.87	2.24	0.89	32.5
PVP	0	30.30	0.86	2.61	0.92	32.9
PVP	0	39.80	0.87	2.88	0.87	32.1
PVP	3.69	0	0.84	1.13	0.71	31.9
PVP	3.81	10.01	0.86	2.21	0.70	32.3
PVP	3.80	20.11	0.86	2.63	0.70	32.0
PVP	3.79	30.26	0.87	2.96	0.71	30.9
PVP	3.76	39.94	0.87	2.95	0.71	30.9
PEO	0	0	0.92	7.69	1.35	40.2
PEO	0	10.19	0.92	8.25	1.42	40.7
PEO	0	20.42	0.92	8.95	1.34	40.7
PEO	0	30.63	0.92	9.04	1.27	39.4
PEO	0	40.08	0.93	9.95	1.32	39.5
PEO	3.83	0	0.93	8.88	1.52	40.2
PEO	3.59	10.08	0.92	9.13	1.45	39.5
PEO	3.80	19.87	0.92	9.18	1.29	40.4
PEO	3.74	30.40	0.92	9.82	1.27	39.2
PEO	3.52	39.84	0.92	10.18	1.30	39.6

Table 3.2—Properties of electrospun PVP or PEO fibers containing MVC and Tween 20. Fiber diameter and material efficiency were dependent upon the formulated concentrations of Tween and maraviroc. All values are taken from single electrospinning experiments (n = 1). Fiber diameter median and coefficient of variation are calculated from measurements of at least 25 fibers per sample. *Fibers seen in SEM had a bimodal distribution of large fibers (~2,000 nm) and small fibers (~400 nm). This behavior was only seen in fibers containing both polysorbate-20 and MVC, and may correlate to decreases in solution viscosity and increases in solution conductivity. **Rough surface morphology suggestive of drug crystallization apparent in SEM micrographs of fibers.

Polymer	Tween 20 (wt%)	MVC (wt%)	Defect-free fibers (Y/N)	Median fiber diameter (nm)	C.V.	Material efficiency (%)
PVP	0	0	Y	2,890	0.16	91.2
PVP	0	9.37	Y	2,422	0.16	93.1
PVP	0	16.9	Y	2,756	0.10	91.0
PVP	0	23.1	Y	2,380	0.17	93.1
PVP	0	28.3	Y	2,101	0.17	90.6
PVP	3.58	0	Y	2,024	0.12	94.3
PVP	3.49	8.74	Y	662*	0.86	94.4
PVP	3.07	16.1	Y	724*	0.73	94.3
PVP	2.83	22.5	Y	586*	0.79	88.6
PVP	2.62	27.8	Y	616*	0.82	89.3
PEO	0	0	Y	417	0.23	95.9
PEO	0	9.25	Y	535	0.22	96.8
PEO	0	16.96	Y	576	0.21	101.8
PEO	0	23.45	Y**	616	0.15	97.9
PEO	0	28.61	Y**	721	0.14	97.2
PEO	3.69	0	Y	396	0.13	97.3
PEO	3.16	8.87	Y	274	0.22	97.6
PEO	3.07	16.07	Y	617	0.15	98.5
PEO	2.79	22.66	Y	596	0.12	97.6
PEO	2.45	27.79	Y	579	0.21	97.8

Table 3.3—Maraviroc loading in PVP or PEO fibers evaluated by HPLC. All encapsulation efficiencies are near 100% and within experimental precision of the HPLC detection method. These data show that maraviroc is loaded efficiently into electrospun fibers. ND = no MVC detected in sample. All values are taken from single experiments (n = 1).

Polymer	Tween 20 (wt%)	Predicted MVC loading (wt%)	Measured MVC loading (wt%)	Encapsulation efficiency (%)
PVP	0	0	ND	ND
PVP	0	9.37	8.93	96.40
PVP	0	16.9	15.92	94.27
PVP	0	23.1	21.44	92.76
PVP	0	28.3	26.52	93.76
PVP	3.58	0	ND	ND
PVP	3.49	8.74	8.13	93.03
PVP	3.07	16.1	15.16	93.89
PVP	2.83	22.5	21.28	94.37
PVP	2.62	27.8	26.48	95.27
PEO	0	0	ND	ND
PEO	0	9.25	9.17	99.17
PEO	0	16.96	16.94	99.87
PEO	0	23.45	22.89	97.61
PEO	0	28.61	28.43	99.35
PEO	3.69	0	ND	ND
PEO	3.16	8.87	8.37	94.37
PEO	3.07	16.07	16.08	100.06
PEO	2.79	22.66	22.01	97.11
PEO	2.45	27.79	26.93	96.88

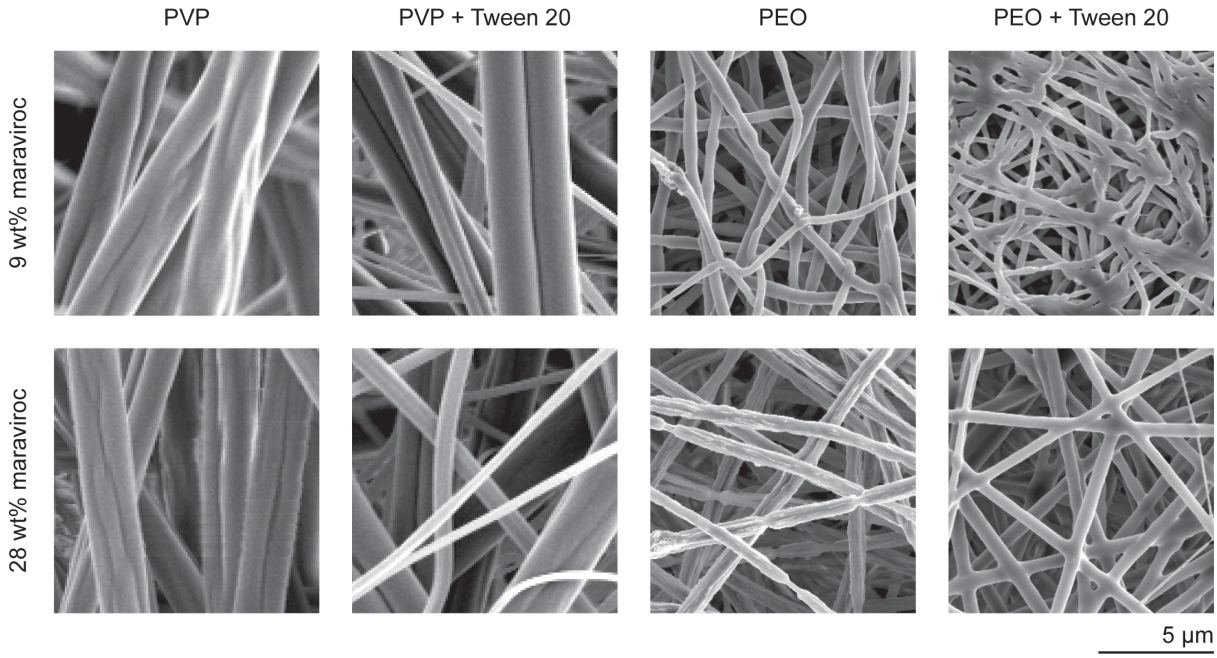

Figure 3.2—Maraviroc may be loaded into PVP and PEO fibers with and without the surfactant Tween 20 up to at least 28 wt%. The size and surface structure of the fibers depend upon the specific combination of polymer choice, drug loading, and surfactant incorporation. SEM images of fibers are organized into a matrix with the row representing either 9 wt% or 28 wt% drug loading, and the column representing the polymer (PVP or PEO) and inclusion of Tween 20. Scale bar = 5 µm.

All PEO solutions containing maraviroc produced electrospun fibers that showed narrow size distributions. Increasing maraviroc content by 4-fold in these PEO formulations also led to higher solution conductivity, but median fiber diameter did not decrease as might be expected. Rather, fiber diameter was positively correlated with maraviroc content in fibers without Tween 20 (Pearson's R = 0.97, P = 0.0042), where we observed up to a 30% change in solution conductivity with increasing maraviroc in solution. In samples containing Tween 20, fiber diameter increased until 16 wt% maraviroc loading, then remained fairly constant at ~600 nm. SEM micrographs of PEO fibers without Tween 20 revealed a rough surface morphology, whereas fibers containing Tween 20 displayed a smooth, highly fused surface morphology (Figure 3.2, Figure 3.3). The observed increase in diameter size by hundreds of nanometers with increasing maraviroc content suggests that a complex interplay of solution characteristics and electrospinning process parameters may make it challenging to predict physical properties of the finished fibers from measuring viscosity, conductivity, and surface tension alone. In summary, our results demonstrate that electrospinning efficiently and reproducibly formulates maraviroc into fibers. We performed all subsequent studies with 9 wt% and 28 wt%

formulations, and final Tween 20 content in fibers ranged from 3.7 wt% to 2.5 wt%, decreasing with increasing maraviroc content (Table 3.3).

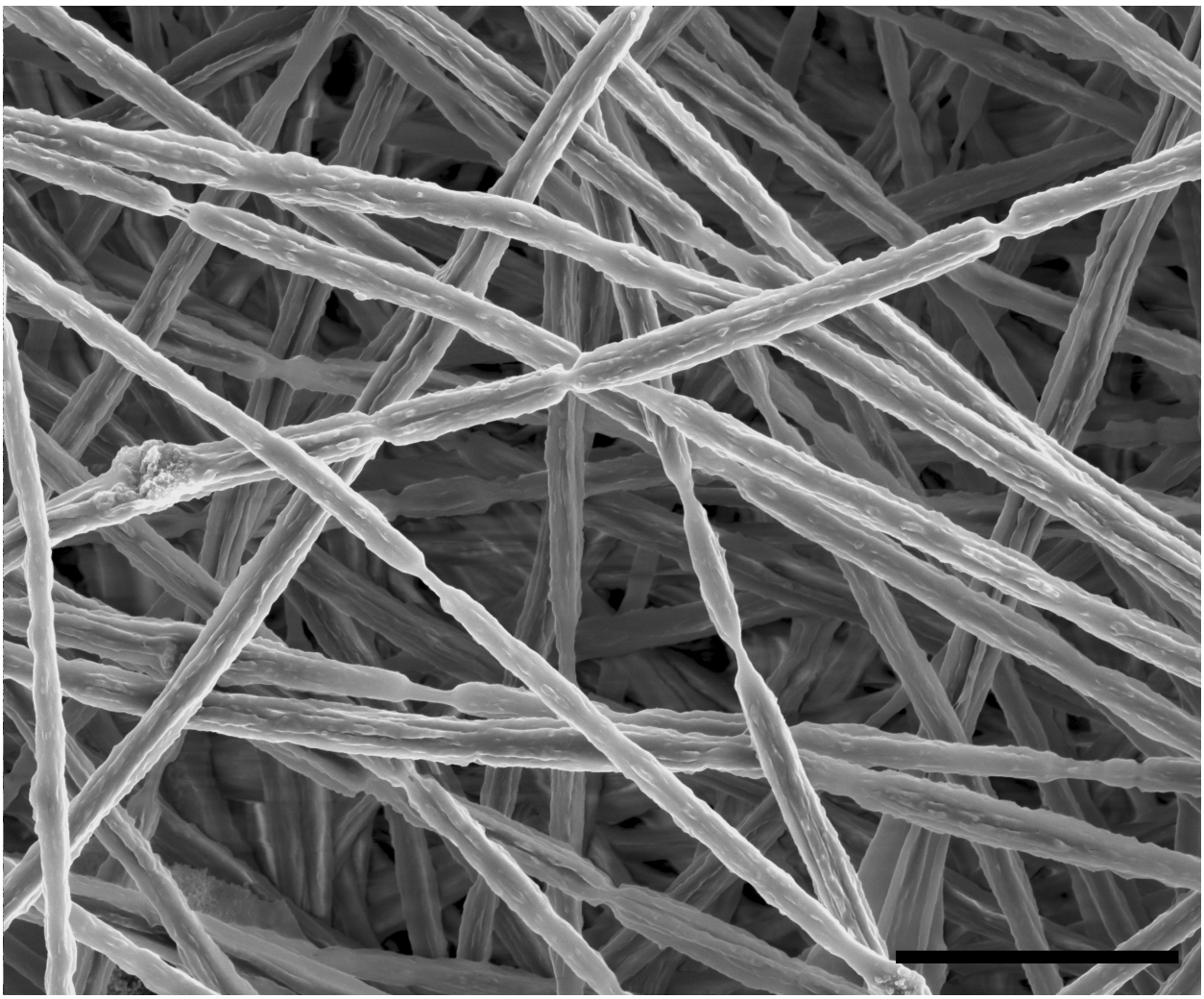

Figure 3.3—Higher resolution image of 28 wt% maraviroc PEO fibers. These fibers show clear signs of drug crystallinity, apparent as a rough surface structure. Scale bar = 5 μm.

3.04.2 Thermal Analysis by Differential Scanning Calorimetry (DSC)

We hypothesized that the extent of drug crystallinity might ultimately affect release rates *in vitro*. DSC analysis of PVP fibers containing maraviroc indicated that PVP and maraviroc were amorphously distributed throughout the electrospun fibers irrespective of Tween 20 content (Figure 3.4). In contrast, drug-loaded PEO fibers displayed melting endotherms near the T_m of pure maraviroc (195°C) (Figure 3.4). There was a significant, positive correlation between drug loading and percent maraviroc crystallinity in PEO fibers with and without Tween 20 (two-sided

Pearson's correlation test, $R > 0.95$, $P < 0.05$, $n = 5, 4$ respectively). For example, drug crystallinity was minimal in PEO fibers loaded at 9 wt% maraviroc but peaked at ~70% in PEO fibers above a loading of 23 wt% maraviroc. Interestingly, PEO formulations containing Tween 20 led to 9.9% greater maraviroc crystallinity in these finished fibers (Figure 3.4, Table 3.4) ($P = 0.035$, $n = 4$). We also observed that the T_m of maraviroc was positively correlated to maraviroc loading in fibers (Pearson's $R = 0.95, 0.95$; $P = 0.053, 0.046$; $n = 5, 5$; for fibers with and without Tween 20, respectively), and increased by 12 °C as maraviroc content went from 9 wt% to 28 wt%. Small exotherms suggestive of maraviroc recrystallization during heating (near 120°C) were present in many PEO fibers containing drug, but they were too minute to accurately integrate and quantify. Therefore, estimates of maraviroc crystallinity may be negligibly overestimated. All PEO fibers had endotherms near 66 °C corresponding to the T_m of PEO (Figure 3.4). The crystallinity of PEO in fibers was estimated to be ~55% and was unaffected by drug loading or inclusion of Tween ($P > 0.05$). However, the T_m of PEO was negatively correlated with maraviroc content in fibers (Pearson's $R = -0.94, -0.97$; $P = 0.0183, 0.0048$; $n = 5, 5$; for fibers with and without Tween 20, respectively) (Figure 3.4, Table 3.4). In summary, thermal analysis of electrospun materials by DSC revealed that maraviroc was amorphous in PVP fibers, semicrystalline in PEO materials, and that the degree of drug crystallinity in PEO increased with drug loading and Tween 20 incorporation.

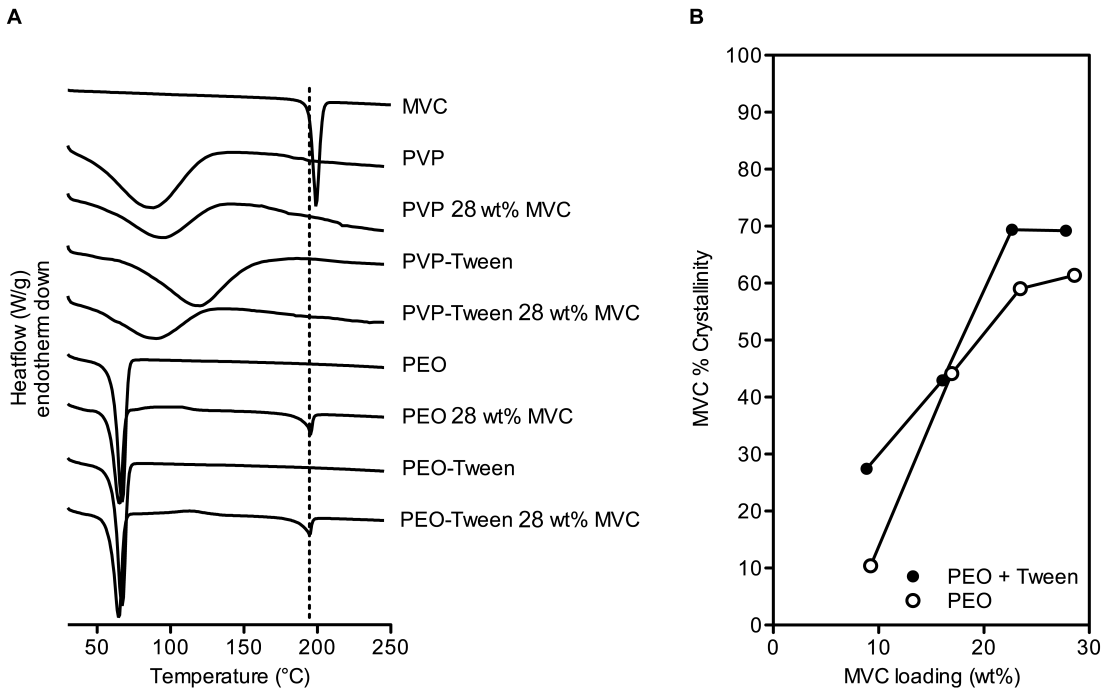

Figure 3.4—Maraviroc exists in different physical states depending upon the polymer choice and drug loading. DSC thermograms are shown in (A). Pure crystalline maraviroc has a melting endotherm around 195 °C (dashed line, A), which is observed in formulations of maraviroc into PEO-based fibers. No maraviroc endotherm was observed in PVP formulations. In PEO fibers, the crystallinity of the drug content was a function of drug loading, and was similar between fibers with and without Tween-20 (B). Data represent values from single experiments.

Table 3.4—Calorimetric analysis of PEO fibers loaded with maraviroc, Tween 20, or both. NA = Not applicable, since no maraviroc was loaded in fibers. All values are taken from single DSC measurements (n = 1).

Loadings		PEO Transition			Maraviroc Transition				
MVC (wt%)	Tween 20 (wt%)	T_m (°C)	ΔH_{fus} (J/g)	PEO % crystallinity = $\frac{\left(\Delta H_{fus}\right)_{meas}}{\omega_{PEO}\left(\Delta H_{fus}\right)_{ref}} \times 100\%$	Recrystallization peak near 120 °C?	Onset temp (°C)	T_m (°C)	ΔH_{fus} (J/g)	Maraviroc % crystallinity = $\frac{\left(\Delta H_{fus}\right)_{meas}}{\omega_{MVC}\left(\Delta H_{fus}\right)_{pure}} \times 100\%$
100.00	0.00	NA	NA	NA	N	195.36	199.13	71.75	100.00
0.00	0.00	67.15	114.80	58.27	NA	NA	NA	NA	NA
9.25	0.00	66.83	97.53	54.55	N	169.64	183.68	0.69	10.39
16.96	0.00	66.46	92.13	56.32	N	177.46	191.30	5.37	44.15
23.45	0.00	65.92	81.06	53.75	Y	183.06	195.39	9.93	59.04
28.61	0.00	65.39	71.73	51.00	Y	192.86	195.61	12.60	61.38
0.00	3.69	69.80	114.40	60.30	NA	NA	NA	NA	NA
8.87	3.16	67.20	104.30	60.18	N	166.50	182.01	1.75	27.42
16.07	3.07	65.28	89.55	56.22	Y	174.36	190.48	5.58	48.39
22.66	2.79	65.11	81.39	55.42	Y	179.80	194.45	11.28	69.37
27.79	2.45	64.91	81.24	59.11	Y	190.47	194.90	13.80	69.21

3.04.3 Fiber surface analysis by X-ray photoelectron spectroscopy (XPS)

XPS of electrospun fibers was used to estimate the degree of enrichment of maraviroc and Tween 20 at the surface (top 100 Å) of electrospun fibers. Atomic percent data for carbon, nitrogen, oxygen, and fluorine showed that the content of maraviroc varied with the polymer type, drug loading, and presence or absence of Tween 20 (Figure 3.5). We observed up to 5.9% fluorine on fiber surfaces, indicating a radially nonhomogeneous distribution of maraviroc within fibers. PVP and PEO fibers showed an approximately two-fold enrichment of maraviroc on the surface of the fibers over expected values for a theoretical fiber with a radially homogeneous distribution of maraviroc. PEO fibers without Tween showed the highest surface concentrations of maraviroc, reaching 100% maraviroc at 17 wt% loading. The surface of PVP fibers with Tween 20 became saturated with maraviroc at the higher loading of 28 wt% maraviroc. However, neither PEO with Tween 20 nor PVP without Tween 20 had maraviroc-saturated surfaces when loaded at 28 wt%. Tween 20 was enriched 4.8 to 7.8-fold on the surface of PVP fibers without maraviroc. We were not able to determine the surface concentration of Tween 20 in either drug loaded PVP fibers or PEO fibers due to limitations in instrument sensitivity. The two-fold surface enrichment of maraviroc in fibers suggests that maraviroc's physicochemical properties may impact the rate of fiber hydration and drug release.

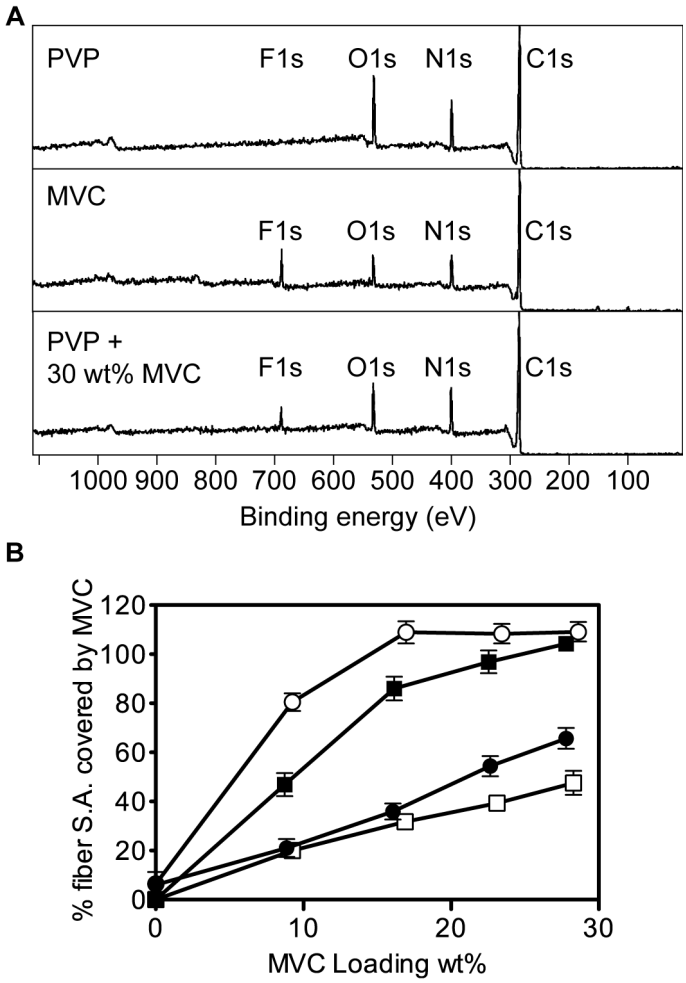

Figure 3.5—Maraviroc content was enriched at the surface of PVP and PEO fibers, as detected by XPS. Representative spectra are shown (A) for pure PVP polymer fibers (Top), pure maraviroc (middle), and PVP fibers loaded to 28 wt% with maraviroc (bottom), showing the shifting of C, N, and O atomic ratios due to the presence of maraviroc in the top 10 nm of the fiber surface. The amount of fluorine detected in samples was normalized to that found in pure maraviroc, and plotted against drug loading as % surface area covered by maraviroc (B). 100% means that the fluorine peak in the sample was as large as that in pure maraviroc samples. Data in (B) represent the mean of n = 3 independent experiments. Error bars represent SD. **O** = PEO, • = PEO + Tween, □ = PVP, ■ = PVP + Tween.

3.04.4 *In vitro* drug release under sink conditions

We tested the solubility limits of maraviroc following incubation of an excess of fibers or pure drug in sodium citrate buffer (10 mM, pH 4.0) for 24 hours (Figure 3.6). There was no change in solution pH after dissolving the fibers in the citrate buffer. Nevertheless, we found that drug solubility differed between all formulations tested ($P = 0.0015$). The solubility limit of pure maraviroc in the absence of polymer or surfactant was 21.3 ± 6.4 mg/mL (n=3). While PVP and

Tween-20 did not affect drug solubility, there was a large decrease in drug solubility after release from PEO formulations with or without Tween 20 ($P < 0.01$) (Figure 3.6). Therefore, in low fluid volumes, PVP fiber formulations maintained drug solubility in pH 4.0 buffer whereas PEO formulations reduced drug solubility, and Tween 20 had no effect on drug solubility with either polymer.

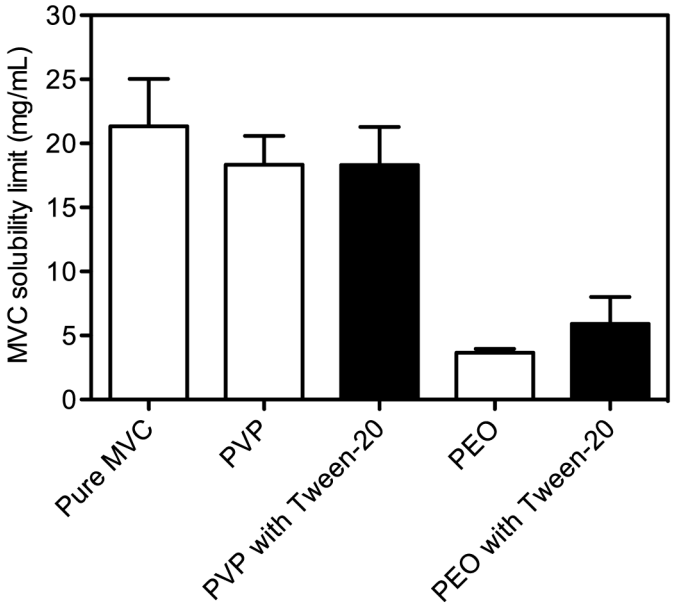

Figure 3.6—The solubility limit of maraviroc after release from fiber formulations into very low fluid volumes is maintained in PVP fiber formulations, but greatly reduced in PEO fiber formulations. Solubility limits were assessed in pH 4.0 10 mM citrate (sodium) buffer at 154 mM ionic strength, 37 °C and 24 h. Data shown as the mean of n = 3 independent experiments. Error bars represent SD.

Drug release into sink conditions at pH 4.0 was evaluated for PVP and PEO fibers loaded with 9 wt% or 28 wt% maraviroc (Figure 3.6). We observed that the time to 100% release of maraviroc from 28 wt% drug materials was 14 min, 6 min, 18 min, and 6 min for PVP, PVP with Tween 20, PEO, and PEO with Tween 20 fibers, respectively (Figure 3.6). All 9 wt% formulations released 100% of the maraviroc within 2-4 min, except for 9 wt% maraviroc in PEO with Tween 20, which required 10 minutes to fully release maraviroc. The time required to release 100% of loaded maraviroc generally increased with higher drug loading. Fibers loaded at 28 wt% maraviroc and 2.5 wt% Tween 20 released maraviroc more rapidly than those fibers without Tween 20. We also examined the effect on release from PVP fibers without Tween by changing the release media from a pH 4.0 citrate buffer, meant to mimic the mildly acidic pH of

the vagina, to a pH 7.0 PBS. The result was that PVP fibers (no Tween 20) required a full 20 minutes to completely release a 28 wt% maraviroc payload and 12 minutes to completely release a 9 wt% maraviroc payload. The time to 100% drug release from fibers was also compared to that from pure maraviroc particles under pH 4.0 and pH 7.0 sink conditions *in vitro*. At pH 4.0, micronized (50 nm to 5 μm) maraviroc particles dissolved completely within 2 minutes despite being 100% crystalline, while it took 20 minutes to dissolve 90% of a 2 mm diameter piece of crystalline maraviroc. At pH 7.0 however, large pieces of crystalline maraviroc required overnight mixing to fully dissolve (visual observations). These results demonstrate that solid dispersion of maraviroc into fibers dramatically accelerated drug dissolution, especially relative to dissolution rates at higher pH. Sink release data demonstrated that all fiber formulations of maraviroc were capable of rapid drug release, but that fibers incorporating Tween 20 as a wetting agent released maraviroc far more rapidly.

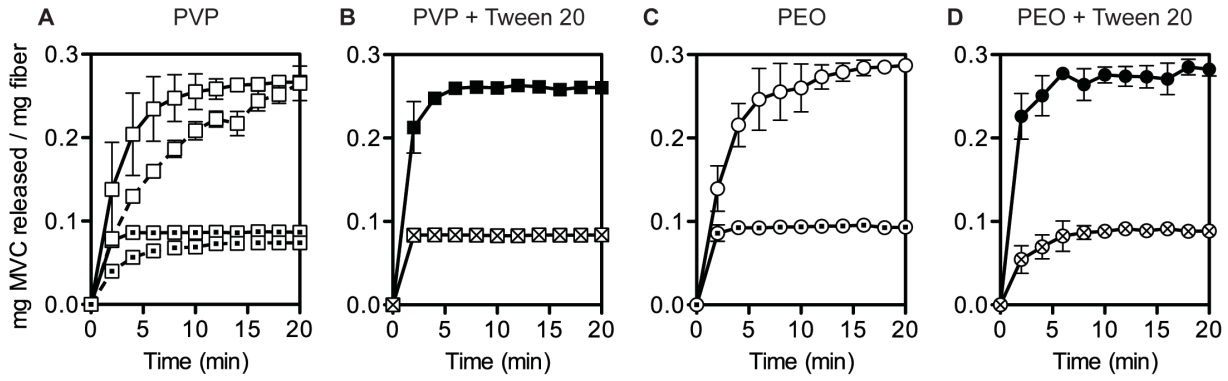

Figure 3.7—The release rate of maraviroc from electrospun fibers in vitro was dependent upon the drug loading, the inclusion of Tween 20, the pH of the release media, and the polymer. (A) Release from PVP fibers with 28 wt% maraviroc (□) into pH 4.0 citrate buffer (solid line) or pH 7.0 PBS (dashed line), and 9 wt% maraviroc (□ with dot) into pH 4.0 citrate buffer (solid line) or pH 7.0 PBS (dashed line); (B) release from PVP fibers with Tween 20 with 28 wt% maraviroc (■) and 9 wt% maraviroc (⊠); (C) release from PEO fibers with 28 wt% maraviroc (O) and 9 wt% maraviroc (⊙); (D) release from PEO fibers with Tween 20 with 28 wt% maraviroc (filled O) and 9 wt% maraviroc (O with x). Data shown as the mean of n = 3 independent experiments. Error bars represent SD.

3.04.5 In vitro dissolution of electrospun fibers on a moist, porous surface

PVP and PEO fibers containing 9 wt% or 28 wt% maraviroc and 0 wt% or 3 wt% Tween 20 were easily visualized as white materials on a black background using black agar plates (Figure 3.8). Fiber hydration was rapid, despite not being immersed in a bath of fluid and not applying pressure to fiber samples on the agar plates. Fibers containing 9 wt% maraviroc significantly hydrated, contracted, or dissolved in fewer than 10 seconds (Figure 3.9). Fibers containing 28 wt% maraviroc had slower hydration rates, and displayed two distinct behaviors depending upon Tween 20 incorporation. Fibers without Tween 20 absorbed water and rapidly contracted within 30 s and then continued to hydrate over 20 minutes, at which point the resulting hydrogel could flow if the agar plate were tipped at an angle. A visible precipitate, thought to be undissolved maraviroc, was present in this gel. In contrast, fibers with Tween 20 hydrated more rapidly than fibers without Tween 20. Between 5 s and 30 s, the fibers wet out in place without significant matrix contraction or shrinkage. By the end of the 20 min monitoring period, no precipitated maraviroc or undissolved polymer was visible. Overall, fibers hydrated more rapidly when they contained less maraviroc or contained Tween 20.

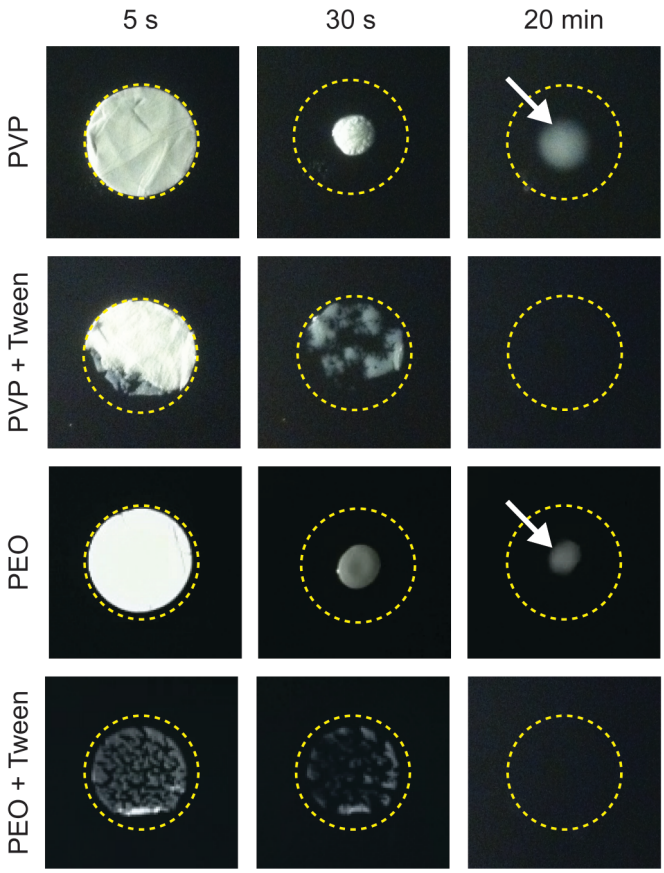

Figure 3.8—Incorporating Tween 20 into PVP or PEO fibers containing 28 wt% maraviroc led to more rapid and total dissolution of fibers and encapsulated maraviroc on a moist porous surface of 1.5% agar at 37 °C. The original perimeters of the 28 wt% maraviroc fiber discs are shown as dashed circles. Images are arranged by fiber type (row) as seen over time (column). A visible precipitate remained in hydrated fiber gels after 20 min for both PVP and PEO fibers without Tween 20 (white arrows). Images are representative samples of n = 3 independent experiments.

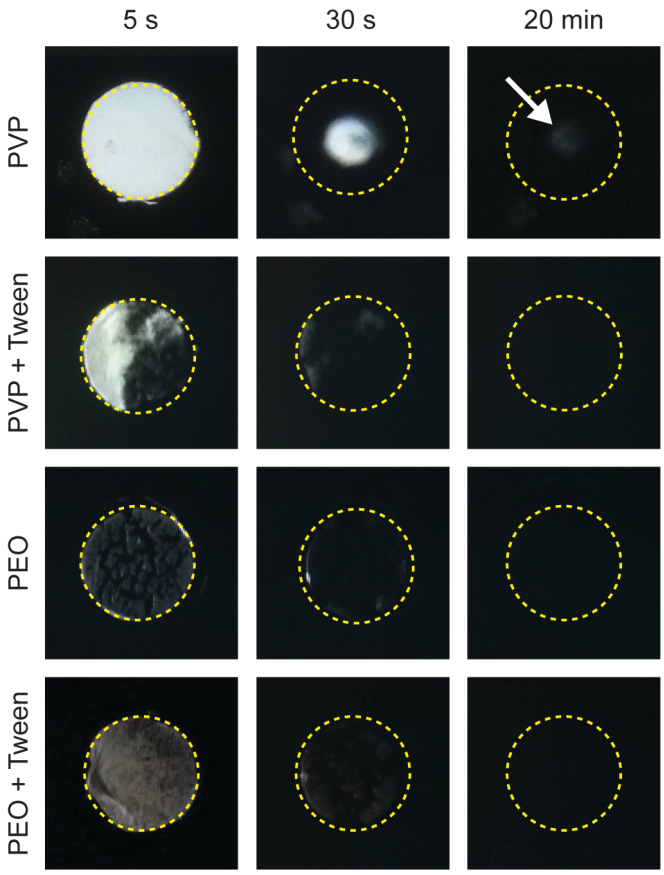

Figure 3.9—Incorporating Tween 20 into PVP or PEO fibers containing 9 wt% maraviroc led to more rapid and total dissolution of fibers and encapsulated maraviroc on a moist porous surface of 1.5% agar at 37 °C. 9 wt% maraviroc discs hydrated more rapidly than corresponding 28 wt% maraviroc discs. The original perimeters of the 9 wt% maraviroc fiber discs are shown as dashed circles. Images are arranged by fiber type (row) as seen over time (column). A visible precipitate remained in hydrated fiber gels after 20 min for PVP fibers without Tween 20 (white arrow). Images are representative samples of n = 3 independent experiments.

3.04.6 Tween 20 cytotoxicity and antiviral activity of maraviroc following sink release

The *in vitro* LD_{50} values of the tested surfactants were: Tween 20 = 0.24 %wt/vol, Tween 80 = 0.32 %wt/vol, glycerol monolaurate = 0.022 %wt/vol, and nonoxynol-9 = 0.0053 %wt/vol when exposed to TZM-bL cells in cDMEM for 24 h (Figure 3.10). The antiviral activities of pure maraviroc and maraviroc released from electrospun formulations were identical *in vitro* (Figure 3.11) and consistent with values reported in literature. No toxic effects due to drug eluates were observed. The estimated IC_{50} values for each individual dose-response curve were not significantly different from one another (P = 0.924). The globally shared best fit IC_{50} value for maraviroc was found to be 6.96 ng/mL, (13.5 nM), which is consistent with previous findings for

maraviroc using this *in vitro* assay [79]. These results show that maraviroc was fully potent following release from electrospun fibers into release media.

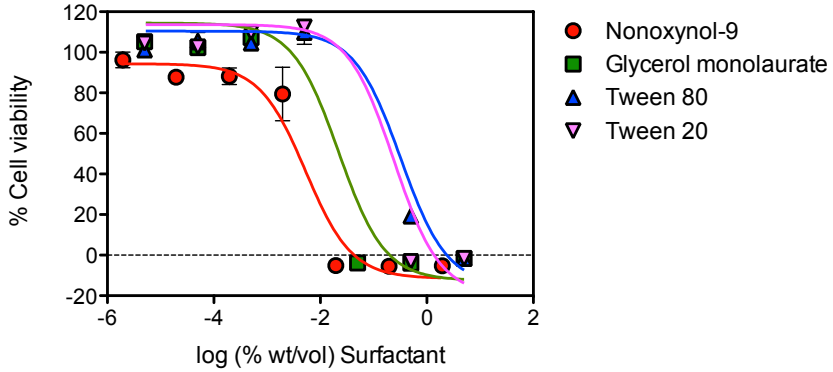

Figure 3.10—We tested the relative toxicity of Tween 20 compared to other surfactant products that have either been used in microbicides (nonoxynol-9 and glycerol monolaurate) or are analogous to Tween 20 (Tween 80). This *in vitro* assay using TZM-bL cells, while far from an *in vivo* test of the surfactants' effect on the cervicovaginal epithelium, suggested that Tween 20 was approximately 50 times less toxic than nonoxynol-9.

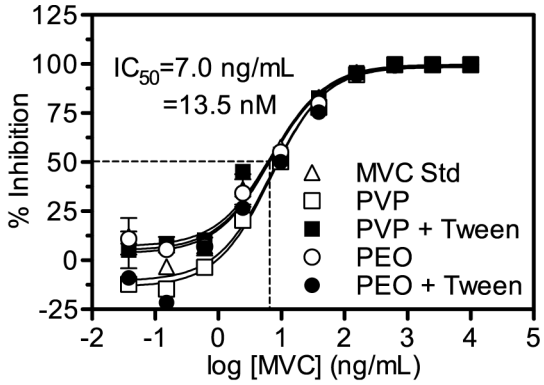

Figure 3.11—Incorporation of maraviroc into electrospun fibers does not decrease drug potency against HIV in vitro. Eluates from 28 wt% maraviroc fibers in pH 4.0 citrate buffer were tested alongside neat maraviroc for antiviral activity against HIV-BaL using a TZM-bL cell reporter assay. There was no difference between the IC_{50} values of neat and formulated maraviroc. All treatments were diluted serially 10 times. Data represent mean values from duplicate wells (n = 2), except for eluates from PVP and PEO + Tween fibers (n = 1). Error bars represent SD.

3.05 Discussion

Maraviroc is promising as a microbicide because of its potency, good toxicity profile, and CCR5-tropism [61,70,117]. In recent years, the pharmacokinetics of maraviroc in nonhuman primates following the administration of maraviroc-containing vaginal gels [61,117,118] and vaginal rings [57,70] have been reported. These pharmacokinetic and efficacy studies have demonstrated that intravaginal maraviroc is rapidly absorbed in macaques and can provide high levels of protection against high dose SHIV-162P3 challenge. However, the efficacy of maraviroc in these trials has been strongly dependent on both the dose and the time of administration. For example, formulations of maraviroc into hydroxyethylcellulose gels poses challenges since a minimum drug loading of 3.3 wt% is required for 100% efficacy, but the drug is not soluble in the gel at this level. Achieving higher doses with a vaginal gel would require greater gel volumes, which would likely result in dose leakage[88]. Solid dosage forms like films could provide higher doses without causing leakage problems, but films have not yet demonstrated high antiretroviral drug loading capacity [51,63]. Furthermore, the efficacy of maraviroc gels decreased when they were applied 1 hour instead of 30 min before challenge[118], suggesting that maraviroc microbicides should be designed for use as close to the time of viral exposure as possible. In other words, a dry dose maraviroc microbicide should dissolve quickly. Since electrospun fibers possess a large surface area for hydration and drug dissolution, they may be ideally suited for pericoital administration of maraviroc.

We showed that electrospun PVP fibers released maraviroc rapidly enough to warrant further investigation as a pericoital anti-HIV microbicide product. Either lowering drug loading or adding Tween 20 as a wetting agent could reduce the time to 100% drug release. Furthermore, the fibers rapidly hydrated in low fluid volumes, transforming the solid fiber dosage into an apparent spreadable gel. Such rapid hydration and drug release might simultaneously accomplish four important tasks. First, rapidly dissolving fibers might be ideally suited for pericoital release of protective levels of maraviroc to the vagina less than 30 minutes before sex, which has been shown in gel efficacy studies to maximize protective efficacy of maraviroc loaded HEC gels [117,118]. Due to the high drug loading in electrospun fibers, 132 mg of maraviroc could be delivered with less than 500 mg of electrospun fibers. Second, rapid hydration rates of fibers may minimize the risk of epithelial abrasions caused by the intravaginal dosage form if applied immediately before sex. The observation that fibers transform into a semi-solid with gel-like properties could prevent the sensation of “dry” sex often attributed to dry dose microbicides[67]. Also, since high molecular weight polymers (M_w > 100 kDa) are utilized for electrospinning, the osmolality of dissolved fibers may be significantly lower than that of

dissolved films incorporating lower molecular weight polymers (PVA with M_w ~10 kDa) and excipients like PEG 400 and glycerol (~10-100 times lower moles of solute per volume in fibers than films). However, this observation depends on several complex factors and should be further tested. Third, since the microbicide products would be applied as a dry dosage form, retention of the drug dose may be higher than if it were applied in a 3-4 mL volume of gel. Finally, fibers may be designed for discreet spontaneous use without the need for partner consent. While the form of a fiber-based microbicide is still undefined, numerous product forms may be envisaged. Fibers could be shaped for insertion with or without an applicator. Disadvantages of an applicator are the added cost, complexity, and potential for abrasions. Likewise, finger insertion may be complicated by moist fingers preventing full insertion of the dose should it hydrate too rapidly. Despite these complexities, the soft, flexible nature of electrospun materials, which resemble fabrics with a microscopically fine texture, may help make them acceptable to users in a number of different delivery formats. For these reasons, local maraviroc delivery from microbicide fibers may fill a gap in the current microbicide product portfolio.

In order to understand the drug release properties from different formulations used in our study, we examined fibers using electron microscopy, chemical analysis, and calorimetric techniques. We observed clear trends in drug distribution, crystallinity, and fiber properties on drug release kinetics, which will be useful for informing the design of future electrospun microbicides. While some of these properties, such as drug crystallinity, had little impact for the delivery of maraviroc from fibers, they have been shown to be of considerable significance for other drugs used in microbicides. For example, Johnson et al. showed that greater crystallinity of tenofovir in the core of an intravaginal ring led to lower daily release rates of the drug [54,55]. In this study, our characterization suggested that water penetration into and subsequent drug release from materials slowed in response to higher drug loading due to a combination of reduced hydrophilicity of maraviroc versus the base polymers, increased drug crystallinity, and drug surface enrichment.

Visual observations of the fibers during release experiments and images of fibers hydrating and disintegrating on agar plates (Figure 3.8, Figure 3.9) revealed correlations between the apparent extent of fiber hydration and the percent of maraviroc released from fibers. While we did not directly measure polymer hydration, swelling, or dissolution, it is worth discussing the role that the composition of the fibers had on the hydration and subsequent release of maraviroc. Our electrospun materials contained high levels of drug, which significantly altered the hydration behavior of the polymer matrix. Maraviroc was formulated into fibers as a neutral

compound, and no salts were present in the electrospinning solutions. Once hydrated, however, protonation would be rapid, and maraviroc would be >99% ionized at pH 4.0. Despite this predicted ionization, increasing the proportion of the drug in PVP and PEO fibers led to longer times to >95% drug release (Figure 3.7), which is likely due to maraviroc being less hydrophilic than either the PVP or PEO base polymers alone. Similar effects of high drug loading on the mechanism of drug dissolution from tablets has been observed using Raman spectroscopy[184].

The impact of media pH on drug release from anti-HIV microbicides is important for evaluating the potential impact of elevated vaginal pH (due to natural variation, infection, the presence of semen, tampon use, heavy menstruation, douching, etc.) on device performance. We found that increasing the pH of release media from 4.0 to 7.0 significantly increased the required time to dissolve micronized maraviroc crystals under sink conditions from less than 2 min to overnight. This might correspond to a decrease in the percentage of maraviroc molecules that are ionized at the tropane ring (pKa = 7.84), and we estimated that only 86% of maraviroc is ionized at pH 7.0, compared to >99% of maraviroc at pH 4.0. In contrast to micronized drug, maraviroc release from PVP fibers with 28 wt% loading required 4.6 min to release 50% drug content at pH 7.0 compared to 1.9 min at pH 4.0 (20 min versus 14 min for >95% release). Thus, while reduced ionization could have slowed hydration and retarded release rates from fibers, especially at loadings as high as 9-28 wt%, solid dispersion within electrospun fibers might offer clear dissolution advantages over the delivery of micronized drug particles. Such pH dependencies imply that release will likely be slower in animal models with higher vaginal pH (e.g., macaques), or if used for rectal application to prevent transmission during receptive anal intercourse among either heterosexual populations or men who have sex with men. Other ionizable antiretrovirals would likely show analogous pH dependencies.

Incorporation of Tween 20 into fibers accelerated drug release (Figure 3.7) and apparent dissolution time on agar plates (Figure 3.8, Figure 3.9). Since Tween 20 did not appear to have a plasticizing effect on PVP or PEO, we expect that this was not the major mechanism behind the accelerated drug release from surfactant-loaded fibers [185]. It is also possible that Tween 20 on or within fibers allowed water to penetrate the matrix more quickly given that Tween 20 is more hydrophilic than maraviroc. While Tween 20 accelerates drug release, it does not seem to enhance maraviroc's solubility in the release media (Figure 3.6). The use of surfactants in a microbicide formulation is a rightly controversial issue, as surfactants may be toxic to epithelial tissue. Increased risk for HIV infection can result from repeated epithelial disruption by detergents such as noonoxynol-9 [21]. Therefore, when designing a vaginal drug delivery system, it is of paramount importance to select a surfactant that poses little to no risk to vaginal and

cervical tissue when applied topically. Tween 20 is a common wetting agent that may be useful for increasing the rate of drug release, and could have an acceptable threshold for toxicity *in vivo* but was not tested here. There is limited but insufficient precedent for the safe repeated use of Tween 20 in vaginal formulations. The gel Conceival (a potential microbicide for lipophilic drug delivery) contains 2-4 wt% Tween 20 and is nontoxic in rabbits and to rabbit and human sperm [186]. Our rationale for formulating Tween 20 into fibers at 4 %wt Tween/wt polymer was to examine the effects of an upper limit of surfactant levels on drug release from fibers. It is possible that much lower concentrations could be used to preserve the beneficial effects of Tween on drug release rates while minimizing concerns about toxicity. Our *in vitro* testing of surfactant cytotoxicity shows that Tween 20 and Tween 80 are tolerated 10 times better than glycerol monolaurate (shown to be safe in macaques [159] but potentially harmful in mice [167]) and 50 times better than nonoxynol-9 by TZM-bL cells, with an LD_{50} for Tween 20 of 0.24 %wt/vol in cell culture media (Figure 3.10). The *in vivo* toxicity of electrospun fibers containing low amounts of Tween-20 remains to be evaluated. Depending upon the required drug dosage and drug loading, it may not be necessary to include wetting agents to achieve rapid delivery with electrospun fibers.

Maraviroc was amorphous in PVP and semi-crystalline in PEO, yet despite this difference in physical state, release of maraviroc was similar from the two polymer types (Figure 3.7). In addition, the crystallinity of maraviroc in electrospun PEO materials had an insignificant impact on the dissolution of maraviroc into pH 4 media on the time scale of 15 min, which we attribute to the small physical size of crystalline drug present in the fibers. Consequently, it can be argued that drug crystallinity was not the principal determinant of the either the rate of hydration or the time to 100% release. Previous work by Peppas et al. has shown that the crystallinity of hydrophilic polymers can have a large effect on drug release rates [187]. Since the crystallinity of the PEO in our fibers was effectively constant over the range of drug loadings tested, neither drug nor polymer crystallinity likely explains the significantly retarded water uptake at higher drug loadings. In fact, our observations imply that as long as the size of the crystalline domains is small and the drug is readily ionizable in the media, the dissolution of maraviroc will not likely be slow due to the crystalline state of the drug.

The highly loaded materials used in this study were electrospun using a mild process with high productivity and material efficiency. In addition to solvent safety, no high temperatures were needed to create these materials, and electrospinning proceeded at ambient conditions (19-23 °C, 40-60% relative humidity). Although electrospinning relies upon high voltage, spinning requires a very low current and therefore little energy. The materials in this study were

successfully loaded with up to 28 wt% maraviroc. Higher drug loading is possible and would result in smaller applied fiber doses, but may be an important cost constraint. Increased drug loading did not reduce productivity, and we observed high material efficiency (88-94% for PVP materials) resulting in a fiber production rate of ~7 mg/min using a bench top instrument with a single nozzle. We recently reviewed the scale up potential and expected cost of electrospun microbicides, finding that current electrospinning technologies are capable of producing up to 6.5 kg of fiber every hour (10-20 million doses annually), at a projected cost of $0.50 to $3.00 per dose depending upon a large number of factors such as initial investments in capital, material costs and production volume [110].

Although this study focused on the intravaginal delivery of maraviroc fibers, similar materials may be developed for rectal delivery or for indications other than HIV prevention. Recent work by Massud et al. suggested that rectal delivery of maraviroc gels lacks efficacy in a macaque SHIV challenge model, and may be complicated by effects of rectally applied maraviroc on populations of $CD3^+/CCR5^+$ cells [115]. It remains to be seen if maraviroc can serve as an effective microbicide in humans, either intravaginally or rectally. Previous work on electrospun microbicides has demonstrated the ability to load and release other APIs, including acyclovir (anti-HSV-2), tenofovir (anti-HIV/HSV-2), glycerol monolaurate (anti-sperm, antimicrobial, anti-inflammatory), and even whole live lactobacilli (anti-bacterial vaginosis) [78,79,188]. We expect that fibers will be capable of delivering a full range of APIs for not only anti-HIV microbicides but also for treatment and prevention of bacterial, fungal, and viral infections.

3.06 Conclusions

Electrospun PVP fibers can deliver a high dose of maraviroc under mildly agitated sink conditions within minutes following initial contact with release media. Maraviroc is currently a lead antiretroviral compound for formulation into anti-HIV topical microbicides including rings and gels. It is highly potent against CCR5-tropic viruses, and has no major side effects. Based on clinical and preclinical studies of the drug's pharmacokinetics and ability to prevent viral transmission, it seems likely that maraviroc will be most effective when incorporated into a microbicide platform that allows for a rapid release of high levels of maraviroc within 30 minutes before viral challenge. In particular, the microbicide product should act locally, achieve high vaginal retention, minimize leakage, and enable coformulation with other APIs. Our current work demonstrates the need for rigorous physical and chemical characterization of new materials in order to better understand and engineer such novel anti-HIV vaginal microbicides.

3.07 Acknowledgements

The authors would like to acknowledge G. Hammer and L. Gamble from NESAC/BIO (NIH P41 EB-002027) for conducting XPS experiments, the UW NNIN for assistance with SEM imaging, and Y. Jiang for performing the *in vitro* anti-HIV activity assay. C.B. was supported by a National Science Foundation Graduate Research Fellowship, and the research was funded by NIH grant AI098648 awarded to K.A.W.

Chapter 4. "Set it and forget it" anti-HIV microbicide fabrics produced by coaxial electrospinning

4.01 Abstract

Current microbicide formulations fail to provide both instant and multi-day sustained antiretroviral delivery with a single dose. Such products could be particularly useful for delivering maraviroc, which is required at high doses for efficacy but absorbed rapidly in the vagina. To address this need, we electrospun a composite fabric that provides both a rapid burst and a multi-day sustained release of maraviroc. Fully tunable sustained release was achieved via coaxially electrospun ethyl cellulose (EC) and polyvinylpyrrolidone (PVP) fiber architectures with up to 37.5 wt% drug loading, and layering with rapid-release fibers allowed independent control over the ratio of burst (20 min) and sustained (120 h) release from composite nanofiber fabrics. This work contributes to our ability to engineer core-shell electrospun fibers for the sustained release of hydrophilic small molecule drugs, and proposes controlled surface wetting of core-shell fibers as the primary mechanism for sustained release from EC/EC and EC/PVP fabrics.

4.02 Introduction

HIV/AIDS is the leading cause of death among women of reproductive age in the world [2]. The majority of new HIV infections in women occur via the genital tract during heterosexual intercourse. Because of the enormity of the HIV epidemic, developing effective prevention technologies, including anti-HIV microbicides, has been a priority for biomedical researchers. Anti-HIV microbicides are topical products, applied vaginally or rectally, that aim to reduce the risk of HIV infection by interfering either nonspecifically or specifically with viral infection [41]. After a series of failed clinical trials testing anti-HIV microbicides with nonspecific mechanisms of action, a Phase IIb clinical trial (CAPRISA 004) of a vaginal gel containing 1% tenofovir, a nucleotide analogue reverse transcriptase inhibitor, was the first to demonstrate a reduction in the risk of contracting HIV [36]. Women in a tenofovir gel group were 39% less likely to be infected by HIV than women in a control gel group. Epidemiological modeling has suggested that such a microbicide might avert millions of new HIV incidences and AIDS deaths [189]. Despite the promise of microbicides, recent trials have continued to yield disappointing results that point to a need for improved efficacy by enhancing user adherence to anti-HIV interventions [42]. It is now

apparent that multiple product types (i.e., drug delivery systems), not just vaginal gels, will be necessary to achieve widespread adoption of and adherence to anti-HIV microbicides.

Current microbicides can be classified into two broad categories based on their intended time of application relative to sexual activity. Coitally dependent (i.e., pericoital) microbicides are meant for use at or around the time of sex. Gels [36,52,190], films [51,63], tablets [66,68], and rapidly dissolving nanofiber fabrics [79,120] are examples of pericoital microbicides. Such products have the advantage of rapid on-demand drug delivery. Disadvantages include historically low user adherence in clinical trials that seems to vary by population and dosing regimen (BAT24, daily, precoital and postcoital). For active agents with short half-lives following intravaginal administration, pericoital products can also suffer from short therapeutic duration [118]. The second category of microbicides, coitally independent (i.e., sustained release) microbicides, are seen as a potential solution to low user adherence and short therapeutic duration, and are meant for up to 90 days of nearly continuous use. Intravaginal rings [53,70,71,73,74] are examples of coitally independent microbicides. The strength of intravaginal rings lies in their ability to remain in the vagina and release antiretroviral compounds over long periods without relying upon frequent application. While rings offer clear technical advantages for HIV prevention, it is unlikely that all women at risk of HIV infection will choose to use them due to cost, concerns about chronic exposure to antiretroviral drugs, and cultural or individual preferences. Recently, interest has grown in developing a third microbicide category to combine the benefits of pericoital products like gels and sustained release products like vaginal rings—products with multiple-day to weeklong release of antiretrovirals.

Recent research on user perceptions and expectations of microbicide products suggests that multiple-day prevention products that also provide instant protection from HIV or other STIs could be popular among women, at least in the United States [76]. Such products could simultaneously provide pericoital protection and enhance efficacy due to replacement of metabolized or excreted drug, leading to the nickname “set it and forget it” microbicides. Many existing microbicide platforms might be adapted for this purpose. For example, vaginal gels (in the form of a silicone elastomer) [61] and tablets (in the form of osmotic pumps) [69] have begun to address this gap. Maraviroc, a CCR5 antagonist that inhibits fusion of CCR5-tropic HIV-1 to target cells [112], might especially benefit from this rapid-then-sustained delivery approach due to its relatively short half-life following intravaginal administration in aqueous gels [117,118]. Here, we develop a new class of microbicide delivery systems using core-shell electrospun nanofiber fabrics to release maraviroc under sink conditions (i.e., drug is freely soluble in release media) over 3 to 5 days *in vitro*. We previously published on electrospun solid dispersions of maraviroc

for rapid drug delivery [120]. Here, we physically combine those rapid-release fibers with ethyl cellulose (EC) and polyvinylpyrrolidone (PVP) coaxial sustained release fibers, and demonstrate that layered fiber composites release maraviroc *in vitro* in a manner that is consistent with the desired release profile for "set it and forget it" microbicides. Similar fiber composites might be applied to deliver multiple drugs in combination while allowing independent control over the rate of drug delivery for each compound. Electrospun fabrics are white, soft, and foldable [79], and represent a truly distinct drug delivery system from existing microbicides. By expanding the choice of available microbicide products, these core-shell electrospun fabrics could one day help expand the prevalence of microbicide use in at-risk populations.

Electrospun fabrics are composed of nano- or microfibers and have diverse applications in drug delivery. Interest in electrospun fabrics for controlled release applications has fostered the development of drug-eluting core-shell fibers. Produced by coaxial electrospinning, core-shell fibers have controlled nano-architectures, allowing active agents to be loaded within a fiber core and sheathed by a release modulating polymer shell. Because coaxial electrospinning localizes active agents to the core of fibers, the resulting fabrics promise to eliminate the burst release often obtained from traditional (uniaxial) electrospun fabrics.

Despite the potential of core-shell fabrics, there is little precedent for demonstrating sustained release of hydrophilic small molecule drugs from highly loaded materials. In most cases, tunable and sustained release has been limited to the delivery of macromolecules (e.g., proteins and nucleic acids) [99,191-193] or hydrophobic small molecules [99,194-196], whose large size, poor solubility, or preferential partitioning into insoluble polymers mediate slow release. For example, Jiang et al. reported on the controlled release of BSA from core-shell fibers with a PEG-PCL shell and a dextran-BSA core in 2006. Increasing PEG concentration led to greater porosity in the PCL shell, which accelerated protein release from the water-soluble dextran core [191]. Six years later, Su et al. reported similar release from a more complicated system of PLLACL-collagen shell and PLLACL-collagen-drug core fibers loaded with BSA, BMP2, and dexamethasone. These fibers achieved sustained release of all three components over 2 weeks. Although dexamethasone is a small molecule drug, it is highly insoluble and hydrophobic, and was only loaded at 0.1 wt% in the core-shell fibers [99].

Minute drug loading is typical of sustained release fibers, since increasing drug loading often increases the tendency of materials to burst. For example, Yu et al. reported on the extended release of ketoprofen, a poorly soluble hydrophobic drug, from core-shell fibers prepared from the corn protein zein (both shell and core). While these materials reached a more significant 9 wt% loading of ketoprofen, they released all of the drug within just 16 h [197].

Similarly, Li et al. prepared core-shell fibers containing 4.7 wt% of the poorly soluble drug naproxen, which burst released from fibers in just 15 h. Placing the drug inside of liposomes that were then further loaded into the cores of core-shell fibers ultimately achieved sustained release, but the resulting drug loading was only 0.48 wt% and 40% of the naproxen burst within 8 h before slowly releasing out to 275 h [196].

Hydrophilic small molecules in particular are usually loaded at extremely low levels into core-shell fibers to avoid burst release, making them impractical for biomedical applications requiring high drug dosing. Where clinically relevant loading has been achieved, the release was usually extended over just 24 h. For example, Viry et al. demonstrated sustained release of the hydrophilic drug levetiracetam from PLGA/PLGA-w/o emulsion core-shell fibers over 20 days *in vitro*, but the drug loading was only 0.28 wt%--far below relevant levels for levetiracetam's clinical application [198]. In contrast, Thitipun et al. loaded amoxicillin into cellulose-acetate shell, gelatin core fibers containing 3 wt% amoxicillin. This system increased drug loading to potentially useful concentrations. However, release was only extended for 24 h [199]. Wang et al. published an extensive report on the formation of core-shell PHB/PDLLA and PDLLA/PHB fibers for the release of the drug dimethyloxalylglycine (>30mg/mL solubility) out to 30 days *in vitro*. Wang et al. also explored the effect of varying the shell-to-core content ratio on drug release and fiber formation, which we replicate in our current work. Despite the level of detail in reporting on aspects of the PDLLA/PHB fiber formation and material properties, Wang et al. did not report the drug loading of their materials and it is uncertain whether this system was capable of achieving high drug content [200]. Sohrabi et al. described the most successful core-shell fibers for sustained hydrophilic drug release wherein PMMA shell and nylon-6 core fibers released 20 wt% ampicillin over 30 days. However, these PMMA/nylon-6 fibers had a significant burst release phase over 6 h [201]. Due to the small number of reports in this area, there is an unmet need to develop practical formulations for sustained hydrophilic small molecule delivery.

Here we aimed to develop core-shell electrospun fabric formulations that might sustain the release of the anti-HIV drug maraviroc to the female reproductive tract with intended use as topical anti-HIV microbicides. As human vaginal pH normally ranges between pH 4 and pH 6 [108], vaginally administered maraviroc behaves as a hydrophilic and slightly soluble drug (logP = -0.32 ± 0.12) [57]. This work makes significant contributions to: 1) loading high amounts of hydrophilic drug into core-shell fabrics, 2) controlling its release from core-shell fabrics, and 3) understanding the important mechanisms governing release. In this work, we electrospin various core-shell fibers from ethyl cellulose (EC) and polyvinylpyrrolidone (PVP) for sustained

release of >0.1 mg/mg maraviroc/core-shell fabric over at least 3 days. Furthermore, we demonstrate tunable release by controlling the nano-architecture of core-shell fibers. Throughout the literature presented above, it is commonly argued that release from core-shell fabrics is sustained relative to release from uniaxial fabrics primarily due to the presence of the polymer shell as an extra barrier to Fickian diffusion of active agents. We believe that while this mechanism is important for sustained release, it is often overemphasized and poorly supported by experimental evidence with regards to small molecules. The extensive literature on drug delivery from polymeric systems suggests that additional mechanisms, including capillary wicking [173], penetrant diffusion into shell and core polymers [202], polymer swelling [203], and matrix or drug ionization [204], likely play important roles in determining release characteristics from coaxially electrospun drug delivery systems. Here, we present experimental evidence that core-shell fabrics sustain hydrophilic drug release by a number of these familiar, interrelated mechanisms, of which shell-limited diffusion of drug is of secondary importance. These insights may be exploited in the design of future core-shell fabrics for controlled release. Additionally, by substituting metronidazole for maraviroc in fiber formulations, we demonstrate that core-shell fibers may serve as a general platform for the sustained release of clinically relevant levels of other hydrophilic small molecules and identify drug-specific challenges for successful formulation.

4.03 Materials and Methods

4.03.1 Formulation and electrospinning

Maraviroc was purchased through the University of Washington's Investigative Drug Services facility, and was purified and recrystallized from Selzentry® (ViiV Healthcare) as described previously [120]. Metronidazole, Ethyl cellulose (EC) with a viscosity of 22 cP at 5% in toluene/ethanol (80:20) and a 48% ethoxyl content, Polyvinylpyrrolidone (PVP) with a M_W of ~1,300,000 Da, and 2,2,2-trifluoroethanol (>99%) were purchased from Sigma Aldrich (St. Louis, MO). 100% ethanol (USP grade) was purchased from the University of Washington's biochemistry supplies store. Glycerol was purchased from ThermoFisher Scientific (Waltham, MA). EC was dissolved at 16% wt/vol in 2,2,2-trifluoroethanol. PVP was dissolved in ethanol at 12% wt/vol. Maraviroc was added to EC solutions at 10%, 20%, 30%, 50%, or 100% wt/wt maraviroc/EC. Maraviroc was added to PVP solutions at 25%, 40%, 50%, 75%, or 100% wt/wt maraviroc/PVP. Metronidazole was added to EC or PVP solutions at 50% or 100% wt/wt

metronidazole/polymer. Glycerol was added to PVP/metronidazole solutions at 0%, 20%, or 100% wt/wt glycerol/metronidazole.

All fibers were electrospun from a total solution volume of = 500 µL per run and collected onto a stationary grounded collector covered in wax paper. Uniaxial EC fibers containing maraviroc were electrospun with the following parameters: 2.54 cm long 25G stainless steel dispensing needle as nozzle, voltage = 15 kV, collection distance = 10 cm, flow rate (Q) = 100 µL/min. Uniaxial PVP fibers containing maraviroc were electrospun using parameters described previously [120]. Core-shell fibers were electrospun using a custom coaxial electrospinning nozzle machined at the University of Washington's physics machine shop. Coaxial fibers with a pure EC shell and a maraviroc-loaded EC core were electrospun with the following parameters: voltage = 19-23 kV, collection distance = 15 cm, total Q = 100 µL/min, ratio of shell solution flow rate (Q_S) and core solution flow rate (Q_C) Q_S/Q_C = 0.5, 1.0, 2.0, or 4.0. Coaxial fibers with a pure EC shell and a maraviroc-loaded PVP core were electrospun with similar parameters, except that the voltage = 19-21 kV and the collection distance = 19 cm. Uniaxial EC fibers containing metronidazole were electrospun with the following parameters: 2.54 cm long 25G stainless steel dispensing needle as nozzle, voltage = 15 kV, collection distance = 20 cm, flow rate (Q) = 50 µL/min. Coaxial fibers with a pure EC shell and a metronidazole-loaded EC core were electrospun with the following parameters: voltage = 24 kV, collection distance = 19 cm, total Q = 100 µL/min, ratio of shell solution flow rate (Q_S) and core solution flow rate (Q_C) Q_S/Q_C = 1.0, 2.0, or 4.0. Coaxial fibers with a pure EC shell and a metronidazole-loaded PVP core were electrospun with similar parameters, except that the voltage = 18-21 kV. Coaxial fibers with a pure EC shell and a metronidazole-loaded PVP/glycerol core were also electrospun with similar parameters, except that the voltage = 16-21 kV. Lower spinning voltages were required for stable coaxial jet formation when core solutions were either more conductive or represented a larger portion of the total flow rate. After electrospinning, fibers were removed from the wax paper, placed into foil packets, and lyophilized for at least 24 h to remove any residual solvent vapor. Fibers were then stored at ambient temperature (23°C ± 1°C) in heat-sealed plastic bags containing desiccant until use.

4.03.2 SEM imaging for fiber morphology and metronidazole stability assessment

Electrospun fibers were examined by SEM using a Sirion SEM (NTUF, UW) as described previously [120]. Fiber diameters were measured in ImageJ (NIH) by bisecting the SEM image diagonally with a line and manually measuring the diameters of fibers that the line intersected.

At least 25 fibers were measured per sample imaged, and fiber diameters were reported using the median and inner quartile range (IQR) as measures of the population's center and distribution, respectively. For images of core-shell fibers in cross section, fibers were cut with a scalpel blade. In order to visualize the core and shell regions of PVP core fibers in cross section, the cut sites were set into distilled water containing 0.1% Liquinox for 5 minutes before drying and imaging. These hollowed-out fibers were used to estimate outer and inner fiber diameters, shell thickness, and the ratio of inner to outer diameter (R_I/R_O). Comparisons between the R_I/R_O of fibers spun from different Q_S/Q_C ratios were made using ANOVA. The stability of metronidazole in core-shell fiber formulations was assessed by imaging a cut site created by scissors over 72 hours.

4.03.3 Mechanical testing

Mechanical tests were conducted on a single column screw-driven Instron 5943 universal materials testing machine (Instron Inc. Canton MA, USA) under 24 ± 1 °C and 45 ± 5 % RH in accordance with ASTM standard D5034-95. Dog-bone tensile specimens (ASTM standard D1708-96, 22 mm in nominal length and 5 mm in width) were prepared for both electrospun fibers and solvent-cast films. A total of 5 specimens were used for each mechanical test. Tensile tests were performed at a strain rate of 0.01 s^{-1}. Load and displacement data were obtained and used to calculate Young's modulus and tensile strength for electrospun materials.

4.03.4 Verification of core-shell structure by chemical surface analysis

XPS was performed using a Surface Science Instruments S-Probe at the University of Washington's NESAC/BIO surface analysis recharge center. Due to the surface sensitivity of XPS measurements, care was taken to prepare samples with no surface contamination. Freshly electrospun materials were collected onto aluminum foil and immediately lyophilized. Samples were analyzed in duplicate and illuminated with low intensity electrons to reduce charging of the insulated materials. Peak assignment and integration were performed using XPS analysis software (CasaXPS).

4.03.5 Construction of "set it and forget it" layered electrospun fiber composites

Composite materials were created using either a solvent weld or mechanical pressure to join materials, and 6 composites of each type were prepared. Solvent welding technique—First, 1" diameter discs of uniaxial maraviroc-loaded PVP fibers and coaxial maraviroc-loaded EC/PVP

fibers were placed on top of one another. Then, the cutting edge of a ¾" metal die (Grainger) was dipped into a shallow bath of ethanol and placed atop the stacked fibers to seal them together at their edges. Mechanical pressure technique—A square of uniaxial maraviroc-loaded PVP fibers and a smaller square of coaxial maraviroc-loaded EC/PVP fibers were cut out from fiber mats using scissors. The EC/PVP fibers were placed on top of the PVP fibers, and the protruding PVP fiber edges were folded over the EC/PVP fibers and firmly pressed for a few seconds using the edge of a blunt plastic ruler to fuse the PVP and EC/PVP materials around their perimeter.

4.03.6 *In vitro* release testing and drug loading measurement

¾" diameter samples were taken from fibers using a metal die. Sample thickness was measured using digital calipers and initial sample mass was measured using an analytical balance (Mettler-Toledo Inc.). Fibers were placed into 50 mL conical tubes with 25 mL of pre-warmed 37°C release media. Fibers were kept at 37°C in a rotary incubator at 200 rpm (VWR). At predetermined time points out to 120 h, 50 µL samples were removed and placed into HPLC vials, which were stored at -80°C prior to analysis. Rapid release of maraviroc from composite materials over the first 20 minutes was measured using a 7 rpm rotisserie shaker (Labquake, Thermo Scientific) as reported previously [120]. Release media included pH 4.0 10 mM citrate (154 mM sodium) buffer, citrate buffer with 0.1% vol/vol Tween 20, vaginal fluid simulant [134], and complete DMEM media (Gibco Life Technologies) containing 10% fetal bovine serum (Hyclone), 1% 200 mM L-glutamine (Invitrogen), and 1% 100x penicillin/streptomycin (Invitrogen). Media pH and surface tension were measured at 37°C. The extent of drug release was calculated as the mass of drug released from fibers relative to the initial fiber mass, as well as the cumulative % release from materials. Data points at < 60% release were used to perform curve fitting using the well-known Peppas equation.

$$\frac{M}{M_{total}} = kt^n$$

M is the amount of drug release as a function of time, M_{total} is the total amount of drug in the sample, and k (units of time^{-n}) and n are parameters estimated by regression using Prism (GraphPad).

The drug loading in the core-shell maraviroc fibers was measured by dissolving 5 mg of fiber samples in 1 mL of ethanol and then adding 9 mL of citrate buffer to precipitate the EC polymer content. After 24 h, samples were filtered through 0.22 µm filters to remove particulates and run through HPLC. Drug loading in 5 of the 24 core-shell maraviroc fiber formulations was

measured from three independently spun fiber samples. Drug loading in remaining formulations was measured with single fiber samples. Spiked controls containing 100% to 50% EC content and 0% to 50% PVP content were prepared in triplicate to validate the measurements. Theoretical drug loadings and fiber compositions were calculated from known mass fractions of polymers and drugs in solution, measured solution densities, and the Q_S/Q_C ratio used in the coaxial electrospinning process according to the equation

$$w_i = \frac{(Q_S/Q_C)\rho_{i,S} + \rho_{i,C}}{(Q_S/Q_C)TDS_S + TDS_C}$$

where w_i is the mass fraction of component i in the final fibers, $\rho_{i,S}$ is the mass concentration (mass per volume) of component i in the shell solution, and $\rho_{i,C}$ is the mass concentration of component i in the core solution.

HPLC analysis was used to quantify maraviroc and metronidazole release as well as measure drug loading from dissolved fiber formulations. A Shimadzu Prominence LC20AD UV-HPLC system equipped with a Phenomenex Kinetex C18 column (5 µm, 250x4.6 mm) and LCSolutions software were used to quantify drug levels in samples. The HPLC mobile phase consisted of a 60% 10 mM KH_2PO_4 buffer and 40% acetonitrile, filtered through 0.45 µm and glass frit filters to remove particulates. Maraviroc and metronidazole were freely soluble in the mobile phase. Maraviroc and metronidazole standard curves were prepared by dissolving 25 mg of maraviroc or 30 mg of metronidazole in appropriate release media to a concentration of 250 µg/mL or 300 µg/mL, respectively, and diluting serially at 1:2 until concentrations of ~100 ng/mL. The maraviroc standard in cDMEM was prepared by serially diluting stock maraviroc from citrate buffer into cDMEM. The maraviroc standard for drug loading determination contained 10% vol/vol ethanol. The maraviroc and metronidazole standards and unknown samples were detected by UV-HPLC as described previously [79,135]. Calibration curves were prepared in Prism (GraphPad) using $1/C^2$ weighting. The linear range was found to be from 64,000 ng/mL to 400 ng/mL for maraviroc and from 150,000 ng/mL to 300 ng/mL for metronidazole.

4.03.7 Measuring water content and mass loss *in vitro*

The water content and mass loss from fibers after 24 h or 120 h in release media was assessed by gravimetry. Fibers with an initial mass m_0 were removed from solution, and excess fluid was removed using a paper towel. The wet fibers were then massed using an analytical balance to assess their wet mass (m_W). Fibers were then stored at 40°C until they reached a

constant mass (24-72 h), which was recorded as their dry mass (m_D). Water content and mass loss were calculated as follows.

$$\%\ \text{water content} = \frac{m_W - m_D}{m_D} \times 100$$

$$\%\ \text{mass loss} = \frac{m_0 - m_D}{m_0} \times 100$$

4.03.8 *In vitro* cytotoxicity and anti-HIV activity of maraviroc

Fiber release eluates in cDMEM were used to verify the biological potency against HIV-BaL of released maraviroc relative to neat drug controls with an *in vitro* TZM-bL cell assay described previously [79,183]. Briefly, TZM-bL cells and HIV-1 BaL isolate were obtained from the NIH AIDS Research and Reference Reagent Program, Division of AIDS, NIAID, NIH (http://www.aidsreagent.org/). TZM-bL cells, a derived HeLa cell line that expresses CD4, CCR5, and CXCR4 [136-139], were added to black 96-well plates (Corning, Corning, NY) with Dulbecco's Modified Eagle Medium (DMEM) (Gibco Life Technologies) with 10% fetal bovine serum (Hyclone), 1% 100X penicillin/streptomycin (Invitrogen), and 1% 200 mM L-glutamine (Invitrogen) with 50 μL/well at a density of 5,000 cells/well. Cells were incubated in 5% CO_2 and 37°C for 24 h prior to exposure to surfactants or fiber eluates. For the antiviral activity assay, treatments were diluted serially. A second operator, blinded to the identity of the treatments, added each in 50 μL volumes into duplicate wells. 100 μL of HIV-BaL (240 TCID/well) was added to wells 1 h after drug treatment. Media was removed from cells after 48 h post-treatment, and 100 μL of phosphate buffered saline (Gibco Life Technologies) and 100 μL of Bright-Glo Luciferase reagent (Promega) were added to wells. Infectious activity was quantified by measuring luminescence on a plate reader (Tecan). IC_{50} values of the drug formulations were estimated using sigmoidal regression in Prism (GraphPad Software, Inc.).

4.03.9 Differential scanning calorimetry

Differential scanning calorimetry was used to investigate the interactions between ethyl cellulose, polyvinylpyrrolidone, and maraviroc in maraviroc-loaded EC/PVP core-shell fibers. Samples from all EC/PVP-maraviroc fiber formulations with a mass of 5-10 mg (n = 1) were placed into aluminum pans (T-Zero, TA Instruments) and analyzed with a TA Auto Q20 DSC instrument (TA Instruments). Samples were heated from 30°C to 250°C at a rate of 10°C/min with a nitrogen flow of 50 mL/min.

4.04 Results

4.04.1 Core-shell fiber formulation, structure, and mechanical properties

A coaxial electrospinning nozzle allowed us to create core-shell fibers with an EC shell and a maraviroc-loaded core of EC or PVP (Figure 4.1). By varying the core drug content and the ratio of the shell to core solution flow rates (Q_S/Q_C), we formulated 24 distinct core-shell maraviroc fabrics. In addition, we formulated 5 uniaxial maraviroc-loaded EC fabrics for comparison in release studies. These formulations are listed along with their drug loading in Table 4.1. Experimentally determined drug loadings were identical to theoretical drug loadings calculated based on solution composition and spinning flow rates (Table 4.2). SEM imaging revealed that core-shell electrospinning successfully formed smooth fibers with regular morphology and without major defects (Figure 4.1). In addition, SEM imaging of fiber cross-sections allowed direct observation of the EC/PVP fibers' core-shell architecture. We found that EC/PVP fibers had elliptic cross-sections and EC shells of uniform thickness (Figure 4.1). Importantly, the ratio of the shell thickness to the outer radius (δ/R_O) was significantly different between fibers spun with variable Q_S/Q_C ($P<0.05$), and the relative shell thickness increased with increasing Q_S/Q_C ($P < 0.05$).

To obtain further evidence of core-shell fiber formation, we used X-ray photoelectron spectroscopy (XPS) to interrogate the surface atomic composition of the EC/PVP fibers formulated 1) with the lowest and the highest concentrations of maraviroc in core PVP solutions, and 2) at the smallest and largest Q_S/Q_C values (Table 4.3). The atomic composition of EC/PVP fibers closely matched that of pure EC. However, at $Q_S/Q_C = 0.5$, small amounts of nitrogen and fluorine were detected on the fiber surface. Furthermore, the fluorine signal increased 2.5-fold in response to a 2.8-fold increase in maraviroc loading between EC/PVP-25 0.5 and EC/PVP-100 0.5 fibers. Thus, thicker EC shells were necessary to completely prevent detectable (XPS is sensitive to ~0.1 atomic %) amounts of maraviroc or PVP from reaching the fiber surface.

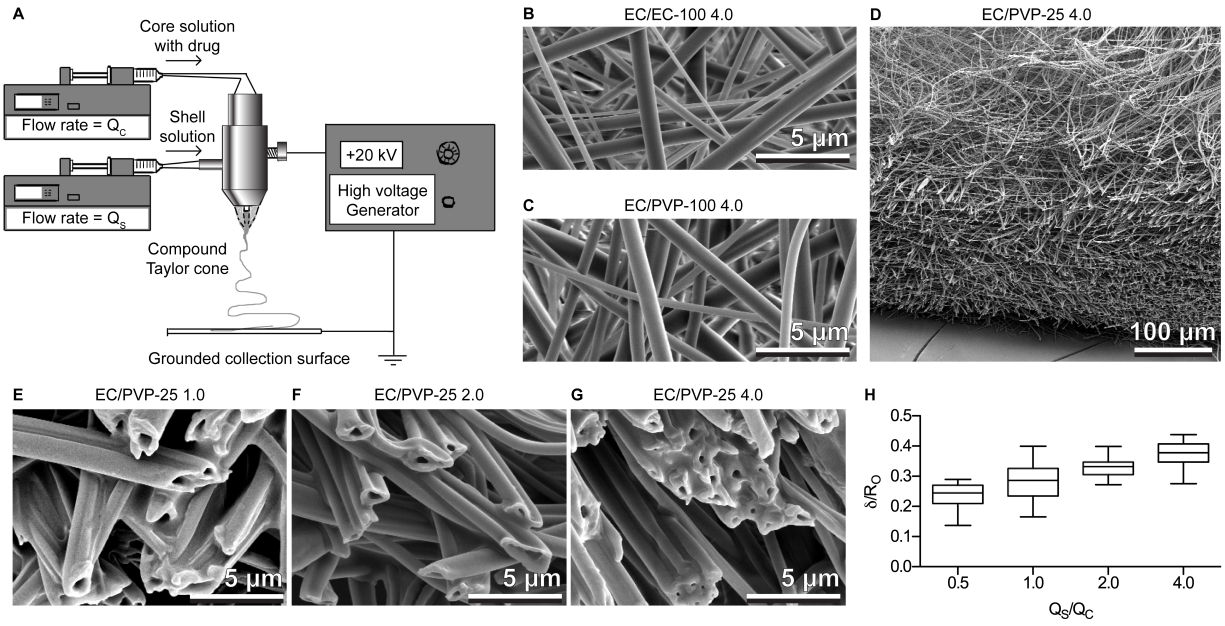

Figure 4.1— Coaxial electrospinning produces core-shell EC/PVP fibers containing maraviroc. A) Setup used for coaxial electrospinning. The core and shell polymer solutions are pumped separately through tubing to the coaxial nozzle, which produces a compound droplet of the two solutions. A high voltage generator induces formation of a compound Taylor cone and coaxial jet to form core-shell fibers. B-C) SEM micrographs at 5,000x magnification of EC/EC-100 4.0 and EC/PVP-100 4.0 fibers show smooth fiber formation. D) Cross-sectional image of EC/PVP-25 4.0 fabric. This SEM image reveals a highly porous network of regularly sized core-shell electrospun fibers. Fabric thickness is approximately 200 μm thick. E-G) SEM micrographs of EC/PVP-25 fibers in cross section, with cores removed, for Q_S/Q_C = 1.0 (E), 2.0 (F), and 4.0 (G). H) Higher Q_S/Q_C during electrospinning lead to thicker fiber shells (δ/R_O). Data are represented as box and whisker plots from min to max measured values, $P < 0.05$, $n > 10$.

Table 4.1—Maraviroc fiber formulations and their drug loading. Bolded formulations enabled sustained release of maraviroc at greater than 0.1 mg drug/mg fiber for at least 72 h in pH 4.0 citrate buffer. MVC = maraviroc. Naming format is “shell polymer / core polymer - %w/w MVC Q_S/Q_C”.

Formulation	Shell solution	Core solution	Q_S/Q_C	Final drug loading (wt%)
EC-10		16% EC + 10% w/w MVC in TFE	Uniaxial	9.09
EC-20		16% EC + 20% w/w MVC in TFE	Uniaxial	16.67
EC-30		16% EC + 30% w/w MVC in TFE	Uniaxial	23.08
EC-50		16% EC + 50% w/w MVC in TFE	Uniaxial	33.33
EC-100		16% EC + 100% w/w MVC in TFE	Uniaxial	50.00
EC/EC-50 0.5	16% EC in TFE	16% EC + 50% w/w MVC in TFE	0.5	24.68
EC/EC-50 1.0	16% EC in TFE	16% EC + 50% w/w MVC in TFE	1.0	19.60
EC/EC-50 2.0	16% EC in TFE	16% EC + 50% w/w MVC in TFE	2.0	13.88
EC/EC-50 4.0	16% EC in TFE	16% EC + 50% w/w MVC in TFE	4.0	8.76
EC/EC-100 0.5	**16% EC in TFE**	**16% EC + 100% w/w MVC in TFE**	**0.5**	**39.19**
EC/EC-100 1.0	16% EC in TFE	16% EC + 100% w/w MVC in TFE	1.0	32.22
EC/EC-100 2.0	16% EC in TFE	16% EC + 100% w/w MVC in TFE	2.0	23.77
EC/EC-100 4.0	16% EC in TFE	16% EC + 100% w/w MVC in TFE	4.0	15.59
EC/PVP-25 0.5	16% EC in TFE	12% PVP + 25% w/w MVC in EtOH	0.5	13.00
EC/PVP-25 1.0	16% EC in TFE	12% PVP + 25% w/w MVC in EtOH	1.0	9.63
EC/PVP-25 2.0	16% EC in TFE	12% PVP + 25% w/w MVC in EtOH	2.0	6.34
EC/PVP-25 4.0	16% EC in TFE	12% PVP + 25% w/w MVC in EtOH	4.0	3.77
EC/PVP-50 0.5	16% EC in TFE	12% PVP + 50% w/w MVC in EtOH	0.5	22.78
EC/PVP-50 1.0	16% EC in TFE	12% PVP + 50% w/w MVC in EtOH	1.0	17.31
EC/PVP-50 2.0	16% EC in TFE	12% PVP + 50% w/w MVC in EtOH	2.0	11.69
EC/PVP-50 4.0	16% EC in TFE	12% PVP + 50% w/w MVC in EtOH	4.0	7.09
EC/PVP-75 0.5	16% EC in TFE	12% PVP + 75% w/w MVC in EtOH	0.5	30.41
EC/PVP-75 1.0	16% EC in TFE	12% PVP + 75% w/w MVC in EtOH	1.0	23.57
EC/PVP-75 2.0	**16% EC in TFE**	**12% PVP + 75% w/w MVC in EtOH**	**2.0**	**16.25**
EC/PVP-75 4.0	16% EC in TFE	12% PVP + 75% w/w MVC in EtOH	4.0	10.03
EC/PVP-100 0.5	16% EC in TFE	12% PVP + 100% w/w MVC in EtOH	0.5	36.53
EC/PVP-100 1.0	**16% EC in TFE**	**12% PVP + 100% w/w MVC in EtOH**	**1.0**	**28.77**
EC/PVP-100 2.0	**16% EC in TFE**	**12% PVP + 100% w/w MVC in EtOH**	**2.0**	**20.20**
EC/PVP-100 4.0	16% EC in TFE	12% PVP + 100% w/w MVC in EtOH	4.0	12.66

Table 4.2—Calculated and measure maraviroc loading in core-shell electrospun fibers. Measurements represent single observations unless noted as mean (SD) of n=3 observations.

Formulation	Theoretical maraviroc loading (wt%)	Measured maraviroc loading (wt%)
EC/EC-50 0.5	24.68	26.23
EC/EC-50 1.0	19.60	20.98
EC/EC-50 2.0	13.88	15.03
EC/EC-50 4.0	8.76	9.00
EC/EC-100 0.5	39.19	38.20
EC/EC-100 1.0	32.22	26.72
EC/EC-100 2.0	23.77	18.35
EC/EC-100 4.0	15.59	14.99
EC/PVP-25 0.5	13.00	14.30
EC/PVP-25 1.0	9.63	9.10
EC/PVP-25 2.0	6.34	6.82
EC/PVP-25 4.0	3.77	3.87
EC/PVP-50 0.5	22.78	23.30
EC/PVP-50 1.0	17.31	17.14 (1.86)
EC/PVP-50 2.0	11.69	12.79
EC/PVP-50 4.0	7.09	7.71
EC/PVP-75 0.5	30.41	30.83
EC/PVP-75 1.0	23.57	24.82 (1.05)
EC/PVP-75 2.0	16.25	17.48 (1.43)
EC/PVP-75 4.0	10.03	11.17
EC/PVP-100 0.5	36.53	35.70
EC/PVP-100 1.0	28.77	28.86 (1.42)
EC/PVP-100 2.0	20.20	19.71 (0.61)
EC/PVP-100 4.0	12.66	11.77

Table 4.3—Chemical surface analysis of core-shell fibers by XPS. Values are listed as the mean (SD) of n = 2 samples

Formulation	% C	% N	% O	% F
Pure EC	64.0 (0.1)	---	36.0 (0.1)	---
Pure PVP	75.4 (0.3)	11.6 (0.4)	13.0 (0.1)	---
Pure MVC	76.1 (0.4)	11.8 (0.2)	5.9 (0.4)	6.1 (0.2)
EC/PVP-25 0.5	67.7 (0.2)	1.7 (0.4)	30.4 (0.3)	0.2 (0.1)
EC/PVP-25 4.0	66.5 (1.9)	---	33.5 (1.9)	---
EC/PVP-100 0.5	68.8 (0.5)	0.8 (0.6)	29.9 (1.1)	0.5 (<0.1)
EC/PVP-100 4.0	68.2 (0.2)	---	31.8 (0.2)	---

Electrospun core-shell fibers produced from core electrospinning solutions with 50% maraviroc were mechanically stretched under a uniaxial load, and the results are shown in Table 4.4. Fiber mechanical properties were dependent on both the core polymer type and Q_S/Q_C, but the effects of Q_S/Q_C were significantly different for EC/EC and EC/PVP fibers ($P<0.05$). The average modulus of EC/EC-50 fibers was minimally affected by Q_S/Q_C, and the tensile strength appeared to decrease slightly as EC shell content increased. In contrast, EC/PVP-50 fibers showed a doubling of the average Young's modulus as Q_S/Q_C increased from 0.5 to 4.0. The average tensile strength of the EC/PVP-50 fibers also increased 1.5-fold as EC shell content increased. Coaxially electrospun fabrics had a thickness of 310 ± 130 μm, a basis weight of 25 ± 3 g/m^2, a density of 0.09 ± 0.03 g/cm^3, and a porosity of 90% ± 3% (mean ± SD). Solvent cast films were significantly stiffer and stronger than maraviroc-loaded core-shell fibers (Table 4.5). This was expected, since the electrospun fabrics had an estimated porosity of 90% ± 3% (mean, SD). Differences between pure polymer and drug-loaded film properties did not correlate with those of core-shell fibers. Altogether, SEM, XPS, and mechanical testing provided strong evidence for core-shell fiber formation and enabled the determination of drug release mechanisms for these materials.

Table 4.4—Mechanical properties of core-shell fibers. Data represent the mean ± SD from n = 5 sample tests.

Formulation	Modulus (MPa)	Tensile Strength (MPa)
EC/EC-50 0.5	21.2 ± 3.2	1.2 ± 0.2
EC/EC-50 1.0	26.1 ± 7.9	1.3 ± 0.2
EC/EC-50 2.0	23.9 ± 3.0	1.0 ± 0.2
EC/EC-50 4.0	18.3 ± 3.2	0.7 ± 0.2
EC/PVP-50 0.5	12.9 ± 3.1	0.9 ± 0.3
EC/PVP-50 1.0	17.0 ± 5.3	1.3 ± 0.3
EC/PVP-50 2.0	18.7 ± 4.8	1.4 ± 0.2
EC/PVP-50 4.0	28.3 ± 4.6	1.4 ± 0.04

Table 4.5—Mechanical properties of solvent-cast polymer films. Data represent the mean ± SD from n = 5 sample tests.

Formulation	Modulus (MPa)	Tensile Strength (MPa)
EC film	1,600 ± 300	51.6 ± 16.3
EC-10 film	2,200 ± 200	22.2 ± 7.4
PVP film	1,100 ± 300	36.4 ± 9.7
PVP-10 film	2,300 ± 300	37.2 ± 8.1

4.04.2 Sink release of maraviroc from electrospun fibers

Our previous work showed that when formulated into uniaxial PVP fibers, maraviroc is released very rapidly as the PVP fibers hydrate, swell, and dissolve [120]. Our current results show that uniaxial EC fibers, in contrast, can provide sustained release of maraviroc for 120 h under sink conditions in pH 4.0 10 mM citrate (154 mM sodium) media (Figure 4.2). Uniaxial EC fibers loaded at or below 23 wt% maraviroc demonstrated very sustained and low levels of drug release over 120 h. However, at higher loadings, maraviroc released much more rapidly from fibers.

Figure 4.2—Sustained release profiles of maraviroc from uniaxial and core-shell fibers. Those formulations that meet ideal product specifications are shaded in green. A) The ideal release profile for an intermediate-term sustained release microbicide delivering maraviroc should achieve greater than 0.1 mg maraviroc released per 1 mg of applied fibers (to keep product size small for ease of vaginal application) by 72 h, and should not plateau prior to 72 h. B) Release

from uniaxial EC fiber formulations EC-10 through EC-100. C-D) Release from core-shell EC/EC fiber formulations with variable core loading and Q_S/Q_C. E-H) Release from core-shell EC/PVP fiber formulations with variable core loading and Q_S/Q_C. Data are shown as the mean and SD (error bars) of three independent release experiments.

We were able to improve the tunability of maraviroc release from uniaxial EC fibers by coating them with a pure EC shell using coaxial electrospinning. All EC/EC fibers sustained the release of maraviroc over at least 120 h (Figure 4.2). Some of the formulations (shaded in green) also met design targets for a sustained release maraviroc product (released > 0.1 mg drug per mg fiber at 72 h). Putting an EC shell around the solutions used to create EC-50 and EC-100 uniaxial fibers eliminated burst release while still allowing high drug loading (EC/EC-50 and EC/EC-100 fibers). Increasing core drug loading from 50% to 100% increased the rate of maraviroc release while increasing Q_S/Q_C reduced the rate of drug release (Figure 4.2, Figure 4.3). Curve fitting showed that maraviroc release from EC/EC fibers was sustained enough that it appeared to be nearly linear over a 120 h period for some formulations, but % release from most fibers was proportional to time$^{\sim 0.5}$. Significant, positive correlations were found between maraviroc content and the % drug release per time (slope, $P<0.05$). No significant correlation was found between maraviroc content and the power law exponent (Figure 4.3).

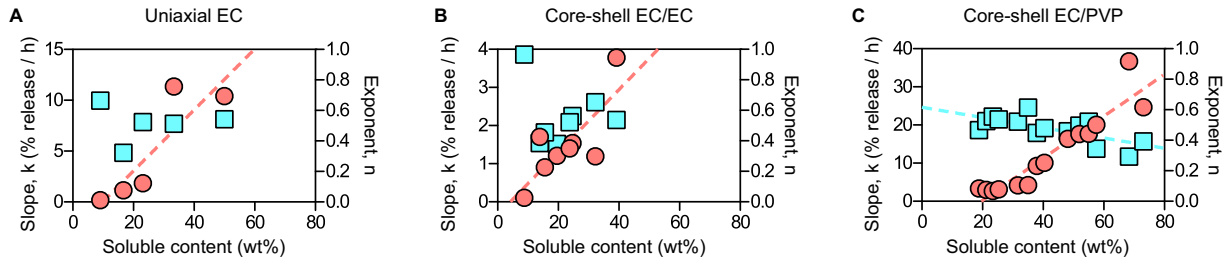

Figure 4.3—Peppas curve fit parameters for fibers releasing maraviroc into pH 4.0 10 mM citrate (154 mM sodium) buffer. The slopes, k, are shown as red circles ●. The exponents, n, are shown as blue squares ■. A) Parameters for uniaxial EC fibers. Significant correlations—k ($P<0.05$). B) Parameters for core-shell EC/EC fibers. Significant correlations—k ($P<0.05$). C) Parameters for core-shell EC/PVP fibers. Significant correlations—k, n ($P<0.05$).

Through the substitution of PVP for the EC core, we were able to increase the rate of drug release from EC shell fibers. These results demonstrate that PVP-maraviroc materials, which normally dissolve in minutes, can provide sustained release of drugs over 24 to 120 h with an EC shell. The magnitude of drug release increased regularly with drug loading. The time to

complete drug release also increased with Q_S/Q_C (Figure 4.2). For example, thin shells (Q_S/Q_C = 0.5) provided only 24 h maraviroc release, while thick shells (Q_S/Q_C = 4) provided at least 120 h maraviroc release. Correlations between the slope, k, or exponent, n, of power law parameters and soluble content (PVP and maraviroc) were significant and positive (k) or negative (n), respectively ($P<0.05$) (Figure 4.3).

4.04.3 Water content and mass loss

We measured the water content and mass loss from electrospun fabric materials after 120 h in citrate media (Figure 4.4). These measurements were also made at 24 h, and were roughly equivalent to those taken at 120 h (Figure 4.5). We found that all materials absorbed significant amounts of water, and that water content increased with total soluble content (maraviroc and PVP). Generally, core-shell EC/EC fibers had the lowest water content, followed by uniaxial EC fibers, and finally core-shell EC/PVP fibers. Since the 48% ethoxyl content EC polymer used in this study is capable of absorbing only 2 wt% water, the data are consistent with water uptake primarily into pores between adjacent fibers. All materials lost mass during release, but there were key differences between EC, EC/EC, and EC/PVP fabrics. While all of the mass loss from EC and EC/EC fabrics was attributable to the release of maraviroc, significant portions of mass loss in EC/PVP fibers with thin shells were attributable to dissolution of the core PVP polymer (Figure 4.4). EC/PVP fibers with thicker shells had little to no mass loss attributable to PVP, despite high water content relative to EC/EC fibers. It is likely that the EC shell is strong enough to resist bursting caused by a swollen PVP core. Based on the results of SEM imaging, XPS characterization, and mechanical testing, it is likely that the shells of EC/PVP fibers electrospun with Q_S/Q_C = 0.5 allowed maraviroc or PVP to reach the fiber surface, resulting in rapid water uptake and a rupture of the fiber shell. This corresponds to the rapid release of maraviroc from EC/PVP, Q_S/Q_C = 0.5 fibers by 24 h (Figure 4.5). PVP mass loss from EC/PVP, Q_S/Q_C = 1.0 fibers is more variable than from any other Q_S/Q_C ratio formulation, and release is intermediate between Q_S/Q_C = 0.5 and 2.0. This likely reflects a transition to complete encapsulation of the core PVP-MVC by the EC shell when Q_S/Q_C = 1.0.

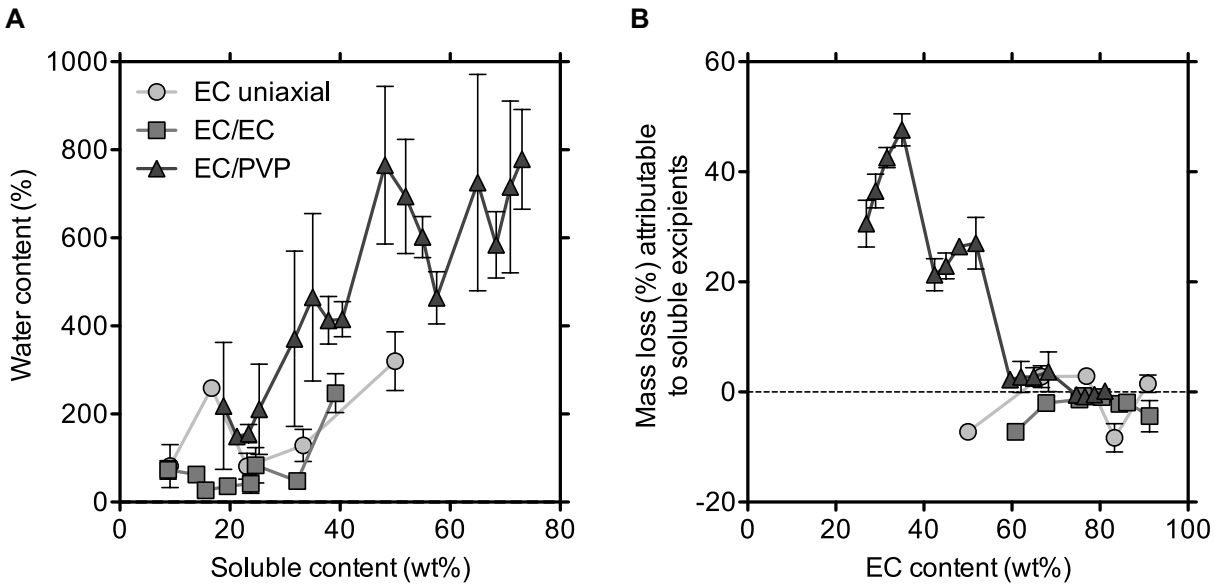

Figure 4.4—The material composition and structure of fibers influences water uptake and mass loss. A) Water content (%) in fabrics after 120 h in citrate release media as a function of total soluble content (maraviroc and PVP). Based on porosity estimates, complete displacement of air by water from fabric materials would result in ~900% water content. B) Mass loss (%) attributable to the loss of PVP or EC from fiber materials after 120 h in citrate release media as a function of total EC content. Note that EC/PVP fibers appear grouped by Q_S/Q_C with Q_S/Q_C = 2.0 or 4.0 experiencing little to no PVP loss. Data represent the mean and SD (error bars) of three independent experiments.

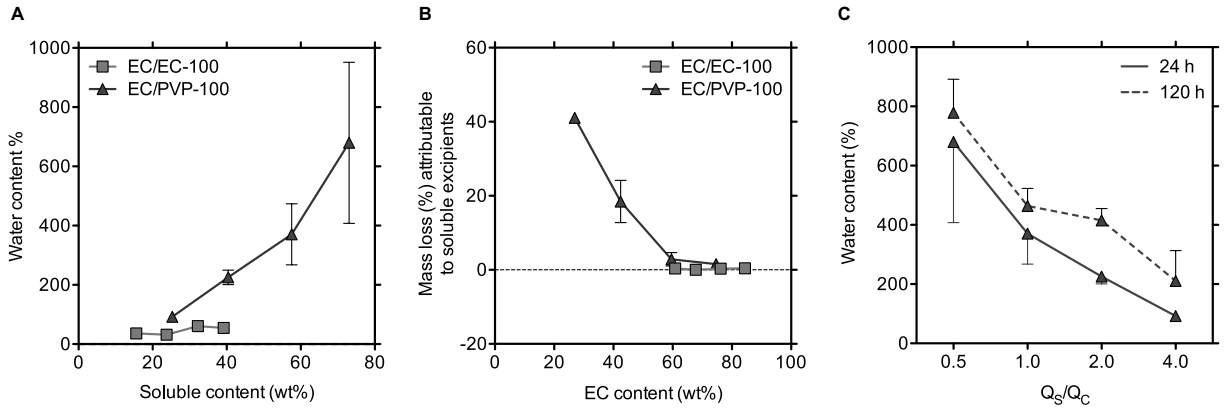

Figure 4.5— The material composition and structure of EC/EC-100 and EC/PVP-100 fibers influences water uptake and mass loss. A) Water content (%) in fabrics after 24 h in citrate release media as a function of total soluble content (maraviroc and PVP). Based on porosity estimates, complete displacement of air by water from fabric materials would result in ~900% water content. B) Mass loss (%) attributable to the loss of PVP or EC from fiber materials after 24 h in citrate release media as a function of total EC content. Note that EC/PVP fibers with Q_S/Q_C = 2.0 or 4.0 experience little to no excipient loss. C) Water content in EC/PVP fabrics was significantly dependent upon Q_S/Q_C and time in release buffer ($P<0.05$, 2-way ANOVA).

EC/PVP-100 fiber data represent the mean and SD (error bars) of three independent experiments. EC/EC-100 fiber data represent single experimental measurements.

4.04.4 Impact of *in vitro* release media on drug release and proposed mechanism

Our results show that shell wettability (surface chemistry), not the shell's presence as a barrier to drug diffusion (bulk property), is the primary determinant of the rate of drug release from core-shell fibers. To evaluate the relative roles of wetting and shell-limited diffusion, we measured release into different release media from maraviroc-loaded uniaxial EC, core-shell EC/EC-100, and core-shell EC/PVP-100 fibers with various Q_S/Q_C ratios. In addition to the citrate media previously mentioned, we chose to repeat release studies using pH 4.0 10 mM citrate (154 mM sodium) buffer with 0.1% vol/vol Tween 20, vaginal fluid simulant (VFS) [134], and cDMEM cell culture media. The surface tension and pH of these media are listed in Table 4.6. The hypothesis was that if the release of maraviroc were sustained primarily by virtue of unfavorable partitioning into or slow diffusion through the ethyl cellulose shell, then performing release studies in low surface tension media, which would cause complete air displacement and wetting out of fiber surfaces, would result in only minor accelerations in drug release.

Table 4.6—Properties of release media that affect the release of maraviroc from electrospun microbicide fabrics.

Media	pH	Surface tension (mN/m)
H_2O (18.2 MΩ-cm)	6.0	72.5
Citrate buffer	4.0	65.3
Citrate buffer + 0.1% Tween 20	4.0	35.8
VFS	4.2	59.1
cDMEM	8.0	57.5

In fact, drug release was dramatically altered in citrate media with 0.1% Tween 20. Uniaxial EC fibers had demonstrated a loading dependent transition from sustained to burst release in Tween-free citrate media (Figure 4.2). In contrast, all uniaxial EC fibers except for EC-10 fibers released their total drug contents within 1-8 hours in citrate media with 0.1% Tween 20 (Figure 4.6). Thus, the threshold drug loading leading to burst release from uniaxial fibers was dramatically reduced. Similarly, EC/EC-100 fibers demonstrated significant amounts of 1 h burst release with Qs/Qc = 0.5 or 1.0. However, release from thicker EC shell fibers remained

sustained out to 48-72 h despite high water content indicative of full fabric wetting (Figure 4.6, Figure 4.7). This suggests that EC may still play a minor role as a barrier to water penetration into or maraviroc diffusion out of core-shell fibers. EC/PVP-100 fibers all burst released a majority of their encapsulated MVC within 1 hour.

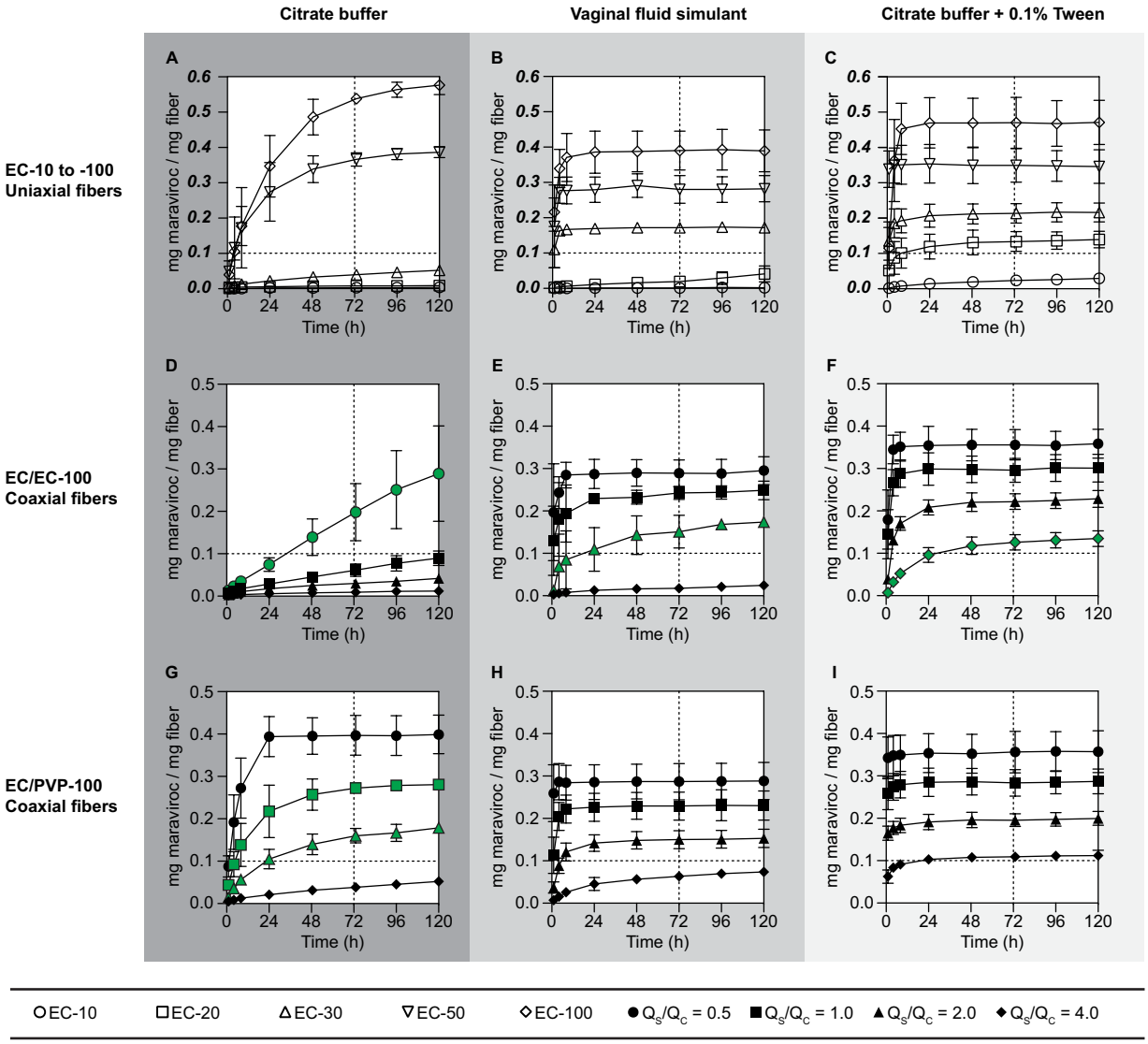

Figure 4.6—Effect of release media on drug release from maraviroc-loaded electrospun microbicides. Row 1: release from uniaxial EC formulations into A) citrate buffer, B) VFS, and C) citrate buffer + 0.1% Tween 20. Row 2: release from core-shell EC/EC-100 formulations into D) citrate buffer, E) VFS, and F) citrate buffer + 0.1% Tween 20. Row 3: release from core-shell EC/PVP-100 formulations into A) citrate buffer, B) VFS, and C) citrate buffer + 0.1% Tween 20. Formulations that meet the release target of > 0.1 mg drug per mg fiber in 72 h within each release media are highlighted in green. Data represent the mean and SD (error bars) from 3 independent release experiments.

Water content and mass loss measurements were taken at 120 h for all fabrics placed into citrate media with 0.1% Tween 20. These data reveal that by 120 h, all fibers had absorbed far more water than in citrate media without Tween 20, and were near their maximum absorbent

capacity based on estimated porosity values (Figure 4.7). Visual observations of fibers during release studies showed that all fibers appeared to wet completely by 8 h. In addition, estimates of mass loss attributable to polymer dissolution suggest that all EC/PVP-100 fibers completely lost their core contents. SEM images of fibers before and after drug release support our understanding of the release of maraviroc and PVP from the core of EC/PVP fibers. In instances where we detected total mass loss of core PVP by 120 h, SEM imaging revealed that the fibers had become flattened, as if hollowed out and then collapsed (Figure 4.8). The degree of fiber collapse depended on the release media, the formulation's shell thickness or integrity, and the core material (PVP or EC). There was no visible collapse of EC/EC fibers.

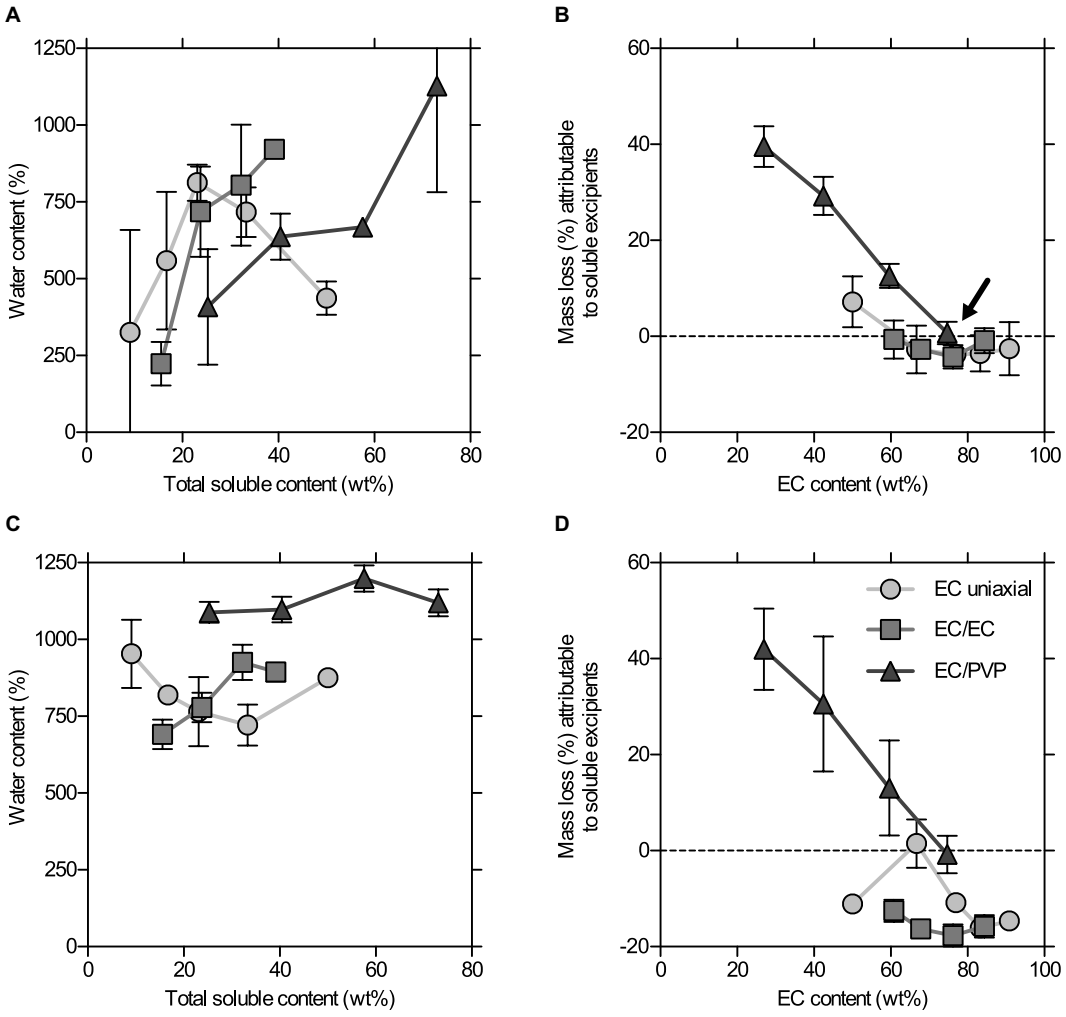

Figure 4.7—The effects of reduced surface tension and biological simulant media on *in vitro* water content and mass loss after 120 h. A) Water content suggests nearly complete pore saturation (~900% water content) in fabrics in citrate + 0.1% Tween 20 release media. B) Mass loss (%) attributable to the loss of PVP or EC from fiber materials after 120 h in citrate + 0.1% Tween 20 release media as a function of total EC content. Nearly all of the formulations had at least one replicate partially disintegrate after 120 h in citrate + 0.1% Tween 20. Note that mass loss in uniaxial EC and core-shell EC/EC-100 fibers is large and negative due to dried salts from the buffer increasing the mass of the dried sample. C) Water content (%) in fabrics after 120 h is highly variable, and is strongly dependent upon formulation structure for core-shell fibers. D) Mass loss data from fibers in VFS suggest that EC/PVP-100 4.0 fibers maintain shell integrity (arrow). Note the return to baseline for mass loss from EC-based fibers. Data represent the mean and SD (error bars) of three independent experiments.

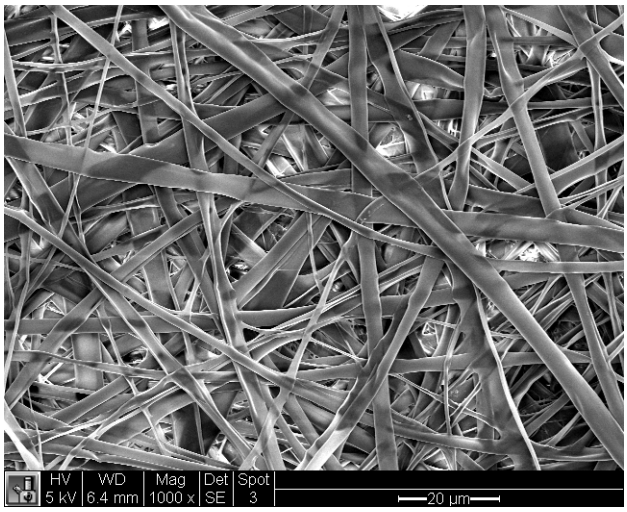

Figure 4.8—SEM image of core-shell EC/PVP-100 0.5 fibers following 120 h in VFS media. The collapsed structure of the core-shell fibers corroborated the large mass loss measured from these materials in VFS media (Figure 4.7).

Drug release into VFS yielded results that were intermediate between release into citrate buffer with and without Tween 20 (Figure 4.6). The threshold loading for burst release from uniaxial EC fibers was an intermediate >17 wt%. EC/EC-100 fibers showed promising sustained, albeit accelerated, release profiles. Finally, EC/PVP-100 fibers with thick shells demonstrated sustained release while those with thinner shells burst encapsulated maraviroc too quickly. Water content and mass loss data were also intermediate between results obtained from release in citrate media with and without Tween 20 (Figure 4.7). These observations were consistent with trends in media surface tension (Table 4.6).

Release from EC/PVP-100 4.0 and EC/EC-100 2.0 fibers into cDMEM illustrated the impact of elevated pH on drug release. cDMEM's surface tension was very similar to that of VFS, but its pH was considerably higher at pH 8.0 instead of pH 4.2 (Table 4.6). As a result, minimal maraviroc was released into cDMEM compared to VFS using otherwise identical release conditions for 120 h. However, steady, nearly zero-order release from core-shell fibers was achievable by vortexing the samples in release media for 10 sec at 30 min and 120 h after the start of the release study to displace air from the fabric pores (Figure 4.9).

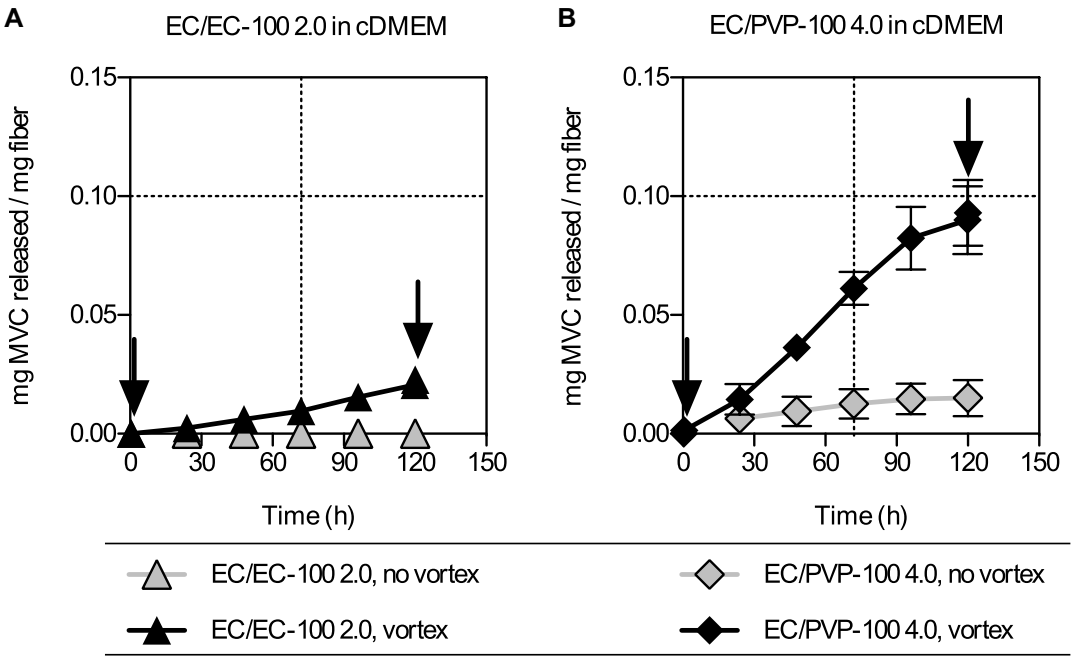

Figure 4.9—Maraviroc release from core-shell fibers into cDMEM was significantly slower than from the same fibers into VFS. Fibers had to be vortexed at the start of the release study to trigger air displacement and encourage drug release. Arrows represent 10 s vortex treatments. Data represent mean and SD (error bars) of 2 independent experiments.

4.04.5 "Set it and forget it" layered composite fabrics for single-dose rapid and sustained maraviroc release

Layered composites meant to provide both rapid and sustained release of maraviroc were created by joining rapidly dissolving PVP fabrics containing 28 wt% maraviroc (previously characterized [120]) with EC/PVP-100 2.0 core-shell fabrics containing 20 wt% maraviroc by solvent welding or mechanical pressure (Figure 4.10). Both construction methods yielded functional composite materials, but each had different effects on efficiency of material use and the dose's final appearance. The ethanol used to solvent weld rapid and sustained release fibers to one another rapidly dissolved the fabrics at the point of contact, resulting in 1-2 mm of reduction in the final dose diameter (~20% reduction in area) and a small loss of fabric material. This would be of minimal concern for samples with larger diameters. After a few seconds, the fibers at the weld dried and remained bonded together. The mechanical pressure joining method allowed for total preservation of the original materials, but resulted in a dose with visible folds on one side that would likely need refinement to avoid attracting attention from a potential user. Both the solvent welding and the folding and pressing techniques created composites that

retained their soft, flexible properties without coming apart if folded and unfolded repeatedly (at least 20 times by hand).

We measured release from these composite materials into citrate media (Figure 4.10). Upon initial contact with release media, the 28 wt% maraviroc PVP fibers rapidly hydrated and released their drug contents in less than 20 minutes without inducing wetting of the sustained release EC/PVP-100 2.0 fabrics. Thus, the dissolution of PVP immediately adjacent to an EC surface did not significantly alter the relationship between EC/PVP-100 2.0 fibers and the release media. This allowed controlled surface wetting and air displacement from EC/PVP-100 2.0 fabrics, providing sustained release of maraviroc over the next 120 h. As a result, release from composite materials was nearly equivalent to the superposition of the individual fabric's release profiles, weighted by their mass fractions in the final composites (Figure 4.10). These stacked composite materials therefore allow for adjustable amounts and timing of burst and sustained release by adjusting the ratio of PVP to EC/PVP fabric and the formulations used. Subtle differences were found between the release characteristics of the two composite types. Initial maraviroc release from folded and pressed composites was slightly slower and continued through the 20 min release time point. Additionally, the sustained release from the folded and pressed composites was less linear than from the solvent-welded composites (Figure 4.10).

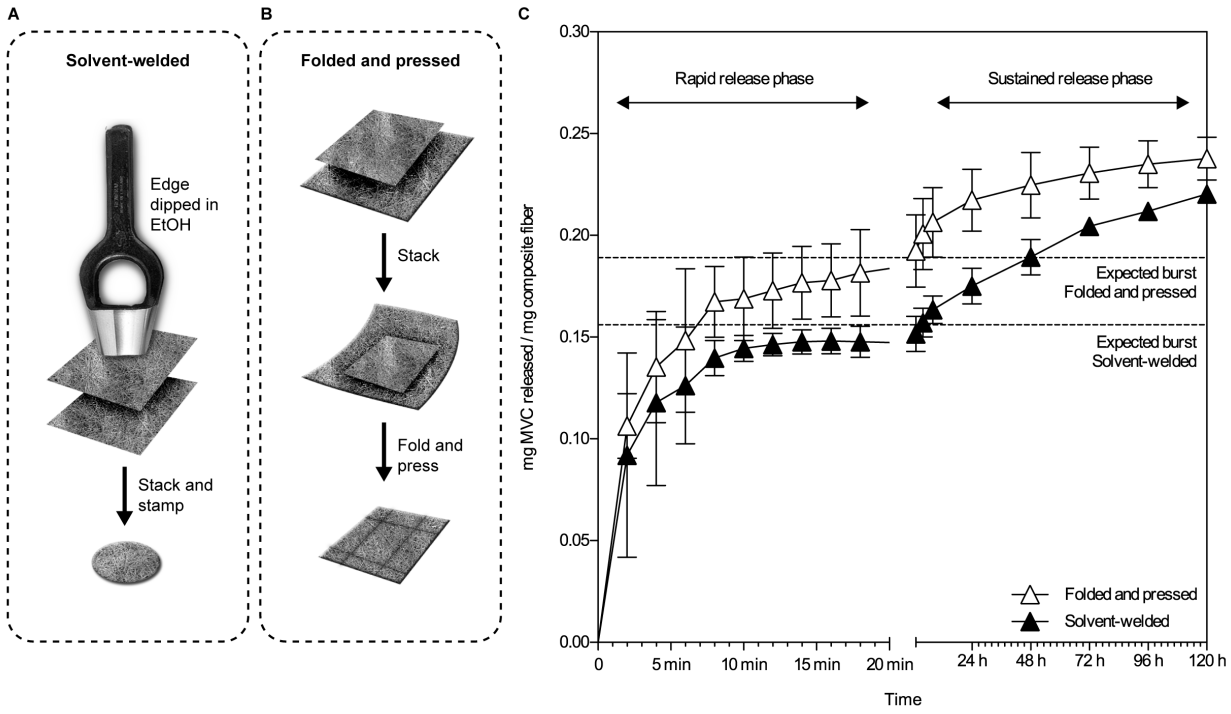

Figure 4.10—"Set it and forget it" composite fabrics demonstrate superposition of component fabrics' release profiles *in vitro*. A) Solvent welding construction method utilizing a punch dipped in ethanol to weld a stacked fiber disc around its perimeter. B) Fold and press construction method by stacking fibers, then folding the bottom fabric over the top fabric, and finally sealing with mechanical pressure along four lines. C) Maraviroc release behavior under sink conditions in 37°C citrate media. The dashed lines represent the mean expected amount of maraviroc release from the rapidly dissolving PVP fabrics with 28 wt% maraviroc based on their contribution to the overall mass of the layered composites. The horizontal axis is split to emphasize the quality of the 2-phase release. Data represent the mean and SD (error bars) of 3 independent experiments.

4.04.6 Formulation toxicity and maraviroc's *in vitro* anti-HIV activity following formulation and release

The eluates from fiber release studies shown in Figure 4.9 were tested for toxicity against TZM-bL cells as a pre-infectious assay check and showed no cytotoxic effects (Figure 4.11). Antiviral testing of fiber eluates with a TZM-bL reporter cell assay confirmed that maraviroc released from fibers into cDMEM for 120 h retained its potency against HIV-BaL *in vitro*. The IC_{50} values of maraviroc in release eluates and neat maraviroc were 5-11 nM, consistent with values seen previously in equivalent assays with HIV-BaL and TZM-bL cells (Figure 4.12) [79,120,183]. Thus, formulation into core-shell fibers and release for 120 h into cDMEM had no impact on the potency of maraviroc.

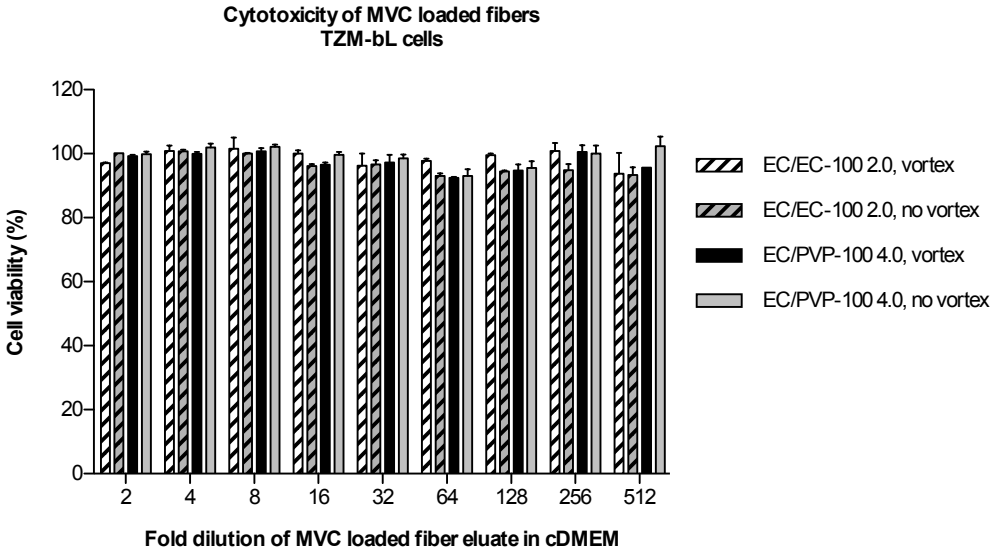

Figure 4.11—Fiber eluates into cDMEM were nontoxic to TZM-bL cells. Thus, antiviral activity was due to specific activity of maraviroc against HIV-BaL

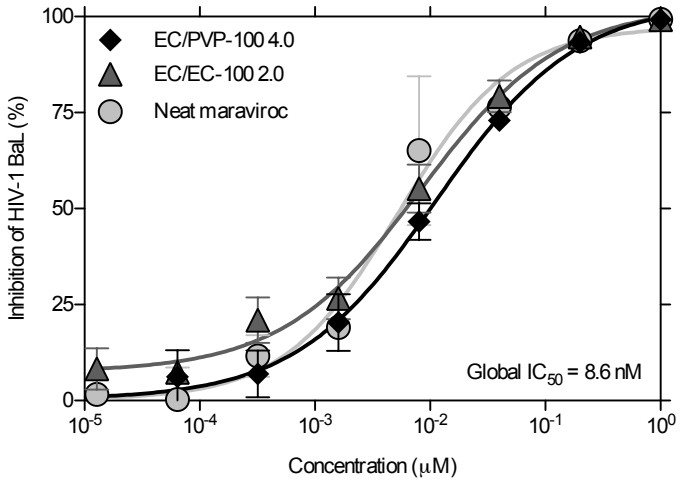

Figure 4.12—The antiviral activity of maraviroc following release from core-shell EC/PVP or EC/EC fibers into cDMEM (Figure 4.9) was equivalent to that of neat maraviroc. Data represent mean and SD from pooled technical duplicate wells of 2 independent release studies.

4.04.7 Extending the core-shell fiber system to metronidazole

In order to test how easily transferable the EC/EC and EC/PVP core-shell fiber systems were to other hydrophilic small molecule drugs, we substituted metronidazole for maraviroc into

electrospinning solutions, creating the formulations listed in Table 4.7. We were able to electrospin uniaxial EC, core-shell EC/EC, and core-shell EC/PVP fibers containing metronidazole, although PVP-metronidazole solutions required the use of a more polar solvent (TFE instead of ethanol) to solubilize the drug, which is permanently ionized. We monitored metronidazole release from EC, EC/EC, and EC/PVP fibers in citrate media for 120 h, and found unexpected release behavior from uniaxial EC and EC/EC fibers (Figure 4.13). With increased metronidazole loading in uniaxial EC fibers, drug release slowed instead of accelerated and released metronidazole continuously for 96 h. Similarly, while there was a clear relationship between Q_S/Q_C and sustained release in EC/EC-50 fibers, no clear trend existed in EC/EC-100 fibers (Figure 4.13). In contrast, EC/PVP core-shell fibers loaded with metronidazole provided sustained, tunable release analogous to behavior seen in maraviroc-loaded fibers (Figure 4.13). As the core drug loading was increased, the total magnitude of drug release rose. In addition, increasing shell thickness extended drug release time out to 48 h. Unlike mass loss from EC/PVP fibers loaded with maraviroc, mass loss from EC/PVP fibers loaded with metronidazole suggested that most, but not all of the PVP core material was lost from core-shell fibers, even those with higher Q_S/Q_C. An explanation for these differences was found upon observation of the fibers with SEM.

Table 4.7—Metronidazole fiber formulations and their drug loadings. Bolded formulations released > 0.1 mg metronidazole per mg fiber over 48 hours. MET = metronidazole. Naming format is “shell polymer / core polymer - %w/w MET - %w/w glycerol Q_S/Q_C.

Formulation	Shell solution	Core solution	Q_S/Q_C	Final drug loading (wt%)
EC-50		16% EC + 50% w/w MET in TFE	Uniaxial	33.33
EC-100		**16% EC + 100% w/w MET in TFE**	**Uniaxial**	**50.00**
EC/EC-50 1.0	16% EC in TFE	16% EC + 50% w/w MET in TFE	1.0	19.60
EC/EC-50 2.0	**16% EC in TFE**	**16% EC + 50% w/w MET in TFE**	**2.0**	**13.88**
EC/EC-50 4.0	16% EC in TFE	16% EC + 50% w/w MET in TFE	4.0	8.76
EC/EC-100 1.0	16% EC in TFE	16% EC + 100% w/w MET in TFE	1.0	32.22
EC/EC-100 2.0	16% EC in TFE	16% EC + 100% w/w MET in TFE	2.0	23.77
EC/EC-100 4.0	16% EC in TFE	16% EC + 100% w/w MET in TFE	4.0	15.59
EC/PVP-50 1.0	16% EC in TFE	15% PVP + 50% w/w MET in TFE	1.0	19.15
EC/PVP-50 2.0	16% EC in TFE	15% PVP + 50% w/w MET in TFE	2.0	13.43
EC/PVP-50 4.0	16% EC in TFE	15% PVP + 50% w/w MET in TFE	4.0	8.41
EC/PVP-100 1.0	16% EC in TFE	15% PVP + 100% w/w MET in TFE	1.0	31.62
EC/PVP-100 2.0	16% EC in TFE	15% PVP + 100% w/w MET in TFE	2.0	23.12
EC/PVP-100 4.0	16% EC in TFE	15% PVP + 100% w/w MET in TFE	4.0	15.03
EC/PVP-50-10 1.0	16% EC in TFE	15% PVP + 50% w/w MET, %10 w/w glycerol in TFE	1.0	18.37
EC/PVP-50-10 2.0	16% EC in TFE	15% PVP + 50% w/w MET, %10 w/w glycerol in TFE	2.0	13.01
EC/PVP-50-10 4.0	16% EC in TFE	15% PVP + 50% w/w MET, %10 w/w glycerol in TFE	4.0	8.21
EC/PVP-100-20 1.0	16% EC in TFE	15% PVP + 100% w/w MET, %20 w/w glycerol in TFE	1.0	29.55
EC/PVP-100-20 2.0	16% EC in TFE	15% PVP + 100% w/w MET, %20 w/w glycerol in TFE	2.0	21.89
EC/PVP-100-20 4.0	**16% EC in TFE**	**15% PVP + 100% w/w MET, %20 w/w glycerol in TFE**	**4.0**	**14.42**
EC/PVP-50 -501.0	16% EC in TFE	15% PVP + 50% w/w MET, %50 w/w glycerol in TFE	1.0	15.81
EC/PVP-50-50 2.0	16% EC in TFE	15% PVP + 50% w/w MET, %50 w/w glycerol in TFE	2.0	11.56
EC/PVP-50-50 4.0	16% EC in TFE	15% PVP + 50% w/w MET, %50 w/w glycerol in TFE	4.0	7.52
EC/PVP-100-100 1.0	16% EC in TFE	15% PVP + 100% w/w MET, %100 w/w glycerol in TFE	1.0	23.44
EC/PVP-100-100 2.0	16% EC in TFE	15% PVP + 100% w/w MET, %100 w/w glycerol in TFE	2.0	18.08
EC/PVP-100-100 4.0	16% EC in TFE	15% PVP + 100% w/w MET, %100 w/w glycerol in TFE	4.0	12.40

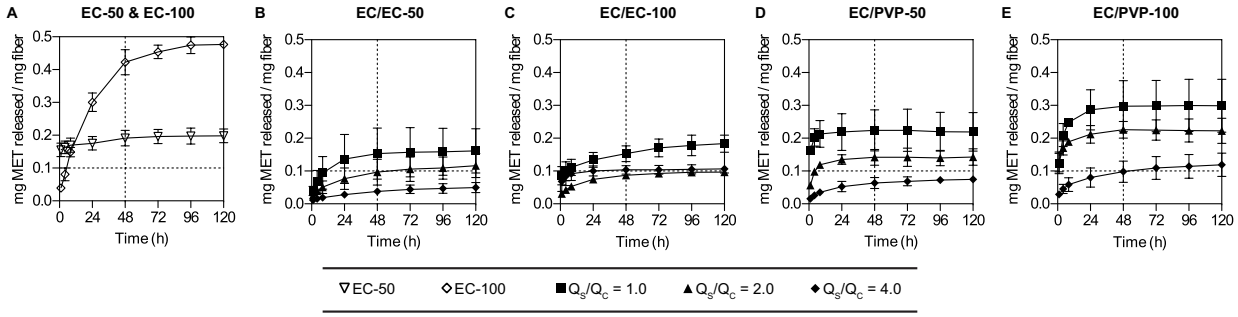

Figure 4.13—Metronidazole release from uniaxial EC fabrics, core-shell EC/EC fabrics, and core-shell EC/PVP fabrics. A) EC-50 fabrics burst released all of their metronidazole within 1 h, while EC-100 fabrics sustained the release of high levels of metronidazole for 96 h. B-C) Release from core-shell EC/EC fiber formulations with variable core loading and Q_S/Q_C. D-E) Release from core-shell EC/PVP fiber formulations with variable core loading and Q_S/Q_C. Data represent the mean and SD of 3 independent release experiments.

SEM imaging revealed that metronidazole was surface crystallizing out of the fibers, forming large drug crystals on the fabric surface (Figure 4.14). This phenomenon occurred more dramatically and more frequently in EC/EC fibers than in EC/PVP fibers, which appeared mostly free of metronidazole crystals except for at aged cut sites. Since the primary mechanism for regular, sustained release of drugs from core-shell fibers is surface-mediated wetting of the fabrics by the release media, the presence of large metronidazole crystals is thought to have caused aberrant release kinetics from EC/EC fibers (Figure 4.13). In contrast to maraviroc, metronidazole is permanently ionized (though net neutral charge), and it readily forms crystals through strong hydrogen bonding and pi-pi interactions [205]. This makes metronidazole less compatible with EC than maraviroc, which is neutral and non-ionized during formulation. While PVP core fibers showed a reasonable ability to stabilize the drug in the fibers, we noted that metronidazole has many hydrogen bond acceptors, but that PVP lacks hydrogen bond donors.

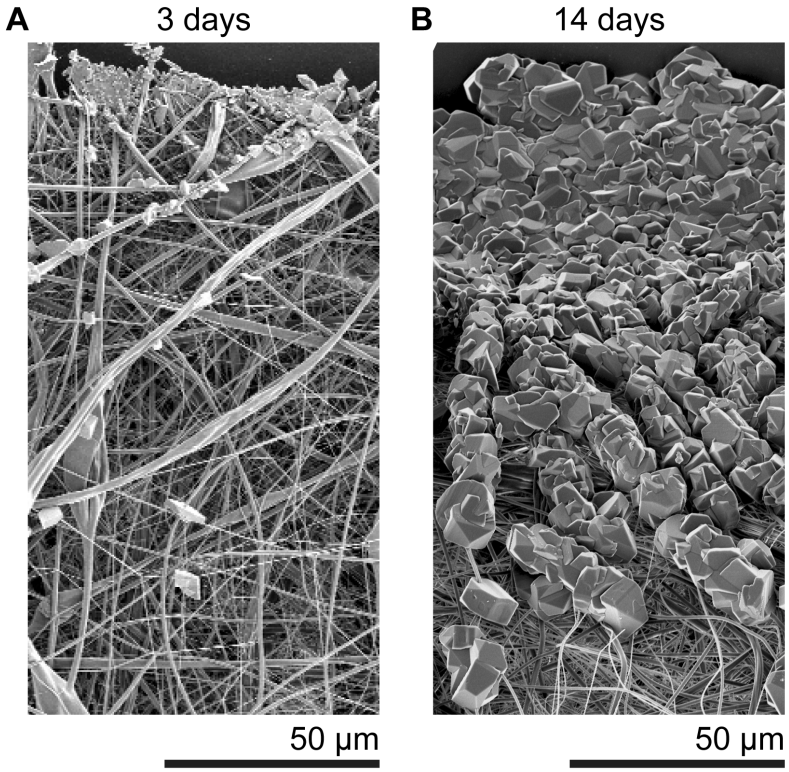

Figure 4.14— Extensive surface crystallization of metronidazole occurs at cut sites (top edge) in EC/EC-100 fibers after A) 3 days and B) 14 days. Scale bar = 50 μm.

We postulated that the addition of glycerol, which has 3 hydroxyl functional groups, to the PVP core would further stabilize metronidazole within the fiber cores via hydrogen bonding. The addition of glycerol dramatically lowered the required voltage for stable coaxial fiber formation and eliminated residual electrostatic charge from the finished fabrics, which had been very apparent in glycerol-free metronidazole-loaded core-shell fibers. SEM images of EC/EC, EC/PVP, and EC/PVP-glycerol core-shell fibers were taken daily for 3 days to monitor the kinetics of metronidazole surface crystallization at cut sites and on the general surface of fibers. We found that although adding glycerol to the core of EC/PVP fibers was insufficient to totally prevent crystal formation, the size of the crystals found in fibers with 1:1:1 mass ratios of PVP, glycerol, and metronidazole after 3 days were significantly reduced compared to the size of crystals in fibers with less or no glycerol content (Figure 4.15). The effect of glycerol incorporation on metronidazole release was readily apparent, and most fibers with glycerol in the core burst released metronidazole within 24 h (Figure 4.16). It is likely that glycerol increased the mobility of the drug in the fiber core or compromised the integrity of the EC shells.

Thus, despite improving fiber formation and improving the stability of metronidazole in solid fibers, glycerol caused burst release.

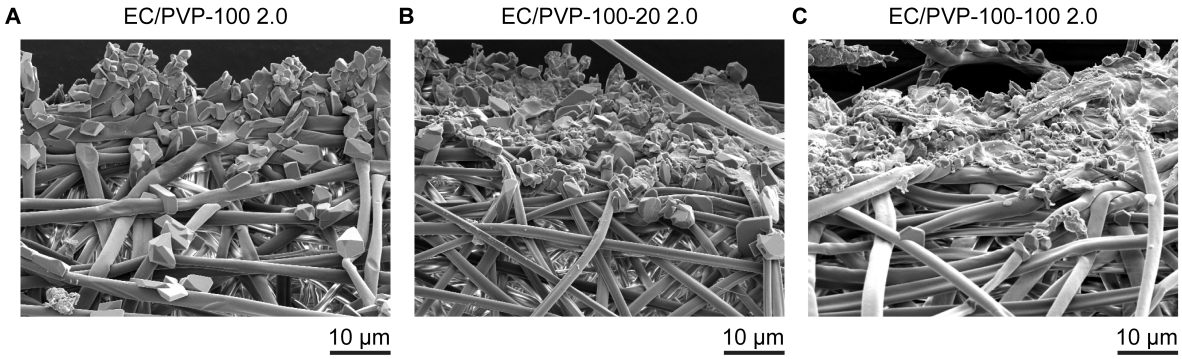

Figure 4.15— A combination of PVP and glycerol in fiber cores reduced metronidazole crystal formation in core-shell fibers. This is apparent in SEM images of 3-day-old cut sites in EC/PVP fabrics with variable glycerol content. A) No glycerol, B) 20% wt/wt metronidazole/glycerol, and C) 100% wt/wt metronidazole/glycerol. Scale bar = 10 μm.

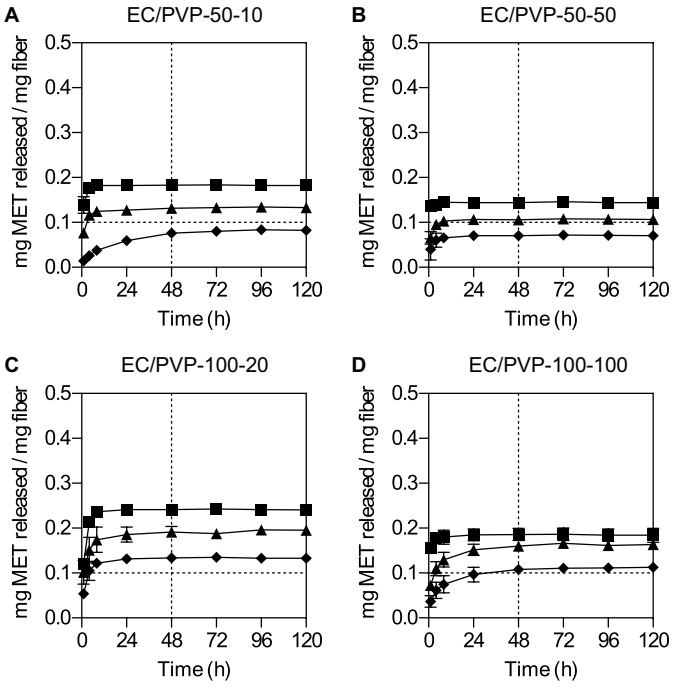

Figure 4.16-- Metronidazole burst released from various core-shell fabrics containing glycerol. A) Release from EC/PVP-50-10 fibers. B) EC/PVP-50-50 fibers. C) EC/PVP-100-20 fibers. D) EC/PVP-100-100 fibers. Data represent the mean and SD (error bars) of 3 independent experiments.

4.05 Discussion

This work significantly contributes to the coaxial electrospinning drug delivery literature by achieving very high drug loading and providing sustained release of maraviroc, a hydrophilic small molecule, for at least 72 h *in vitro*. In comparison to published examples of core-shell fibers for sustained hydrophilic drug release, our materials generally provide much higher drug loading and demonstrate a higher range of tunability [198-201]. For example, extrapolating from observed release trends from our EC/EC-100 4.0 fibers (7.9% ± 1.2% release at 120 h), electrospun fabrics containing 16 wt% maraviroc could take as long as 60 days to release their entire payload into citrate buffer without an initial burst release. If faster release is desired, our results show that reduction of Q_S/Q_C or incorporation of swellable polymers into the cores of fibers can lead to release over 24 h or less (Figure 4.2, Figure 4.3). Because of their controllable nano-architecture (Figure 4.1), core-shell fabrics promise superior controlled release characteristics compared to uniaxial electrospun fabrics, particularly for hydrophilic drug delivery.

Sustained release from core-shell fibers is usually attributed to the rate-limiting effect of drug diffusion through the fibers' polymer shells [171,197-201]. This familiar mechanism explains sustained release phenomena from large reservoir-type drug delivery systems like core-shell intravaginal rings [72]. However, electrospun fibers' small size and our modest ability to alter shell thickness during coaxial electrospinning (Figure 4.1H) make it unlikely that a polymer shell could have facilitated the broad tunability in release rates from our core-shell fabrics (and many of those found in the literature) simply by acting as an additional barrier to hydrophilic small molecule diffusion. Rather, our observations suggest that multiple mechanisms effect sustained release of hydrophilic small molecules from core-shell electrospun fabrics. In our proposed model of controlled release, the diffusional barrier aspect of the shell is seen to be just one part of a larger mechanism that primarily depends upon wicking into fabrics and penetrant transport through individual fibers. To our knowledge, this is the first time that controlled surface wetting has been proposed as the primary mechanism behind sustained hydrophilic drug release from core-shell electrospun fabrics.

Together, properties of electrospun fibers and release media combine to determine the degree of wicking and air displacement from electrospun fabrics. In our study, controlled surface wetting was the most important determinant of sustained release of hydrophilic small molecules from uniaxial EC fabrics and coaxially electrospun EC/EC and EC/PVP fabrics, as evident by comparing the first and last columns of Figure 4.6. Until the recent work of Yohe et al. with uniaxial PCL-based fabrics [173,206], controlled surface wetting was often not appreciated as a

primary mechanism for controlling release from traditional electrospun fabrics. This is in spite of the fact that electrospinning is often utilized to form superhydrophobic materials by virtue of a nano-textured surface that traps air in between water and hydrophobic polymers [207,208]. Besides those core-shell fibers engineered to wet out for tissue engineering purposes [99,102], most core-shell fibers for sustained release possess hydrophobic polymer shells [198-201], and the lack of rapid wicking is likely a key factor in their ability to sustain release. Without wicking, no fluid is in contact with the individual fibers' surfaces, and no drug release can occur. The kinetics of wicking through porous media are governed by Washburn's equation [209]. The electrospun fabric discs used in this study were thin and had a small aspect ratio (thickness/radius = 0.02), so wicking into fabrics either occurred rapidly (dependent upon fiber surface properties and interaction with release media) or at a rate limited by penetrant diffusion (see below). We found that spontaneous wicking was more favorable in low surface tension media and when fiber shells were thin or nonexistent, since low shell content can expose hydrophilic core contents like drugs and swellable polymers on the surface of fibers either via core-shell mixing during spinning or the presence of defects in the shell layer. In light of the observed instability of metronidazole within EC/EC and EC/PVP fabrics, sufficient shell thickness and high core drug loading must be accompanied by drug-core polymer compatibility to prevent surface migration of hydrophilic compounds that can induce capillary action [210]. For drugs like metronidazole that are stabilized by hydrogen bond donors, EC-shell polyvinyl alcohol-core fabrics may be superior to EC/PVP fabrics [211]. To the extent that wicking occurs, water fills the voids in between fibers and comes in direct contact with the fiber surface, releasing any surface drug as an initial burst.

Once the release media is in contact with the fiber surface, water (the penetrant) can diffuse into the fiber shell and further into the fiber core. The drug loading, spatial distribution of drug, and pH-dependent ionization of the drug all play a role in how quickly water penetrates the fiber, plasticizes EC [212], and swells PVP. For example, thicker shells may experience less adulteration with maraviroc from core-shell mixing during electrospinning (Table 4.3), thereby slowing the rate of water penetration into EC. The differences in release profiles among EC/EC fibers with varying shell thickness in citrate buffer with Tween 20 (Figure 4.6F) are most likely due to a large range in the effective diffusivity of maraviroc in shells with different rates of penetrant diffusion and subsequent plasticization, rather than moderate differences in shell thickness. This is analogous to the effects of plasticizers and coating composition on penetrant diffusion and release from aqueous-coated sustained release systems [213]. In addition, drug ionization-dependent water penetration into core-shell fibers has a dramatic effect on the rate of drug release (Figure 4.9). pH-responsive ionization, water penetration, and drug release is often a

characteristic of gastrointestinal delivery systems [214,215], which often employ EC coatings, and the incorporation of ionizable salts or drugs commonly results in pH-dependent release behavior through modulation of water uptake [204]. Future core-shell fibers may be designed explicitly for pH-responsive release or incorporate excipients to ensure pH-independent release rates for ionizable drugs. In our EC/PVP fibers, initially dehydrated PVP cores increased water uptake (Figure 4.4A, Figure 4.7A) by acting as a sponge, providing a sink for water to maintain the diffusive flux of water across the EC shell and into the fibers. While the PVP was not crosslinked, it likely swelled moderately upon hydration [203], which could have contributed to accelerated drug release (Figure 4.2E-H) or cracking of the EC shell and subsequent core polymer loss (Figure 4.4B, Figure 4.7B). Should core-shell fabric systems be adapted for the delivery of hydrophobic antiretrovirals like efavirenz, dapivirine, or saquinavir, they might benefit from formulation with a swellable PVP core, since this would increase the rate of drug release for compounds that have particularly low aqueous solubilities.

Only once water has penetrated the fibers and hydrated the drug molecules may maraviroc then diffuse out of the polymer shell at an appreciable rate. We propose that it is at this point that the commonly cited diffusional barrier mechanism of the shell plays a role in slowing drug release rates. The contribution of penetrant-plasticized EC toward sustained release of maraviroc and other hydrophilic small molecules from nano- or microfibers was most closely reflected in the release characteristics of maraviroc from fully wetted fabrics in citrate buffer with Tween 20 (Figure 4.6), and is generally small (release in < 72 h). By comparison, hindered diffusion of macromolecules through insoluble but porous coaxial fiber shells is significantly slower [99,102]. Thus, one approach to increase the role that shell-limited diffusion plays in controlled release could be to formulate hydrophilic small molecules into fiber cores as high molecular weight drug-polymer or drug-protein conjugates. PVP-drug conjugates have themselves been used to control release rates via hydrolysis rates [216]. Alternatively, more hydrophobic grades of EC, different shell polymers, or varying solvent and electrospinning conditions may be optimized to reduce the effective diffusivity of the drug through the shell.

Finally, we are proposing that penetrant diffusion through core-shell fibers is an important mechanism by which gradual, controlled surface wetting (as opposed to rapid wicking) and subsequent release occurs in thick-shelled core-shell fabrics. Once water is inside the fiber, it can diffuse longitudinally through the material. Penetrant diffusion will be most rapid in the fiber core, which contains hydrophilic maraviroc and sometimes PVP. Such longitudinal water transport will establish a concentration gradient that will drive water back outward toward the shell of the fibers, where it can advance the incursion of water into voids between fibers by

capillary action and encourage more extensive penetrant diffusion and drug release. While we have no direct evidence of this process occurring, our data showing gradual increases in water content from 24 h to 120 h (Figure 4.5C) in EC/PVP fabrics and correlated drug release (Figure 4.2E-H) are consistent with this mechanism and cannot be explained by rapid wicking (Washburn flow) or shell-limited diffusion.

We have presented composite materials for maraviroc release that represent a first step toward developing a new class of microbicide drug delivery systems—"set it and forget it" nanofiber microbicides. Recent research into user perceptions of pericoital microbicides found that U.S. women desire an HIV prevention product that allows them to apply it any time before sex and leave it in place for up to a week to provide protection [76]. Existing microbicide delivery systems might try to accomplish this in different ways. For example, aqueous gels or pericoital films might contain sustained release nanoparticles, and intravaginal rings might contain dissolving "pods" or rapid-release segments. However, there are challenges associated with simultaneously obtaining high drug loading and sustained release of antiretroviral drugs from nanoparticles [155,183], and engineering pericoital release subunits into intravaginal rings seems incongruous with their intended long-term use. In contrast, electrospun microbicides enable high drug loading and combine rapid and sustained delivery *in vitro* with simple post-production processing into composite fabrics (Figure 4.10).

Composite fabrics enabled elegant programming of rapid and sustained maraviroc release *in vitro*. We previously showed that rapid release PVP fibers could be used to rapidly release maraviroc [217]. PVP fibers with maraviroc loading of up to 28 wt% were shown to provide drug release *in vitro* in 2 to 20 min depending upon the drug loading and other formulation characteristics. Here, we showed that core-shell fibers could be used to tune the sustained release of maraviroc. Varying Q_S/Q_C and core solution composition during electrospinning directly impacted the rate of drug release from materials, so the timescale for full release was adjusted from mere hours to more than 5 days (Figure 4.2). Moreover, the final drug loading in fibers ranged from 4 wt% to 40 wt%, so drug release could be partially decoupled from the total mass of fiber used for delivery (Table 4.1). We utilized simple post-electrospinning processes to combine both rapid release and sustained release fibers and linearly superpose their release characteristics (Figure 4.10). Our approach is different from that of Yu et al., who previously utilized EC core, PVP shell fibers to accomplish two-phase release [195], and is more similar to that of Okuda et al., who created stacked composites by sequential electrospinning to achieve two-stage delivery of drugs [218]. Compared to these two strategies, processing prefabricated electrospun fabrics into composites has advantages for scale up, rapid prototyping, and

independent evaluation of component materials. Using solvent welding and mechanical folding and pressing, we combined PVP and EC/PVP fabrics into bilayer composites. Solvent-welded composites in particular maintained the individual release characteristics of the component materials, providing an initial 20 min burst release of maraviroc, followed by sustained release over 120 h (Figure 4.10). Slight differences in release from folded and pressed composites may have been due to the pressure applied on the fibers to seal them together. Mechanical pressure results in fibers fusing into nonporous blocks of polymer, which could delay PVP dissolution. In addition, pressure may compromise the integrity of the EC shell on EC/PVP materials at the pressed seam, resulting in more rapid release from core-shell fibers in areas immediately adjacent to seams. Our approach to constructing electrospun composites may be useful for combination drug delivery in addition to delivery over multiple timescales.

Our choice of maraviroc as a model drug for a “set it and forget it” nanofiber microbicide was based on preclinical observations of the drug’s pharmacokinetics and resulting efficacy profiles against high-dose SHIV challenge (in addition to physicochemical properties). In preclinical studies with nonhuman primates, the efficacy of maraviroc formulated in hydroxyethylcellulose vaginal gels dropped off sharply as the time between dosing and SHIV challenge increased beyond 1 h [117,118]. Rapid drug delivery from a solid delivery system like electrospun fibers might improve efficacy *in vivo* by increasing drug retention, and subsequent sustained release of the compound might ensure that target $CCR5^+$ cells in the genital tract tissue are continuously exposed to the entry inhibitor even if the initial drug dose is diluted during an initial act of coitus [219]. Of course, the current work is limited by the lack of *in vivo* data concerning the pharmacokinetics and efficacy of these electrospun microbicides. These materials must undergo rigorous testing in nonhuman primate models before it can be said how they will impact the type of microbicide delivery systems available to women and men at risk of acquiring HIV by sexual transmission. Our initial *in vitro* testing of fiber eluates confirmed that the maraviroc released from fibers is nontoxic and retains full biological potency after release for 120 h into 37°C cDMEM (Figure 4.11, Figure 4.12).

We felt that it was important to understand how easily the EC/EC and EC/PVP core-shell fiber system could be applied to other drugs for sustained release applications. Metronidazole was chosen as a second hydrophilic small molecule drug with vaginal drug delivery applications. Metronidazole is commonly used to treat bacterial vaginosis (BV) [220-222]—a very common condition characterized by elevated vaginal pH, irritation, odor, and a lack of normal lactobacillus species of bacteria in the vagina. This condition is endemic across Sub-Saharan Africa [223], and very common in the United States as well [224]. It often occurs in response to

repetitive douching of the vagina, and can lead to increased risk of STI acquisition (including HIV), preterm birth, and pelvic inflammatory disease [109,225]. The clinically preferred delivery method for metronidazole is a 5 g (~5 mL) vaginal gel containing 37.5 mg of metronidazole, applied nightly or twice daily for 7 days. We hoped that fibers could provide greater release per mass of delivery vehicle over 48 hours to reduce the risk of vaginal leakage and reduce the required dosing frequency for patients with BV. Our data show that we were able to facilitate excellent sustained release from highly loaded uniaxial EC-100 fibers and 48 h release from core-shell EC/PVP-100 4.0 fibers *in vitro* under sink conditions at pH 4.0 in citrate buffer. Our results for "set it and forget it" microbicide composite fabrics suggests a means for combining these metronidazole fabrics with electrospun fibers containing whole lactobacilli [188] for a combination therapy for BV that could be more effective than either drug or bacteria delivered in isolation [222]. While less successful than our work with maraviroc, this outcome demonstrated that it is at least facile to substitute hydrophilic drugs for maraviroc into core-shell fibers and still produce extended release electrospun fabrics.

From a materials perspective, metronidazole posed more of a challenge than maraviroc in achieving sustained release from fibers. This is because metronidazole contains a nitrous acid functional group. The result is that metronidazole, while uncharged, is permanently ionized. In fact, metronidazole is much more analogous to the microbicide antiretroviral drug UC781 [56]. These drugs have a strong tendency to form crystals via pi-pi and hydrogen bonding interactions, which cause poor shelf-stability in polymers and lead to inconsistent drug release profiles [205]. It is likely that the surface crystallization of drug (Figure 4.14) combined with its increased hydrophilicity compared to maraviroc was responsible for higher levels of wetting and more rapid drug release from fibers (Figure 4.13). Indeed, small amounts of burst release from metronidazole fibers are apparent even in formulations that provided sustained release of the drug. By adding glycerol to the fibers at up to a ~1:1 molar ratio of glycerol to metronidazole, we had hoped to stabilize metronidazole within the PVP core of EC/PVP materials and improve drug release profiles. Clark et al. used a similar strategy in 2012 to inhibit the formation of UC781 crystals on the surface of polyurethane vaginal rings [56]. EC/PVP-glycerol fibers displayed several beneficial characteristics, including reduced surface crystallization of metronidazole via hypothesized secondary interactions between glycerol's hydroxyl groups and metronidazole's nitrous acid group (Figure 4.15). Nevertheless, glycerol-loaded fibers failed to sustain drug release. It is possible that semicrystalline polyvinyl alcohol (PVA), a commonly used electrospinning and vaginal drug delivery polymer, would be more successful than PVP at simultaneously stabilizing metronidazole via hydrogen bonding from hydroxyl groups and

limiting the mobility of drug in the fiber cores [226,227]. Differential scanning calorimetry, wide angle X-ray diffraction, and FTIR may be useful methods for assessing the compatibility of drugs with core polymer candidates for sustained release fiber formulations. We believe that our current EC/EC and EC/PVP core-shell fiber system is best suited for the formulation of non-ionized small molecule antiretrovirals, such as raltegravir, with fewer tendencies to surface crystallize from polymer materials. Should these systems be adapted for the delivery of hydrophobic antiretrovirals like efavirenz, dapivirine, or saquinavir, they might benefit from application with a swellable PVP core, since this would increase the rate of drug release for compounds that have particularly low aqueous solubilities.

4.06 Conclusions

Current microbicides target either pericoital or long-term antiretroviral drug delivery to the genital mucosa. While these technologies are promising, they fail to provide users with a more flexible product type, one that can be utilized either immediately before or as long as 5 days in advance of sexual intercourse. In this work, we have taken the first step toward addressing this gap in the microbicide pipeline. We have shown that electrospinning can be used to create sustained release materials with tunable *in vitro* release kinetics that depend upon material surface chemistry, mechanical properties, drug loading, and process parameters. Furthermore, we have demonstrated that these materials can be combined into layered composites with rapid-release electrospun fibers to provide both instant and extended release of maraviroc for 5 days under sink conditions *in vitro*. Our mechanistic understanding of hydrophilic drug release from coaxial fibers offers a way forward for the development of more robust electrospun microbicides.

4.07 Acknowledgements and Funding

This work was partially supported by a National Science Foundation Graduate Research Fellowship awarded to Cameron Ball and NIH grant A1098648 awarded to Kim A. Woodrow.

Chapter 5. Future directions

5.01 Method development to improve correlations between *in vitro* and *in vivo* release from electrospun microbicides

A major challenge in the field of drug delivery is obtaining meaningful *in vitro* drug release data that informs *in vivo* transport, pharmacokinetics, and efficacy. This is especially true in the specialized field of intravaginal microbicide delivery. *In vitro* systems are useful for evaluating the behavior of pharmaceutical formulations on a rapid, low-cost, and iterative basis. They obviate the excessive use of animals in research and often allow for predictive comparisons of competing formulations, thereby leading to optimized dosage forms to move forward into *in vivo* studies. However, *in vitro* systems are only useful insofar as they can accurately correlate differences between formulations in a dish to differences between the same formulations in a living, breathing organism. Current methods for measuring the release of actives from microbicide products often fail to recapitulate *in vivo* results, even leading to the failure of Phase I clinical studies in humans[75].

Future work on electrospun microbicides (and on vaginal drug delivery more broadly) should prioritize the validation of *in vitro* release methods that accurately predict *in vivo* release behavior. This is very different from developing *in vitro* or even *ex vivo* methods to directly mimic *in vivo* conditions. That approach, apparent in the development of Matek™ vaginal epithelial tissue models, ends up adding dramatically to the cost and complexity of performing *in vitro* drug release assays while still falling far short of recapitulating *in vivo* conditions. Rather, it is my belief that researchers should strive to implement mechanistically enlightened “tricks” to improve correlations between *in vitro* and *in vivo* release systems. Below, I propose some simple methods that may be developed to increase the power of *in vitro* release assays without unduly burdening the research with extra cost or time. The first proposal is to utilize cyclodextrin in release media to provide sink conditions for hydrophobic compounds. The second proposal is to employ animal buccal mucosal tissue in Franz diffusion cells or similar apparatus to study drug release under partial sink conditions. These research efforts might be useful for improving the quality of optimized formulations moving into preclinical *in vivo* experimentation in rabbits, sheep, or nonhuman primates.

5.01.1 Replacing alcohol cosolvents with aqueous cyclodextrin solutions

Methods should be developed and validated for establishing *in vitro* sink conditions without swelling polymeric fiber matrices. Several antiretroviral drugs of interest, including dapivirine, are poorly soluble or nearly insoluble in aqueous media. This necessitates using large volumes for drug dissolution (this presents a problem for detection of very dilute compounds and may alter the mechanism for polymer hydration or dissolution) or performing release studies in aqueous-alcohol mixtures, such as 50:50 solutions of PBS and isopropanol[228]. Alcohols and other organic solvents used to establish sink conditions may cause significant swelling of the polymer matrices and alter release behavior. It has been repeatedly demonstrated that swelling of polymer networks has a dramatic impact on the effective drug diffusivity. As different polymers and APIs have unique degrees of compatibility with solvent mixtures, utilizing a cosolvent release media eliminates the predictive power of *in vitro* release studies comparing formulations with different polymer blends or API coformulation. This is a very important point. Cosolvent media will not lead to optimal formulations utilizing polymer blends or multiple APIs.

How does one increase apparent drug solubility without changing the solvent composition? A potential solution to this problem is adding solubilizing agents, like Kolliphor EL™, to the bath to establish sink conditions[51]. Lipid-based solubilizing agents such as Kolliphor EL, however, form complex structures in solution, with varying degrees of dispersion and interactions with drug compounds. Perhaps a better approach is to utilize water-soluble cyclodextrins to provide sink conditions for drug in release media. Typically, drug solubility increases linearly with cyclodextrin concentration. Once drugs localize within the hydrophobic core of the cyclodextrin molecules, they are still UV-active, and can be detected by HPLC methods. Cyclodextrins were shown previously to increase the aqueous solubility of UC781, a poorly soluble antiretroviral microbicide, by 4,000-fold from < 30 ng/mL to 107 μg/mL[229]. This would be very helpful when studying fiber formulations of dapivirine, for example. For more soluble drugs, like maraviroc, cyclodextrins may be useful for creating sink conditions in even smaller volumes of fluid to study release in low volumes, such as may exist in the vagina or rectum.

Future work would be focused on the following tasks. First, the complexation constant would be assessed from phase solubility studies in aqueous media at various pH values (e.g., 4, 6, 8) using a small number of cyclodextrins. Along with the intrinsic solubility of the drug in these media, this data would allow direct control over the solubility limit of drug in solution by adjusting the cyclodextrin concentration. Second, drug release in media utilizing either isopropanol cosolvent or cyclodextrin should be compared for manifold formulations that feature polymer blends or API coformulation. Third, any apparent differences between *in vitro* release in alcohol

or cyclodextrin media should be attributed to differences in polymer swelling based on partial solubility parameters. If possible, data should be collected from an *in vivo* model to assess which release media provides better correlation between *in vitro* and *in vivo* release results.

5.01.2 Developing inexpensive high-throughput mucosal tissue models

Moving toward assessing drug transport across mucosal tissue models may provide superior correlation between in vitro and in vivo release properties. To date, no electrospun fiber formulations have been evaluated using a Franz diffusion cell or similar apparatus. In general, diffusion cells are not used to study drug release as much as study the permeability of drugs through tissue. Along with drug solubility, permeability in mucosal tissue should be measured as a prerequisite for clinical work. Such data also enable computational modeling of drug PK[92,93]. However, Franz diffusion cells offer unique advantages for studying dynamic processes like drug release from materials in addition to traditional steady-state observations like permeability. In particular, *in vitro* studies with these systems might enable direct comparisons between fibers and alternative dosage forms (e.g., films, gels) for the delivery of ARVs in both rapid and sustained release settings[91]. The challenges for adopting these systems for intravaginal fiber testing include instrumentation costs (Franz cells) and tissue sourcing (nonhuman primate and human cervicovaginal tissue). Franz cell systems, complete with temperature controlled baths, may be purchased for less than $5,000 USD. This cost is negligible compared to the cost of embarking on *in vivo* nonhuman primate studies. Concerning tissue sourcing, buccal mucosa from pigs, obtained fresh from local butcheries, may provide an excellent model for vaginal mucosal tissues. Like the vaginal mucosa, the buccal mucosa also has a stratified, non-keratinized squamous epithelium. Pork cheek is readily available, and could be kept on ice before preparation and mounting in Franz cells for study.

Utilizing Franz cells for release experiments would enable more accurate study of expected *in vivo* release from electrospun fiber formulations. The mucosal tissue would form a barrier between the donor and receptor chambers, simulating the vaginal epithelium in terms of gross anatomical structure. If desired, cervical mucus simulant or vaginal fluid simulant would be applied to the apical side of the tissue. Then, the fiber dose would be placed onto the tissue, and light pressure would be applied from above with a weight to mimic the pressure of collapsed vaginal walls. Drug concentration would be measured in the receptor chamber over time to assess the effect of dosage characteristics on transport through tissue into the plasma

equivalent. This system would have the added benefit of being able to conduct toxicity testing on buccal mucosa.

5.02 Solid dispersions of ARV prodrug and enzyme for rapid mucosal delivery and *in situ* formation of supersaturated drug solutions for enhanced bioavailability of poorly soluble compounds by coaxial electrospinning

In addition to their use in sustained release fabrics, core-shell fibers are promising for application to solid dispersions of poorly soluble drug compounds. In particular, core-shell fibers may enable the use of novel prodrug-enzyme formulations to achieve supersaturated drug levels in the vagina for pericoital protection against STIs, HIV, or unintended pregnancy. This application is proposed briefly below.

Drug delivery systems that increase the bioavailability of poorly soluble compounds may improve upon current pericoital dosage forms. Many ARVs with potent antiviral activity are practically insoluble in aqueous media. Dapivirine, for example, has an extremely low solubility on the order of ~20 ng/mL. As a result, pericoital microbicides containing even low amounts of the drug (1 wt% or less) require long periods of time (~1 hour) to release their protective payload under sink conditions *in vitro*[51]. Incomplete or slow drug release *in vivo* translates to less effective prevention of HIV transmission. Thus, formulating microbicides for the rapid dissolution and absorption of drugs into tissue may improve pericoital prevention outcomes. Electrospun fibers can rapidly accelerate drug delivery compared to film formulations via solid dispersion[91]. In addition, recent groundbreaking work by Mamta Kapoor at the University of Minnesota on prodrug-enzyme delivery has demonstrated that codelivery of highly soluble prodrugs (whose parent drugs are practically insoluble) and cleaving enzymes at mucosal sites can form supersaturated drug solutions *in situ* to increase the flux of compounds up to 6-fold across mucosal membranes[230]. Coaxial electrospinning has a long history of use for the benign encapsulation and release of large proteins with minimal impact of enzymatic activity[193,231]. Furthermore, coaxial spinning would enable physical separation of prodrugs and enzyme during manufacture while maintaining their close physical proximity for rapid mixing and prodrug cleavage upon hydration *in vivo*.

A number of criteria must be met for such a project to be successful. First, an API with poor solubility must be identified that either has a soluble prodrug form or can be modified to create a more soluble prodrug. Second, an enzyme capable of catalyzing the degradation of the prodrug

into the parent drug and solubilizing metabolite must be identified. The primary requirement for such an enzyme would be high activity and a large k_{cat}, since the kinetics of parent drug formation would need to outpace the kinetics of drug crystallization and precipitation in solution. Third, the prodrug and enzyme must be electrospinnable in aqueous solutions of polyvinyl alcohol, polyvinylpyrrolidone, polyethylene oxide, or other common polymers employed for preparing solid amorphous dispersions via electrospinning. Lactose and disintegrants may be added to the dispersions to further accelerate fiber dissolution. The effects of varying the amount of enzyme and prodrug within the fibers on supersaturated drug solution kinetics should be explored. Finally, this system's impact on flux across mucosal membranes and the resulting bioavailability should be measured *in vitro* and *in vivo*.

5.03 Improved core-shell fiber systems for sustained release electrospun microbicides

The core-shell fibers presented in this thesis provide strong rationale for the use of these materials as multi-day microbicide delivery systems. Nevertheless, their direct translation into a clinical product is hindered by a couple of characteristics. First, the fibers release drug differently in response to the surface tension of the media. Second, drug release is dependent upon drug ionization, which is a function of vaginal fluid pH. Third, the fibers contain ethyl cellulose and do not fully dissolve or disintegrate, which may require removal to prevent a site for bacterial growth. Below, I propose future research projects aimed at addressing these shortcomings for sustained release applications.

5.03.1 Engineering wettable core-shell fibers for sustained release

For robust, predictable release behavior *in vivo*, core-shell fibers should wick moisture and release encapsulated drugs with roughly the same kinetics in a range of aqueous media *in vitro*. The surface tension of human vaginal fluid and cervical mucous will depend upon the composition of bodily secretions and the use of vaginal products, including surfactant spermicides like nonoxynol-9. In order to minimize variability of *in vivo* drug release across individuals and sexual encounters, fibers should be designed to eliminate their dependency on external parameters as much as possible. Consequently, fibers should be engineered to wet-out entirely when exposed to aqueous media, irrespective of media surface tension.

Wetting of hydrophobic polymers occurs in the presence of aqueously dispersed surfactants. Surfactant molecules in the media self-assemble into monolayers on the surface of

the hydrophobic polymer, orienting so that oily regions associate with the hydrophobic polymer and hydrophilic regions associate with water. This lowers the contact angle with the fiber material, allowing the ingress of water into the fabric and the displacement of air from the inter-fiber pores. By coating core-shell electrospun fibers with surfactant molecules, either via inclusion in the shell electrospinning solution or post-production dip-coating, it will be possible to ensure fiber wetting regardless of release media characteristics *in vitro* or *in vivo*.

Future work should investigate shell polymer excipients that enable full wetting of electrospun fabrics without posing problems for formulation toxicity *in vivo*. A number of USP grade emulsifiers with a long history of use in vaginal formulations could be screened for this purpose. For example, the company Gattefossé provides dozens of FDA approved, CGMP excipients for vaginal and rectal drug delivery that could be incorporated into shell solutions for electrospinning or dispersed in solution for dip-coating or vacuum filtration coating. Incorporation directly into shell solutions has the benefit of eliminating post-spinning modification, but may cause undesirable plasticization of shell polymers or require higher total levels of excipients to achieve equivalent surface concentrations when compared to dip-coating. Dip-coating could be optimized by dispersing candidate excipients in water across a range of concentrations, then coating fibers via vacuum filtration of the surfactant solution through the fiber membrane to rapidly deposit a monolayer of wetting agent and remove excess fluid from the system for easy drying[**]. Vacuum coating may have the added advantage of reducing the time that materials may release encapsulated drugs into solution, helping to reduce burst release from finished materials.

Quality assessment and quality control of resultant coatings may be assessed by surface analysis techniques and simple wicking experiments. The orientation of wetting excipients and heterogeneity on the fiber surface could be evaluated by TOF-SIMS and XPS methodologies, which can provide 2-D images of mass spectral information and atomic composition. Initial optimization could use uniaxial fibers produced from the shell polymer solution, simplifying the screening process. Fibers would be assessed for water uptake by measuring Washburn coefficients (lateral flow wicking rate) before and after surface treatment in a range of media (e.g., citrate buffer, VFS, VFS with nonoxynol-9). Ideally, water uptake would be roughly equivalent between all media types in post-treatment fibers. In this way, the resulting sustained release fibers could be expected to behave similarly in women with variable vaginal fluid surface tension or extent of fiber wetting due to physical displacement of air.

[**] This method may also prove useful for the formation of release-limiting lipid-based shells. Lipids that form liquid crystalline structures when at body temperature could be heated and applied under vacuum to uniaxial fibers to create a waxy coating that would limit drug release rates form electrospun fabrics.

5.03.2 Engineering pH-independent drug release of ionizable APIs

Human vaginal fluid can range in pH from pH 4 to pH 8 depending upon bacterial communities, genetics, and presence of seminal fluid[108]. In our core-shell fibers containing maraviroc, which is a weakly basic drug, we found that release was greatly slowed when the drug was neutral at pH > 7 (Figure 4.9). This implies that variations in vaginal pH could have a large impact on the release rate of ionizable drug compounds. Similar problems have long been encountered in drug delivery via oral delivery to the gastrointestinal tract. In many cases, it is nontrivial to reduce variations in pH-dependent solubility through the creation of prodrugs. As a result, pharmaceutical researchers have developed a range of polymer products and excipient formulation "tricks" to counteract changes in weakly basic or acidic drug ionization via the inclusion of weak organic acids or bases, respectively. These same techniques may be applied to core-shell fiber systems to ensure pH-independent release rates from coaxial fiber cores.

In the case of maraviroc, which is a weakly basic drug, inclusion of a weak organic acid in the core of the coaxial fiber may provide accelerated release at elevated pH values. Brønsted-Lowry acids are compounds that will donate a proton in a reaction with a Brønsted-Lowry base, resulting in the formation of a conjugate base. The conjugate base is ionized, possessing a negative charge. Incorporation of a neutral Brønsted acid with a pKa similar to that of maraviroc (reported as pKa = 7.3-7.9) into the core solution of fibers containing the drug would mean that ionized species would exist regardless of the pH in hydrated conditions. Carbonic acid, with a pKa of 6.4, might be a good candidate. Alternatively, low MW polymers with pH responsive properties, such as cellulose acetate phthalate (which has antiviral properties[78]) may be mixed with core polymer-drug solutions. Thus, swelling of the fiber polymer matrix in conditions where maraviroc is not ionized would accelerate drug release, hopefully recovering release rates in mildly acidic media. The incorporation of acidic species with basic drugs may also serve the function of stabilizing solid dispersions through hydrogen bonding interactions, improving shelf life of microbicide formulations.

Research efforts would focus on rapidly generating candidate core-shell fiber formulations with varying ratios of the drug and the appropriate acid or base small molecule or polymer inside the fiber cores. Release would be monitored over time at pH 4, 6, and 8 to assess the dependency of drug release on solution pH. FTIR, X-ray diffraction, and DSC methods could be used to assess the molecular and physical interactions between the drug, the pH-responsive excipient, and the polymer base. The ultimate goal of this formulation research would be to

create a core-shell electrospun fabric for sustained release applications that provides similar rates of drug release over a vaginally relevant pH range. Reduced variability in response to environmental factors will lead to less variable release *in vivo* and improved chances of success in preclinical and clinical trials.

5.03.3 Toward fully disintegrable or degradable electrospun fabrics for sustained release

Ethyl cellulose is not a biodegradable polymer. Consequently, ethyl cellulose-based core-shell fibers (Chapter 4) would need to be removed from the vagina after use. This could be difficult, and failure to remove all fiber content could provide a porous substrate for the growth of pathogenic bacteria in the vagina. Past issues with bacterial biofilm formation on woven strings for intrauterine device removal have resulted in pelvic inflammatory disease and infertility in some women (modern IUDs do not have the same issue). While fiber non-degradability poses risks of vaginal infections, it also presents a potential barrier to user adherence, since women would be unlikely to enjoy retrieving used products from the vagina for disposal. While the sustained release materials developed for this thesis provide a proof-of-concept, it is imperative that future formulations enable complete fiber degradation or disintegration on the same timescale as drug release. Even the most common biodegradable polymers, made from PLGA, degrade too slowly for this sort of application. Creative solutions are needed. Below, I briefly propose a number of options for future research in this area.

The most promising solution for addressing this problem is the creation of core-shell poly(ortho ester) (POE) microfibers by coaxial electrospinning. Type IV POEs were developed for the explicit purpose of providing sustained release of APIs via polymer surface erosion. The rate of drug release is directly proportional to the drug loading and the geometry of the delivery system. These polymers are extremely hydrophobic, but undergo acid-catalyzed degradation. Interestingly, their rate of hydrolysis and mechanical properties can be independently tuned by modulating polymer synthesis conditions. For example, POEs can have a degradation time ranging from just hours to months, and mechanical properties that allow for syringe injections or implantable medical plastics. The degradation byproducts of POEs are nontoxic and readily excretable from the blood via the kidneys[106]. These polymers have been FDA approved for use in a small number of applications, and microparticulate POEs have been used for fully degradable delivery of DNA vaccines[232]. Despite their impressive advantages for polymeric drug delivery, their widespread adoption has been hindered by intellectual property restrictions and the need for high-purity monomer used in synthesis of high molecular weight polymers (M_w >50

kDa). While uniaxial electrospinning requires high molecular weight polymers for chain entanglement, coaxial electrospinning enables fiber formation from non-spinnable core materials with the use of spinnable sheath solutions due to viscous entrainment of the fiber core. Thus, POEs with lower molecular weight but extreme hydrophobicity could be formulated with drugs into biodegradable polymer cores. The fiber sheaths could be composed of either water-soluble polymers (e.g., PVP) or rapidly degrading tyrosine-derived polycarbonates[98] with or without drug loading to provide an initial burst release. Such a core-shell fiber system would be well-received by the drug-delivery community and would possess superior properties to ethyl cellulose-based fibers. Fibers could truly become “set it and forget it” formulations with no need for vaginal recovery.

Alternative fiber formulations include core-shell fibers with a core of low molecular weight PLGA or fibers composed primarily of tyrosine-derived polycarbonates. Low molecular weight PLGA (50:50, acid endcap) degrades more quickly and is more readily available than high molecular weight PLGAs. Like low molecular weight POEs, PLGA could be incorporated into core-shell fibers through viscous entrainment by a spinnable shell solution. The key to the success of such a system would be maximizing compatibility between PLGA and the encapsulated drugs. As such, this delivery system will likely be more effective for hydrophobic APIs.

5.04 Integrating contraceptive functionalities into anti-HIV electrospun microbicides for multipurpose prevention

Unsafe sex is the 2nd most important risk factor leading to disease, disability, or death in the developing world, and the 9th in the developed world[1]. Unprotected sex leads not only to exposure to sexually transmitted infections (STIs), but also to unwanted pregnancy. Each year, an estimated 80 million women experience an unintended pregnancy[1], half a million women die from abortions or childbirth complications[233], and 2.5 million people become infected with human immunodeficiency virus (HIV)[2]. The coincidence of HIV with other sexually transmitted infections (STIs) is shockingly high, especially amongst female youth. Within the group of 15-24 year old women, AIDS is the leading cause of death globally[2]. Developing new *multipurpose prevention technology (MPT)* that simultaneously prevents HIV and other STIs and gives women access to safe, reversible contraception is a global research priority. MPTs could revolutionize women’s health on a global scale by providing women with the means to protect themselves from disease

while planning their pregnancies. Current work on developing MPTs has largely come from collaboration between anti-HIV microbicide and family planning researchers.

In clinical trials of microbicides, the majority of women often perceive their risk of acquiring HIV as minimal[39] although it can be quite high—5%[39] or even 9%[36] per woman-year depending on the study population. However, a majority of women of reproductive age throughout Sub-Saharan Africa are all quite aware of the risks associated with having children; there were 162,000 maternal mortalities (10.4% of which were attributable to ADIS) in the region in 2010, and the adult lifetime risk of maternal mortality was 1 in 39[234]. A recent study from Nigeria, a country in which 1 of 23 women will die from pregnancy related complications, reported that 96.3% of women surveyed knew that pregnancy could lead to death, and that 69.1% of those surveyed had experienced at least 1 maternal mortality in their family[235]. This high level of awareness is reflected in the growing number of women who wish to use modern[††] contraceptive methods[233]. It is therefore likely that integrating safe, effective contraception into anti-HIV microbicides would make anti-HIV products more desirable, less stigmatized, and ultimately more effective.

While the desire to access contraceptives has increased in many countries, the majority of women in Sub-Saharan Africa who would like to avoid pregnancy with modern methods lack access (see Table 2). Many women therefore cannot space their pregnancies. Unintended pregnancies often end in seeking unsafe abortion, which contributes substantially to maternal mortality in developing countries[1,233,236]. Other causes of maternal mortality include anemia, insufficient access to obstetric and neonatal care, and hemorrhagic bleeding[234]. For African women, the threat of unintended pregnancy is very real, and is perceived as such. Combining anti-HIV microbicide functionality into a contraceptive product would allow users wishing to avoid pregnancy to also benefit from HIV protection at the time of sex[48,237].

[††] "Modern methods of contraception include female and male sterilization, oral hormonal pills, the intra-uterine device (IUD), the male condom, injectables, the implant (including Norplant), vaginal barrier methods, the female condom and emergency contraception."—United Nations definition, accessed July, 2013.

Table 5.1—The majority of women in Sub-Saharan Africa who wish to use modern contraceptives lack access. Excerpted from Darroch et al., Table 5[238].

Region and Subregion	Number (millions) with unmet need for modern methods			Proportion of women wanting to avoid pregnancy with unmet need for modern methods (%)		
	2003	2008	2012	2003	2008	2012
Sub-Saharan Africa	*43*	*51*	*53*	*68%*	*65%*	*60%*
Eastern Africa	17	19	20	69%	63%	54%
Middle Africa	7	10	10	83%	82%	81%
Southern Africa	2	2	2	25%	25%	17%
Western Africa	15	18	19	78%	78%	74%

A number of contraceptive options are available for integration with microbicides. Many women in Africa choose to rely upon long-term injectable contraceptives like the Depo-Provera (medroxyprogesterone acetate) shot to prevent pregnancy for at least 6 months to 1 year following delivery. While effective at preventing pregnancy, hormonal contraception in the form of an injection, implant, or oral contraception can have unwanted side effects, which may include an elevated risk for acquisition of HIV (although this is still highly controversial)[128,129,239]. Other hormonal methods include intrauterine devices like the Mirena IUD, which deliver low doses of levonorgestrel locally to the uterus and also reduce pain and bleeding associated with menstruation. The ParaGard (copper-T) IUD provides long-term contraception without the need for hormones. Short-term contraception can be provided by barrier methods like the female condom, the diaphragm, or spermicidal gels. Spermicides, as discussed previously, have historically had negative side effects by increasing inflammation in the vagina, leading to modulated immunity that results in increased risk of infection[21].

Over the past four years, I have investigated at least 4 APIs of interest for use as contraceptive agents delivered from fibers. Those were glycerol monolaurate, ferrous gluconate with ascorbic acid, methyl-β-cyclodextrin, and the peptide nisin. Glycerol monolaurate showed significant contraceptive activity against sperm in whole semen, but wasn't nearly potent enough to result in highly effective spermicidal action. In addition, the growing phobia around the use of lipid based excipients with surfactant properties for intravaginal delivery dampened enthusiasm for GML use. Meanwhile, our work with ferrous gluconate, cyclodextrin, and nisin showed poor spermicidal activity from these compounds. Thus, the integration of contraceptive activity into fibers has suffered from a lack of highly effective spermicidal or spermiostatic agents with good toxicity profiles.

Recent work on contraceptive vaccines and immunologically derived anti-sperm biologic agents, such as peptides or anti-sperm antibody fragments, could be formulated into electrospun fibers as a form of nonhormonal, reversible, short to intermediate term contraception. Efforts to find identify such agents will likely continue. In addition, researchers may discover nonhormonal small molecules or biologics that result in thickening of cervicovaginal mucous. Mucus thickeners could serve an essential role in fiber-based contraceptives.

References

1. Glasier, A., Gülmezoglu, A. M., Schmid, G. P., Moreno, C. G. & Van Look, P. F. A. Sexual and reproductive health: a matter of life and death. *Lancet* **368,** 1595–1607 (2006).
2. UNAIDS. *Global Report: UNAIDS Report on the Global AIDS Epidemic 2010 (Joint United Nations Programme on Hiv/Aids (Unaids))*. (World Health Organization, 2011).
3. Sill, T. J. & Recum, von, H. A. Electrospinning: Applications in drug delivery and tissue engineering. *Biomaterials* **29,** 1989–2006 (2008).
4. Teo, W. E. & Ramakrishna, S. A review on electrospinning design and nanofibre assemblies. *Nanotechnology* **17,** R89–R106 (2006).
5. Sharp, P. M. & Hahn, B. H. Origins of HIV and the AIDS Pandemic. *Cold Spring Harbor Perspectives in Medicine* **1,** a006841–a006841 (2011).
6. Gallo, R. C. & Montagnier, L. The Discovery of HIV as the Cause of AIDS. *N Engl J Med* **349,** 2283–2285 (2003).
7. Simon, V., Ho, D. D. & Karim, Q. A. HIV/AIDS epidemiology, pathogenesis, prevention, and treatment. *The Lancet* (2006).
8. Finkel, T. H. & Banda, N. K. Indirect mechanisms of HIV pathogenesis: how does HIV kill T cells? *Curr. Opin. Immunol.* **6,** 605–615 (1994).
9. Ho, D., Neumann, A., Perelson, A. & Chen, W. Rapid turnover of plasma virions and CD4 lymphocytes in HIV-1 infection. *Nature* (1995).
10. Picerno, I., Visalli, G., Lentile, R. & Piedimonte, G. Lymph node involution, T-cell adaptation and T-cell death in HIV infection. *HIV Therapy* **4,** 629–637 (2010).
11. Hunt, P. W. *et al.* The immunologic effects of maraviroc intensification in treated HIV-infected individuals with incomplete CD4+ T-cell recovery: a randomized trial. *Blood* **121,** 4635–4646 (2013).
12. Girard, M. P., Osmanov, S., Assossou, O. M. & Kieny, M. P. Human immunodeficiency virus (HIV) immunopathogenesis and vaccine development: a review. *Vaccine* (2011).
13. Shattock, R. J. & Moore, J. P. Inhibiting sexual transmission of HIV-1 infection. *Nature Reviews Microbiology* **1,** 25–34 (2003).
14. Wu, L. Biology of HIV mucosal transmission. *Current Opinion in HIV and AIDS* (2008).
15. Ganor, Y. & Bomsel, M. HIV-1 transmission in the male genital tract. *Am. J. Reprod. Immunol.* **65,** 284–291 (2011).
16. Quinn, T. C. *et al.* Viral load and heterosexual transmission of human immunodeficiency virus type 1. Rakai Project Study Group. *New England Journal of Medicine* **342,** 921–929 (2000).
17. Cohen, M. S. *et al.* Prevention of HIV-1 Infection with Early Antiretroviral Therapy. *N Engl J Med* **365,** 493–505 (2011).
18. Carlson, J. M. *et al.* Selection bias at the heterosexual HIV-1 transmission bottleneck. *Science* **345,** 1254031–1254031 (2014).
19. Stein, Z. A. HIV prevention: the need for methods women can use. *Am J Public Health* **80,** 460–462 (1990).
20. McGowan, I. Microbicides: A new frontier in HIV prevention. *Biologicals* **34,** 241–255 (2006).
21. Van Damme, L. *et al.* Effectiveness of COL-1492, a nonoxynol-9 vaginal gel, on HIV-1 transmission in female sex workers: a randomised controlled trial. *The Lancet* **360,** 971–977 (2002).
22. Feldblum, P. J. *et al.* SAVVY vaginal gel (C31G) for prevention of HIV infection: a

randomized controlled trial in Nigeria. *PLoS ONE* **3,** e1474 (2008).
23. Mbopi-Keou, F.-X. *et al.* A randomized, double-blind, placebo-controlled Phase II extended safety study of two Invisible Condom formulations in Cameroonian women. *Contraception* **81,** 79–85 (2010).
24. Inácio, Â. S. *et al.* In vitro surfactant structure-toxicity relationships: implications for surfactant use in sexually transmitted infection prophylaxis and contraception. *PLoS ONE* **6,** e19850 (2011).
25. Achilles, S. L., Shete, P. B., Whaley, K. J., Moench, T. R. & Cone, R. A. Microbicide efficacy and toxicity tests in a mouse model for vaginal transmission of Chlamydia trachomatis. *Sexually transmitted diseases* **29,** 655–664 (2002).
26. Pirrone, V., Wigdahl, B. & Krebs, F. C. The rise and fall of polyanionic inhibitors of the human immunodeficiency virus type 1. *Antiviral Research* **90,** 168–182 (2011).
27. Skoler-Karpoff, S. *et al.* Efficacy of Carraguard for prevention of HIV infection in women in South Africa: a randomised, double-blind, placebo-controlled trial. *Lancet* **372,** 1977–1987 (2008).
28. Halpern, V. *et al.* Effectiveness of Cellulose Sulfate Vaginal Gel for the Prevention of HIV Infection: Results of a Phase III Trial in Nigeria. *PLoS ONE* **3,** e3784 (2008).
29. Van Damme, L. *et al.* Lack of effectiveness of cellulose sulfate gel for the prevention of vaginal HIV transmission. *N Engl J Med* **359,** 463–472 (2008).
30. Abdool Karim, S. S. *et al.* Safety and effectiveness of BufferGel and 0.5% PRO2000 gel for the prevention of HIV infection in women. *AIDS* **25,** 957–966 (2011).
31. MSc, D. S. M. *et al.* PRO2000 vaginal gel for prevention of HIV-1 infection (Microbicides Development Programme 301): a phase 3, randomised, double-blind, parallel-group trial. *The Lancet* **376,** 1329–1337 (2010).
32. Carraguard Phase II South Africa Study Team. Expanded safety and acceptability of the candidate vaginal microbicide Carraguard® in South Africa. *Contraception* **82,** 563–571 (2010).
33. Marais, D. *et al.* The effectiveness of Carraguard, a vaginal microbicide, in protecting women against high-risk human papillomavirus infection. *Antivir. Ther. (Lond.)* **16,** 1219–1226 (2011).
34. Fernández-Romero, J. A. *et al.* Zinc acetate/carrageenan gels exhibit potent activity in vivo against high-dose herpes simplex virus 2 vaginal and rectal challenge. *Antimicrobial Agents and Chemotherapy* **56,** 358–368 (2012).
35. Olender, S., Wilkin, T. J., Taylor, B. S. & Hammer, S. M. Advances in antiretroviral therapy. *Top Antivir Med* **20,** 61–86 (2012).
36. Abdool Karim, Q., Abdool Karim, S. & Frohlich, J. Effectiveness and safety of tenofovir gel, an antiretroviral microbicide, for the prevention of HIV infection in women. *Science* (2010).
37. Thigpen, M. C. *et al.* Antiretroviral preexposure prophylaxis for heterosexual HIV transmission in Botswana. *N Engl J Med* **367,** 423–434 (2012).
38. Baeten, J. M. *et al.* Antiretroviral Prophylaxis for HIV Prevention in Heterosexual Men and Women. *N Engl J Med* **367,** 399–410 (2012).
39. Van Damme, L. *et al.* Preexposure prophylaxis for HIV infection among African women. *N Engl J Med* **367,** 411–422 (2012).
40. *VOICE Fact Sheet - Understanding the Results of VOICE*. at <http://www.mtnstopshiv.org/node/2003>
41. Lederman, M. & Offord, R. Microbicides and other topical strategies to prevent vaginal transmission of HIV. *Nature Reviews Immunology* (2006).
42. Rossi, L. Fact Sheet. *www.mtnstopshiv.org* (2013). at <http://www.mtnstopshiv.org/sites/default/files/attachments/Understanding%20VOI

CE%20results_FINAL.pdf>
43. Mahalingam, A. *et al.* Design of a Semisolid Vaginal Microbicide Gel by Relating Composition to Properties and Performance. *Pharm. Res.* **27,** 2478–2491 (2010).
44. Mayer, K. H. *et al.* Safety and tolerability of tenofovir vaginal gel in abstinent and sexually active HIV-infected and uninfected women. *AIDS* **20,** 543–551 (2006).
45. Rohan, L. C. *et al.* In vitro and ex vivo testing of tenofovir shows it is effective as an HIV-1 microbicide. *PLoS ONE* **5,** e9310 (2010).
46. Morrow, K. M. *et al.* Using integrated mixed methods to develop behavioral measures of factors associated with microbicide acceptability. *Qual Health Res* **21,** 987–999 (2011).
47. Moss, D. M., Siccardi, M., Back, D. J. & Owen, A. Predicting intestinal absorption of raltegravir using a population-based ADME simulation. *Journal of Antimicrobial Chemotherapy* **68,** 1627–1634 (2013).
48. Holt, B. Y., Kilbourne-Brook, M., Stone, A., Harrison, P. & Shields, W. C. Multipurpose prevention technologies for reproductive health. (2012).
49. El-Kamel, A., Sokar, M., Naggar, V. & Gamal, Al, S. Chitosan and sodium alginate-based bioadhesive vaginal tablets. *AAPS PharmSci* **4,** E44 (2002).
50. Li, W.-Z. *et al.* Post-expansile hydrogel foam aerosol of PG-liposomes: A novel delivery system for vaginal drug delivery applications. *European Journal of Pharmaceutical Sciences* **47,** 162–169 (2012).
51. Akil, A. *et al.* Development and Characterization of a Vaginal Film Containing Dapivirine, a Non- nucleoside Reverse Transcriptase Inhibitor (NNRTI), for prevention of HIV-1 sexual transmission. *Drug Deliv Transl Res* **1,** 209–222 (2011).
52. Kiser, P. F. *et al.* Design of tenofovir-UC781 combination microbicide vaginal gels. *J. Pharm. Sci.* **101,** 1852–1864 (2012).
53. Johnson, T. J. *et al.* A 90-day tenofovir reservoir intravaginal ring for mucosal HIV prophylaxis. *Antimicrobial Agents and Chemotherapy* **56,** 6272–6283 (2012).
54. Johnson, T. J., Gupta, K. M., Fabian, J., Albright, T. H. & Kiser, P. F. Segmented polyurethane intravaginal rings for the sustained combined delivery of antiretroviral agents dapivirine and tenofovir. *Eur J Pharm Sci* **39,** 203–212 (2010).
55. Malcolm, R. K., Edwards, K.-L., Kiser, P., Romano, J. & Smith, T. J. Advances in microbicide vaginal rings. *Antiviral Research* **88,** S30–S39 (2010).
56. Clark, M. R. *et al.* A hot-melt extruded intravaginal ring for the sustained delivery of the antiretroviral microbicide UC781. *J. Pharm. Sci.* **101,** 576–587 (2012).
57. Malcolm, R. K. *et al.* Sustained Release of the CCR5 Inhibitors CMPD167 and Maraviroc from Vaginal Rings in Rhesus Macaques. *Antimicrobial Agents and Chemotherapy* **56,** 2251–2258 (2012).
58. Garg, S. *et al.* Advances in development, scale-up and manufacturing of microbicide gels, films, and tablets. *Antiviral Research* **88,** S19–S29 (2010).
59. Romano, J., Malcolm, R. K., Garg, S., Rohan, L. C. & Kaptur, P. E. Microbicide delivery: formulation technologies and strategies. *Current Opinion in HIV and AIDS* **3,** 558–566 (2008).
60. Neves, das, J. & Bahia, M. F. Gels as vaginal drug delivery systems. *International Journal of Pharmaceutics* **318,** 1–14 (2006).
61. Forbes, C. J. *et al.* Non-aqueous silicone elastomer gels as a vaginal microbicide delivery system for the HIV-1 entry inhibitor maraviroc. *Journal of Controlled Release* **156,** 161–169 (2011).
62. Yoo, J.-W. & Lee, C. H. Drug delivery systems for hormone therapy. *Journal of Controlled Release* **112,** 1–14 (2006).
63. Ham, A. S. *et al.* Vaginal film drug delivery of the pyrimidinedione IQP-0528 for the prevention of HIV infection. *Pharm. Res.* **29,** 1897–1907 (2012).

64. Garg, S. *et al.* Development and Characterization of Bioadhesive Vaginal Films of Sodium Polystyrene Sulfonate (PSS), a Novel Contraceptive Antimicrobial Agent. *Pharm. Res.* **22,** 584–595 (2005).
65. Rinehart, M. T. *et al.* Time-resolved imaging refractometry of microbicidal films using quantitative phase microscopy. *Journal of Biomedical Optics* **16,** 120510 (2011).
66. Pereira, L. E. *et al.* Pharmacokinetic and safety analyses of tenofovir and tenofovir-emtricitabine vaginal tablets in pigtailed macaques. *Antimicrobial Agents and Chemotherapy* **58,** 2665–2674 (2014).
67. Nel, A. M., Mitchnick, L. B., Risha, P., Muungo, L. T. M. & Norick, P. M. Acceptability of Vaginal Film, Soft-Gel Capsule, and Tablet as Potential Microbicide Delivery Methods Among African Women. *Journal of Women's Health* **20,** 1207–1214 (2011).
68. Joglekar, N. S., Joshi, S. N., Navlakha, S. N., Katti, U. R. & Mehendale, S. M. Acceptability of Praneem polyherbal vaginal tablet among HIV uninfected women & their male partners in Pune, India--Phase I study. *Indian J. Med. Res.* **123,** 547–552 (2006).
69. Rastogi, R., Teller, R. S., Mesquita, P. M. M., Herold, B. C. & Kiser, P. F. Osmotic pump tablets for delivery of antiretrovirals to the vaginal mucosa. *Antiviral Research* **100,** 255–258 (2013).
70. Fetherston, S. M. *et al.* A silicone elastomer vaginal ring for HIV prevention containing two microbicides with different mechanisms of action. *Eur J Pharm Sci* **48,** 406–415 (2012).
71. Smith, J. M., Rastogi, R. & Teller, R. S. Intravaginal ring eluting tenofovir disoproxil fumarate completely protects macaques from multiple vaginal simian-HIV challenges. in (2013). doi:10.1073/pnas.1311355110/-/DCSupplemental
72. Clark, J. T. *et al.* Quantitative evaluation of a hydrophilic matrix intravaginal ring for the sustained delivery of tenofovir. *J Control Release* **163,** 240–248 (2012).
73. Mesquita, P. M. M. *et al.* Intravaginal ring delivery of tenofovir disoproxil fumarate for prevention of HIV and herpes simplex virus infection. *Journal of Antimicrobial Chemotherapy* **67,** 1730–1738 (2012).
74. Romano, J. *et al.* Safety and availability of dapivirine (TMC120) delivered from an intravaginal ring. *AIDS Research and Human Retroviruses* **25,** 483–488 (2009).
75. Rossi, L. First Trial of Combination ARV Vaginal Ring for HIV Prevention Finds Ring Safe but One ARV Carrying the Weight. *www.mtnstopshiv.org* (2014). at <http://www.mtnstopshiv.org/sites/default/files/attachments/MTN-013_CROI_Release_2-28-14%20-Final%20-no%20embargo.pdf>
76. van den Berg, J. J. *et al.* 'Set it and Forget it': Women's Perceptions and Opinions of Long-Acting Topical Vaginal Gels. *AIDS Behav* **18,** 862–870 (2013).
77. Friend, D. ScienceDirect - Antiviral Research : Combining prevention of HIV-1, other sexually transmitted infections and unintended pregnancies: Development of dual-protection technologies. *Antiviral Research* (2010).
78. Huang, C. *et al.* Electrospun cellulose acetate phthalate fibers for semen induced anti-HIV vaginal drug delivery. *Biomaterials* **33,** 962–969 (2012).
79. Ball, C., Krogstad, E., Chaowanachan, T. & Woodrow, K. A. Drug-Eluting Fibers for HIV-1 Inhibition and Contraception. *PLoS ONE* **7,** e49792 (2012).
80. Schiffman, J. D. & Schauer, C. L. A Review: Electrospinning of Biopolymer Nanofibers and their Applications. *Polymer Reviews* **48,** 317–352 (2008).
81. Moghe, A. Co-axial Electrospinning for Nanofiber Structures: Preparation and Applications. *Polymer Reviews* (2008).
82. *Techniques of Solubilization of Drugs*. **12,** (Marcel Dekker, Inc., 1981).

83. Agashe, H., Hu, M. & Rohan, L. Formulation and delivery of microbicides. *Curr. HIV Res.* **10,** 88–96 (2012).
84. Perioli, L., Ambrogi, V., Pagano, C., Massetti, E. & Rossi, C. New solid mucoadhesive systems for benzydamine vaginal administration. *Colloids Surf B Biointerfaces* **84,** 413–420 (2011).
85. Garg, S., Goldman, D., Krumme, M. & Rohan, L. Advances in development, scale-up and manufacturing of microbicide gels, films, and tablets. *Antiviral Research* (2010).
86. Tomar, V. *et al.* Enhancement of Solubility of Acyclovir by Solid Dispersion And Inclusion Complexation Methods. *Der Pharmacia Lettre* **2(5),** 341–352 (2010).
87. Teo, W.-E., Inai, R. & Ramakrishna, S. Technological advances in electrospinning of nanofibers. *Sci. Technol. Adv. Mater.* **12,** 013002 (2011).
88. Barnhart, K., Pretorius, E., Timbers, K. & Shera, D. In vivo distribution of a vaginal gel: MRI evaluation of the effects of gel volume, time and simulated intercourse. *Contraception* (2004).
89. Barnhart, K. T. *et al.* Vaginal distribution of two volumes of the novel microbicide gel cellulose sulfate (2.5 and 3.5 mL). *Contraception* **72,** 65–70 (2005).
90. Rosen, R. K. *et al.* Acceptability of Tenofovir Gel as a Vaginal Microbicide Among Women in a Phase I Trial: A Mixed-Methods Study. *Journal of Women's Health* **17,** 383–392 (2008).
91. Yu, D.-G. *et al.* Solid dispersions in the form of electrospun core-sheath nanofibers. *Int J Nanomedicine* **6,** 3271–3280 (2011).
92. Szeri, A. J., Park, S. C., Verguet, S., Weiss, A. & Katz, D. F. A model of transluminal flow of an anti-HIV microbicide vehicle: Combined elastic squeezing and gravitational sliding. *Phys Fluids (1994)* **20,** 83101 (2008).
93. Geonnotti, A. Compartmental transport model of microbicide delivery by an intravaginal ring. *J. Pharm. Sci.* (2010).
94. Katz, D. F. Cervical mucusProblems and opportunities for drug delivery via the vagina and cervix. *Advanced Drug DeliveryReviews* 1–17 (2002).
95. Schwartz, J. L. *et al.* A Multi-Compartment, Single and Multiple Dose Pharmacokinetic Study of the Vaginal Candidate Microbicide 1% Tenofovir Gel. *PLoS ONE* **6,** e25974 (2011).
96. Hendrix, C. W. *et al.* MTN-001: Randomized Pharmacokinetic Cross-Over Study Comparing Tenofovir Vaginal Gel and Oral Tablets in Vaginal Tissue and Other Compartments. *PLoS ONE* **8,** e55013 (2013).
97. Wang, Y. *et al.* Electrospun composite nanofibers containing nanoparticles for the programmable release of dual drugs. *Polymer Journal* **43,** 478–483 (2011).
98. Macri, L. K., Sheihet, L., Singer, A. J., Kohn, J. & Clark, R. A. F. Ultrafast and fast bioerodible electrospun fiber mats for topical delivery of a hydrophilic peptide. *J Control Release* (2012). doi:10.1016/j.jconrel.2012.04.035
99. Su, Y. *et al.* Controlled release of bone morphogenetic protein 2 and dexamethasone loaded in core-shell PLLACL-collagen fibers for use in bone tissue engineering. *Acta Biomater* **8,** 763–771 (2012).
100. Kim, T. G., Lee, D. S. & Park, T. G. Controlled protein release from electrospun biodegradable fiber mesh composed of poly(epsilon-caprolactone) and poly(ethylene oxide). *International Journal of Pharmaceutics* **338,** 276–283 (2007).
101. Luo, Y. *et al.* Surface functionalization of electrospun nanofibers for detecting E. coli O157:H7 and BVDV cells in a direct-charge transfer biosensor. *Biosensors and Bioelectronics* **26,** 1612–1617 (2010).
102. Jiang, H. *et al.* A facile technique to prepare biodegradable coaxial electrospun nanofibers for controlled release of bioactive agents. *J Control Release* **108,** 237–

243 (2005).
103. Yang, H. & Dong, L. Smart drug delivery using electrospun hollow nanofibers. 308–311 (2010). doi:10.1109/MEMSYS.2010.5442505
104. Chakraborty, S., Liao, I. & Adler, A. Electrohydrodynamics: A facile technique to fabricate drug delivery systems 10.1016/j.addr.2009.07.013 : Advanced Drug Delivery Reviews | ScienceDirect.com. *Advanced drug delivery …* (2009).
105. Magno, M. H. R. *et al.* Synthesis, degradation and biocompatibility of tyrosine-derived polycarbonate scaffolds. *Journal of Materials Chemistry* **20,** 8885 (2010).
106. Heller, J., Barr, J., Ng, S. Y., Abdellauoi, K. S. & Gurny, R. Poly(ortho esters): synthesis, characterization, properties and uses. *Advanced Drug Delivery Reviews* **54,** 1015–1039 (2002).
107. Neurath, A. R., Strick, N., Jiang, S., Li, Y.-Y. & Debnath, A. K. Anti-HIV-1 activity of cellulose acetate phthalate: synergy with soluble CD4 and induction of 'dead-end' gp41 six-helix bundles. *BMC Infectious Diseases 2010 10:331* **2,** 6 (2002).
108. Ravel, J. *et al.* Vaginal microbiome of reproductive-age women. *Proceedings of the National Academy of Sciences* **108 Suppl 1,** 4680–4687 (2011).
109. Kharsany, A. B., Hoosen, A. A. & Moodley, J. Bacterial vaginosis and lower genital tract infections in women attending out-patient clinics at a tertiary institution serving a developing community. *J Obstet Gynaecol* **17,** 171–175 (1997).
110. Blakney, A. K., Ball, C., Krogstad, E. A. & Woodrow, K. A. Antiviral Research. *Antiviral Research* **100,** S9–S16 (2013).
111. Yan, X. *et al.* High-Throughput Needleless Electrospinning of Core-Sheath Fibers. *Controlled Release Society 2013* (2013).
112. Dorr, P. *et al.* Maraviroc (UK-427,857), a Potent, Orally Bioavailable, and Selective Small-Molecule Inhibitor of Chemokine Receptor CCR5 with Broad-Spectrum Anti-Human Immunodeficiency Virus Type 1 Activity. *Antimicrobial Agents and Chemotherapy* **49,** 4721–4732 (2005).
113. Emmelkamp, J. M. & Rockstroh, J. K. Maraviroc, risks and benefits: a review of the clinical literature. *Expert Opin. Drug Saf.* **7,** 559–569 (2008).
114. ViiV Healthcare Company. *Selzentry (maraviroc) tablet, film coated*. (2013). at <http://dailymed.nlm.nih.gov/dailymed/lookup.cfm?setid=46f30ac5-c96b-429e-976d-8c5ee1c0761b#section-1>
115. Massud, I. *et al.* Lack of prophylactic efficacy of oral maraviroc in macaques despite high drug concentrations in rectal tissues. *J. Virol.* (2013). doi:10.1128/JVI.01204-13
116. Dumond, J. B. *et al.* Maraviroc Concentrates in the Cervicovaginal Fluid and Vaginal Tissue of HIV-Negative Women. *JAIDS Journal of Acquired Immune Deficiency Syndromes* **51,** 546–553 (2009).
117. Veazey, R. S. *et al.* Protection of Rhesus Macaques from Vaginal Infection by Vaginally Delivered Maraviroc, an Inhibitor of HIV-1 Entry via the CCR5 Co-Receptor. *J INFECT DIS* **202,** 739–744 (2010).
118. Malcolm, R. K. *et al.* Pharmacokinetics and efficacy of a vaginally administered maraviroc gel in rhesus macaques. *Journal of Antimicrobial Chemotherapy* **68,** 678–683 (2013).
119. Abel, S. *et al.* Assessment of the absorption, metabolism and absolute bioavailability of maraviroc in healthy male subjects. *Br J Clin Pharmacol* **65,** 60–67 (2008).
120. Ball, C. & Woodrow, K. A. Electrospun solid dispersions of maraviroc for rapid intravaginal pre-exposure prophylaxis of HIV. *Antimicrobial Agents and Chemotherapy* (2014). doi:10.1128/AAC.02564-14
121. Abel, S. *et al.* Assessment of the pharmacokinetics, safety and tolerability of

maraviroc, a novel CCR5 antagonist, in healthy volunteers. *Br J Clin Pharmacol* **65 Suppl 1,** 5–18 (2008).
122. Brown, K. C. *et al.* Single and Multiple Dose Pharmacokinetics of Maraviroc in Saliva, Semen, and Rectal Tissue of Healthy HIV-Negative Men. *Journal of Infectious Diseases* **203,** 1484–1490 (2011).
123. Neff, C. P., Ndolo, T., Tandon, A., Habu, Y. & Akkina, R. Oral Pre-Exposure Prophylaxis by Anti-Retrovirals Raltegravir and Maraviroc Protects against HIV-1 Vaginal Transmission in a Humanized Mouse Model. *PLoS ONE* **5,** e15257 (2010).
124. Garcia-Lerma, J. G. *et al.* Intermittent Prophylaxis with Oral Truvada Protects Macaques from Rectal SHIV Infection. *Science Translational Medicine* **2,** 14ra4–14ra4 (2010).
125. Grant, R. M. *et al.* Preexposure Chemoprophylaxis for HIV Prevention in Men Who Have Sex with Men. *N Engl J Med* **363,** 2587–2599 (2010).
126. CAMI. *Multipurpose Prevention Technologies for Reproductive Health*. 1–24 (2012).
127. Major, I. *et al.* A modified SILCS contraceptive diaphragm for long-term controlled release of the HIV microbicide dapivirine. *Contraception* **88,** 58–66 (2013).
128. Blish, C. A. & Baeten, J. M. Hormonal Contraception and HIV-1 Transmission. *American Journal of Reproductive Immunology* **65,** 302–307 (2010).
129. Baeten, J. M., Lavreys, L. & Overbaugh, J. The influence of hormonal contraceptive use on HIV-1 transmission and disease progression. *CLIN INFECT DIS* **45,** 360–369 (2007).
130. Minnis, A. M. & Padian, N. S. Effectiveness of female controlled barrier methods in preventing sexually transmitted infections and HIV: current evidence and future research directions. *Sex Transm Infect* **81,** 193–200 (2005).
131. Herrera, C., Cranage, M. & McGowan, I. Reverse transcriptase inhibitors as potential colorectal microbicides. *Antimicrobial agents …* (2009).
132. Singer, R. *et al.* The nonnucleoside reverse transcriptase inhibitor MIV-150 in carrageenan gel prevents rectal transmission of simian/human immunodeficiency virus infection in macaques. *J. Virol.* **85,** 5504–5512 (2011).
133. Szentivanyi, A., Chakradeo, T. & Zernetsch, H. ScienceDirect.com - Advanced Drug Delivery Reviews - Electrospun cellular microenvironments: Understanding controlled release and scaffold structure. *Advanced drug delivery …* (2011).
134. Owen, D. H. & Katz, D. F. A vaginal fluid simulant. *Contraception* **59,** 91–95 (1999).
135. Notari, S. *et al.* Simultaneous determination of maraviroc and raltegravir in human plasma by HPLC-UV. *IUBMB Life* **61,** 470–475 (2009).
136. Wei, X. *et al.* Emergence of resistant human immunodeficiency virus type 1 in patients receiving fusion inhibitor (T-20) monotherapy. *Antimicrobial Agents and Chemotherapy* **46,** 1896–1905 (2002).
137. Platt, E. J., Wehrly, K., Kuhmann, S. E., Chesebro, B. & Kabat, D. Effects of CCR5 and CD4 cell surface concentrations on infections by macrophagetropic isolates of human immunodeficiency virus type 1. *J. Virol.* **72,** 2855–2864 (1998).
138. Derdeyn, C. A. *et al.* Sensitivity of human immunodeficiency virus type 1 to the fusion inhibitor T-20 is modulated by coreceptor specificity defined by the V3 loop of gp120. *J. Virol.* **74,** 8358–8367 (2000).
139. Takeuchi, Y., McClure, M. O. & Pizzato, M. Identification of gammaretroviruses constitutively released from cell lines used for human immunodeficiency virus research. *J. Virol.* **82,** 12585–12588 (2008).
140. Abner, S. R. *et al.* A human colorectal explant culture to evaluate topical microbicides for the prevention of HIV infection. *J INFECT DIS* **192,** 1545–1556 (2005).
141. Cummins, J. E. *et al.* Preclinical testing of candidate topical microbicides for anti-

human immunodeficiency virus type 1 activity and tissue toxicity in a human cervical explant culture. *Antimicrobial Agents and Chemotherapy* **51,** 1770–1779 (2007).

142. World Health Organization. *WHO Laboratory Manual for the Examination and Processing of Human Semen (Nonserial Publications)*. (World Health Organization, 2010).
143. Ratner, B., Hoffman, A., Schoen, F. & Lemons, J. *Biomaterials science : an introduction to materials in medicine*. 297–308 (Academic Press, 1996).
144. Shive, M. & Anderson, J. Biodegradation and biocompatibility of PLA and PLGA microspheres. *Advanced Drug Delivery Reviews* **28,** 5–24 (1997).
145. Auras, R., Lim, L. & Selke, S. *Poly (lactic Acid): Synthesis, Structures, Properties, Processing, and Applications*. (Wiley, 2010).
146. Saxena, B. B., Singh, M., Gospin, R. M., Chu, C. C. & Ledger, W. J. Efficacy of nonhormonal vaginal contraceptives from a hydrogel delivery system. *Contraception* **70,** 213–219 (2004).
147. Zidovetzki, R. & Levitan, I. Use of cyclodextrins to manipulate plasma membrane cholesterol content: Evidence, misconceptions and control strategies. *Biochimica et Biophysica Acta (BBA) - Biomembranes* **1768,** 1311–1324 (2007).
148. Peterson, M. L. & Schlievert, P. M. Glycerol monolaurate inhibits the effects of Gram-positive select agents on eukaryotic cells. *Biochemistry* **45,** 2387–2397 (2006).
149. Li, Q. *et al.* Glycerol monolaurate prevents mucosal SIV transmission. *Nature* **458,** 1034–1038 (2009).
150. Wald, A. & Link, K. Risk of human immunodeficiency virus infection in herpes simplex virus type 2-seropositive persons: a meta-analysis. *J INFECT DIS* **185,** 45–52 (2002).
151. Graver, M. A. & Wade, J. J. The role of acidification in the inhibition of Neisseria gonorrhoeae by vaginal lactobacilli during anaerobic growth. *Ann. Clin. Microbiol. Antimicrob.* **10,** 8 (2011).
152. Yu, D.-G. *et al.* Third generation solid dispersions of ferulic acid in electrospun composite nanofibers. *International Journal of Pharmaceutics* **400,** 158–164 (2010).
153. Yu, D.-G., Branford-White, C., White, K., Li, X.-L. & Zhu, L.-M. Dissolution Improvement of Electrospun Nanofiber-Based Solid Dispersions for Acetaminophen. *Aaps Pharmscitech* **11,** 809–817 (2010).
154. Kieweg, S. L. & Katz, D. F. Squeezing flows of vaginal gel formulations relevant to microbicide drug delivery. *J Biomech Eng* **128,** 540–553 (2006).
155. Ham, A., Cost, M., Sassi, A. & Dezzutti, C. Targeted delivery of PSC-RANTES for HIV-1 prevention using biodegradable nanoparticles. *Pharmaceutical …* (2009).
156. Fichorova, R. N., Tucker, L. D. & Anderson, D. J. The molecular basis of nonoxynol-9-induced vaginal inflammation and its possible relevance to human immunodeficiency virus type 1 transmission. *J INFECT DIS* **184,** 418–428 (2001).
157. Han, Y. A., Singh, M. & Saxena, B. B. Development of vaginal rings for sustained release of nonhormonal contraceptives and anti-HIV agents. *Contraception* **76,** 132–138 (2007).
158. Boulmedarat, L., Bochot, A., Lesieur, S. & Fattal, E. Evaluation of buccal methyl-β-cyclodextrin toxicity on human oral epithelial cell culture model. *J. Pharm. Sci.* **94,** 1300–1309 (2005).
159. Schlievert, P. M. *et al.* Glycerol Monolaurate Does Not Alter Rhesus Macaque (Macaca mulatta) Vaginal Lactobacilli and Is Safe for Chronic Use. *Antimicrobial Agents and Chemotherapy* **52,** 4448–4454 (2008).
160. Lin, Y.-C. *et al.* Glycerol monolaurate and dodecylglycerol effects on

Staphylococcus aureus and toxic shock syndrome toxin-1 in vitro and in vivo. *PLoS ONE* **4,** e7499 (2009).
161. Projan, S. J., Brown-Skrobot, S., Schlievert, P. M., Vandenesch, F. & Novick, R. P. Glycerol monolaurate inhibits the production of beta-lactamase, toxic shock toxin-1, and other staphylococcal exoproteins by interfering with signal transduction. *The Journal of Bacteriology* **176,** 4204–4209 (1994).
162. Vetter, S. M. & Schlievert, P. M. Glycerol monolaurate inhibits virulence factor production in Bacillus anthracis. *Antimicrobial Agents and Chemotherapy* **49,** 1302–1305 (2005).
163. Strandberg, K. L. *et al.* Glycerol monolaurate inhibits Candida and Gardnerella vaginalis in vitro and in vivo but not Lactobacillus. *Antimicrobial Agents and Chemotherapy* **54,** 597–601 (2010).
164. Yu, D.-G. *et al.* Self-assembled liposomes from amphiphilic electrospun nanofibers. *Soft Matter* **7,** 8239 (2011).
165. Patton, D. L., Kidder, G. G., Sweeney, Y. C., Rabe, L. K. & Hillier, S. L. Effects of multiple applications of benzalkonium chloride and nonoxynol 9 on the vaginal epithelium in the pigtailed macaque (Macaca nemestrina). *Am. J. Obstet. Gynecol.* **180,** 1080–1087 (1999).
166. Watts, D. H., Rabe, L., Krohn, M. A., Aura, J. & Hillier, S. L. The effects of three nonoxynol-9 preparations on vaginal flora and epithelium. *J INFECT DIS* **180,** 426–437 (1999).
167. Moench, T., Mumper, R., Hoen, T., Sun, M. & Cone, R. Microbicide excipients can greatly increase susceptibility to genital herpes transmission in the mouse. *BMC Infectious Diseases 2010 10:331* **10,** 331 (2010).
168. Schlievert, P. M., Deringer, J. R., Kim, M. H., Projan, S. J. & Novick, R. P. Effect of glycerol monolaurate on bacterial growth and toxin production. *Antimicrobial Agents and Chemotherapy* **36,** 626 (1992).
169. Schwartz, J. L. *et al.* SILCS diaphragm: postcoital testing of a new single-size contraceptive device. *Contraception* **78,** 237–244 (2008).
170. Free, M. J., Srisamang, V., Vail, J., Mercer, D. & Kotz, R. Latex rubber condoms: predicting and extending shelf life. *Contraception* (1996).
171. Tiwari, S. K., Tzezana, R., Zussman, E. & Venkatraman, S. S. Optimizing partition-controlled drug release from electrospun core–shell fibers. *International Journal of Pharmaceutics* **392,** 209–217 (2010).
172. Srikar, R., Yarin, A. L., Megaridis, C. M., Bazilevsky, A. V. & Kelley, E. Desorption-Limited Mechanism of Release from Polymer Nanofibers. *Langmuir* **24,** 965–974 (2008).
173. Yohe, S. T., Colson, Y. L. & Grinstaff, M. W. Superhydrophobic materials for tunable drug release: using displacement of air to control delivery rates. *J. Am. Chem. Soc* **134,** 2016–2019 (2012).
174. Cui, W. *et al.* Electrospun fibers of acid-labile biodegradable polymers with acetal groups as potential drug carriers. *International Journal of Pharmaceutics* **361,** 47–55 (2008).
175. Yoon, H. A three-dimensional polycaprolactone scaffold combined with a drug delivery system consisting of electrospun nanofibers - Yoon - 2010 - Journal of Pharmaceutical Sciences - Wiley Online Library. *J. Pharm. Sci.* (2011).
176. Martins, A. *et al.* Osteogenic induction of hBMSCs by electrospun scaffolds with dexamethasone release functionality. *Biomaterials* **31,** 5875–5885 (2010).
177. Roche, M. *et al.* HIV-1 predisposed to acquiring resistance to maraviroc (MVC) and other CCR5 antagonists in vitro has an inherent, low-level ability to utilize MVC-bound CCR5 for entry. *Retrovirology* **8,** 89 (2011).

178. Leuner, C. Improving drug solubility for oral delivery using solid dispersions. *European Journal of Pharmaceutics and Biopharmaceutics* **50,** 47–60 (2000).
179. Brandl, M. *et al.* The amorphous solid dispersion of the poorly soluble ABT-102 forms nano/microparticulate structures in aqueous medium: impact on solubility. *Int J Nanomedicine* 5757 (2012). doi:10.2147/IJN.S36571
180. Dahlberg, C., Dvinskikh, S. V., Schuleit, M. & Furó, I. Polymer swelling, drug mobilization and drug recrystallization in hydrating solid dispersion tablets studied by multinuclear NMR microimaging and spectroscopy. *Mol. Pharmaceutics* **8,** 1247–1256 (2011).
181. Zhao, G.-L. *et al.* Asymmetric Synthesis of Maraviroc (UK-427,857). *Adv. Synth. Catal.* **352,** 2291–2298 (2010).
182. Blaine, R. L. Thermal Applications Note. 1–2 (2002). at <http://www.tainstruments.com/library_download.aspx?file=TN048.pdf>
183. Chaowanachan, T., Krogstad, E., Ball, C. & Woodrow, K. A. Drug Synergy of Tenofovir and Nanoparticle-Based Antiretrovirals for HIV Prophylaxis. *PLoS ONE* **8,** e61416 (2013).
184. Tres, F. *et al.* Journal of Controlled Release. *J Control Release* **188,** 1–8 (2014).
185. Wypych, G. *Handbook of Plasticizers*. (William Andrew, 2013).
186. D'Cruz, O. J., Samuel, P. & Uckun, F. M. Conceival, a novel noncontraceptive vaginal vehicle for lipophilic microbicides. *Aaps Pharmscitech* **6,** E56–64 (2005).
187. Korsmeyer, R. W., Gurny, R., Doelker, E., Buri, P. & Peppas, N. A. Mechanisms of solute release from porous hydrophilic polymers. *International Journal of Pharmaceutics* **15,** 25–35 (2002).
188. Nagy, Z. K. Nanofibrous solid dosage form of living bacteria prepared by electrospinning. *expresspolymlett* **8,** 352–361 (2014).
189. Williams, B. G., Abdool Karim, S. S., Karim, Q. A. & Gouws, E. Epidemiological Impact of Tenofovir Gel on the HIV Epidemic in South Africa. *JAIDS Journal of Acquired Immune Deficiency Syndromes* **58,** 207–210 (2011).
190. McGowan, I. *et al.* Phase 1 randomized trial of the vaginal safety and acceptability of SPL7013 gel (VivaGel) in sexually active young women (MTN-004). *AIDS* **25,** 1057–1064 (2011).
191. Jiang, H., Hu, Y., Zhao, P., Li, Y. & Zhu, K. Modulation of protein release from biodegradable core–shell structured fibers prepared by coaxial electrospinning. *J. Biomed. Mater. Res.* **79B,** 50–57 (2006).
192. Jia, X. *et al.* Sustained Release of VEGF by Coaxial Electrospun Dextran/PLGA Fibrous Membranes in Vascular Tissue Engineering. *J Biomater Sci Polym Ed* **22,** 1811–1827 (2011).
193. Jiang, H., Wang, L. & Zhu, K. ACCEPTED MANUSCRIPT. *J Control Release* 1–32 (2014). doi:10.1016/j.jconrel.2014.04.025
194. Jiang, Y.-N. Y., Mo, H.-Y. H. & Yu, D.-G. D. Electrospun drug-loaded core-sheath PVP/zein nanofibers for biphasic drug release. *International Journal of Pharmaceutics* **438,** 232–239 (2012).
195. Yu, D. G. *et al.* Electrospun biphasic drug release polyvinylpyrrolidone/ethyl cellulose core/sheath nanofibers. *Acta Biomater* **9,** 5665–5672 (2013).
196. Li, Z. *et al.* Carbohydrate Polymers. *Carbohydrate Polymers* **111,** 18–24 (2014).
197. Yu, D. G., Chian, W., Wang, X., Li, X. Y. & Li, Y. Linear drug release membrane prepared by a modified coaxial electrospinning process. *Journal of Membrane …* (2013). doi:10.1016/j.memsci.2012.09.062
198. Viry, L. *et al.* Emulsion-coaxial electrospinning: designing novel architectures for sustained release of highly soluble low molecular weight drugs. *Journal of Materials Chemistry* **22,** 11347 (2012).

199. Kiatyongchai, T., Wongsasulak, S. & Yoovidhya, T. Coaxial electrospinning and release characteristics of cellulose acetate-gelatin blend encapsulating a model drug. *J. Appl. Polym. Sci.* **131,** n/a–n/a (2013).
200. Wang, C., Yan, K.-W., Lin, Y.-D. & Hsieh, P. C. H. Biodegradable Core/Shell Fibers by Coaxial Electrospinning: Processing, Fiber Characterization, and Its Application in Sustained Drug Release. *Macromolecules* **43,** 6389–6397 (2010).
201. Sohrabi, A., Shaibani, P. M., Etayash, H., Kaur, K. & Thundat, T. Sustained drug release and antibacterial activity of ampicillin incorporated poly(methyl methacrylate). *Polymer* **54,** 2699–2705 (2013).
202. Korsmeyer, R. W., Lustig, S. R. & Peppas, N. A. Solute and penetrant diffusion in swellable polymers. I. Mathematical modeling. *J. Polym. Sci. B Polym. Phys.* **24,** 395–408 (1986).
203. Omidian, H. & Park, K. Swelling agents and devices in oral drug delivery. *Journal of drug delivery science and technology* **18,** 83–93 (2008).
204. Siepmann, F., Siepmann, J., Walther, M., MacRae, R. J. & Bodmeier, R. Polymer blends for controlled release coatings. *Journal of Controlled Release* **125,** 1–15 (2008).
205. Ramukutty, S. & Ramachandran, E. Journal of Crystal Growth. *Journal of Crystal Growth* **351,** 47–50 (2012).
206. Yohe, S. T., Freedman, J. D., Falde, E. J., Colson, Y. L. & Grinstaff, M. W. A Mechanistic Study of Wetting Superhydrophobic Porous 3D Meshes. *Adv. Funct. Mater.* n/a–n/a (2013). doi:10.1002/adfm.201203111
207. Ma, M. *et al.* Decorated Electrospun Fibers Exhibiting Superhydrophobicity. *Advanced Materials* **19,** 255–259 (2007).
208. Wang, X., Ding, B., Yu, J. & Wang, M. Engineering biomimetic superhydrophobic surfaces of electrospun nanomaterials. *Nano Today* **6,** 510–530 (2011).
209. Washburn, E. W. The Dynamics of Capillary Flow. *Phys. Rev.* **17,** 273–283 (1921).
210. Zeng, J. *et al.* Influence of the drug compatibility with polymer solution on the release kinetics of electrospun fiber formulation. *Journal of Controlled Release* **105,** 43–51 (2005).
211. Mallapragada, S. K., Peppas, N. A. & Colombo, P. Crystal dissolution-controlled release systems. II. Metronidazole release from semicrystalline poly(vinyl alcohol) systems. *J. Biomed. Mater. Res.* **36,** 125–130 (1997).
212. Aqualon. *AQUALON® Ethylcellulose (EC)Physical and Chemical Properties*. 1–35 (2002).
213. Lecomte, F., Siepmann, J., Walther, M., MacRae, R. J. & Bodmeier, R. Polymer blends used for the aqueous coating of solid dosage forms: importance of the type of plasticizer. *Journal of Controlled Release* **99,** 1–13 (2004).
214. Hariharan, D. & Peppas, N. A. Modelling of water transport and solute release in physiologically sensitive gels. *Journal of Controlled Release* **23,** 123–135 (1993).
215. Lecomte, F., Siepmann, J., Walther, M. & MacRae, R. J. Blends of enteric and GIT-insoluble polymers used for film coating: physicochemical characterization and drug release patterns. *Journal of Controlled …* (2003).
216. D'Souza, A. J. M., Schowen, R. L. & Topp, E. M. Polyvinylpyrrolidone–drug conjugate: synthesis and release mechanism. *Journal of Controlled Release* **94,** 91–100 (2004).
217. Ball, C. & Woodrow, K. A. in *Drug Delivery and Development of Anti-HIV Microbicides* (Neves, das, J.) (Pan Stanford Publishing).
218. Okuda, T., Tominaga, K. & Kidoaki, S. NANOMEDICINE. *J Control Release* **143,** 258–264 (2010).
219. Mesquita, P. M. *et al.* Novel preclinical models of topical PrEP pharmacodynamics

provide rationale for combination of drugs with complementary properties. *Retrovirology* **10,** 1–1 (2013).

220. Ferris, D. G., Litaker, M. S., Woodward, L., Mathis, D. & Hendrich, J. Treatment of bacterial vaginosis: a comparison of oral metronidazole, metronidazole vaginal gel, and clindamycin vaginal cream. *J Fam Pract* **41,** 443–449 (1995).
221. Sobel, J. D. *et al.* Suppressive antibacterial therapy with 0.75% metronidazole vaginal gel to prevent recurrent bacterial vaginosis. *Am. J. Obstet. Gynecol.* **194,** 1283–1289 (2006).
222. Anukam, K. *et al.* Augmentation of antimicrobial metronidazole therapy of bacterial vaginosis with oral probiotic Lactobacillus rhamnosus GR-1 and Lactobacillus reuteri RC-14: randomized, double-blind, placebo controlled trial. *Microbes Infect.* **8,** 1450–1454 (2006).
223. Myer, L., Kuhn, L., Stein, Z. A., Wright, T. C. & Denny, L. Intravaginal practices, bacterial vaginosis, and women's susceptibility to HIV infection: epidemiological evidence and biological mechanisms. *Lancet Infect Dis* **5,** 786–794 (2005).
224. Allsworth, J. E. & Peipert, J. F. Prevalence of bacterial vaginosis: 2001-2004 National Health and Nutrition Examination Survey data. *Obstet Gynecol* **109,** 114–120 (2007).
225. Atashili, J., Poole, C., Ndumbe, P. M., Adimora, A. A. & Smith, J. S. Bacterial vaginosis and HIV acquisition: a meta-analysis of published studies. *AIDS* **22,** 1493–1501 (2008).
226. Varshosaz, J., Jannesari, M., Morshed, M. & Zamani, M. Composite poly(vinyl alcohol)/poly(vinyl acetate) electrospun nanofibrous mats as a novel wound dressing matrix for controlled release of drugs. *Int J Nanomedicine* 993 (2011). doi:10.2147/IJN.S17595
227. Ndesendo, V. M. K. *et al.* A review of current intravaginal drug delivery approaches employed for the prophylaxis of HIV/AIDS and prevention of sexually transmitted infections. *Aaps Pharmscitech* **9,** 505–520 (2008).
228. Blakney, A. K., Krogstad, E. A., Jiang, Y. H. & Woodrow, K. A. Delivery of multipurpose prevention drug combinations from electrospun nanofibers using composite microarchitectures. *Int J Nanomedicine* **9,** 2967–2978 (2014).
229. Yang, H., Parniak, M. A., Isaacs, C. E., Hillier, S. L. & Rohan, L. C. Characterization of cyclodextrin inclusion complexes of the anti-HIV non-nucleoside reverse transcriptase inhibitor UC781. *AAPS J* **10,** 606–613 (2008).
230. Kapoor, M. & Siegel, R. A. Prodrug/Enzyme based acceleration of absorption of hydrophobic drugs: an in vitro study. *Mol. Pharmaceutics* **10,** 3519–3524 (2013).
231. Sakuldao, S., Yoovidhya, T. & Wongsasulak, S. Coaxial electrospinning and sustained release properties of gelatin-cellulose acetate core-shell ultrafine fibres. *ScienceAsia* (2011).
232. Wang, C. *et al.* Molecularly engineered poly(ortho ester) microspheres for enhanced delivery of DNA vaccines. *Nat Mater* **3,** 190–196 (2004).
233. Singh, S. & Darroch, J. E. Adding it up: Costs and benefits of contraceptive services. *Guttmacher Institute and UNFPA* (2012).
234. Geneva, W. *Trends in Maternal Mortality*. (2010).
235. Igberase, G. O., Isah, E. C. & Igbekoyi, O. F. Awareness and perception of maternal mortality among women in a semi-urban community in the Niger Delta of Nigeria. *Ann Afr Med* **8,** 261 (2009).
236. Darroch, J. E. & Singh, S. Estimating unintended pregnancies averted by couple-years of protection (CYP). *New York: Guttmacher Institute* (2011).
237. Harrison, P. F., Hemmerling, A., Romano, J., Whaley, K. J. & Young Holt, B. Developing Multipurpose Reproductive Health Technologies: An Integrated

Strategy. *AIDS Research and Treatment* **2013,** 1–15 (2013).
238. Darroch, J. E. & Singh, S. Trends in contraceptive need and use in developing countries in 2003, 2008, and 2012: an analysis of national surveys. *The Lancet* **381,** 1756–1762 (2013).
239. Morrison, C. S. *et al.* Hormonal contraceptive use and HIV disease progression among women in Uganda and Zimbabwe. *J. Acquir. Immune Defic. Syndr.* **57,** 157–164 (2011).